UNIVERSITY OF BIRMINGHAM

Oral Epithelium in the Pathogenesis of Periodontitis

by

Michael R Milward
BDS, MFGDP, MFDS, FHEA

Thesis submitted to the College of Medical & Dental Sciences, University of Birmingham for the Degree of Doctor of Philosophy

Unit of Periodontology
School of Dentistry
College of Medical &
Dental Sciences
University of Birmingham
February 2010.

Synopsis

Pocket/sulcular epithelium is the first line of defence to plaque bacteria and its potential role in periodontitis is investigated. This thesis describes the development of a model system, utilising an immortal epithelial cell line (H400) in order to investigate responses to periodontal pathogen stimulation (*P. gingivalis* and *F. nucleatum*) in terms of NF-κB activation, differential gene expression and cytokine production. The pathogenesis of periodontitis suggests that susceptible patients exhibit a hyper-inflammatory response to plaque bacteria, so an attempt to modulate the pro-inflammatory epithelial response using a natural di-thiol antioxidant α-lipoate was also investigated.

Data demonstrated that periodontal pathogens *P. gingivalis* and *F. nucleatum* elicited a pro-inflammatory response in the H400 model system. This was confirmed by demonstrating NF-κB activation, gene expression changes and downstream cytokine production. Ontological grouping of gene expression changes revealed a range of gene functions which support the hypothesis that the epithelium may play a role in the initiation and propagation of the periodontal lesion. In addition, α-lipoate was able to modulate this inflammatory response but not completely block this essential defence mechanism. Data obtained indicates the potential of utilising α-lipoate as an adjunct in the management of periodontitis.

Dedication

I dedicate this thesis to my wife Sandra, my son James and my mother Doreen, their love and encouragement has inspired me to complete this study. Sandra has shown unstinting support in whatever I have decided to do in life and this thesis is no exception, without her encouragement I would not have achieved so much and for this I will be forever grateful.

Acknowledgements

I would like to thank Professor Iain Chapple, Dr John Matthews and Dr Paul Cooper for all their help and assistance during this period of study. Their support, guidance and encouragement is much appreciated and has fuelled my continued interest in research, which I hope to take forward in the years to come.

I would also like to thank Kevin Carter, Jane Millard, Iwona Bujalska, John Arrand, Helen Wright and Gareth Griffiths for their help and guidance in teaching me a range of key techniques used during my studies.

My friends and colleagues Sally, Dominic, Lorraine, Keeley, Theresa & Jo have also offered lots of encouragement, and support during this study, as well as having to listen to all the moaning when my experiments went wrong!

Contents:

CHAPTER 2 Materials and Methods PAGE

Abbreviations

ALA	Alpha Lipoate
AO	Antioxidant
AP-1	Activating Protein 1
ATCC	American Type Culture Collection
CCL20	Chemokine Ligand 20
CEJ	Cemento-enamel Junction
CP	Chronic Periodontitis
DAB	Diaminobenzidene
dChip	DNA Chip Analyser
DHLA	Dihydro Lipoic Acid
DMEM	Dulbecco's Modified Eagle's Media
DTT	Dithiothreitol
EC	*Escherichia coli*
EGF	Epidermal Growth Factor
ELISA	Enzyme Linked Immunosorbent Assay
FN	*Fusobacterium nucleatum*
GAPDH	Glyceraldehyde-3-phosphate-dehydrogenase
GCF	Gingival Crevicular Fluid
GM-CSF	Granulocyte-macrophage colony-stimulating factor
GO	Gene Ontology
GSH	Reduced Glutathione
GSSG	Oxidized Glutathione
h	Hour
HMOX	Haemoxygenase
ICC	Immuno Cytochemistry
IHC	Immuno Histochemistry
IκK	IκB Kinase
IL	Interleukin
IVT	*In vitro* Transcription
LOX	Lysyl Oxidase
LPS	Lipopolysaccharide
Min	Minute
MCP	Monocyte Chemo-attractant Protein
MOI	Multiple of Infection
MRP	Migration Inhibitory Factor Related Protein
NF-κB	Nuclear Factor Kappa B
Nrf-2	NE-F2 Related Factor
OD	Optical Density
OEC	Oral Epithelial Cell
PBS	Phosphate Buffered Saline
PCR	Polymerase Chain Reaction
PG	*Porphyromonas gingivalis*
RDD	RPMI DTT and dextrose
RLT	RNeasy lysis buffer
ROS	Reactive Oxygen Species

RPMI	Roswell Park Memorial Institute
RT	Reverse Transcriptase
Sec	Seconds
SOD2	Superoxide Dismutase 2
sq	Semi Quantitative
TAE	Tris-acetate-EDTA
TAOC	Total Antioxidant Concentration
T-EDTA	Trypsin Ethylene Diamine Tetra Acetic Acid
TGF	Transforming Growth factor
TLR	Toll Like Receptors
TMB	Tetramethylbenzidine
TNF	Tumour Necrosis Factor
TSA	Trypticase Soy Agar
TSB	Trypticase Soy Broth
UV	Ultraviolet

CHAPTER 1

Introduction

1.1 Introduction

Periodontitis is a chronic inflammatory disease that affects the supporting structures of the dentition which consists of the alveolar bone, root cementum, periodontal ligament and the investing gingivae (Aisenberg, 1952). A number of forms of periodontitis have been identified the most prevalent being Chronic Periodontitis (CP), which undergoes a chronic course in susceptible individuals with increasing loss of tooth support resulting in tooth mobility and ultimately tooth loss if not appropriately managed (Page and Schroeder, 1976). Whilst the primary aetiological agent is the subgingival microbial biofilm the majority of tissue damage has been shown to be due to an aberrant (exaggerated) response of the host to these bacteria causing collateral tissue damage (Matthews et al., 2007a).

A key interface between plaque bacteria in the subgingival biofilm and the host's periodontal connective tissues is the epithelial lining of the gingival sulcus; the so called "crevicular" and "junctional" epithelia. Epithelia act as a barrier between the external environment and the internalised tissues of the host. Historically, surface epithelium was thought to exist solely as an inert barrier which in certain situations can be lubricated by antimicrobial fluids (saliva or gingival crevicular fluid (GCF) in the oral cavity), however recent research has suggested that rather than simply forming an inert barrier, epithelial tissues may have the potential to play a key role in initiating and propagating the host's inflammatory response.

Therefore, this thesis aims to investigate the ability of the gingival epithelium to respond to periodontal bacteria by production of inflammatory mediators using a model system. In addition, potential methods of modulating an "overactive" inflammatory response are investigated, which may offer potential benefits in managing patients with periodontitis and who exhibit such exaggerated inflammatory responses to plaque bacteria.

It is important to set periodontal diseases in context, and the first part of this introduction aims to provide a background to periodontitis and our current

understanding of its aetiology, prior to focusing specifically on the role of the oral epithelium in the disease process.

1.2 Inflammatory Periodontal Disease

1.2.1 Epidemiology

Inflammatory Periodontal diseases are amongst the most prevalent chronic diseases of man (Papapanou et al., 1991) and have a major impact on the health of the population not only in terms of oral health, but also in terms of their impact on systemic disease (e.g. diabetes) (Seymour et al., 2007). Tooth loss due to advanced periodontitis can impact on a patient's quality of life, but also on their diet, resulting in reduced intake of key micronutrients essential for a wide range of biological processes. Information on the changes in prevalence of periodontitis in the population is therefore key to providing adequate healthcare resources to manage the disease within the community, with the aim of improving the health of the population. Limited data on the prevalence of periodontal disease in the United Kingdom is available from the UK Adult Dental Health Survey 1998 (Morris et al., 2001). In summary, this study showed that across all age groups 54% of the UK population had significant pocketing and 43% significant attachment loss. In the over 65yr old age group these levels were increased with 67% having significant pocketing and 85% significant attachment loss. *(Figure 1.1 & 1.2)*. Therefore older age groups have a higher prevalence of periodontitis and also have higher prevalence of systemic diseases, so the potential impact of toothloss and subsequent reductions in micronutrient intake have the greatest impact on this age group.

One of the limitations of the 1998 UK Adult Dental Health Survey is the "case definition" used. Utilisation of a "single site" with attachment loss is overly sensitive and likely to include cases of incidental attachment loss, leading to a high number of false positives. Equally more stringent case definitions would improve "specificity" of diagnosis but may miss early disease. This issue was debated at

the 5th European Workshop in 2005 when a consensus view was agreed that dual case definitions should be explained in such large scale epidemiological studies one of high and one of lower sensitivity (Tonetti and Claffey, 2005).

Nevertheless the 1998 survey shows that a significant proportion of the UK population exhibit periodontal tissue destruction i.e. periodontitis, which will not only impact on the oral health and therefore quality of life of our society, but also has a major impact on our healthcare system. It has been estimated that treating periodontal diseases costs the National Health Service £0.5 billion per year, and this fails to take into account the costs within the private healthcare sector a growing part of dental health delivery in the UK. These figures are really the 'tip of the iceberg' as they fail to show the potential systemic consequences of periodontal diseases and the increasing demands from an ageing population who now wish to retain their teeth, which will further add to the healthcare burden.

Recent studies have shown potential relationships between periodontal disease and increased risk of atherogenic microvascular diseases and bacterial pneumonia, highlighting the importance of periodontal health in maintaining whole body well being (Fowler et al., 2001).

1.2.2 Classification

Classification systems are employed for the majority of diseases in order for clinicians to design suitable treatment regimes, and periodontal disease is no exception. Classification of periodontal diseases helps with the development of frameworks for study of aetiology and pathogenesis, as well as allowing the international community a way of communicating in a common language. The ideal systems employ use of aetiological agent to classify the disease; an example of this would be Tuberculosis which is classified on the basis of the causative organism *M. tuberculosis*. However, periodontal diseases cannot be classified in this manner due to their complex aetiology which is polymicrobial, polyimmune-inflammatory & polygenetic in nature. Periodontitis is an outcome of complex

interactions between microbial complexes and the hosts inflammatory / immune response; the latter being governed by our genome as well as the environment we live in.

The first classification scheme for periodontal disease was described by Joseph Fox in 1806, since this time a number of classifications for periodontal diseases have been developed as our understanding of the disease has grown. The most recent classification was proposed by 'The International Workshop for the Classification of Periodontal Diseases 1999' and this used the current evidence base to develop a system that best fitted our current understanding of disease pathogenesis, and in so doing addressed a number of issues that were lacking in previous classifications (Armitage, 1999).

The new classification is relatively complex but in summary contains a classification for gingivitis (which was divided into plaque induced and non-plaque induced, *Table 1.1)* and a section covering periodontitis (which was again further subdivided, *Table 1.2)*.

The vast majority of periodontitis seen in the population fits into the category of chronic periodontitis (CP). Whilst CP may start in adolescence (Clerehugh et al., 1990) (Clerehugh et al., 1995) the majority of disease tends to present in older patients (usually over the age of 35yrs), with the amount of periodontal tissue destruction being consistent with local risk factors; for example subgingival calculus which is often a feature. The rate of disease progression tends to be slow, and smoking and stress can impact on the disease, with smoking being a key risk factor for this type of periodontitis (Palmer et al., 2005).

The other major category of periodontitis is 'Aggressive periodontitis,' this is most commonly seen in younger age groups (less than 30 yrs), and is characterised by a rapid or episodic nature of disease progression. There is often a strong family

history of periodontal disease which suggests an underlying genetic background in this type of periodontitis (Tonetti and Claffey, 2005).

Due to the complex aetiology of periodontal diseases and with increasing knowledge of the disease process we can expect this classification to change further.

1.2.3 Anatomy of the periodontal tissues

The periodontal tissues support the teeth within the jaw, allowing the teeth to withstand the forces associated with mastication. Loss of, or disease to the periodontal tissues with periodontal inflammation, can lead to teeth becoming mobile and in advanced cases the teeth are lost.

The periodontal tissues comprise: the gingivae, periodontal ligament, root cementum and alveolar bone. In health the alveolar crest bone lies approximately 1.3mm apical to the cemento-enamel junction (CEJ) with the apical extent of the epithelial attachment close to the CEJ *(Figure 1.3).* In periodontitis, apical migration of the epithelial attachment results in pocket formation and along with alveolar bone loss are key clinical features used in disease diagnosis.

The gingivae are part of the oral mucosa and protect the underlying periodontal apparatus from the oral environment. The gingival tissues can respond to changes in the oral environment and offer a number of defence mechanisms regarded as “mucosal immunity” to protect the host. Examples of mucosal immunity include:-

- Increasing salivary flow (as well as the contents of saliva for example production of IgA and enzymes such as lysozyme).
- Increased rate of cell turnover leading to desquamation of the surface layer of epithelium, and activation of immune mechanisms.
- Expression of adhesion molecules on vascular endothelium which allows migration of inflammatory cells

- Gingival crevicular fluid (GCF) which is a transudate in health, but an inflammatory exudate in disease washing the gingival crevice, and contains immunoglobulins (IgG), complement, and polymorphonuclear cells

The gingivae form a unique junction with the tooth (Orban, 1952), the dentinogingival junction. This epithelial attachment to tooth enamel represents a classic epithelial barrier, protecting the connective tissues from the external environment.
The dentogingival junction can be subdivided into 3 zones *(Figure 1.3)*

- The gingival epithelium running from the mucogingival junction to the gingival margin.
- The crevicular epithelium which runs from the gingival margin and lines the gingival crevice (this also forms the pocket epithelium when periodontal disease is present)
- The junctional epithelium which is found at the base of the crevice. The apical extent of junctional epithelium lies against the cementoenamel junction in health but migrates apically in the presence of periodontitis.

In the presence of periodontal inflammation or trauma the junctional epithelium migrates apically onto the root surface, potentially exposing connective tissue to the oral environment which includes the plaque biofilm, thus creating a vulnerable physiological situation. Production of GCF, which carries components of the innate immune system, attempts to protect the host from the biofilm and oral environment. Microscopic examination of the gingivae shows connective tissue covered with a stratified squamous epithelium. The outer exposed epithelium of the gingivae is normally parakeratinized in man, while the inner or crevicular epithelium is much thinner and non keratinized. As with all epithelial surfaces one of the key functions is to act as a barrier to protect the underlying connective tissues from the external environment. The gingivae have a rich supply of blood allowing rapid mobilisation of inflammatory cells to the area of bacterial challenge.

In periodontitis, the junctional epithelium migrates apically forming a periodontal pocket lined with epithelium. This pocket epithelium is a barrier epithelium and not semi-permeable like junctional epithelium, i.e. a change in epithelial phenotype occurs. Alongside this process periodontal ligament and alveolar bone tissues are lost *(Figure 1.4).*

1.2.4 Natural history of Periodontitis

The natural history of any disease describes the course of the disease over time in the absence of therapeutic intervention. Over the years a number of theories describing periodontitis disease progression have been proposed.

1.2.4.1 Evidence from population studies

There are few studies that have looked at the rate of progression of periodontal disease in a population that have not been exposed to any therapeutic or preventive intervention. One classic landmark study (Loe et al., 1986) was in Sri Lanka which examined 480 male tea workers. This study looked at plaque, calculus, gingivitis and attachment loss in the dentition. These subjects were initially screened in 1970 and then five further examinations were carried out up to 1985 when 161 subjects were left from the initial cohort. During this period the subjects received no treatment and did not perform any conventional oral hygiene. In terms of attachment loss and tooth loss the subjects were subdivided into 3 groups:-

- Rapid periodontal disease progression (8% of subjects)
- Moderate periodontal disease progression (81% of subjects)
- No periodontal disease progression (11% of subjects)

As would be expected due to the lack of oral hygiene measures and subsequent levels of plaque the overall prevalence of periodontal disease were higher. However the data demonstrated different levels of periodontal disease susceptibility, with the percentage of subjects in each group closely following data from other population studies.

1.2.4.2 Evidence from observational cohort studies

Initially it was thought that disease progression followed a linear course, with attachment loss progressing with time (Loe et al., 1978). However in the early 1980's a series of studies from a group in Boston, USA (Goodson et al., 1982) (Haffajee et al., 1983) (Socransky et al., 1984) suggested that the disease followed an irregular pattern of attachment loss and disease activity and this was termed 'the random burst hypothesis' (Socransky et al., 1984). The differences seen in these studies are largely related to the thresholds set for periodontal pocket probing measurements. Further studies during the 1990's (Jeffcoat and Reddy, 1991) have added to the body of evidence with current understanding suggesting that untreated periodontal disease follows a pattern with bursts of disease activity and periods of quiescence, whereas patients who have been treated following a more predictable linear pattern (Claffey et al., 1996).

Clinically, a number of features characterise periodontitis and these include inflammation of the gingival tissues, pocketing of 4mm or more (the base of the pocket will have migrated apically), gingival recession, drifting of teeth, and exposure of furcations *(Figure 1.5).* In addition radiographic examination will show loss of bone supporting the teeth. *(Figure 1.6)*

1.3 The role of the plaque biofilm

Plaque is a complex biofilm that develops on the surface of teeth and oral soft tissues; it consists of a diverse range of bacteria with some 700 species currently identified within the oral environment (Aas et al., 2005), over half of which cannot be cultivated by conventional means and require identification using molecular biology based techniques (ten Cate, 2006). The organisms in this complex microbial community interact with each other both in a synergistic as well as a competitive manner. In addition to the microbial component the biofilm is a matrix of polymers formed by bacteria as well as components derived from saliva.

Research into the aetiological role of dental plaque initially consisted of a series of clinical studies in the 1960's, which showed that accumulation of dental plaque led to local inflammation of the gingival tissues, and subsequent removal resulted in resolution of this inflammation (Loe et al., 1965). It subsequently became widely accepted that the bacterial load directly impacts on the severity of gingivitis. However the link between plaque and periodontitis is more contentious, as patients with high plaque levels do not necessarily develop periodontitis and systemically healthy patients with good plaque control can develop the disease. This may suggest that specific bacterial species are important in the aetiology of periodontitis, a hypothesis known as The Specific Plaque Hypothesis (Loesche, 1976), but to date no one bacterial species has been explicitly implicated as a direct causative pathogen in periodontal disease. A further proposal was made in the 1980's suggesting that it was combinations of bacteria present in a mature plaque biofilm, rather than a single species that were important in disease progression, this was termed 'The Non-specific Plaque hypothesis' (Theilade, 1986). In the early 90's, as understanding of periodontal disease increased, the Environmental Plaque Hypothesis (Marsh, 1991) (Marsh, 1994) was proposed which suggested that the whole sub gingival environment was responsible for disease initiation and progression. Current evidence would support this hypothesis especially with the most common form, chronic periodontitis. Thus the periodontal microflora changes between health and disease; in health it is predominately Gram positive, aerobic and non-motile, whereas in disease the flora shifts to become Gram negative, anaerobic and motile (Socransky, 1970).

Socransky and co-workers investigated the periodontal bacterial flora in health and disease in a classic series of studies (Socransky, 1970), they used plaque samples from multiple patients and showed that certain bacterial species cluster together to produce discrete micro-environments. These studies utilised a DNA-DNA hybridisation checkerboard against 43 periodontal bacteria and allowed bacteria to be assigned into 'coloured complexes' *(Figure 1.7)* which differed in their association with periodontitis (the red complex being strongly associated with

chronic periodontitis). Therefore certain bacteria assigned to the red complex seem to be strongly implicated in the aetiology and progression of periodontitis. However it is now thought that how the host responds to these periodontal pathogens appears to be key to whether, and to what degree, periodontitis develops (Page and Kornman, 1997).

1.4 The role of the host

Current evidence indicates that periodontitis is initiated in predisposed individuals by the subgingival plaque biofilm, and that tissue destruction appears to be largely mediated by an aberrant host response to specific bacteria and their products (Fredriksson et al., 2003). This aberrant response is characterized by exaggerated inflammation, involving the release of excess proteolytic enzymes (Figueredo et al., 2005) and reactive oxygen species (ROS) by inflammatory cells (Matthews et al., 2007b). Neutrophils are recruited to the periodontal tissues in response to cytokines release (Tonetti et al., 1998), and following stimulation by the plaque biofilm, release reactive oxygen species (ROS), proteolytic enzymes and antimicrobial peptides as part of the normal host defence (Matthews et al., 2007b), with the aim of killing the colonizing bacteria. The mechanism by which neutrophils are recruited to the periodontal tissues forms the basis of this thesis, and proposes the epithelium as the key tissue involved (*Figure 1.8* suggests a possible mechanism for this recruitment).

The local release of ROS is balanced by local antioxidant (AO) defense mechanisms, such that in health a balance exists between ROS and AO.

If this balance is disturbed either by excess ROS production and / or reduced levels of extra cellular AO then oxidative stress arises and disease may result (Halliwell et al., 1992). Changes in oxidative stress can lead to either direct damage to the periodontal tissues (large changes in oxidative stress) or by activation of pro-inflammatory genes via activation of REDOX regulated gene transcription factors resulting in further inflammatory cell recruitment (smaller changes in oxidative stress) (Chapple and Matthews, 2007). *(Figure 1.9)*

This tissue damage is caused by:-

- Oxidation of low molecular weight molecules
- Protein oxidation
- Lipid peroxidation
- DNA strand breaks and base hydroxylation

(Chapple and Matthews, 2007)

A growing body of evidence implicates oxidative stress in the pathobiology of chronic periodontitis (Battino et al., 1999, Canakci et al., 2005, Chapple and Matthews, 2007). Several studies have demonstrated increased levels of biomarkers indicative of ROS induced tissue damage in periodontitis patients when compared to controls (Sugano et al., 2000) (Takane et al., 2002) (Panjamurthy et al., 2005). Antioxidant enzymes appear up regulated in inflamed periodontal tissues and in gingival crevicular fluid indicating a response to oxidative stress. (Ellis et al., 1998). Furthermore, extracellular antioxidant scavengers in plasma are depleted both individually (Chapple et al., 2007b) as well as in terms of total antioxidant activity (TAOC). Local levels within GCF are also compromised in periodontitis patients compared to controls (Brock et al., 2004) (Chapple et al., 2007a).

Tissue damage arises directly from oxidative stress and also indirectly via activation of redox-sensitive gene transcription factors like nuclear factor k-B (NF-κB) and Activator protein-1 (AP-1) (Lyakhovich et al., 2006, Schoonbroodt and Piette, 2000), which in turn leads to downstream proinflammatory cytokine/chemokine production (Sandros et al., 2000). The resultant periodontal inflammation creates a low grade inflammatory response detectable within the peripheral vasculature (Loos et al., 2000) (D'Aiuto et al., 2005). Interest has therefore re-emerged in the relationship between antioxidant micronutrients and periodontitis. Studies from the 1970s and 1980s reported conflicting results regarding associations between several individual micronutrients and prevalence of periodontitis (Slade et al., 1976). However, many utilized dietary questionnaires rather than serum biochemistry (Ismail et al., 1983) or intervention studies focused

on chronic gingivitis rather than periodontitis patients (Jacob et al., 1987) (Leggott et al., 1991). The limitations of questionnaire-based approaches to determining antioxidant intake are now recognized (Nishida et al., 2000). Food frequency questionnaires deliver weak associations with serum biochemistry in non-supplement users and only moderate correlations in supplement users (Knutsen et al., 2001). Serum biochemistry is a more robust method of analyzing antioxidant status and a recent analysis of 11,480 patients from the 3rd National Health and Nutrition Examination Survey (NHANES III) demonstrated that increased serum antioxidant concentrations are associated with reduced relative risk of periodontitis even in never smokers. (Chapple et al., 2007b)

1.5 Risk factors for Periodontitis

Risk factors are defined as factors that increase the probability of an individual developing a disease and do not imply cause and effect directly. A number of risk factors have been described for periodontitis which increase the likelihood that an individual may experience disease (Burt, 2005). They can be categorised as local or systemic risk factors. Local risk factors increase levels of plaque adjacent to the periodontium and therefore can initiate and propagate a local inflammatory response. Systemic risk factors on the other hand, act to modify the host response to the plaque adjacent to the periodontium, i.e. they may modulate the inflammatory response to the colonising bacteria. Examples of local risk factors include iatrogenic plaque retentive factors such as deficient restorations (poorly contoured or overhanging / deficient margins), or poorly designed dentures; anatomical factors such as root grooves and local overcrowding. (*Figure 1.10*) Systemic risk factors include smoking and poorly controlled diabetes.

1.6 Managing periodontal disease

Due to our limited understanding of the immune-inflammatory characteristics of periodontitis patients the management of periodontal disease has in general changed very little over the last 50 years. The key to treating periodontitis involves methods largely aimed at reducing the bacterial load adjacent to the periodontal

tissues with the secondary aim of reducing the local inflammatory response. Reduction of plaque can be achieved by instructing patients in methods of plaque removal, as well as professional removal of plaque retentive factors to help patients maintain the reductions in plaque levels. Subgingival calculus an important plaque retentive factor and a frequent finding in patients with chronic periodontitis, requires removal using specialist instruments; such treatment allows removal of the surface layer of endotoxin contaminated cementum, resulting in a root surface which will facilitate healing of the periodontal tissues. Alongside this so called “cause related therapeutic approach” other risk factors should be modified to improve the outcome of treatment. (e.g. smoking cessation).

To date, little attention has been paid to modification of the hyper-inflammatory response, which is widely recognised as being damaging in periodontitis. So there is potential that future management strategies could involve modification of the host response (alongside conventional therapy aimed at reducing plaque levels). One example of such a strategy would be damping down the inflammatory response by blocking activation of NF-κB, a key REDOX sensitive pro-inflammatory transcription factor involved in the inflammatory response (Chapple, 1997) (Van Dyke and Serhan, 2003).

1.7 The role of sulcular / pocket epithelium

Gingival epithelium is a stratified squamous epithelium and can be divided into oral, sulcular and junctional epithelium. The sulcular and junctional epithelium are non-keratinised unlike the oral epithelium, and are in close contact with bacteria present within the gingival sulcus. This area and its interaction with plaque bacteria is thought to play a key role in the initiation and propagation of the inflammatory response and therefore periodontal inflammation. In periodontitis the sulcar and junctional epithelium which are semi-permeable, converts to pocket lining epithelium which is less permeable and possesses rete ridges. Bacteria present in plaque may invade the epithelium, (either by invasion of epithelial cells or by passing between cells) and this is believed to be an important process by which pathogenic bacteria can both avoid the host immune system and inflict local tissue

damage (Han et al., 2000) (Eick et al., 2006). The ability of bacteria to adhere to host cells is important in cell stimulation. Studies *in vivo* have demonstrated a correlation between the number of bacteria attached to the periodontal epithelium and the magnitude of the inflammatory response (Vaahtoniemi et al., 1993). *P. gingivalis* has been shown to attach to a range primary epithelial cell lines, as well as to primary gingival epithelial cells. (Isogai et al., 1988) (Weinberg et al., 1997) (Yilmaz et al., 2002), (Duncan et al., 1993)

A variety of mechanisms exist to allow bacterial adhesion to epithelial cells, these virulence factors include fimbriae, proteases, hemagglutinins, and lipopolysaccharides (LPS) (Lamont and Jenkinson, 1998). Adhesion and invasion of periodontal pathogens is thought to be crucial in the pathogenesis of periodontitis especially in the initial stages, however some studies have suggested that adhesion is more important than invasion in terms of activation of a pro-inflammatory response by epithelial cells (Eaves-Pyles et al., 1999).

As alluded to previously, the role of stratified squamous epithelium was traditionally thought to be purely as a physical barrier to microbial ingress into connective tissues, thus protecting the host from the external environment. However in recent years it has been shown that epithelial cells play an active role in the host response to bacterial infections (Dale, 2002). The epithelium responds to bacterial challenge by helping to initiate the innate immune response. This thesis will focus on the actions of the sulcar/pocket epithelium when challenged with periodontal pathogens in terms of NF-κB activation, downstream changes in gene expression and subsequent pro-inflammatory cytokine production.

1.8 Pro-inflammatory Gene Transcription Factors

Inflammation is a normal physiological response to host injury or infection; it aims to isolate the area of injury or infection as well as mobilising effector cells to stimulate/focus the activity of an immune response leading to elimination/destruction of antigen. An important part of the inflammatory response involves activation of transcription factors, which are intracellular molecules,

usually proteins, which triggers the initiation, stimulation or termination of gene transcriptional events (Adler et al., 1999). Activation of pro-inflammatory transcription factors occur on cell stimulation (e.g. bacteria, oxidative stress etc). Two of the main pro-inflammatory transcription factors are described below:-

(a) Activating protein 1 (AP-1) a group of functionally and structurally similar proteins that play a crucial role in a variety of cellular events including inflammation. Activation of AP-1 is achieved via a wide range of physiological & pathological stimuli (Hess et al., 2004).

(b) Nuclear factor kappa B (NF-kB) a family of nuclear transcription factors that play an active role in almost every aspect of cell regulation including stress responses, apoptosis, differentiation and immune cell activation (Makarov, 2000). Current scientific evidence points to the fact that NF-kB is the most important pro-inflammatory gene transcription factor due to its wide ranging actions (Silverman and Maniatis, 2001). An example of such an effect would be production of pro-inflammatory cytokines which play a key role in orchestrating the inflammatory response. This thesis will therefore focus of NF-kB activation and as a marker of cell activation.

AP-1 and NF-kB are also examples of REDOX sensitive transcription factors i.e. changes in cellular oxidative stress can lead to their activation. Such changes can be induced by a number of factors including bacterial stimulation *(Figure 1.11)*. Alongside these pro-inflammatory pathways other REDOX sensitive transcription factors exists for example nuclear factor erythroid-2 related factor 2, Nrf2, which are similarly regulated by changes in REDOX status but have opposite effects in that they positively regulate the expression of genes encoding antioxidants, and detoxification enzymes, providing protection against oxidative stress. Inactivation of Nrf2 in a mouse model caused increased oxidative stress, with the balance between oxidative stress and pro-inflammatory gene activation is modulated by Nrf2. *(Figure 1.12)* (Rangasamy et al., 2004)

Activation of pro-inflammatory transcription factors triggers gene transcriptional events leading for production of a range of proteins including several pro-inflammatory cytokines (e.g IL-8, TNF-α, IL-1). Alongside this activation a number of regulatory pathways are activated in order to maintain appropriate levels of inflammation relative to the challenge the host is experiencing. The inflammatory response may be acute or chronic in nature, with the chronic response lasting for weeks or months and potentially causing significant collateral tissue damage. Inflammation resulting from chronic exposure to bacteria or their products is central to the pathogenesis of chronic periodontitis.

1.9 NF-κB

NF-κB plays a key role in initiating and regulating the inflammatory response and can be activated by an extensive range of stimuli (Barnes and Karin, 1997). Studies have implicated dysregulation of NF-kB in a wide range of disease processes *Table 1.3)*. Activation of NF-κB can occur via a range of pathways, in terms of bacterial stimulation this is by stimulation of Toll like receptors (TLR) which are expressed by host cells (Zhang and Ghosh, 2001) (Banerjee and Gerondakis, 2007). Studies have shown that TLR's play a crucial role in the recognition of bacterial pathogens. To date, in the region of 13 TLR's have been described, each having a specific receptor profile. NF-kB can also be activated by a whole range of factors, for example oxidative stress. Different pathways of activation can lead to different gene expression changes and thus different down stream peptide synthesis.

NF-κB is the collective name for a group of Rel proteins which act as transcription factors, 5 members of the Rel family are currently known, specifically Rel A (p65), Rel B, c-Rel, NF-κB1 (p50) and NF-κB2 (p52). If these proteins are found as homo or hetro-dimers they are termed NF-κB. The classic dimer is a p65/p50 combination. In most resting "un-stimulated" cells NF-κB resides in the cell cytoplasm in an inactive form bound to its inhibitor IκB. IκB is a family of inhibitor proteins that include p100, p102, Bcl-3, IκBε, IκBγ, IκBβ, IκBα (Barnes, 1997, Chen

and Ghosh, 1999). Binding of NF-κB to IκB prevents activation of NF-κB by masking a region called the nuclear localization signal. This region, if exposed, allows NF-κB to cross the nuclear membrane and to bind to DNA and activate genes downstream of the binding sites.

Activation of NF-κB initially requires activation of IκB kinase (IκK), present in the cell cytoplasm, which causes phosphorylation of IκB, marking IκB out for ubiquitination. Ubiquitination is a process by which ubiquitin, a small molecule, is attached to the target protein and acts as a tag which signals the protein-transport machinery to transport the ubiquinated protein to the proteasome where it is broken down. On breakdown of IκB, the resulting free NF-κB can translocate to the cell nucleus, bind to the nuclear DNA via its κB binding site and cause changes in gene expression (Barnes, 1997, May and Ghosh, 1997) (*Figure 1.13).* The regulation of NF-κB is achieved via a number of auto-regulatory mechanisms which limit the duration and intensity of NF-κB activation. One such mechanism is the production of IκB on NF-κB activation (Hayden and Ghosh, 2004). The freshly synthesised IκB enters the cell nucleus and acts to remove NF-κB from the DNA and transport it out of the nucleus back into the cytoplasm in its inactive form bound to IκB. Another mechanism of NF-κB regulation is via IκB kinase , where the active IκK enzyme auto phosphorylates in order to limit its own activity and hence limit the duration of NF-κB activation (Hayden and Ghosh, 2004) (*Figure 1.14).* These mechanisms are in place to ensure that NF-κB activation is only transient on cell stimulation. However, reactive oxygen species can inhibit this regulatory feedback pathway leading to further activation of NF-κB. *(Figure 1.14)*

As previously discussed, NF-κB can be activated by a wide variety of stimuli which will include oxidative stress, bacterial/viral proteins and their by-products, cytokines as well as a range of physical stimuli (e.g. temperature changes, radiation, pH changes etc) (Hayden and Ghosh, 2004). Activation of NF-κB is rapid, taking only a few minutes and results in transcriptional changes with downstream production

of a whole range of cytokines, chemokines, growth factors and adhesion molecules (Perkins, 2007).

NF-κB activation occurs in the majority of cells including those which take part in the innate or acquired immune response (e.g. neutrophils, macrophages, lymphocytes, endothelium, epithelium and mesenchymal cells) being part of the normal inflammatory response. However, if NF-κB is activated in an abnormal or excessive manner the inflammatory response may be perpetuated and this has been implicated in chronic inflammatory diseases. Research has thus implicated NF-κB in terms of initiation and propagation of chronic inflammation (*Table 1.3*). So some way of dampening down NF-κB activation in cells where its activation is disproportionate may have utility in managing chronic inflammatory diseases in general and in terms of this thesis periodontal disease in particular. As the pathway to activation of NF-κB, downstream changes to gene expression and subsequent protein production are extremely complex, involving a number of interactions with other molecules, a wide range of opportunities arise to block or down regulate the NF-κB pathway. As research into the actions of NF-κB continues to gather pace the number of identified exogenous inhibitors of NF-κB have grown over recent years, from 125 in 1999 to around 785, with this number set to rise further in the coming years. These inhibitors encompass natural products, chemicals, metabolites, synthetic compounds, peptides and proteins *(Figure 1.15).*

Despite the suggestion 13 years ago that NF-κB modulation may be a key therapeutic strategy in managing periodontal inflammation (Chapple, 1997) there are few papers reporting NF-κB activation in patients with periodontitis. To date only one study has examined gingival tissue samples collected from patients with CP and compared them to healthy controls. This paper had a number of drawbacks but suggested increased levels of NF-κB activation in the gingival epithelium of diseased sites when compared to the healthy controls (Ambili et al., 2005)

1.9.1 Inhibitors of NF-κB activation

These inhibitors can be categorised in a variety of ways, one of which is by site of action in the NF-κB pathway. By using this method the inhibitors can be divided into a number of distinct groups:-

1.9.1.1 Upstream of IκB kinase (IkK)

The IkK complex is the point at which a number of activation pathways for NF-κB merge, so blocking pathways prior to activation of IκK gives potential to inhibit downstream NF-κB activation, examples of this would be blocking the TNF NF-κB activation pathway by using TNF antibodies or blocking the TNF receptor, as well as blocking other compounds in this pathway prior to IkK activation (Blackwell et al., 1996).

1.9.1.2 Directly on the IκB kinase complex

This complex plays a central role in the NF-κB pathway and it therefore offers an important target for blockage. A whole range of kinase inhibitors have been developed to block IKK activity (e.g β-Carbolines, (Castro et al., 2003)) and these have been shown to have therapeutic potential (May et al., 2000).

1.9.1.3 IκB phosphorylation

IκB when bound to NF-κB causes inactivation of NF-κB, thus mechanisms that promote synthesis or prevent breakdown of IκB would help to prevent activation of NF-κB. A range of compounds that achieve this have been cited (e.g. Doxazosin). Up regulating IκB has been achieved by various peptides e.g β-amyloid peptide (Bales et al., 1998).

1.9.1.4 Ubiquitination or proteasomal degradation of IκB

Inhibitors of either the ubiquitination of IκB by SCF-β-TrCP ubiquitin ligase complex or subsequent proteosomal degradation of ubiquitinated (e.g. Ro106-9920) IκB results in suppression of NF-κB activation by stabilising IκB (Swinney et al., 2002).

1.9.2 Nuclear translocation of NF-κB

This is another potential target for inhibiting the actions of NF-κB, even if NF-κB becomes active in the cell cytoplasm, in order to be effective it needs to enter the nucleus. One possible mechanism to block nuclear translocation is by saturating the nuclear import mechanism which transports NF-κB into the nucleus. A range of peptides have been reported to have this ability, an example being SN-50 (an inhibitory peptide) which has been shown to block nuclear uptake of NF-κB. (Torgerson et al., 1998)

1.9.3 NF-κB DNA binding

Once NF-κB has translocated into the cell nucleus it needs to bind to DNA in order to induce gene transcriptional changes. This is the target step in the activation pathway for the largest group of NF-κB antagonists which prevent DNA binding by a variety of mechanisms. An example of a blocking mechanism is by the use of decoy oligonucleotides which have κB binding sites which compete with NF-κB for DNA binding sites (Kupatt et al., 2002). This mechanism has demonstrated therapeutic benefits in animal models of inflammation (Tomita et al., 2003).

1.9.4 NF-κB gene transcription

The final step in the NF-κB pathway is transactivation (an increased rate of production of genes), this step gives the potential for modifications to specific levels of gene expression by NF-κB. A number of molecules have been shown to specifically inhibit gene transactivation. Several mechanisms have been cited, which include phosphatidylcholine-phospholipase C inhibition achieved by D609, protein kinase C inhibition via RO31-8220 and p38 MAPK inhibition by SB203580, all of which have been shown to inhibit gene transactivation via NF-κB. (Gilmore and Herscovitch, 2006)

1.9.5 Antioxidants

Oxidant stimulation of NF-κB has been demonstrated in a range of cell types. A number of authors have demonstrated that antioxidants can block this activation

(Bubici et al., 2006, Gloire et al., 2006). However, the exact target for antioxidant action and the pathway by which they act has yet to be fully elucidated. It seems that antioxidants act on different parts of the pathway depending upon the cell type. *(Figure 1.16)*

A range of antioxidant species have been shown to block NF-κB activation, these include thiols (which includes α-lipoic acid (ALA)) and vitamins. These potentially act by direct scavenging of reactive oxygen species (ROS), suppression of ROS production or by stimulating over expression of other antioxidant enzymes. (for example catalase which can block TNF-α activation of NF-κB; (Manna et al., 1999, Manna et al., 1998, Schulze-Osthoff et al., 1993).

In broad terms there are 2 main antioxidant actions in blocking the NF-κB pathway:
1) Direct scavenging of ROS, which have the ability to activate the pathway via signalling molecules (Haddad et al., 2000).
2) Direct inhibition of IκK activity limiting breakdown of IκB and thus preventing activation of NF-κB (Gloire et al 2006, Bubici et al 2006).

The literature shows that antioxidants have anti-inflammatory properties in animal models and in humans (Na and Surh, 2006). Because of it's central role in inflammation (Aggarwal et al., 2007) it would seem appropriate to investigate NF-κB as a potential therapeutic target in dampening down the "hyper inflammatory" response, moreover inhibitors of NF-κB could modulate the pathway at a single or multiple points. For the majority of compounds reported to block NF-κB, the exact mode of inhibition has yet to be fully determined.

1.10 Antioxidants and periodontitis

Damage to the supporting tissues of the teeth is a feature of periodontitis and is, in the main, caused by an inappropriate response of the host to microbial plaque. A shift in the homeostatic balance causes disease, due to excess ROS and proteolytic enzyme release by neutrophils. Current evidence suggests that

periodontitis is manifested in individuals who have an exaggerated inflammatory response to microbial plaque (Gustafsson et al., 2006) The literature suggests that neutrophils, which migrate to the area as part of the normal defence mechanism, are hyper reactive (Matthews et al., 2007b) and hyper active (Matthews et al., 2007a) producing excess ROS and enzymes (Fredriksson et al., 1998); this alongside the reduced local antioxidant defences seen in these patients. Several studies have investigated levels of antioxidant in periodontal tissues (Chapple et al., 2002, Panjamurthy et al., 2005) and demonstrated reduced levels, which in the presence of excess ROS may result in periodontal tissue damage (Chapple and Matthews, 2007).

1.11 α-Lipoate

α-lipoate (ALA), which is also known as α-lipoic acid or thiocytic acid, was initially isolated from bovine liver in 1950 (Reed, 1957) with some 10 tons of liver yielding 30mg of pale yellow crystals. ALA is an eight carbon dithiol containing an asymmetric carbon atom. It exists in two forms, the R enantiomer being found naturally whereas the synthetic form contains both R & S enantiomers (*Figure 1.17*). ALA is an essential group found in mitochondria being part of the α-keto acid dehydrogenase complex, and having a pivotal role in energy metabolism (Schmidt et al., 1969). In recent years ALA has attracted considerable attention due to its beneficial antioxidant properties, having the ability to directly scavenge free radicals, chelating transition metals in biological systems, preventing membrane lipid peroxidation and protein damage via regeneration of other antioxidants (e.g. vitamin C and E), as well as increasing intracellular levels of reduced glutathione (GSH) (Packer et al., 1995); (Matsugo et al., 1996).

1.11.1 Direct Radical Scavenging

A number of studies have shown that ALA is highly reactive to a range of reactive oxygen species. Concentrations of ALA in the range of 0.05-1 mM have been shown to scavenge hydroxyl radicals, hypochlorous acid and singlet oxygen (Packer et al., 1995). The reduced form of ALA, dihydro-lipoic acid (DHLA) in the

concentration range 0.01-0.5mM can, in addition, scavenge peroxyl and superoxide radicals (Packer et al., 1995) (Matsugo et al., 1996).

1.11.2 Redox interactions with other antioxidants

ALA/DHLA has been shown to regenerate other antioxidants from their oxidized or reduced forms. For example DHLA is able to directly reduce oxidized glutathione (GSSG) to its reduced form GSH (Jocelyn, 1967). Animal studies using rats have demonstrated that ALA administration increases GSH levels in a range of tissues (Busse et al., 1992); (Khanna et al., 1999). Studies have also investigated the action of ALA on human cells in culture and demonstrated that following exposure, it was rapidly taken up by the cells and reduced to DHLA before being released (Handelman et al., 1994). DHLA reduces the amino acid cystine to cysteine, which is then taken up by amino acid transporters and used in the synthesis of reduced glutathione. The ability of ALA to increase the intracellular availability of cysteine (the central amino acid in the tripeptide GSH) has been proposed as the mechanism by which ALA increases intracellular GSH (Han et al., 1997); (*Figure 1.18)*. In addition to the effect of ALA on intracellular GSH levels, it has also been reported that ALA may contribute to regeneration of vitamin B, C and E from their oxidized forms in biological systems (Packer and Suzuki, 1993, Packer et al., 1995), (*Figure 1.19)*

1.11.3 In vivo antioxidant activity

A number of experimental models have provided evidence that supplementation with ALA decreases oxidative stress as well as restoring levels of other antioxidants. One such study supplemented healthy human subjects with 600mg per day of ALA over a 2 month period. Results from this study showed a decrease in urinary F2-α isoprostane, a biomarker of lipid peroxidation, caused by oxidative stress (Marangon et al., 1999). In a separate study, the oxidative stress induced by exercise was assessed using rats administered with intragastric ALA (150mg/kg body weight per day). Rats administered with ALA showed protection against oxidative stress-induced heart, liver and muscle damage, as well as increased

levels of glutathione (Khanna et al., 1999). Further evidence for a potential role for exogenous ALA in preventing oxidative damage can been seen with ageing. One of the proposed mechanisms of ageing is the accumulation of DNA, lipid and protein damage from reactive oxygen species (Finkel and Holbrook, 2000). A study supplementing old rats with ALA (0.2% weight per weight) for 2 weeks showed a reduction in age-associated oxidant production in cardiac monocytes, restored myocardial ascorbic acid levels and reduced oxidative DNA damage in cardiac tissue (Suh et al., 2001). Other studies have shown that ALA prevents age related cerebral lipid peroxidation, and age-related decreases in ascorbic acid, vitamin E and GSH (Arivazhagan et al., 2000).

1.11.4 Other biological actions of ALA and DHLA

Studies using animal models of diabetes and in humans with type 2 diabetes have demonstrated that ALA has the ability to reduce elevated glucose levels (Midaoui et al., 2003, Packer et al., 2001). At a cellular level, cultured insulin responsive cells exposed to ALA (2.5mM) showed rapid glucose uptake via activation of the insulin signaling pathway (Yaworsky et al., 2000). The mechanism highlighted is believed to be due to the insulin signaling pathway being sensitive to REDOX status, with oxidation of thiol groups causing activation of insulin signaling (Schmid et al., 1999). Experiments pre-incubating adipocytes with ALA demonstrated increased glucose uptake and intracellular glutathione levels. (Moini et al., 2002)

Therefore, ALA has been shown to increase antioxidant activity both in the laboratory, in animal models, and in patients. Provision of exogenous ALA to patients who exhibit a REDOX imbalance (Moini et al., 2002), diabetes (Packer et al., 2001), auto-immune disease (Morini et al., 2004), hypertension (Takaoka et al., 2001),(Vasdev et al., 2000) as well as a number of other inflammatory diseases (e.g. atherosclerosis) has produced improved clinical outcomes. However the exact mode of activity of ALA on different biological systems has yet to be fully determined, and only then can its true efficacy in a particular inflammatory disease be established.

1.12 Cytokines

Cytokines are defined as soluble factors that are produced by cells and act on a target cell to cause a change in cellular behaviour. This target cell can be a second cell or the same cell (autocrine action). Cytokines act on a wide range of biological processes including development of the embryo, inflammatory and malignant disease pathogenesis, non-specific responses to infection, specific antigen responses, and host ageing. The term “cytokine” encompasses a number of groups of cell signaling molecules: interferons, interleukins, chemokines, mesenchymal growth factors, tumor necrosis factors and adipokines. To date, there are in excess of 100 separate genes coding for cytokine-like activities many of which have overlapping functions.

Cytokines are key to the host’s innate immunity, which is required for host survival. However, dysregulated cytokine production has been implicated in disease aetiology where inappropriate levels of cytokine production can cause excess levels of inflammation (Opal et al., 2005), (Konstan and Berger, 1997). Classically, during infection a whole range of pro-inflammatory cytokines are produced with the aim of generating an inflammatory / immune response and therefore defending the host from infection. As the infection resolves, cytokine production is reduced and inflammation subsides. However, when cytokine genes fail to shut down or when the infective agent persists, chronic inflammation results (Opal et al., 2005).

1.12.1 Cytokines and periodontal disease

Periodontal tissue homeostasis is achieved by a delicate balance between cellular activity (including cell migration, proliferation and differentiation) along with the production of extracellular matrix. Strong evidence exists that cytokines play a pivotal role in ensuring that homeostasis is maintained (Moscatelli et al., 1986), (Garlet et al., 2006). Research has demonstrated that in healthy periodontal tissues a range of growth factors are expressed, examples of which include epidermal growth factor (EGF), platelet derived growth factor (PDGF) and transforming growth factor β (TGF-β) (Okada and Murakami, 1998). In addition low

levels of expression of inflammatory cytokines are detected at healthy sites (e.g. IL-1, IL-6, TNF-α), but at levels much lower than those seen in inflamed sites. This array of cytokines detected at healthy sites suggests that cytokines are important in maintaining homeostasis within the periodontal tissues.

In patients with CP, histological examination of the periodontal tissues reveals an inflammatory cell infiltrate (Page and Schroeder, 1976). Thus, an important aspect of disease is how these cells are attracted to the area. A number of cytokines have been implicated in the initiation and progression of periodontal inflammation, the majority of which are pro-inflammatory in nature. Recent studies using epithelial cells removed from healthy and diseased sites revealed expression of IL-1β, IL-6, IL-8, TNF-α and TGF-β (Lundqvist et al., 1994) with the expression profiles being similar between healthy and diseased sites. *In vitro* studies using an epithelial cell line showed increased production of IL-1β, IL-6, IL-8, TNF-α and monocyte chemo-attractant protein (MCP-1), when stimulated by *P.gingivalis* LPS (Kou et al., 2008, Okada and Murakami, 1998). The increased production of IL-8 and MCP-1 is of particular interest as they are chemotactic for neutrophils, suggesting the epithelium may have a role in the initial recruitment of inflammatory cells to the periodontium.

These ‘pro-inflammatory cytokines’ are also prominent regulators of tissue homeostasis, so a normal baseline level of expression is expected (Okada et al., 1996), however this appears to be significantly increased in the inflammatory lesion. At sites of disease, cytokines are produced by immuno-competent cells (T cells and monocytes) that have infiltrated the tissues. In addition, resident cells such as epithelial cells and fibroblasts also produce cytokines, which play an important role in the inflammatory response. This thesis investigates the role of pocket/sulcar epithelium in orchestrating this inflammatory response seen in periodontitis, using an oral gingival epithelial cell model system.

There are a number of cytokines implicated in periodontitis and 3 key pro-inflammatory cytokines closely related to the pathogenesis of periodontitis (i.e. IL-1, IL-8 & TNF-α) will be discussed in more detail in the following section.

1.12.2 Interleukin 1 (IL-1)

IL-1 has a wide range of biological activities in tissue homeostasis, immunity, inflammation (Okada et al., 1996) and tissue breakdown (Dinarello, 1997, Mizel, 1989, Schmidt et al., 1982, Stashenko et al., 1987) It can be produced by a number of cells once they become activated. Two forms exist IL-1α and IL-1β. In terms of amino acid composition they only share 27% homology but have similar modes of action. IL-1α has been shown to remain closely cell associated, whilst IL1-β is released from the cell (Hazuda et al., 1988). IL1-α and IL1-β act via the same cell surface receptor, which has been demonstrated on a wide range of cell types.

In healthy tissues IL-1 stimulates cell proliferation (keratinocytes, fibroblasts, and endothelial cells) as well as fibroblast synthesis of collagen, hyaluronate, fibronectin and prostaglandins. In diseased tissues, excess production can lead to local tissue damage. In the periodontal tissues IL-1 can stimulate production of other pro-inflammatory cytokines, and enzymes which may be responsible for tissue destruction and therefore loss of attachment. IL-1 has thus been implicated as a key factor in periodontal disease pathogenesis.

1.12.3 Interleukin 8 (IL-8)

IL-8 acts as a potent chemo-attractant for neutrophils (Bickel, 1993, Skerka et al., 1993); It has been reported to be produced by a range of cell types including monocytes, fibroblasts and endothelium. In inflamed gingival tissue it is seen to be produced by macrophages and epithelial cells (Bodet et al., 2005, Milward et al., 2007, Sfakianakis et al., 2002). Neutrophils are implicated in the initiation and progression of periodontal disease, and with local IL-8 production found in periodontal tissues this suggests a potential important role for IL-8 in neutrophil recruitment to the periodontal tissues and therefore disease pathogenesis. Subjects with systemic neutrophil dysfunction (e.g. Chediak-Higashi syndrome) show increased severity of periodontal disease, which suggests that the infiltration

of neutrophils to the periodontal lesion plays an important role in first line defence. However, if the production of IL-8 becomes chronic and at elevated levels, it will potentially cause excess neutrophil recruitment and activation. This may be an important factor in local tissue destruction. The production of IL-8 is downstream of the NF-κB pathway (Roebuck, 1999) and is widely accepted to be a surrogate marker of NF-κB pathway activation, so methods of blocking this pathway have the potential to reduce the amount of IL-8 produced (Pease and Sabroe, 2002).

1.12.4 Tumor necrosis factor alpha (TNF-α)

TNF-α is mainly secreted by monocytes and macrophages. It has a number of pro-inflammatory effects, inducing collagenase production, bone resorption and has been implicated in periodontal tissue breakdown (Alexander and Damoulis, 1994, Chaudhary et al., 1992, Elias et al., 1987). TNF-α has been demonstrated to activate osteoclasts as well as inducing IL-1 production by macrophages (Johnson et al., 1989). TNF-α has been shown to act synergistically with IL-1 to enhance its bone resorption activities (Bertolini et al., 1986, Johnson et al., 1989, Mundy, 1989, Pfeilschifter et al., 1989, van der Pluijm et al., 1991). In addition, *in vitro* stimulation of fibroblasts by TNF-α has induced their ability to breakdown collagen (Meikle et al., 1989). It has been shown that Gram negative bacterial lipopolysacharide (LPS) can induce TNF-α production in peripheral blood monocytes (Van Dyke et al., 1993).

1.13 Aims and Objectives

This thesis will investigate the role of sulcar/pocket epithelium in the initiation of inflammation when stimulated with periodontal pathogens, as well as potential methods of blocking the pro-inflammatory response. Studies will utilise a model system to investigate genomic and proteomic changes as well as exploring a possible method of modulating the inflammatory response seen periodontitis. The key stages in attempting to achieve this goal are:-

1. Development and characterisation of an *in vitro* oral epithelial cell model.

2. Induction of NF-κB activation via different microbial stimuli demonstrating nuclear translocation using immuno-histochemistry (IHC).
3. Determining the effects of microbial stimulation on this model system in terms of global gene expression using both high throughput microarray technology and confirmatory PCR.
4. Assessment of cytokine production downstream of gene transcription changes.
5. Investigating methods of blocking NF-kB activation using α-lipoate, determined by IHC, PCR and cytokine ELISA's.

In summary the effects of periodontal pathogens upon oral epithelial cell (OEC) behaviour will be examined by analysing NF-κB activation in a model system, specific cellular events analysed will be:- *(Figure 1.20)*

A. Translocation of NF-kB to the nucleus
B. Changes in gene expression
C. Cytokine production

CHAPTER 2

Materials & Methods

2.1 Bacterial culture preparation

This section describes the reagents and preparation of the bacteria used to stimulate the epithelial model system.

2.1.1 Mycoplasma broth (Difco laboratories, USA)

This commercially available powder requires re-hydrating and sterilizing by autoclave prior to use. 21g of the mycoplasma broth powder was added to 700ml of distilled water; thoroughly mixed and autoclaved at 121°C for 15 minutes. After cooling the broth was stored at +4^{o}C prior to use.

2.1.2 Trypticase soy broth (TSB)

40g of trypticase soy base powder (Difco laboratories, USA) was dissolved in 1 litre of distilled water, dispensed into bijou bottles and autoclaved at 121^{o}C for 15 minutes. The broth was allowed to cool and stored at + 4^{o}C prior to use.

2.1.3 Trypticase Soy Agar (TSA)

40g of trypticase soy base powder was added to 1 litre of distilled water along with 15g agar base, after mixing it was autoclaved at 121^{o}C for 15 minutes, and whilst still molten, was dispensed into Petri dishes. Once the agar had set, plates were stored at + 4^{o}C prior to use.

2.1.4 Blood agar

This was prepared using a TSA base (as previously described) to which 5% defibrinated sheep blood was added. The sheep blood was added to the TSA whilst still in its liquid state just above its setting temperature in order to prevent lysis of the red blood cells. Once mixed it was poured into Petri dishes, allowed to set, and the plates stored at +4^{o}C prior to use.

2.1.5 Bacterial stimulants

This thesis utilised whole dead periodontal pathogens as well as *E. coli* lipopolysaccharide (EC LPS) to stimulate the model epithelial cell system. LPS is a major structural and functional component of the outer membrane of Gram-negative bacteria, which is known to interact with a variety of cells producing a wide array of inflammatory responses including NF-κB activation.

2.1.5.1 Bacterial cultivation

Fusobacterium nucleatum (ATCC 10953) and *Porphyromonas gingivalis* (ATCC 33277) were purchased as lyophilized stocks from the American Type Culture Collection (ATCC, Rockville, MD). These were reconstituted using mycoplasma broth (Difco Laboratories, USA) then plated out onto a trypticase soy agar supplemented with sheep blood and incubated at 37°C anaerobically (anaerobic chamber – Don Whitley, UK atmosphere 80% nitrogen, 10% carbon dioxide, 10% hydrogen) *(Figure 2.1)*. The resulting bacterial colonies were checked to ensure purity by Gram staining and subculture. Subsequent morphologically identical colonies were seeded into 10 ml trypticase soy broth, which was incubated at 37°C in an anaerobic chamber for 24 hours. Following incubation the bacterial suspension was centrifuged to produce a bacterial cell pellet. This pellet was washed three times in sterile phosphate buffered saline (PBS) and then heat-inactivated at 100ºC for 10 minutes. The optical density (OD) of the resultant suspension was measured at 600nm in a Jenway, Spectrophotometer, (Dunmow,UK) using 1ml semi-micro cuvettes (Sarstedt, UK). By using a standard curve (OD vs. bacterial count), the bacterial concentration was then adjusted using sterile PBS in order to produce a suspension containing $4x10^8$ bacterial cells per ml. Heat inactivation of the bacterial suspension was confirmed by lack of growth on a blood agar plate after 48h anaerobic culture. Bacterial suspensions were stored in aliquots at -30ºC prior to use.

2.1.5.2 E. coli LPS

Escherichia coli LPS serotype 026:B6 was purchased commercially (Sigma, UK, cat number L-8274) as a powder. This was dissolved in DMEM tissue culture media to produce a 250µg/ml stock solution that was stored at -30ºC prior to use

2.2 Cell culture

2.2.1 Culture media and reagents:

2.2.1.1 Supplemented Dulbecco's modification of Eagle's medium (DMEM)

This was used as a standard growth media for culturing the oral keratinocyte cell line and was available in 500ml sterilised bottles (Invitrogen,UK). The media was supplemented with L-glutamine (Sigma; final concentration 2mM), hydrocortisone (Sigma; 0.25mg per 500ml medium) and foetal calf serum (10% v/v; Labtech) prior to use, all reagents being added aseptically. In order to ensure sterility, 10ml of supplemented media was removed and incubated at 37^{o}C in 5% CO_2 for 24h, and checked for turbidity and pH change, both of which would indicate bacterial / fungal contamination. Supplemented growth media was stored at 4^{o}C prior to use. Once supplemented the media has a 9 month shelf life, however all media was used within 3 months.

2.2.1.2 Trypsin ethylenediaminetetraacetic acid (T-EDTA)

This was used for disruption of the cell monolayer producing a single cell suspension allowing reseeding of the cell line. This commercial reagent (Gibco,UK) contained 0.5g/l trypsin (1:250) and 0.2g/l EDTA•4Na in Hanks' balanced salt solution. On delivery the solution was aseptically distributed into 4ml aliquots prior to storing at -20^{o}C.

2.2.1.3 Dulbecco's phosphate buffered saline (D-PBS) without calcium & magnesium

This buffered saline solution was used to wash the cell monolayer prior to application of trypsin EDTA. It is commercially available (Gibco,UK) and contains KCl 0.2g/l, KH_2PO_4 0.2g/l, NaCl 8.0g/l, Na_2HPO_4 anhydrous 1.15g/l. This solution on delivery is stored at room temperature, but once opened is kept at 4^{o}C.

2.2.2 Oral epithelial cell culture

Experiments utilised an oral epithelial cell (OEC) line H400 which was a kind donation from S.Prime at Bristol University, UK. This human immortal cell line was derived from a squamous cell carcinoma (20-40mm, stage 2, moderately differentiated, node negative tumour) of the alveolar process in a 55 year old female patient, and has been well characterised (e.g. cytokeratins) indicating close similarities to gingival epithelium (Prime et al., 1990) and represents a suitable cell line for use in the model system. All experiments were performed between passages 4-20.

Cell culture is a technique sensitive discipline in which careful, aseptic manipulation of the cells is required in order to produce consistent results. All cell culture based experimental work was conducted in a positive flow biological hood (MSC12, Themo Scientific, USA) *(Figure 2.2)* in order to help minimise potential contamination. The practice of supplementing cell culture growth media with antibiotics in order to suppress bacterial contamination is widespread. This approach is required when using contaminated biological samples, however when using an immortal cell line this is an unwanted confounder having the potential to influence experimental results. It can give a 'false sense of security' masking poor aseptic technique. All experiments in this thesis were conducted without the use of antibiotic supplemented media.

2.2.2.1 Cell storage and recovery

Preservation of cells for future use was achieved by preparing a 1ml suspension of $1x10^6$ cells containing 20% (v/v) heat inactivated foetal calf serum (Labtech, UK) and 10% (v/v) dimethyl sulphoxide (BDH, UK). Suspensions were slowly frozen to -80^oC overnight before long term storage under liquid nitrogen. H400 cells were initially supplied after being preserved and stored as described above.

When required cell aliquots were removed from liquid nitrogen and rapidly defrosted in a water bath at 37^oC. Once defrosted the suspension was transferred to 9ml of pre-warmed (37^oC) DMEM cell culture media and gently mixed. This suspension was centrifuged at between 600-800rpm for 10 minutes, the supernatant gently removed using a Pasteur pipette to prevent disruption of the cell pellet, and re-suspended in 1ml of fresh pre warmed (37^oC) DMEM. Following gentle mixing the resultant suspension was used to seed a 75cm^2 cell culture flask containing 9ml of pre-warmed (37^oC) DMEM. The flask was then incubated at 37^oC in 5% CO_2 for 4 days. On day 4 the flask is inspected for bacterial / fungal contamination (turbidity / pH change), as well as being examined microscopically (inverted microscope – Leica, Germany) to look at cell growth (cell numbers and morphology). Cells are then fed with 10ml of fresh pre heated (37^oC) DMEM following removal of the old DMEM. The flask was then re-incubated at 37^oC for a further 2-3 days (time dependent on cell growth rate), with passage performed when the cells became near confluent and the pH is neutral (as indicated by the phenol read indicator present in DMEM). If the cells are left too long, cell growth results in exhaustion of nutrients in the media and an acidic swing in pH which leads to cell death.

2.2.2.2 Cell passage

Maintenance of a cell line requires the cells to undergo passage as they near confluence. This technique disrupts the cell monolayer to produce a single cell suspension, which is subsequently diluted and reseeded into a new flask, starting the process of monolayer growth again.

Cell passage was achieved by firstly removing the old media from the cell monolayer and washing with warm (37^{o}C) D-PBS. The D-PBS was then removed, 4ml of T-EDTA added and incubated for 10 minutes at 37^{o}C with occasional mixing. Dissociation of the monolayer was confirmed microscopically. If this had not occurred at 10 min incubation was continued until dissolution was complete. The resultant suspension was transferred to a sterile universal container containing 4ml of warm (37^{o}C) DMEM (stops further action of T-EDTA). After mixing, the cell suspension was centrifuged at 150g for 10 minutes, the resultant supernatant was removed and discarded, and the cell pellet re-suspended in 5ml warm (37^{o}C) DMEM. Cells were counted and flasks seeded at various cell concentrations (*Table 2.1*)

Table 2.1 Cell counts for seeding a range of cell culture receptacles

Receptacle	Volume DMEM	Cell number
25cm^2 cell culture flask	5ml	2x10^5
75cm^2 cell culture flask	10ml	5x10^5
Petri dish	15ml	4x10^5
96 well plate	150µl (per well)	8x10^3

After initial seeding (day 0) cells were fed on day 4. Old DMEM was removed and replaced with fresh warmed (37^{o}C) DMEM and incubation continued. All experiments were performed between passage 4-20.

2.2.2.3 Growing cells on glass multi well slides

For experiments with an immuno-cytochemical end point, cells were grown on multi well glass slides *(Figure 2.3*). Glass slides printed with 4 wells (C.A Hendley Ltd, UK) were sterilized using a hot air oven (OP Series, AWOP30-U, Appleton Woods, UK) (150^{o}C for 2 hours), allowed to cool, aseptically transferred to sterile plastic Petri dishes (Appleton Woods, UK) and 15ml of warmed (37^{o}C) DMEM was

added. The dish was placed into a square plastic dish to help prevent contamination and evaporation of DMEM. Following passage, $4x10^5$ cells were seeded into the Petri dish and incubated at 37°C in 5% CO_2.

2.2.2.4 Growing cells in 96 well plates

Following passage cells were seeded ($8x10^3$ cells in 150µl DMEM per well) into flat bottomed 96 well plates (Costar,UK). Cells were grown for between 24 and 48 hours until a semi confluent monolayer was achieved, and then treated depending on the experiment being performed.

2.2.2.5 Cell counts and viability

Cell counts were determined using a haemocytometer (modified Neubauer). Cells were counted on each of the 4 quadrants. The total numbers of cells from these 4 quadrants were then divided by 4. The results from this calculation gave a cell count $x10^4$ per ml.

Cell viability was determined using a trypan blue (0.4%; Gibco, UK) exclusion test. This technique utilizes the principal that viable cells have intact cell membranes and will therefore exclude trypan blue whereas non viable cells lack cell membrane continuity and take up trypan blue.

The following protocol was used:-

1. A suitable cell suspension was produced (i.e. a cell number which could be easily counted using a haemocytometer, approximately $4x10^5$ cells per ml; suspensions with higher cell concentrations were diluted). Ideally cells should be suspended in a serum free media to prevent non specific staining of the serum proteins.
2. A mix of 1 part trypan blue (0.4%) with 1 part cell suspension was made and incubated for 2-3 minutes at room temperature
3. The resulting suspension was introduced to a counting chamber and the numbers of stained and unstained cells determined
4. A calculation was performed to determine the percentage of viable cells (number viable cells/ total number of cells x 100)

2.3 Immunocytochemistry of cells grown on multi-well slides

Immunocytochemistry (ICC) is based on the interaction of an antibody with an insoluble immunoreactive tissue or cellular antigen, then localisation of the site using a label (e.g. an enzyme or fluorescent marker). Detection is dependent on the label used, and can be by ultra-violet, light or electron microscopy. There are a number of methods used with antigens being localised using direct, indirect and multilayer techniques. These differ in the way in which the label is located at the site of the tissue antigen/antibody reaction. (Van Noorden et al., 1986) (Ordronneau et al., 1981)

The method used in this thesis is the biotin-streptavidin amplified technique (StrAviGen, Biogenex). This technique involves the primary antibody binding to the antigen, this is followed by use of multi-link which is biotin labelled goat anti-mouse/rabbit immunoglobulin which specifically binds to the primary monoclonal antibody. The next stage involves use of label, in this case peroxidase linked to streptavidin and binds to the multi-link. The cells are then exposed to diaminobenzidene (DAB) which changes colour from clear to brown. The change in colour occurs as a result of oxidation from exposure to peroxidase in the label. The outcome of these steps is to deposit a coloured complex at the site of the antigen which can be visualised by light microscopy.

In order to ensure that this staining technique was specific for the target protein (NF-κB) a number of controls were used, these included use of a known positive section, replacing primary antibody with (i) non-immune serum, (ii) antibody known to have a different localisation pattern, (iii) buffer, as well as pre-absorbed primary antibody with (i) purified homologous antigen, (ii) non-cross reacting antigen (negative controls). These controls were run during development of the NF-κB staining technique, once specificity had been ascertained, subsequent staining of samples used a positive staining control (Ki-67) and a negative control which used primary antibody replaced by diluent.

The mechanism and the practical steps involved are summarised in *Figures 2.4 & 2.5* and are described below.

2.3.1 Staining procedure

All procedures were performed at room temperature and PBS (pH7.6) was used for washing stages and reagent dilution.

When the glass multi-well slides were ready for staining they were removed from the DMEM and washed in PBS (3x2mins), prior to fixing in dry acetone (15 minutes at room temperature). Slides were air dried (10 mins) and then placed in a darkened humidified box where all subsequent incubations were performed. Monoclonal antibody to NF-κB p65 subunit (clone F-6, Santa Cruz Biotechnology, US; 1:100), a positive staining control Ki-67 was included (clone MM1; Novacastra™, UK; 1:100) as well as a negative staining control which consisted of replacement of the primary antibody with PBS. These monoclonal antibodies and controls were applied to appropriate slide wells. Following 60 minute incubation the slides were washed in PBS (3x2mins), dried to remove excess moisture from around the wells then overlayed with Multilink (biotin-labelled goat anti-mouse/rabbit Ig, 1:50 dilution. Biogenex) and incubated for a further hour. Following this incubation the slides were washed in PBS (3x2mins) and then overlaid with label (peroxidase linked to avidin. 1:50 dilution. Biogenex) and incubated for 1h. After washing in PBS (3x2mins) excess PBS was removed and the slides overlaid with freshly prepared diaminobenzidene (DAB) reagent (10mg in 20ml PBS - filtered then 25µl H_2O_2 added - used immediately $\leq$5mins). Slides were incubated for 5mins then washed for 2 mins in water, before applying copper sulphate solution (0.5% w/v in NaCl) for a further 5 mins – this step darkens the brown end product allowing easier visualisation. After further washing the cells were counterstained for 30 secs using Meyer's haematoxylin. After a final wash the slides were dehydrated in graded alcohols, cleared in xylene and mounted in XAM.

2.3.2 Quantification of cell translocation

Cell counts were performed on cell monolayers after 1h bacterial stimulation and histochemically stained as previously outlined. A binocular microscope (Leica,

Germany) fitted with an eyepiece graticule divided into 10 x 10 squares. The slides were viewed at x100 magnification. For cells to be classified as demonstrating NF-κB activation (i.e. nuclear translocation) the presence of nuclear staining for p65 was required with no visible staining present within the cytoplasm, where any ambiguity existed cells were recorded as negative. Preliminary analysis of 8 slides indicated that counts from a total of 30 randomly selected microscope fields would provide a representative cell count for a given specimen. This was determined using Hunting curves which plotted cell count per square against field number (*Figure 2.6)*. All cells within a 30 graticule squares were counted, (i.e. 1 square represents 0.01mm^2) and recorded as positive or negative. The total and mean number of positive cells for each specimen was determined and used to calculate the percentage of cells demonstrating NF-κB activation.

2.4 High throughput immuno-cytochemistry

In addition to detection of nuclear translocation of NF-κB by standard immuno-cytochemistry, high throughput technology was also used to determine NF-κB activation. This had the advantage of analysing NF-kB translocation in a quantitative way, with the additional benefit of high through put of samples. The basic principal of the method is similar to the staining techniques previously described (section 2.3) but uses a fluorescent marker rather than horseradish peroxidase. However, the main difference is the way in which the resulting stained images are analysed. This technology utilises an automated fluorescence microscopic imaging system which is computer driven allowing rapid cell identification as well as quantification of a vast array of parameters (e.g. cell size, number, shape, nuclear intensity, cytoplasmic intensity). Its use in this context allows determination of levels of p65 staining in the nuclei and the surrounding cytoplasmic area.

Cells were grown in black 96 well tissue culture grade flat bottom plates (Corning, UK) as described in section 2.2.2.4 Cells were then treated depending on the particular experimental protocol.

2.4.1 Fixing of cell monolayer

Following removal of growth media from the wells, the monolayer was fixed for 20min using a 1% formaldehyde solution, the formaldehyde was then removed and the cells were washed twice with 100µl PBS, before filling the wells to the top with PBS. A sealing film (Jencons, UK) was then applied to cover the wells which were then stored at 4^{o}C prior to analysis.

2.4.2 Staining

Plates were washed with PBS prior to staining, then incubated with 100µl (per well) primary antibody (anti-NF-κB p65 monoclonal antibody (F-6) (Santa Cruz, USA) diluted 1:100 in 0.1M phosphate buffer pH 7.8 with 0.1% bovine serum albumin) for 1 hour at room temperature. Cells were then washed three times in wash buffer and incubated with the secondary antibody (anti-STAT1 rabbit polyclonal immunoglobulin – conjugated to a fluorescent label - Santa Cruz, USA) for a further hour. Following this stage detergent buffer (Cellomics, UK) was added to the wells for 15 mins. After washing with PBS, 200µl of detergent buffer added to each well prior to analysis.

2.4.3 Data acquisition and analysis

Data acquisition utilized ArrayScan HCS imaging cytometer (Cellomics, UK) (*Figure 2.7)*. This is an automated fluorescent imaging microscope that allows collection of data on the spatial distribution of the fluorescent marker. The scanner reads multiple fields in order to build up a picture of each of the multi-wells. The software then allows identification of individual cells which are then subdivided into nuclear and cytoplasmic compartments. The software can identify the edge of the nucleus and then creates areas 2 pixels either side of this line, therefore producing a nuclear and cytoplasmic compartment (*Figure 2.8*). The fluorescent intensity can then be acquired for each. The number of cells counted or the area covered can be defined by the operator. The software used for data acquisition and analysis was ArrayScan II Data Acquisition and Data Viewer 3.0 (Cellomics,UK). The

localization of NF-κB was thus determined by analysis of nuclear and cytoplasmic fluorescence.

2.5 RNA isolation and preparation of cDNA

2.5.1 RNA isolation

RNA was extracted from cells grown in cell culture flasks using a commercially available extraction kit (RNeasy® protect mini kit, Qiagen UK). Cell culture media was removed and replaced with 350µl of RLT lysis buffer, containing 1% β-Mercaptoethanol (β-ME). β-ME is a reducing agent that induces cell lysis whilst protecting DNA and RNA from degradation. Culture flasks were agitated to ensure complete lysis of the cell monolayer (confirmed using an inverted microscope (Leica, Germany). The resulting lysate was transferred to a 2ml microcentrifuge tube and homogenised thoroughly using an Ultra-Turrax T8 tissue disrupter (Fisher Scientific, UK). The lysate was vortexed for 30 seconds to help shear genomic DNA as well as reducing the viscosity. Ethanol was then added to allow binding of RNA to the RNeasy® membrane. The resultant sample was pipetted onto an RNeasy® spin column and this was then placed in a 2ml collection tube. The column assembly was then spun in a 5415D microcentrifuge (Eppendorf, UK) for 15 seconds at 10,000g. Following centrifugation 350µl of wash buffer (RW1) was pipetted onto the RNeasy® column and centrifuged for a further 15 secs at 10,000g. At this point a DNase digestion was applied to remove any DNA contamination from the sample which would interfere with downstream analysis. This was achieved using the RNase-free DNase® kit (Qiagen, UK). Samples were treated using 10µl of DNase 1 which was mixed with 70µl of buffer RDD, pipetted onto the column and incubated at room temperature for 15 mins. The DNase 1 solution was then removed from the column by washing with 350µl of buffer RW1 and then centrifuged for 15 secs at 10,000g. Further washing was performed using 500µl of buffer RPE and centrifuged for 15 secs at 10,000g, re-washed with 500µl of buffer RPE and finally centrifuged for 2 mins at 15,000g to dry the silica membrane. RNA attached to the column membrane was eluted by the addition of

30µl of RNase-free water directly onto the silica membrane followed by centrifugation for 1 min at 10,000g. This step resulted in RNA being removed from the membrane and present in the water.

2.5.2 Reverse transcription (RT)

Reverse transcription (RT) or first strand synthesis of RNA samples was performed in order to generate a DNA strand complementary to the mRNA (cDNA) present within the sample of total RNA. RT reactions were carried out using the Omniscript reverse transcriptase® kit (Qiagen, UK) coupled with an oligo (dT) primer (Ambion, UK) and an RNase inhibitor (Promega, UK). An oligo (dT) primer was used as it incorporates a run of 15-20 Thymine bases that is complementary to the sequence of Adenine bases (poly-A tail) found at the 3' end of eukaryotic mRNA molecules. This ensured that only mRNA species within the total RNA sample were reverse transcribed as RNA species other than mRNA do not possess poly-A tails.

First strand synthesis was carried out in accordance with the manufacturer's instructions, *Table 2.2* shows volume and final concentrations of components used in the RT reaction. Template RNA and oligo (dT) primers were initially incubated in a heated block (Eppendorf, UK) at 80°C for 10 mins in order to remove any secondary structure from the RNA sample, and then placed on ice for 5 mins. The remaining components of the RT reaction were then added, gently mixed and then incubated at 37°C for 60 mins. This step allowed extension of the transcription product. The reverse transcriptase enzyme was then inactivated by heating at 93°C for 5 mins followed by rapid cooling on ice.

Table 2.2: RT reaction set-up

Component	Volume	Final concentration
10X RT buffer	2.0µl	1X
5mM dNTP mix	2.0µl	0.5mM
10µM Oligo (dT)	2.0µl	1µM
RNase inhibitor (40 units/µl)	0.3µl	10 units
Reverse transcriptase	1.0µl	4 units
Template RNA	variable	50ng-2µg
RNase-free water	to a total volume of 20µl	
Total volume	**20µl**	

2.5.3 Concentration and purification of cDNA

This stage aims to remove unincorporated RT reaction components, which could interfere with downstream analysis, and to concentrate the cDNA samples. These samples were diluted with 500µl dH_2O and centrifuged for 6 minutes at 10,000g using a Microcon YM-30 centrifugal filter unit (Millipore, UK). This filter unit retains cDNA molecules greater than 60 nucleotides in length whilst contaminants were eluted with the water. Samples were washed with a further 500µl dH_2O and centrifuged at 10,000g for 8 mins to concentrate cDNA into 30µl of solution. The cDNA was then collected by inverting the filter into a fresh 1.5ml collection tube and centrifuging for 3 mins at 1000g. Recovered cDNA was quantified using a spectrophotometer.

2.5.4 Quantification of RNA and DNA

Following extraction, RNA and DNA were quantified spectrophotometrically using a Biophotometer (Eppendorf, UK). This was achieved by producing a dilution of 1µl of sample with 69µl of RNase-free water, which was then transferred to a cuvette (Eppendorf, UK). The absorbance at 260nm was then used to determine the concentration of RNA in the sample. An absorbance value of 1 unit at 260nm corresponds to 40µg/ml of RNA or single stranded DNA. In addition the sample

purity was determined by assessing the ratio between readings taken at 260nm and 280nm (A_{260}/A_{280}), with high purity RNA signified by a A_{260}/A_{280} of 1.8-2.1.

2.6 Polymerase chain reaction (PCR)

2.6.1 PCR conditions

All PCRs were set-up on ice to limit primer dimer formation and avoid reactions starting prematurely. All PCR assays were performed using the RedTaq PCR system (Sigma, UK) in 50µl reaction volumes containing; 25µl RedTaq ready reaction mix, 20µ dH_2O, 2.5µl 25µM forward primer and 2.5µl 25µM reverse primer. Reactions were amplified in a Thermal Cycler (Mastercycler Gradient, Eppendorf, UK or GeneAmp 2700 PCR system, Perkin-Elmer, UK). A standard PCR programme is shown in *Table 2.3*, with a schematic diagram of the PCR process in *Figure 2.9*. Annealing temperatures varied according to specific primers used and cycle numbers varied between assays depending on relative abundance of the target sequence or efficiency of the specific reaction. Resulting PCR products were visualised using agarose gel electrophoresis.

Table 2.3: Thermal cycler programme for PCR

Reaction stage	Temperature	Time	
Denaturation	94°C	5 mins	
Denaturation	94°C	30 secs	Cycle n^o dependant upon abundance of target sequence
Annealing	Primer Dependant	30 secs	
Polymerisation	72°C	30 secs	
Polymerisation	72°C	10 mins	

2.6.2 Sample normalisation

In order to effectively compare gene expression levels between control and experimental samples, glyceraldehyde-3-phosphate-dehydrogenase (GAPDH) expression levels were normalised between all samples. PCRs were performed using GAPDH primers with the products being visualised using agarose gel electrophoresis. Images of the resulting gels were taken and band intensity determined using AIDA image analysis software (Fuji, UK). This allowed calculation of the amount of cDNA required for addition to subsequent PCRs, in order to produce bands of equal intensity for each sample. One sample was chosen from each sample set to which all others in the set were normalised. Calculations were performed using the equation below:-

$$\frac{\text{Intensity of test}}{\text{Intensity of band to normalise}} \times \text{Volume of sample} = \text{Volume of cDNA required to normalise}$$

The process of normalisation is repeated until all bands are of similar intensity, thus ensuring the same amount of cDNA is added to each subsequent reaction.

2.6.3 Agarose gel electrophoresis

PCR products, extracted RNA and genomic DNA were visualised using agarose gel electrophoresis. 1.5% agarose gels were prepared by mixing 0.6g agarose (Bioline, UK) with 40ml 1X Tris-acetate-EDTA (TAE) buffer solution (Helena Biosciences, UK). After mixing it was heated to boiling point using a microwave in order to dissolve the agarose. Following this the solution was briefly cooled and 10mg/ml ethidium bromide (e.g. 1µl for a 40ml gel) was added to enable visualisation of nucleic acids upon exposure to ultra-violet (UV) light. The gel was subsequently formed using a gel tray whilst the sample wells were formed using a plastic sample comb *(Figure 2.10)*. The gel was allowed to set at room temperature and if not used immediately was stored at 4^{o}C for a maximum period

of 2-3 h. For use the gel was placed in an electrophoresis tank containing sufficient 1X TAE buffer to cover the gel and wells. The sample comb was removed producing sample wells which were flooded with TAE buffer and PCR products were loaded into each well (The RedTaq system has a dye to allow tracking of the PCR products on the gel). Hyperladder IV, a 100bp ladder (Bioline, UK) was added to a separate well to enable size determination of DNA products. Electrophoresis was performed at 80-120 Volts. The tracking dye (present in RedTaq mix) can be visualised and has a low molecular weight when compared to DNA. The gel is run for sufficient time to allow good separation of sample, but ensuring tracking dye is not run off the plate (dye will run further than DNA so if tracking dye is still on the plate so will DNA products). Following electrophoresis, gel images were captured using the Electrophoresis Documentation and Analysis System (EDAS) (Kodak, UK) under exposure to UV light (300nm) and analysed with AIDA image analysis software (Fuji, UK).

2.7 DNA laddering

2.7.1 Genomic DNA extraction and analysis

In order to look for apoptotic DNA laddering in the cell line, DNA was extracted from cell cultures using the Wizard® SV Genomic DNA Purification System (Promega, UK) according to manufacturers' instructions. Cell culture samples were lysed in 275µl SV lysis buffer, transferred to 1.5ml microcentrifuge tubes containing a mini spin column (Qiagen,UK) then centrifuged at 13000g for 3 mins, DNA binds to the membrane of the mini spin column. The filtrate was discarded and 650µl of SV wash solution added to the column and further centrifuged at 13000g for 1 minute. The filtrate was again discarded and samples washed a further five times with 650µl wash solution as previously described. Following the final wash, samples were spun for a further 2 mins to dry, before transferring the column to a fresh collection tube. Elution solution (2µl RNAse A, 100µl nuclease free water) was then added and the column incubated at room temperature for 5 mins before centrifugation at 13000g for 1 min in order to elute the DNA from the mini spin column membrane.

To determine whether extracted genomic DNA was intact or had fragmented (suggesting apoptosis), samples were visualised using 1% agarose gels (as described previously) using 2µl orange G as a loading dye. Gels were imaged under UV illumination for indications of 180 bp DNA laddering which is a specific indicator of early apoptosis. One of the early events following induction of apoptosis is DNAase activation, condensation of chromatin and a characteristic pattern of DNA fragmentation (laddering) (Khodarev et al., 1998)

2.8 Microarray analysis of gene expression

This high throughput technique allowed analysis of multiple gene expression changes in H400 cells stimulated with periodontal pathogens *P. gingivalis & F. nucleatum*. This technology utilises microarray chips which are spotted with many thousands of DNA oligonucleotide probes to which fragmented labelled cRNA is hybridised. The degree of hybridisation is detected and analysed giving an insight into the level of a particular gene expressed in the sample (*Figure 2.11*)

Gene expression in epithelial cells grown in 25cm^2 cell culture flasks (Corning,UK) and stimulated with a) *P. gingivalis* [10^9 cfu/ml], b) *F. nucleatum* [10^9 cfu/ml], and c) Media alone (negative control) were analyzed using human Affymetrix HG_U133A oligonucleotide arrays.

For microarray analysis DNA free RNA was extracted from H400 cells (method as described in section 2.5)

2.8.1 First strand synthesis of cDNA from total RNA:

This was performed using the SuperScript Choice kit (Invitrogen, UK) and GeneChip promoter primer kit (Applied Biosystems, UK). To 5µg of total RNA extracted from H400 cells 2µl of 50µM HPLC purified T7-Oligo (dT) primer was added to give a final concentration of 100 pmol. The resulting samples were then incubated for 10 minutes at 70^{o}C to allow primer hybridisation. Following incubation, 4µl of 5x first strand cDNA buffer, 2µl 0.1DTT and 1µl of 10 mM dNTP mix were added resulting in final concentrations of 1x, 10mM and 500µM respectively. The mixture was briefly vortexed and incubated at 42^{o}C for 2 mins.

Following incubation, first strand cDNA was synthesised by adding 1µl SuperScript II RT (200 U/µl) and further incubated at 42^{o}C for 60 mins.

2.8.2 Second strand cDNA synthesis

To the first strand synthesis was added (*Table 2.4*):-

Table 2.4: Reagents used for second strand cDNA synthesis

Reagent	Volume added	Final concentration
5x second strand reaction buffer	30µl	200µM
dNTP mix	3µl	200µM
10U/µl *E.coli* DNA ligase	1µl	10U
10U/µl *E.coli* DNA polymerase 1	4µl	40U
2U/µl *E.coli* RNase H	1µl	2U

The resulting mixture was adjusted to 150µl by the addition of 91µl of RNase free water and then incubated for 2 h at 16^{o}C. On completion of incubation 2 µl (10U) of T4 DNA polymerase was added to the reaction mix and the incubated for a further 5 mins at 16^{o}C. To complete second strand cDNA synthesis, 10 µl of 0.5M EDTA was added to the samples and sample integrity verified by electrophoresis (1µl sample).

2.8.3 Purification of double stranded cDNA

This was achieved by mixing the samples with 162 µl of a mixture of phenol, chloroform, isoamyl alcohol in a ratio of 25:24:21. This was then transferred to a phase lock gel tube (Eppendorf, UK) and centrifuged (Eppendorf 5415D - Eppendorf, UK) for 2 mins at 12,000g. Using these tubes allows a distinct separation of the organic and aqueous phases, with the resulting aqueous phase being transferred to a new 1.5 ml Eppendorf tube. To this was added 0.5 volume of 7.5M ammonium acetate and 2.5 volumes 100% ethanol prior to mixing and

centrifugation (5 mins at 12,000g). The supernatant was removed, the remaining pellet dried (Speedvac – Savant,UK) for 2 minutes prior to rehydration with 12 µl of RNase free water with overnight incubation at 4^{o}C to ensure complete dissolution. From the resulting solution 1 µl was taken for gel electrophoresis to confirm cDNA integrity.

2.8.4 Synthesis of biotin labelled cRNA

This stage for synthesis of biotin labelled cRNA utilised reagents supplied in a the Enzo BioArray high yield *in vitro* transcription (IVT) labelling kit (Affymetrix, UK).
To each sample of 10 µl of purified double stranded cDNA were added (*Table 2.5*)

Table 2.5: Reagents used for synthesis of biotin labelled cRNA

Reagent	**Volume added (µl)**
RNAse free water	variable
10X reaction buffer.	4
10X Biotin-labelled ribonucleotides	4
10X DTT (Dithiothreitol)	4
10X RNase inhibitor	4
20X T7 (promoter sequence) RNA polymerase	2

Following these additions the volume was adjusted to 40 µl by the addition of 12 µl RNase free water. Samples were mixed and incubated for 5h at 37ºC, with gentle mixing by inversion every 30-40 mins throughout the incubation. Sample integrity was confirmed using 1 µl of biotin labelled cRNA and analysing by gel electrophoresis.

2.8.5 Purification of Biotin labelled cRNA

All reagents and materials required for purification of biotin labelled cRNA were supplied in the gene chip sample clean-up module (Affymetrix, UK).

To the biotin labelled cRNA synthesised in the previous step was added (*Table 2.6*):

Table 2.6: Reagents used for synthesis of biotin labelled cRNA

Reagent	Volume added (µl)
RNase free water	60
IVT cRNA binding buffer	350
100% ethanol	250

Samples (700µl) were vortexed for 5 secs, and then applied to an IVT cRNA clean-up spin column placed in a 2 ml collection tube and centrifuged for 15 secs at 8,000g. The filtrate was discarded and the spin column transferred to a fresh 2 ml collection tube. 500 µl of IVT cRNA wash buffer was applied to the spin column and centrifuged for 15 sec at 12,000g. Then 500 µl of 80% ethanol was added to the spin column and samples centrifuged for 15 secs at 12,000g. The filtrate was discarded, the cap of the spin column opened and samples centrifuged for 5 mins at 12,000g to ensure complete drying of the filter membrane. The spin column was then transferred to a fresh 1.5 ml Eppendorf tube, 100 µl RNase free water applied directly to the spin column membrane and then centrifuged for 1 min at 12,000g to elute the sample. 4 µl of the resulting solution underwent spectrophotometric analysis with the remainder being reduced to 40 µl in a Speedvac.

2.8.6 Quantification of biotin labelled cRNA:

In order to ensure that quantities and purity of cRNA were adequate, spectrophotometric analysis was used as previously described (section 2.5.4). An absorbance value of 1 at 260 nm corresponds to 40 µg/ml cRNA, and a A_{260}/A_{280} ratio of 1.9 to 2.1 was acceptable for sample purity. For quantification of cRNA when using total RNA as starting material, an adjusted cRNA yield was calculated to reflect carryover of unlabelled total RNA.

The formula below was used to determine adjusted cRNA yield assuming 100% carryover:

$$\text{Adjusted cRNA yield} = RNA_m - (\text{total } RNA_i)(y)$$

where

RNA_m = amount of cRNA measured after IVT (µg)

Total RNA_i = starting amount of total RNA (µg)

y = Fraction of cDNA reaction used in IVT

2.8.7 Fragmentation of cRNA

To obtain optimal microarray hybridisation, fragmentation of cRNA targets was performed. 8 µl of 5X fragmentation buffer, which was supplied with the GeneChip sample clean-up module (Affymetrix, UK), was added to 20 µg of cRNA target and the volume adjusted to 40 µl with RNase free water. Reactions were subsequently incubated for 35 mins at 94ºC. This allowed fragmentation of full-length cRNA targets to 35-100 base fragments, this was achieved using fragmentation buffer by a process of metal induced hydrolysis. From the resulting samples 1µl was removed and analysed by gel electrophoresis.

2.8.8 Target hybridisation

5 µg of fragmented cRNA was initially hybridised to GeneChip Test3 arrays (*Figure 2.12*) in order to confirm sample integrity. Following confirmation of sample quality from these test arrays, 15 µg of sample was hybridised in duplicate onto Human Genome U133A arrays [HG U133A, (Affymetrix, UK)].

The following components were added to fragmented cRNA samples to create a hybridisation cocktail either for GeneChip Test3 or HG U133A arrays (*Table 2.7*)

Table 2.7: Reagents used for cRNA preparation prior to hybridisation onto GeneChip Test3 or HG U133A microarray.

Reagent	Volume added (µl)	Final concentration
Fragmented cRNA	15	0.05µg/µl
Control oligonucleotide B2 (3nM)	5	50ρM
20x Eukaryotic hybridization controls (bioB, bioC, bioD, cre)	15	1.5, 5, 25 and 100ρM respectively
Herring sperm DNA (10mg/ml)	3	0.1mg/ml
BSA (50mg/ml)	3	0.5mg/ml
2x Hybridization buffer	150	1x
DMSO	30	10%
H_2O	To final volume of 300	
Final volume	**300**	

The final reaction volume was adjusted to 100 µl (300 µl) with RNase free water, and the hybridisation cocktail incubated for 5 mins at 99ºC. Whilst the hybridisation cocktail was incubating, the room-temperature equilibrated arrays were filled with 80 µl (200 µl) of 1X hybridisation buffer through the array septa to wet the probe array (*Figure 2.13*) and incubated for 10 mins at 45ºC, rotating at 60 rpm in a hybridisation oven 640 (Affymetrix, UK). The hybridisation cocktail was incubated for a further 5 mins at 45ºC and centrifuged for 5 min at 12,000g to remove any insoluble material. The 1X hybridisation buffer was removed from the array and 80 µl (200 µl) hybridisation cocktail added via the septa. The arrays were incubated for 16 hours at 45ºC, rotating at 60 rpm.

2.8.9 Probe array wash and stain

Following 16h of hybridisation, the hybridisation cocktail was removed from the array and replaced with 100 µl wash buffer A. The arrays were then loaded onto a primed fluidics station (Affymetrix, UK) and run through an automated washing and staining cycle. This cycle was controlled via microarray suite software (Affymetrix, UK) installed on a workstation computer The protocol for this washing/staining protocol can be seen in *Table 2.8*:

Table 2.8: Affymetrix wash and stain protocol for GeneChip Test3 and HG U133A microarrays.

Procedure	**Protocol**	**Reagent**	**Temperature (^{o}C)**
Post hybridisation wash 1	10 cycles of 2 mixes/cycle with wash	Wash buffer A (6x SSPE, 0.01% Tween 20)	25
Post hybridisation wash 2	4 cycles of 15 mixes/cycles with wash	Was buffer B (100mM MES, 0.1M Na^{+}, 0.01% Tween-20)	50
Stain	10mins	SAPE solution (1xMES stain buffer, 2mg/ml BSA, 10µg/ml streptavidin)	25
Post stain wash	10 cycles of 2 mixes/cycle	Wash buffer A	25
2^{nd} stain	10mins	Antibody solution	25
3rd stain	10mins	SAPE solution	25
Final wash	15 cycles of 2 mixes/cycle	Wash buffer A	30

2.8.10 Array scan

On completion of staining the arrays were scanned at 488nm using a GeneArray scanner and software package (Affymetrix, UK). The scanning process was controlled by Affymetrix Microarray Suite 4.0 (AMS v4) software package. Each array was scanned in duplicate, this process took 5 mins for GeneChip Test3 arrays and 20 mins for HG U133A arrays. Once scanning was complete, the software calculated a mean of the two scanned images, by measuring intensity for each cell. Duplicate scanning results in improved sensitivity and reduction in background noise.

2.8.11 Array analysis

A number of software packages are available in order to analyse the large amount of data produced from microarray analysis, thus allowing comparisons between different samples. The raw data produced from microarray scanning results in an image, where the colour and intensity of the fluorescence reflect the extent of hybridisation of the sample to the probes present on the chip. Colours are used to show whether the sample has hybridised to one of the two probes (red), the other probe (green) and if both hybridise then resultant image is yellow (green + red). Initial data processing aims to produce a gene expression table. Due to redundancy within the microarray, each gene may be represented by several spots corresponding to different sequences of the same gene; controls are included with deliberate gene mismatch, which allows validation of gene presence. A single gene may correspond to around 30-40 spots.

The analysis of the generated microarray data was performed using the DNA-Chip analyser (dChip) software package (Havard School of Public Health, USA). Array normalization to adjust overall brightness was performed by default selecting an array with median overall intensity as the baseline array against which all other arrays were normalized at probe intensity levels. The Invariant Set of Normalization method was used to identify a subset of probes with small, within subset rank, differences in the different arrays to serve as the basis for fitting a normalization curve. Following normalization, we identified genes differentially

expressed between the control, *F. nucleatum,* & *P. gingivalis* stimulated OEC samples. Based on previous experiences, Affymetrix and dCHip recommendations and published literature (Fan et al., 2005) (Corradi et al., 2008) the criteria we used to identify differentially expressed genes were that they showed at least a 2-fold change in expression level and had an absolute difference of more than 100 in the expression level between the samples on the control vs. test arrays. In addition, the following criteria were used in the analysis: the p-value threshold was set at 0.05 (per default), filtering genes that differ within the group means with a two-tail p-value 0.05.

To classify genes according to standardized Gene-Ontology (GO), vocabulary for the categories of biological process information from the NetAffx software (Affymetrix, UK) was utilised or entire datasets were imported into the Onto-Express software (http://vortex.cs.wayne.edu/projects.htm). The default binomial probability distribution and Bonferroni multiple experiment correction settings of the software were used for data analysis. Microsoft Access (Microsoft, US) database queries were used to compare genes in *P. gingivalis* and *F. nucleatum*.

In addition to utilisation of dChip bioinformatics software package, the data were analysed by a second bioinformatics software package GeneSpring (Agilent Technologies, USA). This commercially available program and is often considered the gold standard for micro array data analysis (Dresen et al., 2003). As well as analysing the data into lists of differentially expressed genes, (similar to dChip) it has the added benefit of having the ability to perform a wide range of advanced microarray analysis functions. This protocol was used to ensure that no differentially expressed genes were missed by utilising just one software package to analyse the data. In this thesis it was used to produce lists of differentially expressed genes using similar parameters to those used for dChip analysis.

2.9 Determination of cytokine levels in culture supernatants

2.9.1 *Enzyme linked immunosorbent assay (ELISA)*

Commercially available kits (IDS Limited, UK) were used for cytokine determination within the cell culture media removed from H400 cell monolayers. The assays were based upon sandwich ELISA methodology which allows sensitive and specific detection and quantification of soluble cytokines and chemokines. This method uses a highly-purified anti-cytokine antibody coated onto the walls of a plastic multiwell plate. The antibody specifically captures cytokine molecules present in the cell culture media introduced into the wells. Following washing of the wells to remove unbound material, the bound cytokine molecules are detected by biotin-conjugated anti-cytokine detection antibodies, followed by an enzyme-labeled avidin or streptavidin stage. The final stage is the addition of a chromogenic substrate, which results in the formation of a coloured end product which can be quantified spectrophotometrically. The amount of colour produced is proportional to the amount of cytokine present in the cell culture media. All kits included an appropriate standard protein which is serially diluted producing a range of standards dilutions. These are included on the multiwell plate and allow production of a standard curve allowing sample quantification.

The following protocol was used for cytokine assay of cell culture media.

1. Cell culture media was removed from the cell monolayer and filtered through a 0.2 micron filter in order to remove any residual cellular debris.
2. Media was then immediately stored in 1ml aliquots at -80^{o}C prior to use
3. On day of assay samples were removed from storage, quickly defrosted and thoroughly mixed before immediate use.
4. Samples and reagents used in the assay were equilibrated to room temperature prior to use.
5. All assays (samples, controls, standards and blanks) were run in duplicate.

6. 100µl of standard was taken and serial diluted in the wells to produce a suitable standard dilution range.
7. 100µl of sample, or blank was added to appropriate wells.
8. 50µl of diluted biotinylated anti-body (specific to cytokine being tested e.g. IL8) was added to all wells
9. The plate was then covered and incubated at room temperature (18-25^{o}C) for 1 h.
10. Following incubation the plate was washed 3 times
11. 100µl of avidin peroxidase was added to all wells, the plate was recovered and incubated at room temperature for 30 mins
12. Following incubation wells were aspirated and the washed 3 times.
13. 100µl of Tetramethylbenzidine (TMB) was added to all wells and incubated in the dark at room temperature for 12-15 mins.
14. Following incubation the reaction is stopped by adding 100µl of 1.8N sulphuric acid to all wells
15. Absorbance was immediately read at 450nm.
16. A standard curve was drawn and this was used to determine sample concentrations which were expressed in pg/ml.

It should be remembered that all sample values should fall within the standard curve, and the curve should not be extrapolated beyond the highest standard as this would invalidate the results. If samples were in excess of the maximum standard then they were diluted prior to assay, values falling below the minimum standard may require addition of more sample, concentration or the assay may not be sensitive enough for sample assay.

CHAPTER 3

Development & Validation of an *in vitro* Oral Epithelial Model System

3.1 Introduction

Initial experiments involved the development, validation and characterisation of a model system to investigate the potential role of oral epithelium in the establishment of inflammatory responses to colonising bacterial species. An immortal oral epithelial cell line (H400) was chosen because it is currently one of the best characterised oral epithelial cell lines available (Prime et al., 1990). This facilitated a range of relevant experimental procedures to be employed (summarised in *Figure 3.1*) without the need for basic re-characterisation studies. Cells were exposed to a variety of bacterial stimulants and downstream cellular responses were characterised at the gene and protein expression levels. Specifically, activation of NF-κB, changes in expression of key pro-inflammatory genes and downstream cytokine production were studied.

This chapter describes the characterisation of H400 cells in terms of growth characteristics on a range of substrates (cell culture flasks, glass slides and 96 well plates) necessary for the proposed investigations and initial studies to determine the effect of *E. coli* LPS on activation of NF-κB.

3.2 Establishing cell growth characteristics

3.2.1 H400 cell growth characteristics in cell culture flasks

In order to establish a cell culture flask-based model for the H400 cells, growth characteristics needed to be determined, which would optimise survival, growth, and production of a semi-confluent monolayer, thus permitting subsequent experimentation to determine the effect of microbial challenge.

The aim was to achieve sufficient cells to allow detection of cellular changes, prior to development of a confluent monolayer, since this results in altered cell phenotype (Jiang et al., 2004) and ultimately induces cellular quiescence (Gos et al., 2005). Excessive cell growth also potentiates nutritional exhaustion of the growth media, inducing changes in media pH and accumulating metabolic waste

products. These changes invoke cellular stress and ultimately cell death. In order to avoid such confounding factors, a time point must be established where cells are semi-confluent and still actively growing in a buffered, nutritionally rich medium. For these reasons it was decided that the ideal level of confluence would be in the region of 70-80%.

Cells were seeded in 25cm^2 culture flasks (passage 11) at a density of 2x10^5 cells per flask in 5ml of DMEM and incubated for 2-4 days (37^{o}C, 5% CO_2). Triplicate flasks were included for each time point and cell counts performed after 2, 3 and 4 days incubation (*Figure 3.2*). In order to determine non-adherent cell counts, cell culture media was removed, counts performed and viability determined using trypan dye exclusion as described in section 2.2.2.5. Adherent cells were then trypsinized to produce a cell suspension, which was counted and viability determined.
Cells grew well with cell counts increasing 5-fold by day 4. Microscopic analysis revealed typical epithelial cell morphology and confluence was estimated to be in the region of 30-40% (*Figure 3.3*).

The results clearly showed that these culture conditions did not produce the desired 80% confluence. Therefore, a second culture experiment was performed extending the time course to 9 days (each time point run in duplicate) and also determining cell viability and the number of non-adherent cells at each time point. Due to the likelihood of media exhaustion over this extended experiment, media was removed and replaced with fresh DMEM (+10% FCS) on days 4 and 7. The pH of the growth media removed at each time point was also determined.

Adherent cell number continued to increase over the 9 day period but the rate of increase was reducing by day 9 (*Figure 3.4*) and a semi-confluent cell monolayer in the region of 80% was achieved between days 5 and 7 (*Figure 3.5*). Interestingly, the numbers of adherent cells counted on days 2, 3 and 4 were similar to those obtained in the previous experiment (*Figure 3.2*). The percentage

of adherent, non-viable cells peaked at day 4 (11.25 %), corresponding with the greatest fall in media pH (*Figure 3.6*). The numbers of unattached cells were extremely low throughout the experiment (*Figure 3.7*) and varied between 0.006-0.6% of the total cell count.

These data demonstrated that to achieve the required level of confluence (~80%) with a high level of cell viability (>90%) for subsequent experiments, 25cm^2 flasks should be inoculated with 2x10^5 cells in 5ml DMEM, supplemented with 10% FCS, and incubated for between 5 and 7 days at 37°C in 5% CO_2, with the media being changed on day 4.

3.2.2 Oral epithelial cell growth on glass slides

In order to allow immuno-cytochemical analysis of H400 cells they would need to be grown on multi-well glass microscope slides, so growth characteristics were determined, thus allowing studies to demonstrate the cellular localisation of NF-κB. Glass represents a markedly different substrate from cell culture plastic ware, which has coated surfaces to aid cell adhesion and subsequent growth. Therefore this series of experiments aimed to determine the optimal growth characteristics of H400 cells on glass slides.

Sterile glass multi-well slides in Petri dishes (2 slides per dish) containing 15ml of DMEM were seeded with H400 cells at 3x10^5, 4x10^5, and 5x10^5 cells per dish. Cells were cultured for 6 days with the media being changed on day 4, slides were examined using an inverted microscope (x10) each day to estimate cell confluence. Results (*Table 3.1; Figure 3.8*) demonstrated that the initial inoculum size was inversely related to the time taken to attain 80% confluence. The use of an initial inoculum of 4x10^5 resulted in 80% confluence at 5 days and was was adopted for all subsequent experiments involving stimulation of cell monolayers with bacteria and *E. coli* LPS. This allowed for media replacement with fresh DMEM at day 4 and, if required, pre-incubated at this time with NF-κB modulators.

3.2.3 Oral epithelial cell growth in 96 well plates

96 well, flat bottomed plates were used for the high throughput fluorescence immunocytochemical analyses and thus studies were performed to determine the growth characteristics of H400 cells in this plate format to attain a semi-confluent monolayer at around 80%.

Pilot experiments were performed that investigated initial seeding of wells with 3, 6 and 8 $x10^3$ cells and growth for 5 days (being fed on day 4 with fresh DMEM). Microscopic examination of wells from the middle and edge of the plate were performed daily to estimate levels of confluence. Results suggested that 80% confluence was achieved at day 5 with an initial inoculum of $6x10^3$ cells per well**.** This allowed for media replacement with fresh DMEM at day 4 (and, if required, pre-incubated at this time with NF-κB modulators). Counts of 20 individual wells following trypsinisation were performed and demonstrated a mean cell number of 4164.9±513.2 (range of 2610 – 4898). Two wells showed low cell numbers (2610 and 3278); their exclusion resulted in a mean count of 4292.9±313.5. These results suggested that, under these culture conditions, suitable monolayers of H400 cells within microwells could be produced for the high throughput immunocytochemistry studies.

3.3 A model of NF-κB translocation

This section reports the development of a model system, based on H400 cells, to identify NF-κB within the cytosol of un-stimulated cells (inactive form of NF-κB) and/or within the nuclei of stimulated cells (active form of NF-κB). This aim was to demonstrate nuclear translocation (activation) of NF-κB in H400 cells after stimulation/treatment with oral bacteria. Initial proof of principal studies utilised *E. coli* LPS, a recognised activator of NF-κB (Prince et al., 2004). Studies investigated size of stimulus and length of stimulation to produce maximal nuclear translocation of NF-κB in this H400 model system.

3.3.1 Determination of nuclear translocation of NF-κB in H400 cells

H400 cells grown for 5 days on glass slides were stimulated with *E. coli* LPS (10μg/ml; n=4) or DMEM, as the negative control (n=4), for 1h. Immunocytochemical staining of the cells for NF-κB after acetone fixation revealed cytoplasmic staining in cells treated with DMEM but extensive nuclear localisation in cells exposed to *E. coli* LPS *(Figure 3.9)*. Cell counts to determine the percentage of cells showing NF-κB nuclear translocation demonstrated that under these conditions nuclear translocation had occurred in 50% of cells treated with *E. coli* LPS (*Figure 3.10*).

3.3.2 Effect of stimulation time

The following studies aimed to determine the optimal stimulation time required to produce maximal nuclear translocation of NF-κB. Cells grown on slides were stimulated with *E. coli* LPS (10μg/ml) or DMEM (negative control) for 30, 45, 60, 75 and 90 mins. The percentage of cells showing nuclear translocation of NF-κB changed with time of stimulation and was maximal (54.2±23.2%) at 60 mins (Figure 3.11). By contrast, control cells challenged with medium exhibited very low levels of nuclear staining (range 0.98 – 2.11%), which did not vary with time of treatment. Interestingly, treatment of cells for 30 minutes with *E. coli* LPS did not stimulate activation of NF-κB above the low level seen in medium-challenged controls.

3.3.3 Effect of E. coli LPS concentration on NF-κB activation

Initial experiments utilised 10 μg/ml of *E.coli* LPS because this is a frequently reported standard concentration used for cell stimulation, however it appeared that this level produced in the region of 50% NF-κB stimulation in this model system. Therefore in an attempt to increase the levels of translocation H400 cells were stimulated with *E. coli* LPS at 10 and 20 μg/ml for 1h. The percentage of cells showing nuclear translocation of NF-κB increased from 45.5±22.6% to 98.5±8.49% when the LPS concentration was doubled to 20μg/ml (*Figure 3.12*). As a result, all

subsequent experiments using *E. coli* LPS were performed using the higher concentration of 20µg/ml due to the enhanced levels of NF-κB activation.

3.3.4 Effect of cell confluence on E. coli LPS stimulated NF-κB translocation

Another potential variable on NF-κB translocation in H400 cells was the effect of the degree of cell confluence. To investigate this Petri dishes containing 2 glass slides were seeded with a range of cell concentrations (3, 4 & 5 x 10^5 cells) and after 4 days growth they were stimulated for 1h with *E. coli* LPS (20µg/ml) or growth media as a negative control.

Cell confluence was estimated as 30%, 40% and 70% for initial seeding suspensions of 3, 4 & 5x10^5 cells respectively, by day 4. There appeared to be no differences between levels of translocation (*Figure 3.13*) following stimulation at confluence levels between 30-70% (range of NF-κB translocation 97.6 – 98.7%). Similarly, control levels of translocation were at a similar level to previous experiments and unaffected by percentage confluence (range 2.3 – 4.2%).

3.3.5 Effect of time from passage (seeding) on NF-κB translocation

Another potential confounder, which may influence epithelial cellular responses, was the time from cell passage or seeding prior to stimulation. As previously described, the passage protocol involves trypsinisation of cells in order to detach them from the culture plate substrate and produce a single cell suspension. This may involve significant cellular stress and it was hypothesised that this may affect cell responses to stimulation. In addition it may also cause stimulation of NF-κB in "un-stimulated" cells at earlier time points thus masking the effects of bacterial stimulation. To investigate this, cells were seeded into Petri dishes containing growth media and multi-well slides at a concentration of 4x10^5 cells and cultured for between 3 – 6 days. At each time point (days 3, 4, 5 & 6) slides were either stimulated with 20µg/ml of *E. coli* LPS for 1h or media (negative control). Slides were then removed, fixed, stained and the percentage nuclear translocation determined as previously described (*Figure 3.14*). The levels of NF-κB activation in

un-stimulated cells remained low during the course of the experiment suggesting that at day 3 there is no detectable residual NF-κB activation resulting from initial passage. However, there was an increase in the percentage of cells showing nuclear translocation of NF-κB from day 3 (59.8±12.5%) to day 6 (86.8±7.6%). In terms of developing the model system day 5 or day 6 post-seeding showed high levels of NF-κB activation (79.2% and 86.8% respectively) and thus deemed appropriate time points for investigation of NF-κB activation.

3.3.6 Conclusions

Data from this series of experiments which aimed to develop an H400 model system to demonstrate NF-κB translocation support the following conclusions:

1. NF-κB translocation can be induced in the H400 cells when stimulated with *E. coli* LPS at 10 & 20µg/ml.
2. *E. coli* LPS induces nuclear translocation in almost 100% of cells when 20µg/ml LPS is used for 1 hour.
3. Nuclear localisation of NF-κB peaks at about 60 minutes post stimulation.
4. There appears to be no effect of cell confluence level (30-70%) in terms of the percentage of cells demonstrating NF-κB activation.
5. Levels of NF-κB translocation appear to increase with time post-passage (days 3-6).

By utilizing the data generated from this series of experiments a model system has been developed and validated using a known NF-κB activator (*E. coli* LPS).

3.4 Effect of periodontal pathogens *P. gingivalis* (PG) & *F. nucleatum* (FN) on NF-κB translocation in H400 cells

After establishing a model system for NF-κB translocation using *E. coli* LPS, the following experiments aimed to determine the effect of whole heat-killed

periodontal pathogens *P. gingivalis* and *F. nucleatum* upon activation of NF-κB in H400 cells.

3.4.1 Quantitative analysis of NF-κB activation with P. gingivalis and F. nucleatum using manual counting methods

H400 cells, grown on glass slides for 4 days, were stimulated for 1 hr using whole dead bacteria at a concentration of $1x10^9$ bacteria per ml (Multiple of infection (MOI) of 1:100, i.e. 100 bacteria per epithelial cell). Following stimulation cells were washed, fixed and stained for NF-κB.

Levels of nuclear translocation of NF-κB in medium-stimulated negative controls were low (2.8±1.2%; *Figure 3.15*). By contrast, stimulation with *P. gingivalis* and *F. nucleatum* produced increased levels of NF-κB translocation when compared to negative controls with *F. nucleatum* inducing higher levels of translocation (98.1±2.2%) than *P. gingivalis* (16.6±9.7%)

3.4.2 Quantitative analysis of NF-κB with P .gingivalis and F. nucleatum by high throughput fluorescent immunocytochemistry

The previous experiment clearly demonstrated that both *P. gingivalis* and *F. nucleatum* could stimulate nuclear translocation of NF-κB in H400 cells and suggested quantitative differences in the ability of these two bacteria in activating this transcription factor. However this relied upon time consuming manual counting methods (*Material and methods, section 2.3.2*) limiting the number of replicates possible. Therefore, in order to further confirm the actions of the periodontal pathogens tested, high throughput quantitative analysis of NF-κB translocation was performed (*Materials and methods, section 2.4*). This methodology allows analysis of large numbers of cells, and results can be normalised based on cell number, and expressed as relative intensity of cytoplasmic relative to nuclear NF-κB staining.

The data obtained confirmed that derived from manual methods demonstrating that *E. coli* LPS (20μg/ml), *F. nucleatum* (MOI of 100:1) and *P. gingivalis* (MOI of

100:1) all stimulated increased nuclear translocation of NF-κB verses un-stimulated (negative) controls (*Figure 3.16*). Both bacteria stimulated greater NF-κB activation than *E. coli* LPS, with *P. gingivalis* demonstrating higher mean of NF-κB activation levels than *F. nucleatum.* This result differed from the result obtained by manual counting, which relied only on nuclear staining rather than a ratio of nuclear to cytoplasmic staining.

3.4.3 NF-κB activation time course with P. gingivalis & F. nucleatum

Experiments in which H400 cells were stimulated by *E. coli* LPS suggested that the optimal time for maximal nuclear translocation of NF-κB was about 60 mins, but this may differ for intact bacteria. In order to address this issue, the high throughput fluorescence technique for quantification of NF-κB activation was used to investigate H400 stimulation by both *P. gingivalis* (MOI of 100:1) and *F. nucleatum* (MOI of 100:1) at the time points of 0, 30, 45, 60, 90, 120 and 240 mins. The data generated (*Figure 3.17*) demonstrated that both bacteria caused high levels of NF-κB activation at 60 mins, which was the peak time for *P. gingivalis*. *Fusobacterium nucleatum* appeared to stimulate maximal nuclear translocation of NF-κB over a wider time range, peaking between 60 – 90 mins after challenge. However, the mean maximal level of stimulation (ratio of nuclear to cytoplasmic staining) attained with *F. nucleatum* (mean$\pm$SD) was lower than that found with *P. gingivalis*. At 240 mins after challenge, activated levels of NF-κB approached un-stimulated control levels.

3.4.4 Conclusions

These data demonstrated that:

- Heat treated whole *P. gingivalis* and *F. nucleatum* activate NF-κB in the H400 cell model.
- Levels of NF-κB activation differed between the two techniques employed; manual counting, based on assessing nuclear staining alone, showed higher levels of activation of NF-κB by *F. nucleatum*, compared to *P. gingivalis,* whereas the

high throughput analysis showed equivalent or higher levels of activation by *P. gingivalis* compared to *F . nucleatum*.

- Time course experiments demonstrated that NF-κB activation peaked at around 60-90 mins, and there appeared to be a slight lag in activation with *F. nucleatum* compared to *P. gingivalis,* but *F. nucleatum* showed prolonged activation.
- Levels of *P. gingivalis* and *F. nucleatum* induced NF-κB activation approached baseline (un-stimulated control) levels at 240 mins.

3.5 Chapter summary

The aim of this chapter was to develop a model system for investigating oral epithelial responses to the periodontal pathogens *P. gingivalis* and *F. nucleatum*. Experiments were separated into two main areas firstly, characterisation of H400 cell growth patterns on a range of substrates, and secondly to determine if stimulation of these cells demonstrated activation of key pro-inflammatory REDOX sensitive transcription factor NF-κB. The results of these experiments are summarised below:

1. Cell growth characteristics aimed at achieving 80% confluence are listed below:

- 25 cm^2 plastic culture plates; seeded at $2x10^5$ cells in 5ml DMEM and grown for 5-7 days.
- Glass slides in Petri dishes; seeded at $4x10^5$ cells in 15ml DMEM and grown for 5 days.
- 96 well plates; seeded at $6x10^3$ cells per well in 150µl of DMEM.

2. The effect of H400 cells stimulation on NF-κB activation:

- Stimulation of H400 cells with a known activator (*E. coli* LPS) of NF-κB showed nuclear translocation with optimal levels seen with 20µg/ml of *E.coli* LPS for 60 mins.

- Stimulation of H 400 cells with intact, heat-killed *P. gingivalis* and *F. nucleatum* at an MOI of 100:1 demonstrated NF-κB nuclear translocation, which was maximal between 60-100 mins after challenge.

The data generated suggests both qualitative and quantitative differences in activation of NF-κB in H400 cells stimulated by these two periodontal pathogens.

Having established the model system the next stage was to determine whether activation of NF-κB reported could be modulated using the natural antioxidant (α-lipoate), experiments to investigate this possibility are discussed in subsequent chapters.

CHAPTER 4

Effects of α-lipoate
on
H400 epithelial cells

4.1 Introduction

The previous chapter described the development of an epithelial model system which on epithelial cell stimulation activated NF-κB. This chapter aimed to determine whether the antioxidant α-lipoate was able to modulate the activation of NF-κB.

Initial pilot experiments suggested that α-lipoate at certain concentrations may reduce cell number and levels of attachment. These observations could be explained by a number of factors, including growth inhibition, cytotoxicity, or effects on cell attachment mechanisms reducing levels of cell adhesion (epithelial cells are unable to grow if they are not attached to a substrate). Experimentation was directed initially at characterising these observations and secondly at determining a suitable concentration / exposure time of H400 cells to α-lipoate to minimise these effects.

4.2 Effect of α-lipoate on H400 cell viability and adherence

4.2.1 Concurrent cell seeding / growth with α-lipoate

Initially, experiments investigated H400 cells seeded into cell culture flasks containing media supplemented with α-lipoate. Flasks were seeded in duplicate for each time point (2, 3, 4, 7 and 9 days) with $2x10^5$ H400 cells containing either 1mM α-lipoate supplemented DMEM or vehicle control (DMEM, no α-lipoate) and incubated at 37°C in 5% CO_2. At each time point growth media was removed, cells washed and trypsinized to produce a single cell suspension. Cell counts and viability were performed on growth media (unattached cells) and trypsinized cell suspensions (attached cells).

Results from this experiment indicated that α-lipoate at a concentration of 1mM in DMEM inhibited proliferation of H400 cells over a 9 day period when compared to cells incubated with DMEM containing vehicle (negative control) (*Figure 4.1*). Increases in detached cell number were also seen during the 9 days this

experiment was run (*Figure 4.2*). Up to day 5 there was little difference in the viability of detached cells between those grown in the presence or absence of 1mM α-lipoate, this suggests that although detached cells are unable to proliferate they do retain viability (up to day 5) as determined by trypan blue staining. However a difference in levels of cell viability was seen on day 7 with considerably lower levels observed with α-lipoate treatment (63.8%) compared to those cells grown in plain growth media (89.4%) (*Figure 4.3*). When investigating attached cell viability on days 2, 3 & 9 there appeared to be little difference between cells grown with or without α-lipoate, however on days 4, 5 & 7 a difference was seen which suggested that attached cells supplemented with α-lipoate demonstrated higher levels of viability (*Figure 4.4*).

4.2.2 The effect of α-lipoate on an established cell monolayer

In order to determine the effect of α-lipoate on the H400 cell model system (i.e. glass multi-well slides with cells grown to 80% confluence), an initial pilot experiment was performed with α-lipoate added to growth media providing a final concentration of 4mM (negative control without α-lipoate was included). Slides were incubated under standard conditions for 24h and then microscopically examined (*Figure 4.5*). Results demonstrated reductions in levels of confluence with α-lipoate (number of attached cells) compared to controls. In addition, high numbers of unattached cells were present within the media. This suggested that incubating an established monolayer of H400 cells with 4 mM α-lipoic for 24h effected cell growth and/or attachment.

To determine if the observed changes with cells exposed to 4 mM α-lipoate were reversible, the media was removed; the remaining attached cells were washed in sterile PBS and then incubated under standard conditions with fresh growth media (no α-lipoate). Microscopic examination over the next 3 days showed a return to normal epithelial cell growth patterns. In addition, the media removed from the treated monolayer (which contained free cells) was centrifuged with the resulting cell pellet being washed, re suspended in growth media and seeded into a cell

culture flask. These cells reattached and grew normally. Taken together these observations suggest that the changes induced in cell attachment by α-lipoate are reversible and that this may be due to cell adhesion mechanisms rather than inducing cell death.

The previous experiment indicated that 4mM α-lipoate had a significant effect upon H400 cell growth and adhesion over 24h, In order to determine the effects of α-lipoate on the model system in terms of activation of NF-κB, experimental conditions that minimised these cellular effects were required.

To achieve this goal 2 options were considered:-

1. Reduction in the concentration of α-lipoate used.
2. Reduce the cellular exposure time to α-lipoate.

4.2.3 Effects of varying α-lipoate concentrations upon H400 cell growth

Semi-confluent H400 cells were incubated with a range of α-lipoate acid concentrations (4, 2, 1, 0.5, 0.25, 0.125 and 0.0624 mM) for 24h and cell growth was examined. Duplicate cultures were run with a negative control included (no α-lipoate-vehicle control).

Results indicated a dose response between increasing concentrations of α-lipoate and reductions in cell count (*Figure 4.6*). Incubation with 4mM α-lipoate for 24h resulted in a 92.9% reduction in cell count. There appeared to be a marked difference between 1mM and 0.5mM α-lipoate, with an increase from 43.7% to 85.5% of the control cell count.

This data suggested that the use of 0.5mM α-lipoate (or less) would be a suitable concentration to employ for 24h incubation studies with H400 cells, with $\geq$ 85% of cells remaining attached

4.2.4 The effect of varying the exposure time of H400 cells to α-lipoate on cell attachment

Cells were seeded onto glass multi-well slides (in duplicate) and grown to semi confluence before exposure to 4mM α-lipoate or control solution (no α-lipoate). Slides were then incubated under standard growth conditions and examined every 30 mins over a 3h period. At each time point, cells were examined microscopically with a comparison made between cells incubated with α-lipoate and the negative controls.

Microscopic examination revealed no discernable difference between cells incubated with 4mM α-lipoate acid and those without, additionally no observed increase in the numbers of detached cells were seen. This suggested that short term incubation ($\leq$ 3 hours) with 4 mM α-lipoate avoided the reduction in attached cell number seen with longer term exposure at this concentration.

The results from these two experiments suggested 2 potential methods for exposing the H400 cells to α-lipoate whilst minimising reductions in cell growth / loss of cell adhesion seen in previous experiments:

1. Exposure of H400 cells to $\leq$ 0.5mM α-lipoate over 24h

or

2. Exposure of H400 cells to 4mM α-lipoate for $\leq$ 3h

Although these methods would allow further experimentation utilising the model system, the loss of attachment seen was an interesting phenomenon that was deemed worthy of further investigation.

4.2.5 α-lipoate and apoptosis in H400 cells

One potential reason for poor attachment and growth of H400 cells in the presence of α-lipoate was the induction of apoptosis. This possibility was investigated by

determining DNA fragmentation patterns and the expression of caspase 3, both characteristic signatures of apoptosis.

4.2.5.1 DNA laddering:

H400 cells were grown to semi confluence (~80% confluence) and exposed to a range of α-lipoate concentrations (0.125, 1, 4mM) for 24h (n=2 per concentration). Cells were then trypsinized and harvested into lysis buffer (duplicate flasks were pooled for each concentration). The extracted DNA was then separated by agar gel electrophoresis and examined under ultra violet light *(Figure 4.7).*

No evidence of DNA laddering was detected, suggesting that α-lipoate was not inducing apoptosis in H400 cells.

4.2.5.2 Caspase 3 expression:

H400 cells were grown in 96 well plates seeded at $5x10^3$ cells per well to semi-confluence and incubated with a range of α-lipoate concentrations and vehicle control for 48h (n=3 for each concentration). After fixation, caspase 3 expression was determined by high throughput immunocytochemistry.

Control (non-treated) cells exhibited no detectable caspase 3 expression and no significant change in caspase 3 expression was induced by 0.25 and 0.5mM α-lipoate after 48h incubation. By contrast, cells incubated with 1mM α-lipoate showed substantial increases in caspase activity (*Figure 4.8 & 4.9*).

Results from these 2 experiments suggested that apoptosis does not appear to be induced in H400 cells on incubation with $\leq$ 4mM α-lipoate for 24h, or $\leq$ 0.5mM for 48h, however 48h incubation with 1mM α-lipoate produced substantial increases in levels of apoptosis.

4.2.6 Methods of increasing α-lipoate treated H400 cell adherence.

This section investigates potential methods of increasing cell adherence and growth of H400 cells treated with high concentrations of α-lipoate. Although the previous section suggested potential protocols to overcome this issue, this section

will investigate methods of increasing cell adherence and potentially allowing higher concentrations of α-lipoate to be used.

4.2.6.1 Calcium supplementation

Calcium plays a key role in cell attachment (Ko et al., 2001) both to substrates and adjacent cells, resulting in the development of classic tissue architecture (or monolayers seen in cell culture). This is achieved by calcium modulation of a family of molecules central to cellular interactions and adherence (cadherins, selectins and integrins). So the possibility exists that increasing the concentration of calcium in DMEM may be a potential method of increasing cell adhesion. Interestingly α-lipoate has been reported to chelate a range of divalent metallic cations (e.g. zinc, copper) (Ou et al., 1995). Although not yet published within the literature, it is possible that α-lipoate could chelate calcium, reducing levels available to cells and therefore reducing levels of cell-cell and cell-substrate attachment.

Calcium in the form of $CaCl_2$ is present in DMEM at a concentration of 1mM, and so a range of concentrations (1, 2, 3, and 4mM) were investigated by additional supplementation of $CaCl_2$ +/- 1mM α-lipoate. H400 cells were grown to semi-confluence then incubated with 1mM α-lipoate for 24h (n=2). Following incubation, monolayers were examined microscopically. Thereafter, they were washed in PBS to remove any non-adherent cells, trypsinized and counts performed on the resulting cell suspensions (*Figure 4.10, 4.11*)

Increasing the levels of $CaCl_2$ from a baseline of 1mM (present in DMEM) to 4mM in H400 cells grown to semi-confluence (without α-lipoate) resulted in a substantial reduction in attached cell count from $163.6x10^5$ to $116.0x10^5$. By contrast, increasing the levels of $CaCl_2$ to 4mM in DMEM increased mean attached cell number after exposure to 1mM α-lipoate for 24h to control levels. (*Figure 4.11*). However, supplementation with $CaCl_2$ at 4mM effectively reduced cell attachment

levels to those resulting from treatment with 1mM α-lipoate, rather than increasing attachment levels to those of non-supplemented ($CaCl_2$ or α-lipoate) controls.

This experiment suggested that by increasing the levels of $CaCl_2$ in DMEM in the presence of α-lipoate had little beneficial effect on the number of attached cells; however when levels of calcium were increased without α-lipoate a reduction in attached cell number occurred. The net effect of $CaCl_2$ supplementation (1-4 mM) was a reduction in attached cell number in un-supplemented cells, with a slight increase in cell attachment in the presence of 1mM α-lipoate with both 3 and 4 mM $CaCl_2$ supplementation, but overall numbers of cells attached were greatly reduced when compared to un-supplemented $CaCl_2$ controls without α-lipoate. Therefore it was concluded that the there would be little benefit in adopting this technique for future experimentation.

4.2.6.2 Glass slide surface treatments

The surfaces of cell culture flasks are normally treated (hydrophilic and ionic surface treatment in manufacture) to help cell attachment and monolayer development. The glass multi-well slides used to determine NF-κB activation in this model system were not treated in this manner and, as discussed, cell attachment was a particular issue in the presence of certain α-lipoate concentrations. In an attempt to improve cell adhesion two approaches were investigated.

1. The use of commercially available electro-statically charged slides (Super Frost, Jencons,UK).
2. The use of poly-L-lysine (0.1%)-treated slides.

H400 cells suspended in DMEM were seeded into Petri dishes with (a) untreated slides, (b) Superfrost slides and (c) slides pre-treated with poly-L-lysine. Cells were grown to semi confluence before 24h exposure to 4mM α-lipoate or control solution (DMEM).

All control slides (no α-lipoate) showed intact semi-confluent monolayers, whereas near complete loss of cell adherence was seen in those exposed to α-lipoate. There was no microscopically discernable difference in cell attachment between plain slides, Superfrost & 0.1% poly-L-lysine treated slides in the presence of α-lipoate. These results demonstrate that the treated slides investigated offered no benefit in increasing levels of cell attachment in the presence of this concentration of α-lipoate.

4.2.7 Conclusions about the effect of α-lipoate on H400 cell viability and adherence

Results from the reported series of experiments suggested that either reducing the exposure time or reducing the concentration of α-lipoate was the best method to adopt in the H400 cell model system in order to maintain cell adherence and growth. The other variables investigated demonstrated no benefit and may potentially result in the introduction of other confounding factors.

Although the effect of α-lipoate on H400 cell adherence, and therefore cell proliferation, is substantial at concentrations greater than 0.5mM, its effect on cell viability is less marked. Indicating that:

- Attached cells had similar levels of viability to cells not exposed to α-lipoate (>95%).
- Unattached cells had similar levels of viability (dye exclusion) up to day 5 of growth, however levels of viability reduced (~64%) with α-lipoate compared to untreated controls (~90%) on day 7.
- Unattached cells exposed to α-lipoate for up to 5 days were able to attach and grow normally after reseeding into α-lipoate free media.

4.3 Effect of α-lipoate on post stimulation NF-κB translocation

Previous experiments aimed to determine the effects of α-lipoate on H400 cells in terms of cell attachment and apoptosis, with results suggesting the maximal levels of α-lipoate that could be used, whilst minimising issues surrounding loss of cell adhesion were 0.5mM for 24h incubation and up to 4mM for short term incubation

(≤3h). This resulted in a model system that could be treated with α-lipoate prior to bacterial stimulation, allowing investigations into the effect of α-lipoate on NF-κB activation.

4.3.1 Effect of α-lipoate on NF-κB nuclear translocation in LPS-stimulated H400 cells

In order to determine whether α-lipoate was able to modulate levels of NF-κB activation, H400 cells were grown to semi-confluence on multi-well glass slides, pre-incubated with and without α-lipoate and than stimulated with *E.coli* LPS (20μg/ml). NF-κB nuclear translocation was detected immunocytochemically after 1h stimulation using an NF-kB monoclonal antibody to the p65 subunit (clone F-6, Santa Cruz Biotechnology, USA; diluted 1:100) Staining controls included omission of the primary antibody (negative control) and use of clone MM1 (Ki67; positive control). Semi-quantitative analysis was performed using cell counts to determine percentage of cells exhibiting nuclear translocation of NF-κB.

4.3.1.1 Effect of pre-incubation with 4mM α-lipoate (1h) prior to stimulation

Un-stimulated cells showed cytoplasmic localisation of NF-κB both when pre-incubated with vehicle (DMEM) or α-lipoate, with less than 2% of cells showing nuclear staining (*Figure 4.12*). In contrast, stimulated cells pre-incubated with vehicle showed high levels of nuclear localisation of NF-κB (95.8%). Pre-incubation of cells with α-lipoate prior to stimulation caused a >80% reduction in nuclear localisation of NF-κB compared to cells stimulated without α-lipoate.

4.3.1.2 Effect of pre-incubation with 0.5mM α-lipoate (24h) prior to stimulation

Un-stimulated cells showed cytoplasmic localisation of NF-κB with <1% cells showing nuclear localisation (*Figure 4.13*). Stimulated cells showed high levels of nuclear localisation of NF-κB (mean=50.2%). As seen in the previous experiment, pre-incubation with α-lipoate reduced levels of *E.coli* LPS stimulated nuclear NF-κB translocation (mean=11.2%)

The results of these experiments confirmed that un-stimulated levels of NF-κB nuclear translocation were low and that stimulation with *E.coli* LPS induced high levels of nuclear translocation which were similar to those seen in previous experiments. However, the key finding was that pre-incubation with either 4mM α-lipoate for 1h or 0.5mM for 24h prior to stimulation, induced reductions in nuclear translocation of between 84.6 and 77.7% respectively when compared to positive, non-α-lipoate controls. It was also noted that pre-incubation with α-lipoate (by either method) did not return levels of NF-κB activation to un-stimulated levels. This is a potentially important finding, as *in vivo* activation of NF-κB is key to the immune/inflammatory response, and the challenge in anti-inflammatory therapy would be to dampen down pro-inflammatory gene transcription in hyper inflammatory periodontitis patients rather than completely blocking activation of this essentially defence process.

4.3.2 Effect of different concentrations of α-lipoate on NF-κB nuclear translocation on LPS-stimulated H400 cells

To determine the effects of α-lipoate concentration on the overnight dosing model, H400 cells were grown to semi-confluence on multi-well glass slides and incubated overnight with a range of concentrations (0.25, 0.5 and 1mM) to determine if lower levels could be used to block LPS induced (1h) NF-κB translocation. Following stimulation, cells were fixed and immunocytochemically stained prior to performing cell counts to determine levels of NF-κB translocation.

Both microscopic inspection of slides (*Figure 4.14*) and cells counts *(Figure 4.15)* clearly showed a dose related trend in levels of NF-κB translocation, with 2mM producing a 91% reduction and 0.25mM a 65% reduction in the levels seen in the vehicle treated control.

This series of experiments demonstrated that 0.5mM α-lipoate incubated for 24h with H400 cells is a suitable concentration and time scale to use for future experiments. This was concluded because this protocol:

- had minimal effect on cell adhesion, with 85.5% cell attachment
- did not induce apoptosis
- blocked 78% of LPS induced nuclear NF-κB translocation

4.3.3 The effect of α-lipoate on periodontal pathogen-induced NF-κB translocation.

Previous results have shown that α-lipoate can modulate NF-κB activation in H400 cells when stimulated by *E.coli* LPS. The following experiments, based upon high throughput immunocytochemistry, aimed at determining whether a similar result was obtained after stimulation with periodontal pathogens. H400 cells were grown to semi–confluence in 96-well plates, pre-incubated with 0.5mM α-lipoate for 24h prior to stimulating with *F. nucleatum* or *P. gingivalis* (whole dead bacteria, MOI 1:100) for 1h. Following fixing, wells were stained for NF-κB and resulting images analysed for NF-κB translocation using image analysis software.

4.3.3.1 P. gingivalis stimulation

Un-stimulated (vehicle control) cells demonstrated cytoplasmic NF-κB localisation whereas cells stimulated with *P. gingivalis* showed nuclear localisation (*Figure 4.16*). However, when cells were pre-incubated with 0.5mM α-lipoate for 24h prior to stimulation levels of NF-κB activation approached those of un-stimulated controls (*Figure 4.17*). Statistically significant differences were noted between un-stimulated control and *P. gingivalis* stimulated cells ($p=0.0016$); and between stimulated cells and stimulated cells with α-lipoate ($p=0.0026$)

4.3.3.2 F. nucleatum stimulation

Stimulation with *F. nucleatum* caused NF-κB activation and nuclear translocation whereas NF-κB in un-stimulated (vehicle control) cells remained within the cytoplasm (*Figure 4.18*). When cells were pre-incubated with 0.5mM α-lipoate for 24h and stimulated with *F. nucleatum,* levels of NF-κB activation approached un-stimulated control levels (*Figure 4.19*). Statistically significant differences were noted between un-stimulated control and *F .nucleatum* stimulated cells ($p=0.02$); and between stimulated cells and stimulated cells with α-lipoate ($p=0.008$).

These data suggest that, in addition to α-lipoate modulating *E.coli* LPS NF-κB activation, it also has the ability to reduce activation when stimulated with intact dead whole periodontal pathogens such as *P. gingivalis* and *F. nucleatum*.

This chapter has determined suitable conditions to culture H400 cells in the presence of α-lipoate in order to minimise issues surrounding cell adherence. The methods investigated have resulted in conditions that allow investigation of α-lipoate in the H400 model system. In addition, it has been shown that at lower concentrations of α-lipoate, cells do not appear to undergo apoptosis. Furthermore, results have shown that α-lipoate can modulate the activation of NF-κB in this model system when stimulated with *E.coli* LPS, *F. nucleatum* and *P. gingivalis*. This phenomenon may be important in down regulating the hyper-inflammatory response to plaque seen in patients with chronic periodontitis.

Activation of the pro-inflammatory transcription factor NF-κB represents an early stage in the cellular response to stimulation and a range of downstream changes in gene expression will inevitably follow. Changes in gene expression resulting in mRNA production can ultimately lead to production of cytokines which are key to the initiation and propagation of the immune/inflammatory response.

The following chapter will investigate the next stage of this process i.e. downstream changes in gene expression subsequent to NF-κB activation.

CHAPTER 5:

Gene expression changes in periodontal pathogen stimulated H400 cells

5.1 Introduction

Results from previous chapters have demonstrated the ability of *E. coli LPS*, *P. gingivalis* and *F. nucleatum* to activate NF-κB in an oral epithelial model system. Activation of this key pro-inflammatory transcription factor is an early response to cell stress (in this case bacterial stimulation) resulting in phosphorylation of the NF-kB-IkB cytoplasmic complex, ubiquitination of IkB resulting in translocation of NF-κB into the nucleus, binding to DNA and gene transcription.

Therefore the next stage of this study aimed to examine changes in gene expression invoked by microbial stimulation. Such gene expression changes are a precursor to changes in cell protein production including cytokines, which play a key role in cellular immune / inflammatory responses.

A variety of techniques exist to investigate changes in gene expression e.g. (i) PCR: which investigates genes using specific gene primers, therefore this technique only allows investigation of individual pre-selected genes and does not allow high throughput screening of large numbers of genes, thus limiting the amount of information on cellular response to stimulation. (ii) Microarray analysis: this technique allows for screening of many thousands of individual genes, and may identify novel genes that have an important but as yet not identified role in the cellular inflammatory/immune response.

5.2 Verification of gene expression changes in stimulated H400 cells

Prior to microarray analysis, experiments utilizing sq-RT-PCR were performed to ensure gene expression changes could be seen in this model system. As changes in gene expression are downstream of NF-κB activation, a decision was made to look at 2 time points, 4h and 24h post bacterial stimulation. Genes that might be expected to be differentially expressed because of their involvement in the inflammatory response (IL-1β, TNF-α, IL-8 and GM-CSF) were chosen. H400 cells were grown to semi-confluence, stimulated with non-viable *F. nucleatum, P. gingivalis* or media (negative control), cells were harvested, RNA extracted and

processed to cDNA. Gene expression was determined by sq-RT-PCR normalised against the house keeping gene GAPDH.

Results from these experiments demonstrated that stimulation with media (negative control) produced low levels expression of these selected genes (no detectable expression of TNF-α) (*Figures 5.1, & 5.2*). *P. gingivalis* and *F. nucleatum* stimulation resulted in increased levels of gene expression at both 4 & 24h when compared to media controls. When comparing stimulation with *P. gingivalis* or *F. nucleatum*, it was noted that *F. nucleatum* stimulated higher levels of gene expression compared to *P. gingivalis* for all 4 genes investigated and at both time points. Gene expression changes for both *P. gingivalis* and *F. nucleatum* tended to be higher at 24h compared to 4h (however this was not the case for IL-8 in cells stimulated with *P. gingivalis* where relative expression dropped from 55.1% at 4h to 31.1% at 24h).

These data confirmed that gene expression changes could be seen in the stimulated H400 model system and that the 24h post stimulation time point generally produced greater changes in gene expression when compared to 4h. In view of the increased expression at 24h and the hypothesis that this time point better represented molecular changes occurring *in vivo* (i.e. interactions and feedback mechanisms seen in chronic disease), this time point was chosen for subsequent microarray analysis.

5.3 Microarray analysis of gene expression in stimulated H400 cells

Changes in gene expression in H400 cells grown to semi confluence and stimulated with non-viable *P. gingivalis, F. nucleatum* or media alone were determined using human U133A oligonucleotide arrays.

Prior to microarray analysis, the quality of RNA extracted from the stimulated cells was determined by using agarose gel electrophoresis (*Figure 5.3*). The gel showed 2 sharp 28s and 18s RNA bands with increased intensity at 28s (which should be

twice as intense as the 18s). This suggested intact RNA was present in all samples, as denatured RNA would lack the sharp 28s and 18s bands and show a low molecular weight smear. The latter would not be suitable for further processing. The quality and integrity of RNA was further confirmed by spectrophotometry utilizing the 260/280 ratio, all sample ratios were >1.8 indicating suitable RNA quality. RNA was then processed to fragmented labelled cRNA. The efficiency of fragmentation and target labelling was confirmed using gel electrophoresis (*Figure 5.4*), which revealed a bright band close to the end of the gel. The resulting labelled cRNA was initially hybridised onto Test3 GeneChips to confirm sample integrity and quality. Data from the test chips was within manufacturer's recommended parameters as outlined by Affymetrix. Thereafter, 15µg of cRNA was hybridised onto the U133 Affymetrix microarrays, stained and analysed.

5.4 Bioinformatic analysis of microarray data

Scanning of microarrays produced a vast quantity of gene expression data from the samples analysed. Analysis of this data is key to understanding the biological processes taking place at the genomic level, and is termed "bioinformatics". Data generated from this study was analysed using the software package DNA-Chip analyser (dChip). This allowed identification of differentially expressed genes between media (negative control) and *P. gingivalis* or *F. nucleatum* stimulated cells. Based on recommendations from the literature, (Seo et al., 2006) the criteria used to determine differentially expressed genes were that they demonstrated a 2-fold change in expression levels with an absolute difference of more than 100 units in levels of expression between samples on the control and test arrays. Additionally, the *P*-value threshold for statistical significance was set at 0.05, for between group means using a two-tailed test (two sample t-test)

By utilising the dChip package, lists of differentially expressed genes (both up-regulated & down-regulated) between test (*P. gingivalis* or *F. nucleatum*) and control (media) were generated (*Tables 5.1, 5.2, 5.3, 5.4, 5.5 & 5.6*). Analysis of

this data indicated that *P. gingivalis* and *F. nucleatum* stimulation resulted in differential expression of 409 and 609 genes respectively. Cells stimulated with *P. gingivalis* showed 170 genes up-regulated and 239 down-regulated. By comparison, stimulation with *F. nucleatum* produced 247 up-regulated and 362 down-regulated genes. To determine commonality between *F. nucleatum* and *P. gingivalis* differential gene regulation, data was analysed using a Microsoft Access database with the Affymetrix Probe ID as the primary key. This indicated that from a total of 1018 differentially expressed genes only 91 were common to both datasets, with 47 up-regulated and 44 down-regulated (*Figure 5.5*). Results demonstrated a number of genes that have been widely reported as important in immune/inflammatory responses in other epithelial based systems, however it also highlighted a number of other genes, so called novel genes, that have not previously been associated with periodontal disease. In order to represent this data in a biologically relevant format and to more thoroughly characterise sets of functionally related genes, the data was organised into gene ontological groupings by using the Onto-Express software package. This approach allowed the determination of biological processes that were up or down regulated following stimulation with periodontal pathogens. This data is summarised in *Figures 5.6, 5.7 & 5.8*.

Analysis of data and ontological grouping demonstrated that gene expression changes seen in this stimulated epithelial cell model were consistent with functions that may indicate a role of pocket epithelium in disease pathogenesis such as neutrophil chemotaxis, neutrophil activation and the inflammatory response. These findings lend support to the hypothesis that gingival epithelium may play a role in the initiation and orchestration of the exaggerated inflammatory response which characterises the periodontitis phenotype.

5.5 Confirmatory sq-RT-PCR to validate microarray results

The results obtained from microarray analysis were supported by the initial gene expression changes utilising sq-RT-PCR (*Figures 5.1 & 5.2*). However to further validate the microarray results, additional sq-RT-PCRs were performed for genes selected using the following criteria:-

- Previously not described as being induced in oral epithelial cells by periodontal pathogens or reported as being involved in periodontal disease pathogenesis
- Genes differentially expressed by either *P. gingivalis* or *F. nucleatum*
- Genes that may have a role in periodontal disease pathogenesis

Based upon these selection criteria, sq-RT-PCR was performed to determine levels of expression of genes coding for haemoxygenase (HMOX), lysyl oxidase (LOX), superoxide dismutase 2 (SOD2), chemokine (C-C motif) ligand 20 (CCL20), migration inhibitory factor related protein 8 (MRP8 / S100A8) and migration inhibitory factor related protein 14 (MRP14 / S100A9).

- *Haemoxygenase:* has a key role in cellular protection against injury caused by reactive oxygen species and oxidative stress and was differentially expressed in the microarray data (up-regulated by *P. gingivalis* +21.1 not differentially expressed by *F. nucleatum*)
- *Lysyl oxidase*: an extracellular enzyme that catalyses the cross-linking of collagen and elastin, essential for stabilization of collagen fibrils and for the integrity and elasticity of elastin. (down regulated by both *P. gingivalis* and *F. nucleatum*, -6.07 and -4.14 respectively)
- *Superoxide dismutase 2:* the mitochondrial superoxide dismutase which catalyzes the break down of superoxide into oxygen and hydrogen peroxide and therefore is an important antioxidant cellular defence mechanism. (up-regulated in *P. gingivalis* and *F. nucleatum*, +2.7 and +4.69 respectively)

- *Chemokine (C-C motif) ligand 20:* a chemotactic cytokine for lymphocytes and neutrophils, induced by lipopolysaccharide and TNF-α (up-regulated in *P. gingivalis* and *F. nucleatum*, +6.39 and +5.7 respectively)
- *Migration inhibitory factor related protein 8 (S100A8) & 14 (S100A9):* Members of the S100 protein family. Increased levels of this protein are seen in inflammatory lesions. Functionally they have antibacterial properties implicated in protection against invading bacteria. Reactive oxygen species (ROS) implicated in periodontal disease pathogenesis, induce production of Migration inhibitory factor related proteins (MRP) which has been reported to offer host cell protection to ROS. These genes have interesting properties in terms of periodontal disease pathogenesis and epithelial barrier function. MRP-8 was not differentially expressed in the microarray data on stimulation with *F. nucleatum* but with *P. gingivalis* showed reduced levels of expression (-4.15 fold change). MRP-14 was up-regulated by *F. nucleatum* (+2.49 fold change) but down regulated by *P. gingivalis* (-2.56 fold change)

5.5.1 Results

This section will present the results of analysis of individual genes by sq-RT-PCR (*Figure 5.9*) and compare with individual gene microarray data.

SOD-2 and CCL-20 gene expression showed the same trend for both RT-PCR and microarray analysis with both *P. gingivalis* and *F. nucleatum* stimulation increasing levels of gene expression. S100A8 and S100A9 showed a similar trend between these two techniques, with *F. nucleatum* stimulation causing increased gene expression. *P. gingivalis* reduced gene expression as tested by microarray analysis, and showed little difference over un-stimulated controls when utilising sq-RT-PCR. *Fusobacterium nucleatum* stimulation resulted in little change in HMOX gene expression when compared to controls for either technique, however stimulation with *P. gingivalis* did increase HMOX gene expression. In the case of LOX, high levels of un-stimulated gene expression were seen by both microarray and sq-RT-PCR techniques, stimulation with *P. gingivalis* or *F. nucleatum* resulted

in reductions in gene expression. These reductions were large for *P. gingivalis* and *F. nucleatum* (microarray analysis) and *P. gingivalis* (sq-RT-PCR), however when sq-RT-PCR was used to determine *F. nucleatum* stimulated gene expression this change was small.

In an attempt to compare the data obtained by these two techniques (RT-PCR & microarray), individual graphs were plotted for each gene which included data from both microarray and RT-PCR (*Figure 5.9*). Data from microarray analysis included negative values (indicating gene down regulation) and therefore all microarray gene data was normalised to the most negative value, which allowed a more meaningful graphical representation, facilitating identification of trends between methodologies. From these graphs, microarray analysis produced similar trends to the confirmatory PCR data. There were 2 results that contradicted the microarray results – (a) *F. nucleatum* stimulation on S100A8 (not differentially expressed in microarrays but increased expression in PCR analysis). (b) *P. gingivalis* stimulation on S100A9 (down-regulated in microarrays but up-regulated when assessed by PCR). There may be a number of reasons for this discrepancy which include different methods of RNA processing required for each technique, bioinformatic handling of data from microarray analysis, different levels of sensitivity between the two techniques and interference between RNA within the sample (Ach et al 2008). Apart from these 2 outlying results, microarray and PCR data showed close similarities in gene expression and increased confidence in the validity of the microarray results.

5.6 Conclusions

This chapter has demonstrated that stimulation of H400 cells with the periodontal pathogens *F. nucleatum* and *P. gingivalis* results in differential effects at a molecular level. Analysis of these gene expression changes allows increased understanding of the pathways induced by microbial stimulation and highlights potential mechanisms underpinning the pathogenesis of chronic periodontal disease. Examples of such mechanisms are the recruitment and activation of

immune system cells (e.g. IL-8, TNF-α, IL-1β and GM-CSF), and genes having an important role in cellular protection (e.g. HMOX, and S100A8/S100A9).

In addition to confirming a pro-inflammatory response microarray analysis allowed identification of a number of novel genes not previously described in periodontitis, and which may play an important role in disease pathogenesis, and are worthy of further investigation (e.g. S100A8/A9, LOX, HMOX, CCL-20, SOD-2).

The changes in gene regulation reported in this chapter do not tell the whole story in terms of cellular responses to stimulation; regulatory changes in gene expression are not always represented by protein production (e.g. cytokines) and ultimately responsible for immune/inflammatory effects. The following chapter aims to address this issue by investigating downstream stimulated cell cytokine production.

Chapter 6

The effects of α-lipoate on H400 gene expression & cytokine production

6.1 Introduction

Previous chapters have reported the ability of *F. nucleatum* and *P. gingivalis* to activate NF-κB within oral epithelial cells. A wide range of pro-inflammatory gene expression changes have also been demonstrated, a number of which have been reported as downstream to NF-κB activation. The most widely reported gene up-regulated post NF-κB activation is IL-8, which has been termed a 'surrogate marker' of NF-κB activation. Data from this thesis has indicated that on stimulation with *P. gingivalis* and *F. nucleatum* H400 cells demonstrated large increases in IL-8 gene expression at both 4 and 24h post stimulation. In addition a number of other key pro-inflammatory genes associated with NF-κB activation were up-regulated e.g. IL-1β, TNF-α, and GM-CSF. Immuno-cytochemical analysis has demonstrated the ability of α-lipoate to reduce NF-κB activation in H400 cells following stimulation with *P. gingivalis* and *F. nucleatum;* however the effect of α-lipoate on pro-inflammatory gene expression has yet to be determined. Thus the first part of this chapter reports upon studies that investigate the action of pre-incubation with α-lipoate on *P. gingivalis* and *F. nucleatum* stimulated H400 gene expression. The choice of genes for these experiments was based on those having a potential role in periodontal disease pathogenesis e.g. pro-inflammatory genes and genes involved in bacterial recognition (Toll-like receptors). In addition, novel genes detected by microarray analysis of stimulated H400 cells, which may have an as yet unreported role in periodontal disease pathogenesis were also included.

The second part of this chapter examines whether the gene expression changes detected are manifest at a protein level i.e. that they are potentially biologically relevant. These cytokines are produced downstream of cell stimulation and are bioactive end products which may have a role in periodontal disease pathogenesis. Results thus far have shown a variety of gene expression changes in H400 cells stimulated with *P. gingivalis* and *F. nucleatum*, however gene expression changes do not necessarily equate with cytokine production. Therefore this section will investigate post-stimulation cytokine production with or without α-lipoate pre-incubation. A range of cytokines known to be important in the

inflammatory response, and whose gene expression have previously been shown to be up-regulated were chosen for analysis i.e. IL-8, GM-CSF, TNF-α, & IL-1β.

6.2 Effect of α-lipoate on gene expression by sq RT-PCR

H400 cells were pre-incubated for 24h ± α-lipoate (0.5mM), and then stimulated with *P. gingivalis, F. nucleatum* or media (un-stimulated control) for a further 24h. RNA was extracted from the H400 cells and processed to cDNA then normalised to the house keeping gene GAPDH prior to sq RT-PCR.

Results from this series of experiments are grouped ontologically, based on the reported main function of each gene, as described below. Electrophoresis gel images of individual genes are shown in *Figure 6.1*

6.2.1 Pro-inflammatory genes

Interleukin 8, GM-CSF, TNF-α, and IL-1β *(Figure 6.2)* demonstrated increases in gene expression when stimulated with both *P. gingivalis* and *F. nucleatum* and compared to un-stimulated controls. The levels of gene expression were higher with *P. gingivalis* stimulation compared to *F. nucleatum* for these pro-inflammatory genes. Pre-incubation with α-lipoate prior to stimulation with *P. gingivalis* or *F. nucleatum* resulted in reduced levels of gene expression. However, reduced expression levels were still higher than those of un-stimulated controls, suggesting that α-lipoate did not completely block bacterial stimulation of these pro-inflammatory genes.

6.2.2 Bacterial recognition (Toll-like receptors)

Gene expression of TLR-2 and TLR-9 (*Figure 6.3*) in un-stimulated H400 cells was relatively high; in contrast to un-stimulated levels of TLR-4 which were low. Pre-incubation with α-lipoate without stimulation, resulted not change in TLR-2 gene expression, however significant increases in TLR-9 (increase of 51.3 to 85.7%) and TLR-4 (increase of 2.1 to 87.7%) expression. When cells were stimulated with *F. nucleatum* or *P. gingivalis* increased gene expression was noted for TLR-2 (increase from 87.2 to 100 or 92.9% respectively) and TLR-4 (increase from 2.1 to

29.6 or 61.0% respectively). By contrast *F. nucleatum* or *P. gingivalis* stimulation caused a reduction in TLR-9 expression (reduced from 51.3 to 44.5 or 25.0% respectively). Pre-incubation of H400 cells with α-lipoate prior to *F. nucleatum* or *P. gingivalis* stimulation resulted in a small reduction in gene expression for TLR-2, however in contrast a marked increase in expression was seen for TLR-4 (*F. nucleatum* from 29.6 to 93.6%; *P. gingivalis* from 61.0 to 82.1%) and TLR-9 (*F. nucleatum* from 44.5 to 100%; *P. gingivalis* from 25.0 to 74.0%). The increases in TLR-4 and 9 gene expression in both un-stimulated and periodontal pathogen stimulated cells pre-incubated with α-lipoate is a novel and interesting finding and suggests it's addition may increase the efficacy of cellular bacterial recognition.

6.2.3 Epithelial protection

Two members of the S100 protein family (Calprotectin – S100A8 & S100A9) were differentially expressed in previous experiments (*Section 5.4*). PCR analysis demonstrated high baseline (un-stimulated) gene expression levels of these proteins (*Figure 6.4*). *Fusobacterium nucleatum* stimulation caused increases in both S100A8 and S100A9 (both showing an approximate 30% increase over un-stimulated control). *Porphyromonas gingivalis* stimulation appeared to result in little difference from the baseline levels of gene expression. Pre-incubation with α-lipoate for both of these genes resulted in substantial reductions in gene expression for both un-stimulated and stimulated cells.

6.2.4 Antioxidant defence

Cellular antioxidant levels have a major impact on pro-inflammatory responses via NF-κB. Analyses were performed on two genes important in antioxidant defence (SOD-2 & HMOX) and differentially expressed in the microarray analysis (*Section 5.4*). SOD-2 *(Figure 6.5*) gene expression levels increased after stimulation with *P. gingivalis* and *F. nucleatum* when compared with un-stimulated controls (increase from 29.2 to 84.3 or 94.1% respectively). The addition of α-lipoate to un-stimulated cells resulted in a small increase in gene expression. The addition of α-lipoate to cells stimulated with *P. gingivalis* and *F. nucleatum* made little difference to levels

of SOD-2 gene expression, (*P. gingivalis* a small reduction and *F. nucleatum* a small increase). Baseline H400 cell HMOX gene expression in un-stimulated cells was relatively high *(Figure 6.5)*, and stimulation with *F. nucleatum* resulted in little change in expression. Stimulation with *P. gingivalis* resulted in increased gene expression when compared to un-stimulated controls. α-lipoate appeared to have little effect on un-stimulated cells, however, its effects on gene expression of stimulated cells were variable. Pre-incubation with α-lipoate reduced *P. gingivalis* stimulated gene expression (reduced from 100 to 63.3%), but increased (from 60.6 to 75.8%) *F. nucleatum* induced gene expression.

6.2.5 Tissue repair

From the microarray data, one of the genes that was strongly down-regulated following stimulation with both *P. gingivalis* (-6.9 fold) and *F. nucleatum* (-4.1 fold) that was the gene that codes for lysyl oxidase (LOX). The gene product has been shown to be a key enzyme in the biogenesis of connective tissues, acting via cross linking of collagen and elastin. This enzyme may therefore play a role in the formation and repair of the periodontal tissues. RT-PCR analysis revealed high levels of basal un-stimulated LOX gene expression (*Figure 6.6)*. Stimulation with *F. nucleatum* caused little effect on gene expression. By contrast stimulation with *P. gingivalis* resulted in a large reduction in expression, when compared to control levels (reduced from 100 to 20.2%). Similarly, pre-incubation of cells in α-lipoate resulted in a reduction in LOX gene expression (reduced from 100 to 15.1%). Pre-incubation of cells with α-lipoate prior to stimulation with *F. nucleatum* reduced levels of gene expression (from 94.2 to 34.3%). α-lipoate had little effect on the levels of LOX gene expression resulting from stimulation with *P. gingivalis*.

6.2.6 Other genes

The effects of periodontal pathogen stimulation, and pre-incubation with α-lipoate were determined for three other genes, NF-κB_1, CCL-2 & CCL-20.

6.2.6.1 CCL-2 & CCL-20

These chemokines both have chemo attractant properties for inflammatory cells. Stimulation with *P. gingivalis* and *F. nucleatum* resulted in increased expression for both of these genes. Pre-incubation with α-lipoate resulted in reduced gene expression of CCL-20 in both stimulated and un-stimulated cells. CCL-2 showed a similar trend for un-stimulated and *P. gingivalis* stimulated cells, however pre-incubation with α-lipoate and stimulation with *F. nucleatum* resulted in no differences *(Figure 6.7)*.

6.2.6.2 NF-κB$_1$

NF-κB$_1$ is a precursor protein of NF-κB subunit p50, and therefore has a key role in the maturation of NF-kB. Expression of this gene was high in un-stimulated cells, and these levels increased further on stimulation with *P. gingivalis* and *F. nucleatum*. Pre-incubation with α-lipoate resulted in a reduction in gene expression both in un-stimulated cells as well as *P. gingivalis* and *F. nucleatum* stimulated cells (*Figure 6.8*).

6.3 Pro-inflammatory cytokine production

6.3.1 ELISA cytokine analysis

Commercially available cytokine ELISA kits (*Section 2.9*) were used to determine supernatant (DMEM growth media) levels of IL-8, GM-CSF, TNF-α, & IL-1β. Growth media was removed, filtered and stored at -80^{o}C prior to analysis. Each sample was run in duplicate, with a range of standards included to produce a standard curve All standard curves were shown to exhibit straight line relationships (IL-8 R^2=0.986; TNF-α R^2=0.998; GM-CSF R^2=0.987 & IL-1β R^2=0.992).

6.3.1.1 Effect of P. gingivalis & F. nucleatum stimulation

Un-stimulated H400 cells produced low levels of IL-1β (5.61, 9.06 ρg/ml) and GM-CSF (17.06, 18.58 ρg/ml), compared to IL-8 (325.6, 309.33 ρg/ml). By contrast, basal levels of TNF-α were not detectable. Stimulation of H400 cells with *F.*

nucleatum caused increased levels of all of the tested cytokines when compared to un-stimulated controls (*Figure 6.9)*. In each case the levels seen were higher than those produced with *P. gingivalis.* Stimulation with *P .gingivalis* also resulted in increased levels of IL-8, GM-CSF & IL-1β over un-stimulated controls. However *P. gingivalis* failed to stimulate production of detectable levels of TNF-α.

6.3.1.2 Effect of α-lipoate pre-incubation

Pre-incubation of H400 cells with 0.5mM α-lipoate resulted in reductions in the levels of IL-8, GM-CSF and IL-1β, stimulated by *P. gingivalis* and *F. nucleatum*. In addition α-lipoate appeared to cause a small reduction in un-stimulated levels of cytokine production. In the case of TNF-α, pre-incubation with α-lipoate reduced levels of the *F. nucleatum* stimulated cytokine. In all cases, the reduced cytokine production elicited by α-lipoate did not completely remove the cellular response, as levels were still greater than those produced by un-stimulated cells. Thus, α-lipoate reduced but did not stop *P. gingivalis* and *F. nucleatum* stimulating cytokine production by H400 cells

6.4 Conclusions

This chapter aimed to investigate the effect of α-lipoate on the H400 model system in terms of changes in gene expression and cytokine production. Data from these experiments demonstrated the ability of *F. nucleatum* & *P. gingivalis* to produce changes in gene expression as well as enhanced production of a range of key pro-inflammatory cytokines. H400 cell pre-incubation with α-lipoate demonstrated a range of variable effects including reduction of key pro-inflammatory gene expression levels and cytokine production in stimulated cells.

Interestingly, when comparing gene expression changes in IL8, TNF-α, GM-CSF and IL1-β with cytokine production, differences were evident. The trend is for higher gene expression levels post *P. gingivalis* stimulation compared to *F .nucleatum*, however the reverse is true when assessing cytokine production levels. These differences may be due to gene expression changes not being represented in protein production (gene expression changes don't necessarily

equate to protein production), assessment at a single time point (24h) different result may be evident if a longer time course was investigated, the two bacteria may activate other cell processes causing feedback mechanisms preventing or down regulating protein production. Both PCR and cytokine production of these cytokines in stimulated H400 cells is reduced when pre-incubated with α-lipoate.

The effect of α-lipoate on TLR receptors is of interest with a slight reduction in gene expression of TLR-2, but increases in expression of TLR-4 & 9, and may suggest that α-lipoate increases levels of TLR 4 & 9, therefore increasing the ability of the cells to detect periodontal pathogens. Interestingly, when α-lipoate pre-incubation has reduced periodontal pathogen stimulated effects on epithelial cells it does not return to un-stimulated levels. This finding may be of considerable significance, as complete blocking of this key first line epithelial defence response to bacterial challenge may render the host susceptible to infection. Rather α-lipoate appears to modulate the stimulated response, therefore having potential in modulating the hyper-inflammatory response seen in periodontitis.

CHAPTER 7

Concluding discussion

7.1 Introduction

This thesis proposed a biological role for crevicular/pocket epithelium in periodontal disease pathogenesis. The results obtained are now discussed with specific reference to those that underpin this proposal (*Figure 7.1*) including novel findings that may augment our current understanding of periodontal disease pathogenesis. In addition, modulation of this process with a novel antioxidant dithiol, α-lipoate is discussed.

7.2 Epithelial cell activation

Individual stages in epithelial cell activation are discussed in terms of NF-κB activation (*Figure 7.1: label 1*), induction of gene expression changes (*Figure 7.1: label 2*) and cytokine production (*Figure 7.1: label 3*). Data from this thesis demonstrating the activation of H400 epithelial cells for each of these stages is presented.

7.2.1 Bacterial recognition / Toll-like receptor expression.

Toll-like receptors (TLR) are important pattern recognition receptors which are present on cell surfaces and have the ability to recognise bacterial components. Once stimulated these receptors cause cell activation via a range of pathways including NF-κB (Zhang and Ghosh, 2001). Gene expressions of three Toll-like receptors were investigated in this thesis (TLR-2, 4 and 9; *Results section 6.2.2*). Baseline expression of these receptors in un-stimulated H400 cells appeared to vary, however all were identified as being expressed. Stimulation with *P. gingivalis* or *F. nucleatum* resulted in a relatively large increase in expression of TLR-4 (small increase in TLR-2), and a decrease in TLR-9 expression. Increased expression of TLR-4 by microbial stimulation, and specifically Gram negative bacterial lipopolysaccaride (LPS), may be due to autocrine feedback mechanisms in response to TLR activation by *P. gingivalis* and *F. nucleatum*. This increased TLR-4 gene expression (which may translate to increased surface receptor expression) may enhance epithelial responses to LPS. Moreover as bacterial clearance from cells may also be regulated by this receptor (Song et al., 2009),

elevated levels of TLR-4 may also contribute *in vivo* to cellular sensitivity to facilitate removal of intracellular pathogens such as *P. gingivalis*.

The data presented in this thesis suggest a difference in levels of TLR-4 activation between *P. gingivalis* and *F. nucleatum*, with *F. nucleatum* stimulating lower levels of gene expression when compared to *P. gingivalis.* Potentially, this difference could confer an advantage to *F. nucleatum in vivo*, as reduced TLR-4 expression may facilitate evasion of detection by the host's immune system (Wolfe et al., 2009).

Interestingly, a recent study has reported that *P. gingivalis* interacts with TLR-2 (more commonly associated with Gram positive bacteria, viruses and yeasts) to stimulate epithelial cells rather than via TLR-4, the classic Gram negative LPS receptor (Kocgozlu et al., 2009). The increased expression of the TLR-2 gene in H400 cells stimulated by *P. gingivalis*, perhaps indicates that this organism has the ability to up-regulate pro-inflammatory responses of epithelial cells to itself and other bacteria within the subgingival biofilm. Such a property would support the role of this "red-complex" organism (Socransky, 1970) and crevicular/pocket epithelium in the aetiology and pathogenesis of periodontitis. Whilst it is important to remember that gene expression data may not be reflected in changes in levels of cellular TLRs, the data does suggest that two organisms present in the subgingival biofilm are associated with periodontitis have the potential to increase epithelial responses to bacteria, viruses and yeasts by modulating expression of these important cell receptors.

7.2.2 NF-κB activation

Initial experiments using a 'gold standard' NF-κB activator [*E.coli* LPS; (Prince et al., 2004)] demonstrated nuclear translocation of NF-κB in the H400 cell model system. Additionally, immunocytochemistry (individual slide and high-throughput data) demonstrated the ability of both *F. nucleatum* and *P. gingivalis* to activate NF-κB as indicated by nuclear translocation (*Results section 3.3*). *Porphyromonas*

gingivalis and *F. nucleatum* stimulated maximal nuclear translocation of NF-κB at 60-90 mins post stimulation, which was in agreement with time course data obtained using *E. coli* LPS stimulation. Thus, periodontal bacteria clearly have the ability to activate the epithelial NF-κB pathway, which has a central role in promoting expression of pro-inflammatory genes (Silverman and Maniatis, 2001). This step is likely to be crucial for subsequent synthesis and secretion of the epithelial-derived cytokines necessary to initiate and/or propagate a local inflammatory response within the periodontal tissues.

Assessment of the temporal differences in NF-κB activation between the periodontal pathogens appeared to indicate that *P. gingivalis* caused maximal activation of NF-κB at a marginally earlier time-point, and at a higher level of induction compared with *F. nucleatum*. In addition, activation by *F. nucleatum* also appeared more prolonged (*Results section 3.4.3*). These findings may have important implications for disease pathogenesis as they could indicate that *P. gingivalis* initiates epithelial cell activation and downstream pro-inflammatory responses, whereas subsequent *F. nucleatum* stimulation prolongs this response. This data suggests that these two bacteria, as part of the plaque biofilm, may synergistically activate the epithelium thereby contributing to the exaggerated inflammatory response observed in periodontitis patients. Time course experiments demonstrated that activated NF-κB returned to levels comparable with those of un-stimulated cells 4h post stimulation. The reduction in NF-κB activation at this time point, occurred in the presence of chronic bacterial exposure, which notably mimics the situation present within the periodontal pocket. These findings pose further important questions which include i) does NF-κB require further stimulation to become re-activated?, or ii) is a time lag necessary to allow the biological system to recycle itself prior to further NF-κB reactivation? As the data indicate that there is a time period when NF-κB is not reactivated despite the stimulant still being present, the length of this ‘refractory’ period may be of considerable importance in chronic inflammatory diseases. Hypothetically it may be that this period is reduced in patients with periodontal disease, leading to

increased frequency of NF-kB activation which may therefore contribute to chronic hyper-inflammation. Review of the literature currently demonstrates little research into this phenomenon, and this therefore represents an important area for future study.

7.2.3 Gene expression analyses

NF-κB nuclear translocation and subsequent promoter binding results in gene expression which in turn leads to the production of proteins, especially pro-inflammatory cytokines, implicated in the inflammatory and immune responses.

7.2.3.1 Pro-inflammatory cytokine gene expression

Initial sq-RT-PCR confirmed that stimulation of H400 cells with either *P. gingivalis* or *F. nucleatum* for 4 and 24h caused up-regulation of key pro-inflammatory genes (including IL-1β, TNF-α, IL-8 and GM-CSF), with the largest changes seen at 24h. Further microarray analysis confirmed these findings and demonstrated that the majority of up-regulated genes were associated with immune/inflammatory and chemotaxis responses (*Results section 5.4*). The stimulated up-regulation of pro-inflammatory genes demonstrated both with sq-RT-PCR and microarray analysis, fits well with the hypothesis that the epithelial lining of gingival crevice/pocket can mount and regulate a pro-inflammatory response following interaction with bacteria within the subgingival plaque biofilm.

Analysis of microarray data for the two periodontal bacteria examined identified relatively few differentially expressed genes common to both organisms (91 up- and down-regulated), and the majority of differentially regulated genes were specific to either *P. gingivalis* or *F. nucleatum*. Ontological grouping of the commonly up-regulated genes demonstrated a predominance of transcripts involved in regulating inflammatory functions including cell proliferation, cell signalling, protein metabolism, signal transduction and apoptosis (*Figure 7.2*). Further investigation of this dataset may provide a better understanding of the epithelium's molecular response to the complex bacterial challenge induced by

biofilm exposure, rather than individual organisms. However investigation of genes that are specific to either *P. gingivalis* or *F. nucleatum* epithelial stimulation may also provide a better understanding of the role of specific bacteria in periodontal disease pathogenesis.

It may be hypothesised that a balanced non-pathogenic plaque biofilm may induce a relatively low level of epithelial inflammation, enabling the existence of homeostasis between the host and biofilm. However if certain key periodontal pathogens dominate (e.g. *P. gingivalis* or *F. nucleatum*) then the gene transcriptional changes associated with these bacteria could predominate causing an elevated pro-inflammatory response, along with other changes that could effect healing of the periodontal lesion and of epithelial barrier function. Further study of the molecular interactions between the epithelium and single bacteria or complex biofilms would help to determine the validity of this hypothesis and its relevance to periodontal disease pathogenesis.

7.2.3.2 Potential importance of other genes identified in periodontitis

Microarray analysis also identified genes (*Results section 5.4*) which may play a role in the pathogenesis of periodontitis that are part of the specific disease model under investigation (*Figure 7.2*). Haemoxygenase (HMOX) was up-regulated by *P. gingivalis* but not *F. nucleatum,* and notably this molecule has been implicated in cellular protection against reactive oxygen species (Hisada et al., 2000) which are now considered important in the pathogenesis of periodontitis (Chapple and Matthews, 2007). In addition, increased HMOX production has been reported to decrease TNF-α induced inflammation via reduction in NF-κB activation in airway smooth muscle cells (Lee et al., 2009). The differential expression of the HMOX gene between these two organisms may be of particular interest. Whilst *P. gingivalis* increased HMOX gene expression, suggesting that it may induce anti-inflammatory pathways activated via HMOX, in contrast *F. nucleatum* stimulation did not increase HMOX gene expression. These data indicate that *P. gingivalis* may have the capacity to modulate the pro-inflammatory response and thereby

evade host defence mechanisms, thus aiding it's colonisation of the periodontal tissues.

Superoxide dismutase (SOD) is a key enzyme important in antioxidant defence (Sasaki et al., 2000), and was up-regulated in H400 cells stimulated with *P. gingivalis* and *F. nucleatum*. Recent reports indicate elevated SOD levels can reduce levels of IL-8 production in stimulated cells (Mulligan et al., 2009). This effect may be due to its antioxidant action influencing the intracellular REDOX status and acting via the REDOX sensitive transcription factors such as NF-κB. Notably reduced levels of SOD have recently been reported in patients with chronic periodontitis (Akalin et al., 2009, Akalin et al., 2008). These studies compared SOD levels in GCF, serum and gingival biopsy samples, with results indicating a statistically significant difference in levels between chronic periodontitis patients and healthy controls. The reduced levels seen in periodontitis patients may indicate compromised host antioxidant defence mechanisms in chronic periodontitis. Combined data indicate that it is therefore possible that SOD activity may play an important role in epithelial cell defence as well as periodontal disease pathogenesis.

The Lysyl oxidase (LOX) gene, which encodes an enzyme important in collagen maturation (Rodriguez et al., 2008), exhibited decreased epithelial cell expression following exposure to *P. gingivalis* and *F. nucleatum.*. The finding that both bacteria down-regulated its expression may be of importance in periodontitis, as maturation of collagen is important in the wound healing and tissue repair processes (Lau et al., 2006). Whilst it is acknowledged that collagen is mainly produced by fibroblasts and is a key component of the submucosa (Grinnell, 2008) reduction in LOX levels by the epithelium may impact deleteriously on the supporting periodontal tissues. Moreover whilst LOX expression was examined here in epithelial cells it is known that fibroblasts express TLR-2 and -4 (Hirao et al., 2009) and therefore it is logical to speculate that periodontal infection may also lead to reductions in fibroblast LOX levels. Combined, the data suggest that

reductions in the production of tissue derived LOX, due to periodontal pathogen infection, may lead to a frustrated healing response and contribute to the pathogenesis of periodontitis.

Chemokine ligand 20 (CCL20) is an important cytokine implicated in neutrophil and lymphocyte trafficking and recent research has highlighted its role in T(H)17 cell chemotaxis. This newly characterised T(H) cell contributes to host defence via its actions on extracellular bacteria (Louten et al., 2009). T(H)17 encompasses a subset of T-helper cells, producing a range of cytokines, two of the most interesting being interleukin 17, which orchestrates pro-inflammatory responses (Miossec et al., 2009), and interleukin 22, which acts via epithelial cells to produce anti-microbial peptides (Aujla and Kolls, 2009). These proteins are important in microbial immunity at epithelial/mucosal barriers, with reduced levels implicated in opportunist infections (Pitta et al., 2009). As both *P. gingivalis* and *F. nucleatum* up-regulated CCL20 gene expression in H400 cells, it is possible that crevicular/pocket epithelium may play an important role in mediating local host defences to the subgingival bacterial biofilm via T(H)17 cells.

The genes for Migration inhibitory factors 8 and 14 (MRP-8/-14 also known as S100A8 and S100A9 respectively) encode multifunctional proteins which form heterodimers with antibacterial properties and which have been implicated in host defence against invasive bacteria (Nisapakultorn et al., 2001) . In addition they have been implicated in neutrophil recruitment and activation and therefore behave in a pro-inflammatory manner (Foell et al., 2008). Whilst periodontal pathogen stimulation did not appear to give rise to differential expression for MRP-8, increased gene expression of MRP-14 following *F. nucleatum* stimulation was detected, although *P. gingivalis* reduced gene expression levels. As has previously been discussed for HMOX the reduced gene expression of MRP-14 by *P. gingivalis* afford this bacterium protection from the innate immune system by its modulation of the inflammatory response.

As the role of several of the genes identified by microarray analysis and discussed above have not been studied in periodontitis pathogenesis, further studies on these molecules with respect to periodontitis are warranted.

7.2.4 Cytokine production

Whilst activation of NF-κB and regulation of gene expression have been demonstrated in stimulated H400 cells, these changes do not necessarily translate to downstream protein production. Subsequently, therefore, levels of cytokines important in the inflammatory response (eg. TNF-α, GM-CSF, IL-8, and IL-1β) were investigated in cell culture supernatants. Stimulation with *P. gingivalis* and *F. nucleatum* resulted in increased production of these cytokines when compared to unstimulated controls. Stimulation with *F. nucleatum* generated higher levels of cytokines compared with *P. gingivalis*, and this data might indicate that *F. nucleatum in vivo* stimulates elevated levels of inflammation. It is therefore logical to interpret this finding in several ways, which include i) *F. nucleatum* is more important in promoting the inflammatory response which could result in more efficient bacterial killing, or ii) *P. gingivalis* may be able to modulate the host's inflammatory response to enable evasion and further unchecked infection. *Fusobacterium nucleatum* has the ability to adhere to a wide range of plaque bacteria and acts as a bridge between early and late colonizers (Uitto et al., 2005). Therefore *F. nucleatum* may have a central role in the transition between health and disease (Krisanaprakornkit et al., 2000).

These data demonstrate the ability of oral epithelial cells to produce pro-inflammatory cytokines on stimulation with periodontal pathogens, these key proteins have a central role in innate immunity, and their production lends support to the hypothesis that epithelia initiate and orchestrate the local inflammatory response to colonising bacteria.

7.2.5 Summary

Data presented in this thesis has shown that the periodontal pathogens *P. gingivalis* and *F. nucleatum* can stimulate key stages in epithelial cell activation (*Figure 7.1, labels 1,2 & 3*), i.e. NF-κB translocation, gene expression changes and cytokine production. This suggests that stimulated crevicular/pocket epithelium plays a role in the initiation and propagation of periodontal inflammation, thus supporting the proposed hypothesis.

7.3 Action of α-lipoate on epithelial cell activation

Our current understanding of periodontal disease pathogenesis suggests that in susceptible individuals the exaggerated inflammatory response causes the tissue damage seen in periodontitis; with 80% being host mediated and only 20% directly attributable to bacteria (Grossi et al., 1994). Initial results have demonstrated the ability of periodontal pathogens to stimulate oral epithelium to mount a pro-inflammatory response. The second stage was to investigate a method of "dampening down" this inflammatory response as a potential novel therapeutic strategy in periodontitis patients where an exaggerated host inflammatory response underpins disease. NF-κB is a REDOX sensitive transcription factor activated by changes in intracellular REDOX status, so a natural dithiol antioxidant, α-lipoate, which boosts intracellular antioxidant levels was chosen in an attempt to modulate NF-κB activation. As Toll like receptor activation is key to NF-κB activation and subsequent pro-inflammatory gene expression, initial experiments were performed to determine whether α-lipoate affected expression of these receptors, prior to investigating effects on gene expression and cytokine production.

7.3.1 Bacterial recognition / Toll-like receptor gene expression

Three key Toll-like receptors were investigated by sq-RT-PCR. Pre-incubation of H400 cells with α-lipoate generated a small reduction in TLR-2 gene expression and large increases in expression of TLR-4 and TLR-9 transcripts. These changes, detected in un-stimulated, *P. gingivalis* and *F. nucleatum* stimulated cells, if

translated into cellular TLR protein expression, suggests that α-lipoate may have the ability to increase cellular sensitivity to bacterial challenge, or indeed increase the pro-inflammatory response. Potentially, this may not be beneficial to the periodontally susceptible host where excess inflammation may result in local tissue damage.

7.3.2. NF-κB activation

Immunocytochemical analysis of H400 cells pre-incubated with α-lipoate and stimulated with *E. coli* LPS, *P. gingivalis* or *F. nucleatum* showed reduced levels of NF-κB activation when compared to controls (no α-lipoate). This is a key finding suggesting that irrespective of changes induced in the TLR transcriptome α-lipoate is able to reduce periodontal pathogen induced activation of this important pro-inflammatory transcription factor. As previously described, NF-κB is REDOX sensitive, so a potential mechanism by which α-lipoate reduces NF-κB activation is via changes in intracellular antioxidant levels. The literature reports the ability of α-lipoate to increase levels of reduced glutathione (GSH) a key intra-cellular thiol antioxidant (Sen et al., 1997), therefore as NF-κB is activated by oxidative stress, it seems plausible that α-lipoate, reduces intra-cellular oxidative stress by boosting intracellular GSH levels thereby reducing NF-κB activation. Indeed α-lipoate has been shown to reduce levels of NF-κB activation in a range of cell types (Packer et al., 1995) (Zhang and Frei, 2001). A recent paper demonstrated the ability of α-lipoate to down-regulate NF-κB activation, and boost antioxidant levels in lung tissue in septic shock (Cadirci et al., 2009).

7.3.3 Gene expression

As discussed earlier periodontal pathogen stimulation demonstrated a range of gene transcription changes, this section therefore discusses how pre-incubation with α-lipoate effects gene expression

7.3.3.1 Pro-inflammatory gene expression

Pre-incubation with α-lipoate resulted in a reduction in stimulated transcript levels of pro-inflammatory genes IL-8, GM-CSF, IL-1β and TNF-α. These genes possess a range of functions important in the initiation and propagation of the inflammatory response and clearly, if extrapolated to cytokine production, indicate that α-lipoate is able to reduce the pro-inflammatory response of epithelium to periodontal pathogens.

Chemokine ligand 2 (CCL-2) and 20 (CCL-20) genes were down-regulated by *P. gingivalis* and *F. nucleatum* stimulation when pre-incubated with α-lipoate, the exception being CCL-2 in *F. nucleatum* stimulated cells which showed little change. The down-regulation seen with α-lipoate, if this indeed does equate to reduced production of cytokines, would result in an anti-inflammatory response.

7.3.3.2 Potential importance of other genes identified in periodontitis

The effect of α-lipoate pre-incubation on gene expression for the antioxidant enzymes, superoxide dismutase (SOD) and haemoxygenase (HO) were investigated. Results revealed little change in terms of un-stimulated levels of these two genes. Stimulated levels showed little change for SOD, a small increase in levels for *F. nucleatum* stimulated HO, with α-lipoate causing a reduction in *P. gingivalis* stimulated levels (HO). These results are somewhat difficult to interpret and whether α-lipoate has beneficial or detrimental effects on expression of these genes remains unclear.

As previously discussed, lysyl oxidase is an important enzyme in collagen maturation, pre-incubation of cells with α-lipoate led to reduced gene expression in both stimulated and un-stimulated cells. Stimulation with *P. gingivalis* or *F. nucleatum* caused reduced gene expression and this reduction was further enhanced by α-lipoate. Stimulation by these pathogens and and/or pre-incubation with α-lipoate could prevent collagen maturation and thus frustrate healing within the periodontal tissues leading to promotion of a chronic inflammatory lesion. It

would appear that α-lipoate may not be beneficial in this regard. Recent research has suggested that excess production of lysyl oxidase may be an important factor, and prognostic indicator, in oral squamous cell carcinoma (Albinger-Hegyi et al., 2009). To date the role of lysyl oxidase in periodontal disease pathogenesis remains unclear and further investigation into this role is warranted.

Two genes important in cellular protection, neutrophil recruitment and activation are MRP-8 (S100A8) and MRP-14 (S100A9). α-lipoate pre-incubation reduced both stimulated and un-stimulated expression levels of these genes. These reductions may reduce cellular protection to bacterial challenge, which may not be beneficial to host defence, however in terms of reduced chemotaxis this may result in reduced inflammatory response. In addition a recent publication suggests that combined increased expression of these two genes is implicated in ROS mediated transcription pathway activation (Nemeth et al., 2009) which, along with reduced neutrophil recruitment, and activation may suggest that α-lipoate may be beneficial in reducing the hyper-inflammatory response associated with tissue damage.

7.3.3.3 NF-κB

Gene expression was investigated for NF-κB$_1$ (p50) a component of the NF-κB complex. Results indicated high un-stimulated levels of expression in H400 cells. Stimulation with *P. gingivalis* or *F. nucleatum* resulted in increased expression of this gene, whereas pre-incubation with α-lipoate caused reduced expression in both stimulated and un-stimulated cells. These reductions in expression may equate to reduced cellular levels of NF-κB levels potentially diminishing cellular activation and the downstream pro-inflammatory response. Interestingly, the reductions in stimulated levels of NF-κB$_1$ with α-lipoate, did not completely block transcription of this gene, but reduced it to un-stimulated levels. This is potentially of importance as complete blocking of the cells pro-inflammatory response may lead the host exposed to bacterial challenge.

7.3.4 Cytokine production

The effect of pre-incubation of H400 cells with α-lipoate prior to stimulation with *F. nucleatum* or *P. gingivalis* was to reduce subsequent production of levels of the cytokines investigated (IL-1β, GM-CSF, and IL-8; this was also the case for *F. nucleatum* stimulated TNF-α production, but *P. gingivalis* stimulation was below the levels of detection). Interestingly, the reductions seen with α-lipoate did not return levels to those of un-stimulated cells. This finding may be due to α-lipoate changing the intracellular REDOX potential of the cell either directly due to its antioxidant properties, or indirectly via boosting the key intracellular antioxidant glutathione. Boosting antioxidants will reduce intracellular oxidative stress resulting in reduced phosphorylation of IκK, subsequent activation of NF-κB and downstream cytokine production.

7.3.5 Summary

Pre-incubation with α-lipoate induced a number of cellular changes in H400 cells in terms of NF-κB activation, gene expression and cytokine production. Taken as a whole the results show a reduction in pro-inflammation post stimulation with periodontal pathogens *P. gingivalis* and *F. nucleatum,* however α-lipoate does not completely block pro-inflammatory cascades. This has important ramifications biologically, as the aim of any new anti-inflammatory therapeutic agent is to reduce exaggerated levels of inflammation seen in patients with periodontitis, rather than completely inhibiting the inflammatory response. The epithelial response to bacteria is an important first line of defence against bacterial invasion and complete blocking may render the host susceptible to bacterial colonisation, virulence expression and indeed invasion.

7.4 Future work

The data presented in this thesis suggests a role for epithelium in peridodontal disease pathogenesis, however further study is required to firstly underpin and better understand the mechanisms of activation in epithelia, and secondly

determine the efficacy of inflammatory modulation in disease management. In order to address these questions it is proposed that three key areas of research will be explored in future work:-

7.4.1 Explant epithelium

Current experimentation has focused on an immortal H400 gingival epithelial cell line, how this relates to the *in vivo* situation would be of considerable interest and would allow further validation of this model system. Additionally comparisons of epithelium from patients with chronic periodontitis and comparison with healthy controls may demonstrate differences in epithelial response to bacterial challenge thereby predisposing patients to disease.

7.4.2 Other transcription factor pathways

This thesis focused on the REDOX sensitive transcription factor NF-κB which is thought to be the key pro-inflammatory transcription factor responsible for cell activation; however other transcription factors have been described which are pro and anti-inflammatory. Investigation of such pathways may result in a better understanding of the mechanisms of bacterial cell activation, and offer further therapeutic targets to modulated the exaggerated inflammatory response. Two other pathways have been identified and worthy of investigation:

7.4.2.1 Nrf-2: (NE-F2 related factor)

This is also a REDOX sensitive transcription factor, and regulates the cell antioxidant response to oxidative stress. This response involves two major REDOX system regulators i.e. glutathione & thioredoxin, these systems acts to dampen down the cellular pro-inflammatory response.

7.4.2.2 AP-1 (activator protein 1)

As with NF-κB this transcription factor orchestrates the expression of a range of genes involved in inflammation, as well as a number of other functions. Although activation of NF-κB and AP-1 are via different mechanisms, it appears that they are activated by similar stimuli. The literature suggests that some genes are only differentially expressed when both these transcription factors are activated.

7.4.3 Clinical trials

Research over the last few years has demonstrated the hyper-inflammatory nature of periodontitis and how this can cause collateral tissue damage and its importance in disease pathogenesis. Results obtained in this thesis suggest α-lipoate may be able to modulate this hyper-inflammatory response. Randomised controlled clinical trials would aim to determine the efficacy of α-lipoate in managing chronic periodontitis.

7.5 Concluding remarks

This thesis reports the development of a model system to investigate the potential role of periodontal / sulcar epithelium in the initiation and propagation of the exaggerated inflammatory/immune response seen in periodontitis. The data generated clearly show that the epithelial lining of the sulcus/pocket, which accumulates subgingival plaque, is capable of mounting a pro-inflammatory response to the bacterial biofilm and therefore could play a crucial role in the initiation and propagation of the hyper inflammation seen in periodontitis patients. α-lipoate has the ability to modulate this pro-inflammatory response, but importantly, does not completely block this key defence process. Treatment of periodontal disease has changed little over the last 50 years, with management focusing on reducing the bacterial load and thereby reducing tissue damage caused by the exaggerated inflammatory response seen in periodontitis patients. As our understanding of this fascinating and complex disease grows, opportunities will arise to modulate this exaggerated response. The findings of this thesis

suggest the potential for developing new, locally applied anti-inflammatory therapies for managing periodontitis.

References

Aas, J.A., Paster, B.J., Stokes, L.N., et al. (2005) Defining the normal bacterial flora of the oral cavity. **J Clin Microbiol***,* 43: (11): 5721-5732.

Adler, V., Yin, Z., Tew, K.D., et al. (1999) Role of redox potential and reactive oxygen species in stress signaling. **Oncogene***,* 18: (45): 6104-6111.

Aggarwal, B.B., Banerjee, S., Bharadwaj, U., et al. (2007) Curcumin induces the degradation of cyclin E expression through ubiquitin-dependent pathway and up-regulates cyclin-dependent kinase inhibitors p21 and p27 in multiple human tumor cell lines. **Biochem Pharmacol***,* 73: (7): 1024-1032.

Aisenberg, M.S. (1952) Histology and physiology of the supporting structures. **J Am Dent Assoc***,* 44: (6): 628-632.

Akalin, F.A., Baltacioglu, E., Alver, A., et al. (2009) Total antioxidant capacity and superoxide dismutase activity levels in serum and gingival crevicular fluid in pregnant women with chronic periodontitis. **J Periodontol***,* 80: (3): 457-467.

Akalin, F.A., Isiksal, E., Baltacioglu, E., et al. (2008) Superoxide dismutase activity in gingiva in type-2 diabetes mellitus patients with chronic periodontitis. **Arch Oral Biol***,* 53: (1): 44-52.

Albinger-Hegyi, A., Stoeckli, S.J., Schmid, S., et al. (2009) Lysyl oxidase expression is an independent marker of prognosis and a predictor of lymph node metastasis in oral and oropharyngeal squamous cell carcinoma (OSCC). **Int J Cancer**.

Alexander, M.B. and Damoulis, P.D. (1994) The role of cytokines in the pathogenesis of periodontal disease. **Curr Opin Periodontol***,* 39-53.

Ambili, R., Santhi, W.S., Janam, P., et al. (2005) Expression of activated transcription factor nuclear factor-kappaB in periodontally diseased tissues. **J Periodontol***,* 76: (7): 1148-1153.

Arivazhagan, P., Thilakavathy, T. and Panneerselvam, C. (2000) Antioxidant lipoate and tissue antioxidants in aged rats. **J Nutr Biochem***,* 11: (3): 122-127.

Armitage, G.C. (1999) Development of a classification system for periodontal diseases and conditions. **Ann Periodontol***,* 4: (1): 1-6.

Aujla, S.J. and Kolls, J.K. (2009) IL-22: a critical mediator in mucosal host defense. **J Mol Med***,* 87: (5): 451-454.

Bales, K.R., Du, Y., Dodel, R.C., et al. (1998) The NF-kappaB/Rel family of proteins mediates Abeta-induced neurotoxicity and glial activation. **Brain Res Mol Brain Res**, 57: (1): 63-72.

Banerjee, A. and Gerondakis, S. (2007) Coordinating TLR-activated signaling pathways in cells of the immune system. **Immunol Cell Biol**, 85: (6): 420-424.

Barnes, P.J. (1997) Nuclear factor-kappa B. **Int J Biochem Cell Biol**, 29: (6): 867-870.

Barnes, P.J. and Karin, M. (1997) Nuclear factor-kappaB: a pivotal transcription factor in chronic inflammatory diseases. **N Engl J Med**, 336: (15): 1066-1071.

Battino, M., Bullon, P., Wilson, M., et al. (1999) Oxidative injury and inflammatory periodontal diseases: the challenge of anti-oxidants to free radicals and reactive oxygen species. **Crit Rev Oral Biol Med**, 10: (4): 458-476.

Bertolini, D.R., Nedwin, G.E., Bringman, T.S., et al. (1986) Stimulation of bone resorption and inhibition of bone formation in vitro by human tumour necrosis factors. **Nature**, 319: (6053): 516-518.

Bickel, M. (1993) The role of interleukin-8 in inflammation and mechanisms of regulation. **J Periodontol**, 64: (5 Suppl): 456-460.

Blackwell, T.S., Blackwell, T.R., Holden, E.P., et al. (1996) In vivo antioxidant treatment suppresses nuclear factor-kappa B activation and neutrophilic lung inflammation. **J Immunol**, 157: (4): 1630-1637.

Bodet, C., Chandad, F. and Grenier, D. (2005) Modulation of cytokine production by Porphyromonas gingivalis in a macrophage and epithelial cell co-culture model. **Microbes Infect**, 7: (3): 448-456.

Brock, G.R., Butterworth, C.J., Matthews, J.B., et al. (2004) Local and systemic total antioxidant capacity in periodontitis and health. **J Clin Periodontol**, 31: (7): 515-521.

Bubici, C., Papa, S., Dean, K., et al. (2006) Mutual cross-talk between reactive oxygen species and nuclear factor-kappa B: molecular basis and biological significance. **Oncogene**, 25: (51): 6731-6748.

Burt, B.A. (2005) Concepts of risk in dental public health. **Community Dent Oral Epidemiol**, 33: (4): 240-247.

Busse, E., Zimmer, G., Schopohl, B., et al. (1992) Influence of alpha-lipoic acid on intracellular glutathione in vitro and in vivo. **Arzneimittelforschung**, 42: (6): 829-831.

Cadirci, E., Altunkaynak, B.Z., Halici, Z., et al. (2009) Alpha-lipoic acid as a potential target for the treatment of lung injury caused by cecal ligation and puncture-induced sepsis model in rats. **Shock**.

Canakci, C.F., Cicek, Y. and Canakci, V. (2005) Reactive oxygen species and human inflammatory periodontal diseases. **Biochemistry (Mosc)***,* 70: (6): 619-628.

Castro, A.C., Dang, L.C., Soucy, F., et al. (2003) Novel IKK inhibitors: beta-carbolines. **Bioorg Med Chem Lett***,* 13: (14): 2419-2422.

Chapple, I.L. (1997) Reactive oxygen species and antioxidants in inflammatory diseases. **J Clin Periodontol***,* 24: (5): 287-296.

Chapple, I.L., Brock, G., Eftimiadi, C., et al. (2002) Glutathione in gingival crevicular fluid and its relation to local antioxidant capacity in periodontal health and disease. **Mol Pathol***,* 55: (6): 367-373.

Chapple, I.L., Brock, G.R., Milward, M.R., et al. (2007a) Compromised GCF total antioxidant capacity in periodontitis: cause or effect? **J Clin Periodontol***,* 34: (2): 103-110.

Chapple, I.L. and Matthews, J.B. (2007) The role of reactive oxygen and antioxidant species in periodontal tissue destruction. **Periodontol 2000***,* 43: 160-232.

Chapple, I.L., Milward, M.R. and Dietrich, T. (2007b) The prevalence of inflammatory periodontitis is negatively associated with serum antioxidant concentrations. **J Nutr***,* 137: (3): 657-664.

Chaudhary, L.R., Spelsberg, T.C. and Riggs, B.L. (1992) Production of various cytokines by normal human osteoblast-like cells in response to interleukin-1 beta and tumor necrosis factor-alpha: lack of regulation by 17 beta-estradiol. **Endocrinology***,* 130: (5): 2528-2534.

Chen, F.E. and Ghosh, G. (1999) Regulation of DNA binding by Rel/NF-kappaB transcription factors: structural views. **Oncogene***,* 18: (49): 6845-6852.

Claffey, N., Kelly, A., Bergquist, J., et al. (1996) Patterns of attachment loss in advanced periodontitis patients monitored following initial periodontal treatment. **J Clin Periodontol***,* 23: (6): 523-531.

Clerehugh, V., Lennon, M.A. and Worthington, H.V. (1990) 5-year results of a longitudinal study of early periodontitis in 14- to 19-year-old adolescents. **J Clin Periodontol***,* 17: (10): 702-708.

Clerehugh, V., Worthington, H.V., Lennon, M.A., et al. (1995) Site progression of loss of attachment over 5 years in 14- to 19-year-old adolescents. **J Clin Periodontol***,* 22: (1): 15-21.

Corradi, L., Fato, M., Porro, I., et al. (2008) A Web-based and Grid-enabled dChip version for the analysis of large sets of gene expression data. **BMC Bioinformatics***,* 9: 480.

D'Aiuto, F., Parkar, M. and Tonetti, M.S. (2005) Periodontal therapy: a novel acute inflammatory model. **Inflamm Res***,* 54: (10): 412-414.

Dale, B.A. (2002) Periodontal epithelium: a newly recognized role in health and disease. **Periodontol 2000***,* 30: 70-78.

Dinarello, C.A. (1997) Interleukin-1. **Cytokine Growth Factor Rev***,* 8: (4): 253-265.

Dresen, I.M., Husing, J., Kruse, E., et al. (2003) Software packages for quantitative microarray-based gene expression analysis. **Curr Pharm Biotechnol***,* 4: (6): 417-437.

Duncan, M.J., Nakao, S., Skobe, Z., et al. (1993) Interactions of Porphyromonas gingivalis with epithelial cells. **Infect Immun***,* 61: (5): 2260-2265.

Eaves-Pyles, T., Szabo, C. and Salzman, A.L. (1999) Bacterial invasion is not required for activation of NF-kappaB in enterocytes. **Infect Immun***,* 67: (2): 800-804.

Eick, S., Reissmann, A., Rodel, J., et al. (2006) Porphyromonas gingivalis survives within KB cells and modulates inflammatory response. **Oral Microbiol Immunol***,* 21: (4): 231-237.

Elias, J.A., Gustilo, K., Baeder, W., et al. (1987) Synergistic stimulation of fibroblast prostaglandin production by recombinant interleukin 1 and tumor necrosis factor. **J Immunol***,* 138: (11): 3812-3816.

Ellis, S.D., Tucci, M.A., Serio, F.G., et al. (1998) Factors for progression of periodontal diseases. **J Oral Pathol Med***,* 27: (3): 101-105.

Fan, W., Pritchard, J.I., Olson, J.M., et al. (2005) A class of models for analyzing GeneChip gene expression analysis array data. **BMC Genomics***,* 6: (1): 16.

Figueredo, C.M., Fischer, R.G. and Gustafsson, A. (2005) Aberrant neutrophil reactions in periodontitis. **J Periodontol***,* 76: (6): 951-955.

Finkel, T. and Holbrook, N.J. (2000) Oxidants, oxidative stress and the biology of ageing. **Nature***,* 408: (6809): 239-247.

Foell, D., Wittkowski, H., Ren, Z., et al. (2008) Phagocyte-specific S100 proteins are released from affected mucosa and promote immune responses during inflammatory bowel disease. **J Pathol***,* 216: (2): 183-192.

Fowler, E.B., Breault, L.G. and Cuenin, M.F. (2001) Periodontal disease and its association with systemic disease. **Mil Med***,* 166: (1): 85-89.

Fredriksson, M., Gustafsson, A., Asman, B., et al. (1998) Hyper-reactive peripheral neutrophils in adult periodontitis: generation of chemiluminescence and intracellular hydrogen peroxide after in vitro priming and FcgammaR-stimulation. **J Clin Periodontol***,* 25: (5): 394-398.

Fredriksson, M.I., Gustafsson, A.K., Bergstrom, K.G., et al. (2003) Constitutionally hyperreactive neutrophils in periodontitis. **J Periodontol***,* 74: (2): 219-224.

Garlet, G.P., Cardoso, C.R., Silva, T.A., et al. (2006) Cytokine pattern determines the progression of experimental periodontal disease induced by Actinobacillus actinomycetemcomitans through the modulation of MMPs, RANKL, and their physiological inhibitors. **Oral Microbiol Immunol***,* 21: (1): 12-20.

Gilmore, T.D. and Herscovitch, M. (2006) Inhibitors of NF-kappaB signaling: 785 and counting. **Oncogene***,* 25: (51): 6887-6899.

Gloire, G., Legrand-Poels, S. and Piette, J. (2006) NF-kappaB activation by reactive oxygen species: fifteen years later. **Biochem Pharmacol***,* 72: (11): 1493-1505.

Goodson, J.M., Tanner, A.C., Haffajee, A.D., et al. (1982) Patterns of progression and regression of advanced destructive periodontal disease. **J Clin Periodontol***,* 9: (6): 472-481.

Gos, M., Miloszewska, J., Swoboda, P., et al. (2005) Cellular quiescence induced by contact inhibition or serum withdrawal in C3H10T1/2 cells. **Cell Prolif***,* 38: (2): 107-116.

Grinnell, F. (2008) Fibroblast mechanics in three-dimensional collagen matrices. **J Bodyw Mov Ther***,* 12: (3): 191-193.

Grossi, S.G., Zambon, J.J., Ho, A.W., et al. (1994) Assessment of risk for periodontal disease. I. Risk indicators for attachment loss. **J Periodontol***,* 65: (3): 260-267.

Gustafsson, A., Ito, H., Asman, B., et al. (2006) Hyper-reactive mononuclear cells and neutrophils in chronic periodontitis. **J Clin Periodontol***,* 33: (2): 126-129.

Haddad, J.J., Olver, R.E. and Land, S.C. (2000) Antioxidant/pro-oxidant equilibrium regulates HIF-1alpha and NF-kappa B redox sensitivity. Evidence for inhibition by glutathione oxidation in alveolar epithelial cells. **J Biol Chem***,* 275: (28): 21130-21139.

Haffajee, A.D., Socransky, S.S. and Goodson, J.M. (1983) Comparison of different data analyses for detecting changes in attachment level. **J Clin Periodontol***,* 10: (3): 298-310.

Halliwell, B., Gutteridge, J.M. and Cross, C.E. (1992) Free radicals, antioxidants, and human disease: where are we now? **J Lab Clin Med***,* 119: (6): 598-620.
Han, D., Handelman, G., Marcocci, L., et al. (1997) Lipoic acid increases de novo synthesis of cellular glutathione by improving cystine utilization. **Biofactors***,* 6: (3): 321-338.

Han, Y.W., Shi, W., Huang, G.T., et al. (2000) Interactions between periodontal bacteria and human oral epithelial cells: Fusobacterium nucleatum adheres to and invades epithelial cells. **Infect Immun***,* 68: (6): 3140-3146.

Handelman, G.J., Han, D., Tritschler, H., et al. (1994) Alpha-lipoic acid reduction by mammalian cells to the dithiol form, and release into the culture medium. **Biochem Pharmacol***,* 47: (10): 1725-1730.

Hayden, M.S. and Ghosh, S. (2004) Signaling to NF-kappaB. **Genes Dev***,* 18: (18): 2195-2224.

Hazuda, D.J., Lee, J.C. and Young, P.R. (1988) The kinetics of interleukin 1 secretion from activated monocytes. Differences between interleukin 1 alpha and interleukin 1 beta. **J Biol Chem***,* 263: (17): 8473-8479.

Hess, J., Angel, P. and Schorpp-Kistner, M. (2004) AP-1 subunits: quarrel and harmony among siblings. **J Cell Sci***,* 117: (Pt 25): 5965-5973.

Hirao, K., Yumoto, H., Takahashi, K., et al. (2009) Roles of TLR2, TLR4, NOD2, and NOD1 in pulp fibroblasts. **J Dent Res***,* 88: (8): 762-767.

Hisada, T., Salmon, M., Nasuhara, Y., et al. (2000) Involvement of haemoxygenase-1 in ozone-induced airway inflammation and hyperresponsiveness. **Eur J Pharmacol***,* 399: (2-3): 229-234.

Ismail, A.I., Burt, B.A. and Eklund, S.A. (1983) Relation between ascorbic acid intake and periodontal disease in the United States. **J Am Dent Assoc***,* 107: (6): 927-931.

Isogai, H., Isogai, E., Yoshimura, F., et al. (1988) Specific inhibition of adherence of an oral strain of Bacteroides gingivalis 381 to epithelial cells by monoclonal antibodies against the bacterial fimbriae. **Arch Oral Biol***,* 33: (7): 479-485.

Jacob, R.A., Omaye, S.T., Skala, J.H., et al. (1987) Experimental vitamin C depletion and supplementation in young men. Nutrient interactions and dental health effects. **Ann N Y Acad Sci***,* 498: 333-346.

Jeffcoat, M.K. and Reddy, M.S. (1991) Progression of probing attachment loss in adult periodontitis. **J Periodontol***,* 62: (3): 185-189.

Jiang, H., Weyrich, A.S., Zimmerman, G.A., et al. (2004) Endothelial cell confluence regulates cyclooxygenase-2 and prostaglandin E2 production that modulate motility. **J Biol Chem***,* 279: (53): 55905-55913.

Jocelyn, P.C. (1967) The standard redox potential of cysteine-cystine from the thiol-disulphide exchange reaction with glutathione and lipoic acid. **Eur J Biochem***,* 2: (3): 327-331.

Johnson, R.A., Boyce, B.F., Mundy, G.R., et al. (1989) Tumors producing human tumor necrosis factor induced hypercalcemia and osteoclastic bone resorption in nude mice. **Endocrinology***,* 124: (3): 1424-1427.

Khanna, S., Atalay, M., Laaksonen, D.E., et al. (1999) Alpha-lipoic acid supplementation: tissue glutathione homeostasis at rest and after exercise. **J Appl Physiol***,* 86: (4): 1191-1196.

Khodarev, N.N., Sokolova, I.A. and Vaughan, A.T. (1998) Mechanisms of induction of apoptotic DNA fragmentation. **Int J Radiat Biol***,* 73: (5): 455-467.

Knutsen, S.F., Fraser, G.E., Linsted, K.D., et al. (2001) Comparing biological measurements of vitamin C, folate, alpha-tocopherol and carotene with 24-hour dietary recall information in nonhispanic blacks and whites. **Ann Epidemiol***,* 11: (6): 406-416.

Ko, K.S., Arora, P.D., Bhide, V., et al. (2001) Cell-cell adhesion in human fibroblasts requires calcium signaling. **J Cell Sci***,* 114: (Pt 6): 1155-1167.

Kocgozlu, L., Elkaim, R., Tenenbaum, H., et al. (2009) Variable cell responses to P. gingivalis lipopolysaccharide. **J Dent Res***,* 88: (8): 741-745.

Konstan, M.W. and Berger, M. (1997) Current understanding of the inflammatory process in cystic fibrosis: onset and etiology. **Pediatr Pulmonol***,* 24: (2): 137-142; discussion 159-161.

Kou, Y., Inaba, H., Kato, T., et al. (2008) Inflammatory responses of gingival epithelial cells stimulated with Porphyromonas gingivalis vesicles are inhibited by hop-associated polyphenols. **J Periodontol***,* 79: (1): 174-180.

Krisanaprakornkit, S., Kimball, J.R., Weinberg, A., et al. (2000) Inducible expression of human beta-defensin 2 by Fusobacterium nucleatum in oral epithelial cells: multiple signaling pathways and role of commensal bacteria in innate immunity and the epithelial barrier. **Infect Immun***,* 68: (5): 2907-2915.

Kupatt, C., Wichels, R., Deiss, M., et al. (2002) Retroinfusion of NFkappaB decoy oligonucleotide extends cardioprotection achieved by CD18 inhibition in a preclinical study of myocardial ischemia and retroinfusion in pigs. **Gene Ther***,* 9: (8): 518-526.

Lamont, R.J. and Jenkinson, H.F. (1998) Life below the gum line: pathogenic mechanisms of Porphyromonas gingivalis. **Microbiol Mol Biol Rev***,* 62: (4): 1244-1263.

Lau, Y.K., Gobin, A.M. and West, J.L. (2006) Overexpression of lysyl oxidase to increase matrix crosslinking and improve tissue strength in dermal wound healing. **Ann Biomed Eng***,* 34: (8): 1239-1246.

Lee, I.T., Luo, S.F., Lee, C.W., et al. (2009) Overexpression of HO-1 protects against TNF-alpha-mediated airway inflammation by down-regulation of TNFR1-dependent oxidative stress. **Am J Pathol***,* 175: (2): 519-532.

Leggott, P.J., Robertson, P.B., Jacob, R.A., et al. (1991) Effects of ascorbic acid depletion and supplementation on periodontal health and subgingival microflora in humans. **J Dent Res***,* 70: (12): 1531-1536.

Loe, H., Anerud, A., Boysen, H., et al. (1986) Natural history of periodontal disease in man. Rapid, moderate and no loss of attachment in Sri Lankan laborers 14 to 46 years of age. **J Clin Periodontol***,* 13: (5): 431-445.

Loe, H., Anerud, A., Boysen, H., et al. (1978) The natural history of periodontal disease in man. The rate of periodontal destruction before 40 years of age. **J Periodontol***,* 49: (12): 607-620.

Loe, H., Theilade, E. and Jensen, S.B. (1965) Experimental Gingivitis In Man. **J Periodontol***,* 36: 177-187.

Loos, B.G., Craandijk, J., Hoek, F.J., et al. (2000) Elevation of systemic markers related to cardiovascular diseases in the peripheral blood of periodontitis patients. **J Periodontol***,* 71: (10): 1528-1534.

Louten, J., Boniface, K. and de Waal Malefyt, R. (2009) Development and function of TH17 cells in health and disease. **J Allergy Clin Immunol***,* 123: (5): 1004-1011.

Lundqvist, C., Baranov, V., Teglund, S., et al. (1994) Cytokine profile and ultrastructure of intraepithelial gamma delta T cells in chronically inflamed human gingiva suggest a cytotoxic effector function. **J Immunol***,* 153: (5): 2302-2312.

Lyakhovich, V.V., Vavilin, V.A., Zenkov, N.K., et al. (2006) Active defense under oxidative stress. The antioxidant responsive element. **Biochemistry (Mosc)***,* 71: (9): 962-974.

Makarov, S.S. (2000) NF-kappaB as a therapeutic target in chronic inflammation: recent advances. **Mol Med Today***,* 6: (11): 441-448.

Manna, S.K., Kuo, M.T. and Aggarwal, B.B. (1999) Overexpression of gamma-glutamylcysteine synthetase suppresses tumor necrosis factor-induced apoptosis and activation of nuclear transcription factor-kappa B and activator protein-1. **Oncogene***,* 18: (30): 4371-4382.

Manna, S.K., Zhang, H.J., Yan, T., et al. (1998) Overexpression of manganese superoxide dismutase suppresses tumor necrosis factor-induced apoptosis and activation of nuclear transcription factor-kappaB and activated protein-1. **J Biol Chem***,* 273: (21): 13245-13254.

Marangon, K., Devaraj, S., Tirosh, O., et al. (1999) Comparison of the effect of alpha-lipoic acid and alpha-tocopherol supplementation on measures of oxidative stress. **Free Radic Biol Med***,* 27: (9-10): 1114-1121.

Marsh, P.D. (1991) Sugar, fluoride, pH and microbial homeostasis in dental plaque. **Proc Finn Dent Soc***,* 87: (4): 515-525.

Marsh, P.D. (1994) Microbial ecology of dental plaque and its significance in health and disease. **Adv Dent Res***,* 8: (2): 263-271.

Matsugo, S., Konishi, T., Matsuo, D., et al. (1996) Reevaluation of superoxide scavenging activity of dihydrolipoic acid and its analogues by chemiluminescent method using 2-methyl-6-[p-methoxyphenyl]-3,7-dihydroimidazo-[1,2-a]pyrazine-3-one (MCLA) as a superoxide probe. **Biochem Biophys Res Commun***,* 227: (1): 216-220.

Matthews, J.B., Wright, H.J., Roberts, A., et al. (2007a) Hyperactivity and reactivity of peripheral blood neutrophils in chronic periodontitis. **Clin Exp Immunol***,* 147: (2): 255-264.

Matthews, J.B., Wright, H.J., Roberts, A., et al. (2007b) Neutrophil hyper-responsiveness in periodontitis. **J Dent Res***,* 86: (8): 718-722.

May, M.J., D'Acquisto, F., Madge, L.A., et al. (2000) Selective inhibition of NF-kappaB activation by a peptide that blocks the interaction of NEMO with the IkappaB kinase complex. **Science**, 289: (5484): 1550-1554.

May, M.J. and Ghosh, S. (1997) Rel/NF-kappa B and I kappa B proteins: an overview. **Semin Cancer Biol**, 8: (2): 63-73.

Meikle, M.C., Atkinson, S.J., Ward, R.V., et al. (1989) Gingival fibroblasts degrade type I collagen films when stimulated with tumor necrosis factor and interleukin 1: evidence that breakdown is mediated by metalloproteinases. **J Periodontal Res**, 24: (3): 207-213.

Midaoui, A.E., Elimadi, A., Wu, L., et al. (2003) Lipoic acid prevents hypertension, hyperglycemia, and the increase in heart mitochondrial superoxide production. **Am J Hypertens**, 16: (3): 173-179.

Milward, M.R., Chapple, I.L., Wright, H.J., et al. (2007) Differential activation of NF-kappaB and gene expression in oral epithelial cells by periodontal pathogens. **Clin Exp Immunol**, 148: (2): 307-324.

Miossec, P., Korn, T. and Kuchroo, V.K. (2009) Interleukin-17 and type 17 helper T cells. **N Engl J Med**, 361: (9): 888-898.

Mizel, S.B. (1989) The interleukins. **Faseb J**, 3: (12): 2379-2388.
Moini, H., Tirosh, O., Park, Y.C., et al. (2002) R-alpha-lipoic acid action on cell redox status, the insulin receptor, and glucose uptake in 3T3-L1 adipocytes. **Arch Biochem Biophys**, 397: (2): 384-391.

Morini, M., Roccatagliata, L., Dell'Eva, R., et al. (2004) Alpha-lipoic acid is effective in prevention and treatment of experimental autoimmune encephalomyelitis. **J Neuroimmunol**, 148: (1-2): 146-153.

Morris, A.J., Steele, J. and White, D.A. (2001) The oral cleanliness and periodontal health of UK adults in 1998. **Br Dent J**, 191: (4): 186-192.

Moscatelli, D., Presta, M., Joseph-Silverstein, J., et al. (1986) Both normal and tumor cells produce basic fibroblast growth factor. **J Cell Physiol**, 129: (2): 273-276.

Mulligan, R.M., Atkinson, C., Vertegel, A.A., et al. (2009) Cigarette smoke extract stimulates interleukin-8 production in human airway epithelium and is attenuated by superoxide dismutase in vitro. **Am J Rhinol Allergy**.

Mundy, G.R. (1989) Local factors in bone remodeling. **Recent Prog Horm Res**, 45: 507-527; discussion 527-531.

Na, H.K. and Surh, Y.J. (2006) Intracellular signaling network as a prime chemopreventive target of (-)-epigallocatechin gallate. **Mol Nutr Food Res***,* 50: (2): 152-159.

Nemeth, J., Stein, I., Haag, D., et al. (2009) S100A8 and S100A9 are novel nuclear factor kappa B target genes during malignant progression of murine and human liver carcinogenesis. **Hepatology***,* 50: (4): 1251-1262.

Nisapakultorn, K., Ross, K.F. and Herzberg, M.C. (2001) Calprotectin expression in vitro by oral epithelial cells confers resistance to infection by Porphyromonas gingivalis. **Infect Immun***,* 69: (7): 4242-4247.

Nishida, M., Grossi, S.G., Dunford, R.G., et al. (2000) Dietary vitamin C and the risk for periodontal disease. **J Periodontol***,* 71: (8): 1215-1223.

Okada, H. and Murakami, S. (1998) Cytokine expression in periodontal health and disease. **Crit Rev Oral Biol Med***,* 9: (3): 248-266.

Okada, H., Murakami, S., Kitamura, M., et al. (1996) Diagnostic strategies of periodontitis based on the molecular mechanisms of periodontal tissue destruction. **Oral Dis***,* 2: (1): 87-95.

Opal, S.M., Girard, T.D. and Ely, E.W. (2005) The immunopathogenesis of sepsis in elderly patients. **Clin Infect Dis***,* 41 Suppl 7: S504-512.

Orban, B. (1952) Histology and physiology of the gingiva. **J Am Dent Assoc***,* 44: (6): 624-628.

Ordronneau, P., Lindstrom, P.B. and Petrusz, P. (1981) Four unlabeled antibody bridge techniques: a comparison. **J Histochem Cytochem***,* 29: (12): 1397-1404.

Ou, P., Tritschler, H.J. and Wolff, S.P. (1995) Thioctic (lipoic) acid: a therapeutic metal-chelating antioxidant? **Biochem Pharmacol***,* 50: (1): 123-126.

Packer, L., Kraemer, K. and Rimbach, G. (2001) Molecular aspects of lipoic acid in the prevention of diabetes complications. **Nutrition***,* 17: (10): 888-895.

Packer, L. and Suzuki, Y.J. (1993) Vitamin E and alpha-lipoate: role in antioxidant recycling and activation of the NF-kappa B transcription factor. **Mol Aspects Med***,* 14: (3): 229-239.

Packer, L., Witt, E.H. and Tritschler, H.J. (1995) alpha-Lipoic acid as a biological antioxidant. **Free Radic Biol Med***,* 19: (2): 227-250.

Page, R.C. and Kornman, K.S. (1997) The pathogenesis of human periodontitis: an introduction. **Periodontol 2000***,* 14: 9-11.

Page, R.C. and Schroeder, H.E. (1976) Pathogenesis of inflammatory periodontal disease. A summary of current work. **Lab Invest***,* 34: (3): 235-249.

Palmer, R.M., Wilson, R.F., Hasan, A.S., et al. (2005) Mechanisms of action of environmental factors--tobacco smoking. **J Clin Periodontol***,* 32 Suppl 6: 180-195.

Panjamurthy, K., Manoharan, S. and Ramachandran, C.R. (2005) Lipid peroxidation and antioxidant status in patients with periodontitis. **Cell Mol Biol Lett***,* 10: (2): 255-264.

Papapanou, P.N., Wennstrom, J.L. and Johnsson, T. (1991) Extent and Severity Index based on assessments of radiographic bone loss. **Community Dent Oral Epidemiol***,* 19: (6): 313-317.

Pease, J.E. and Sabroe, I. (2002) The role of interleukin-8 and its receptors in inflammatory lung disease: implications for therapy. **Am J Respir Med***,* 1: (1): 19-25.

Perkins, N.D. (2007) Integrating cell-signalling pathways with NF-kappaB and IKK function. **Nat Rev Mol Cell Biol***,* 8: (1): 49-62.

Pfeilschifter, J., Chenu, C., Bird, A., et al. (1989) Interleukin-1 and tumor necrosis factor stimulate the formation of human osteoclastlike cells in vitro. **J Bone Miner Res***,* 4: (1): 113-118.

Pitta, M.G., Romano, A., Cabantous, S., et al. (2009) IL-17 and IL-22 are associated with protection against human kala azar caused by Leishmania donovani. **J Clin Invest***,* 119: (8): 2379-2387.

Prime, S.S., Nixon, S.V., Crane, I.J., et al. (1990) The behaviour of human oral squamous cell carcinoma in cell culture. **J Pathol***,* 160: (3): 259-269.

Prince, L.S., Okoh, V.O., Moninger, T.O., et al. (2004) Lipopolysaccharide increases alveolar type II cell number in fetal mouse lungs through Toll-like receptor 4 and NF-kappaB. **Am J Physiol Lung Cell Mol Physiol***,* 287: (5): L999-1006.

Rangasamy, T., Cho, C.Y., Thimmulappa, R.K., et al. (2004) Genetic ablation of Nrf2 enhances susceptibility to cigarette smoke-induced emphysema in mice. **J Clin Invest***,* 114: (9): 1248-1259.

Reed, L.J. (1957) The chemistry and function of lipoic acid. **Adv Enzymol Relat Subj Biochem***,* 18: 319-347.

Rodriguez, C., Rodriguez-Sinovas, A. and Martinez-Gonzalez, J. (2008) Lysyl oxidase as a potential therapeutic target. **Drug News Perspect***,* 21: (4): 218-224.

Roebuck, K.A. (1999) Regulation of interleukin-8 gene expression. **J Interferon Cytokine Res***,* 19: (5): 429-438.

Sandros, J., Karlsson, C., Lappin, D.F., et al. (2000) Cytokine responses of oral epithelial cells to Porphyromonas gingivalis infection. **J Dent Res***,* 79: (10): 1808-1814.

Sasaki, H., Akamatsu, H. and Horio, T. (2000) Protective role of copper, zinc superoxide dismutase against UVB-induced injury of the human keratinocyte cell line HaCaT. **J Invest Dermatol***,* 114: (3): 502-507.

Schmid, E., Hotz-Wagenblatt, A., Hacj, V., et al. (1999) Phosphorylation of the insulin receptor kinase by phosphocreatine in combination with hydrogen peroxide: the structural basis of redox priming. **Faseb J***,* 13: (12): 1491-1500.

Schmidt, J.A., Mizel, S.B., Cohen, D., et al. (1982) Interleukin 1, a potential regulator of fibroblast proliferation. **J Immunol***,* 128: (5): 2177-2182.

Schmidt, U., Grafen, P., Altland, K., et al. (1969) Biochemistry and chemistry of lipoic acids. **Adv Enzymol Relat Areas Mol Biol***,* 32: 423-469.

Schoonbroodt, S. and Piette, J. (2000) Oxidative stress interference with the nuclear factor-kappa B activation pathways. **Biochem Pharmacol***,* 60: (8): 1075-1083.

Schulze-Osthoff, K., Beyaert, R., Vandevoorde, V., et al. (1993) Depletion of the mitochondrial electron transport abrogates the cytotoxic and gene-inductive effects of TNF. **Embo J***,* 12: (8): 3095-3104.

Sen, C.K., Roy, S., Han, D., et al. (1997) Regulation of cellular thiols in human lymphocytes by alpha-lipoic acid: a flow cytometric analysis. **Free Radic Biol Med***,* 22: (7): 1241-1257.

Seo, J., Gordish-Dressman, H. and Hoffman, E.P. (2006) An interactive power analysis tool for microarray hypothesis testing and generation. **Bioinformatics***,* 22: (7): 808-814.

Seymour, G.J., Ford, P.J., Cullinan, M.P., et al. (2007) Relationship between periodontal infections and systemic disease. **Clin Microbiol Infect***,* 13 Suppl 4: 3-10.

Sfakianakis, A., Barr, C.E. and Kreutzer, D.L. (2002) Localization of the chemokine interleukin-8 and interleukin-8 receptors in human gingiva and cultured gingival keratinocytes. **J Periodontal Res***,* 37: (2): 154-160.

Silverman, N. and Maniatis, T. (2001) NF-kappaB signaling pathways in mammalian and insect innate immunity. **Genes Dev***,* 15: (18): 2321-2342.

Skerka, C., Irving, S.G., Bialonski, A., et al. (1993) Cell type specific expression of members of the IL-8/NAP-1 gene family. **Cytokine***,* 5: (2): 112-116.

Slade, E.W., Jr., Bartuska, D., Rose, L.F., et al. (1976) Vitamin E and periodontal disease. **J Periodontol***,* 47: (6): 352-354.

Socransky, S.S. (1970) Relationship of bacteria to the etiology of periodontal disease. **J Dent Res***,* 49: (2): 203-222.

Socransky, S.S., Haffajee, A.D., Goodson, J.M., et al. (1984) New concepts of destructive periodontal disease. **J Clin Periodontol***,* 11: (1): 21-32.

Song, J., Bishop, B.L., Li, G., et al. (2009) TLR4-mediated expulsion of bacteria from infected bladder epithelial cells. **Proc Natl Acad Sci U S A***,* 106: (35): 14966-14971.

Stashenko, P., Dewhirst, F.E., Rooney, M.L., et al. (1987) Interleukin-1 beta is a potent inhibitor of bone formation in vitro. **J Bone Miner Res***,* 2: (6): 559-565.

Sugano, N., Kawamoto, K., Numazaki, H., et al. (2000) Detection of mitochondrial DNA mutations in human gingival tissues. **J Oral Sci***,* 42: (4): 221-223.

Suh, J.H., Shigeno, E.T., Morrow, J.D., et al. (2001) Oxidative stress in the aging rat heart is reversed by dietary supplementation with (R)-(alpha)-lipoic acid. **Faseb J***,* 15: (3): 700-706.

Swinney, D.C., Xu, Y.Z., Scarafia, L.E., et al. (2002) A small molecule ubiquitination inhibitor blocks NF-kappa B-dependent cytokine expression in cells and rats. **J Biol Chem***,* 277: (26): 23573-23581.

Takane, M., Sugano, N., Iwasaki, H., et al. (2002) New biomarker evidence of oxidative DNA damage in whole saliva from clinically healthy and periodontally diseased individuals. **J Periodontol***,* 73: (5): 551-554.

Takaoka, M., Kobayashi, Y., Yuba, M., et al. (2001) Effects of alpha-lipoic acid on deoxycorticosterone acetate-salt-induced hypertension in rats. **Eur J Pharmacol***,* 424: (2): 121-129.

ten Cate, J.M. (2006) Biofilms, a new approach to the microbiology of dental plaque. **Odontology***,* 94: (1): 1-9.

Tomita, N., Ogihara, T. and Morishita, R. (2003) Transcription factors as molecular targets: molecular mechanisms of decoy ODN and their design. **Curr Drug Targets**, 4: (8): 603-608.

Tonetti, M.S. and Claffey, N. (2005) Advances in the progression of periodontitis and proposal of definitions of a periodontitis case and disease progression for use in risk factor research. Group C consensus report of the 5th European Workshop in Periodontology. **J Clin Periodontol**, 32 Suppl 6: 210-213.

Tonetti, M.S., Imboden, M.A. and Lang, N.P. (1998) Neutrophil migration into the gingival sulcus is associated with transepithelial gradients of interleukin-8 and ICAM-1. **J Periodontol**, 69: (10): 1139-1147.

Torgerson, T.R., Colosia, A.D., Donahue, J.P., et al. (1998) Regulation of NF-kappa B, AP-1, NFAT, and STAT1 nuclear import in T lymphocytes by noninvasive delivery of peptide carrying the nuclear localization sequence of NF-kappa B p50. **J Immunol**, 161: (11): 6084-6092.

Uitto, V.J., Baillie, D., Wu, Q., et al. (2005) Fusobacterium nucleatum increases collagenase 3 production and migration of epithelial cells. **Infect Immun**, 73: (2): 1171-1179.

Vaahtoniemi, L.H., Raisanen, S. and Stenfors, L.E. (1993) Attachment of bacteria to oral epithelial cells in vivo: a possible correlation to gingival health status. **J Periodontal Res**, 28: (4): 308-311.

van der Pluijm, G., Most, W., van der Wee-Pals, L., et al. (1991) Two distinct effects of recombinant human tumor necrosis factor-alpha on osteoclast development and subsequent resorption of mineralized matrix. **Endocrinology**, 129: (3): 1596-1604.

Van Dyke, T.E., Lester, M.A. and Shapira, L. (1993) The role of the host response in periodontal disease progression: implications for future treatment strategies. **J Periodontol**, 64: (8 Suppl): 792-806.

Van Dyke, T.E. and Serhan, C.N. (2003) Resolution of inflammation: a new paradigm for the pathogenesis of periodontal diseases. **J Dent Res**, 82: (2): 82-90.

Van Noorden, S., Stuart, M.C., Cheung, A., et al. (1986) Localization of human pituitary hormones by multiple immunoenzyme staining procedures using monoclonal and polyclonal antibodies. **J Histochem Cytochem**, 34: (3): 287-292.

Vasdev, S., Ford, C.A., Parai, S., et al. (2000) Dietary lipoic acid supplementation prevents fructose-induced hypertension in rats. **Nutr Metab Cardiovasc Dis**, 10: (6): 339-346.

Weinberg, A., Belton, C.M., Park, Y., et al. (1997) Role of fimbriae in Porphyromonas gingivalis invasion of gingival epithelial cells. **Infect Immun***,* 65: (1): 313-316.

Wolfe, D.N., Buboltz, A.M. and Harvill, E.T. (2009) Inefficient Toll-like receptor-4 stimulation enables Bordetella parapertussis to avoid host immunity. **PLoS One***,* 4: (1): e4280.

Yaworsky, K., Somwar, R., Ramlal, T., et al. (2000) Engagement of the insulin-sensitive pathway in the stimulation of glucose transport by alpha-lipoic acid in 3T3-L1 adipocytes. **Diabetologia***,* 43: (3): 294-303.

Yilmaz, O., Watanabe, K. and Lamont, R.J. (2002) Involvement of integrins in fimbriae-mediated binding and invasion by Porphyromonas gingivalis. **Cell Microbiol***,* 4: (5): 305-314.

Zhang, G. and Ghosh, S. (2001) Toll-like receptor-mediated NF-kappaB activation: a phylogenetically conserved paradigm in innate immunity. **J Clin Invest***,* 107: (1): 13-19.

Zhang, W.J. and Frei, B. (2001) Alpha-lipoic acid inhibits TNF-alpha-induced NF-kappaB activation and adhesion molecule expression in human aortic endothelial cells. **Faseb J***,* 15: (13): 2423-2432.

Figures

Figure 1.1: The prevalence of significant periodontal pocketing in the UK population (1998) by age

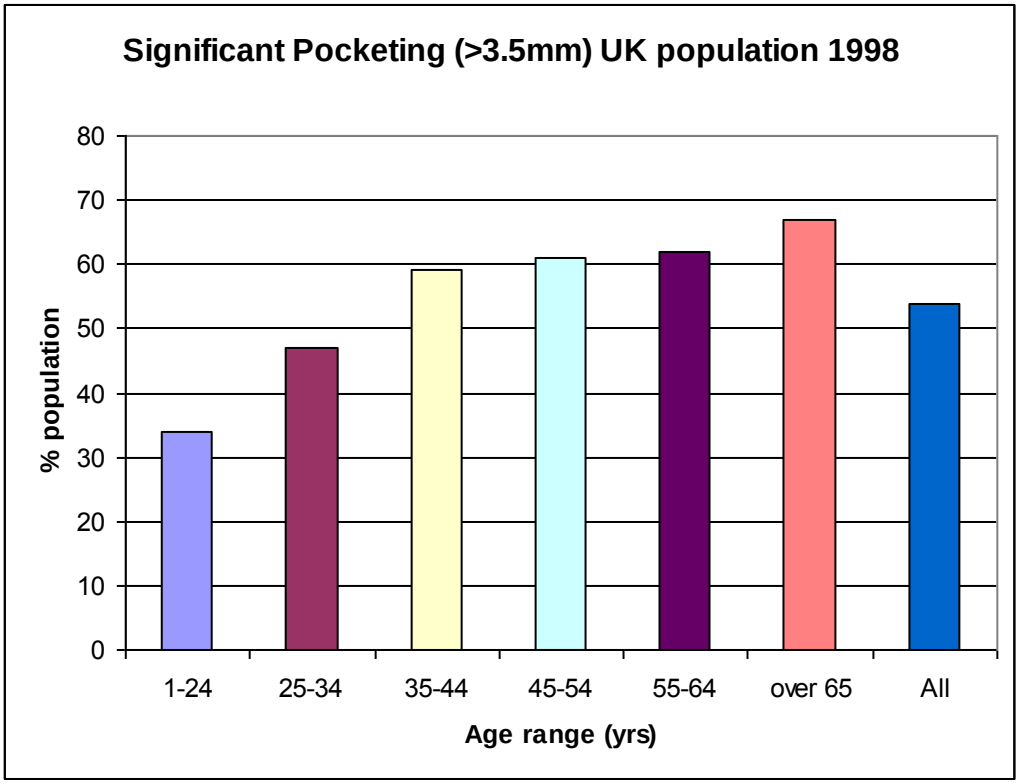

Figure 1.2: The prevalence of significant periodontal attachment loss in the UK population (1998) by age

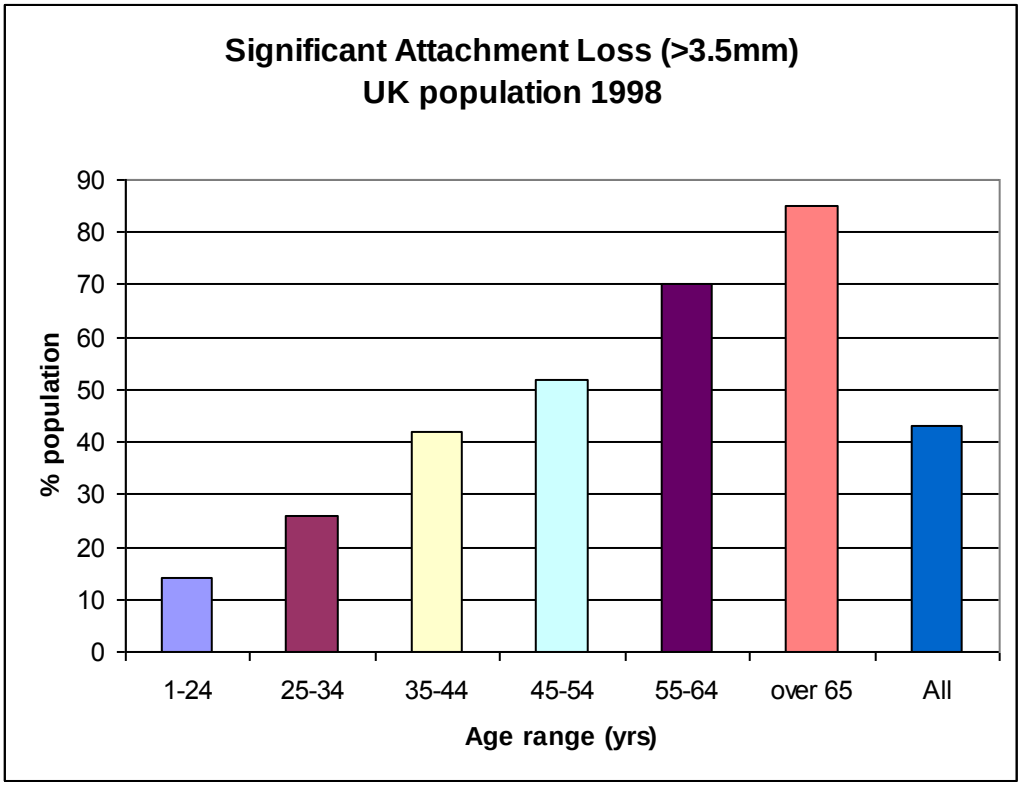

Table 1.1: Classification of Gingival diseases

Dental Plaque Induced Gingival Disease	Gingivitis associated with dental plaque only.
	Gingival disease modified by systemic factors.
	Gingival disease modified by medication.
	Gingival disease modified by malnutrition.
Non-plaque Induced Gingival Lesions	Gingival disease of bacterial origin
	Gingival disease of viral origin
	Gingival disease of fungal origin
	Gingival disease of genetic origin
	Gingival manifestations of systemic conditions
	Traumatic lesions
	Foreign body reactions
	Not otherwise specified

Table 1.2: Classification of Periodontitis

Chronic periodontitis	Localised (<30% of sites)
	Generalised (>30% of sites)
Aggressive Periodontitis	Localised
	Generalised
Periodontitis as a manifestation of systemic disease	Associated with systemic disorders
	Not otherwise specified
Necrotising Periodontal Disease	Necrotising Ulcerative Gingivitis
	Necrotising Ulcerative Periodontitis
Abscess of the Periodontium	Gingival abscess
	Periodontal abscess
	Pericoronal abscess
Periodontal lesions associated with endodontic lesions	Combined periodontal – endodontic lesions
Developmental or Acquired deformities or conditions	Localised tooth related factors that modify or predispose to plaque induced periodontitis
	Mucogingival deformities & conditions around teeth
	Mucogingival deformities & conditions on edentulous ridges
	Occlusal trauma

Figure 1.3: A diagrammatic representation of a tooth section (longitudinal) showing normal (healthy) periodontal tissue architecture

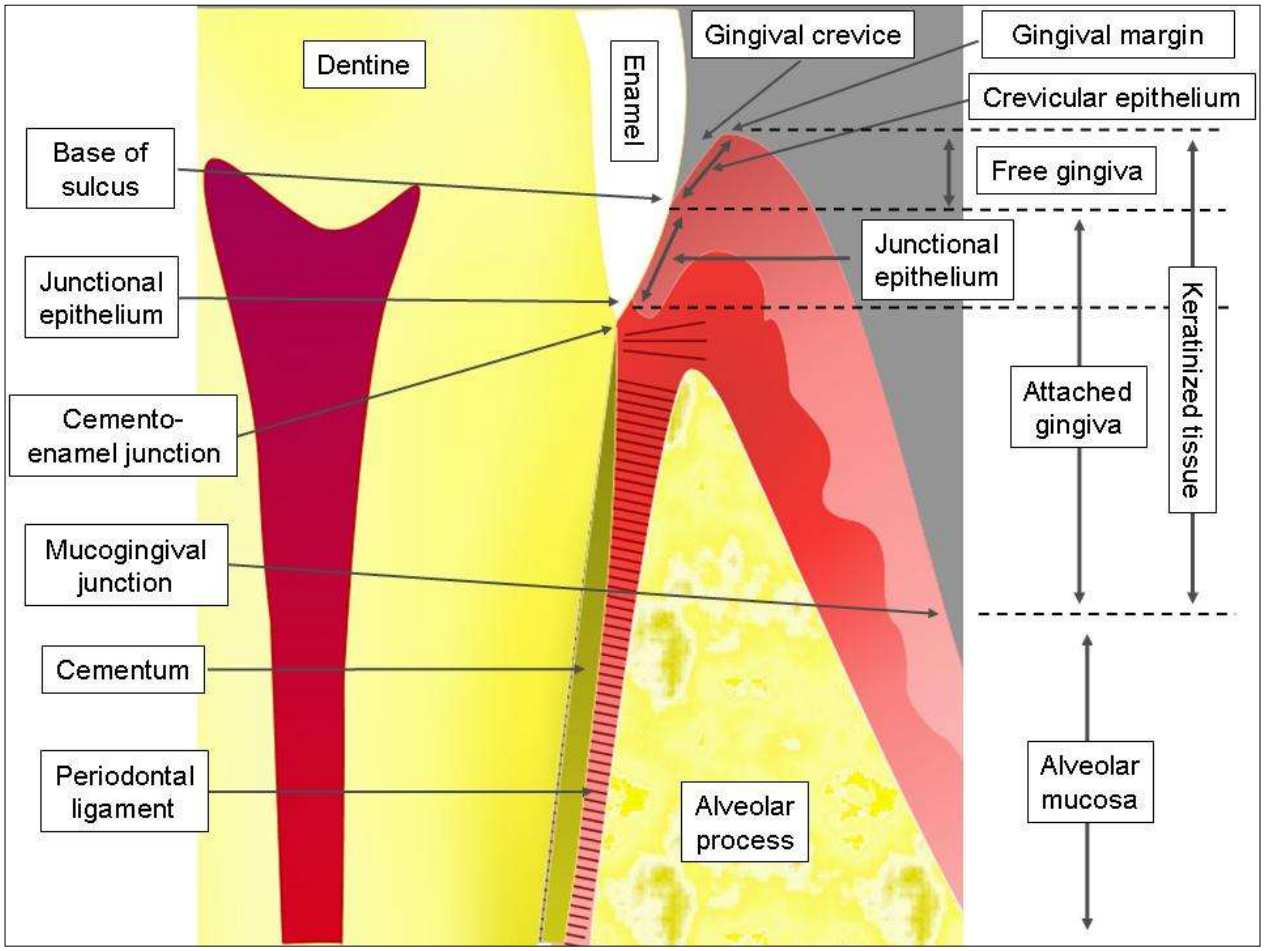

Figure 1.4: A diagrammatic representation of a tooth section (longitudinal) showing periodontitis

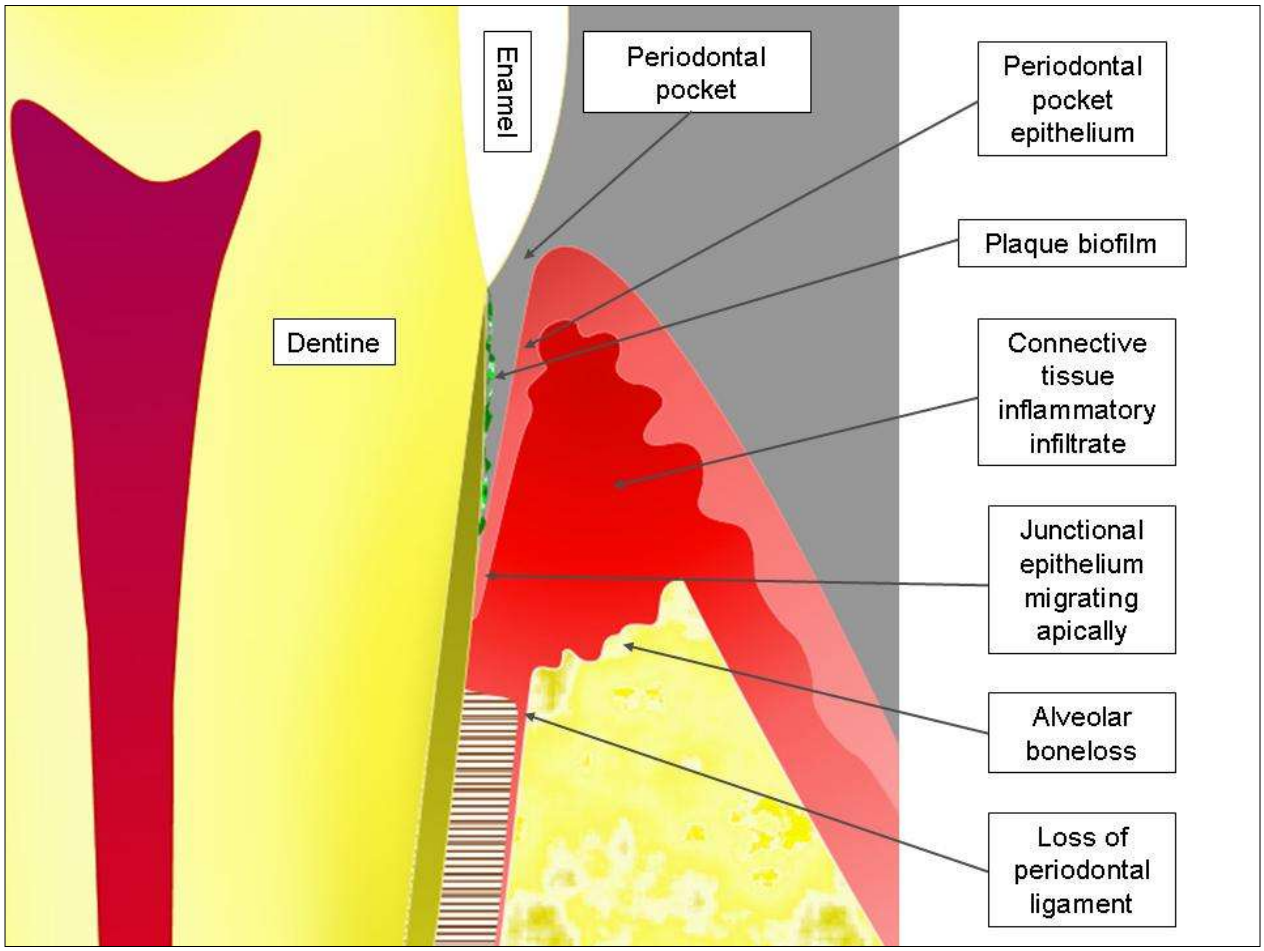

***Figure 1.5*:** Clinical photograph showing patient with chronic periodontitis

Figure 1.6: Full mouth long cone periapical radiographs, showing generalised severe bone loss in a chronic periodontitis patient

Figure 1.7: Socransky's coloured complexes showing association with periodontitis

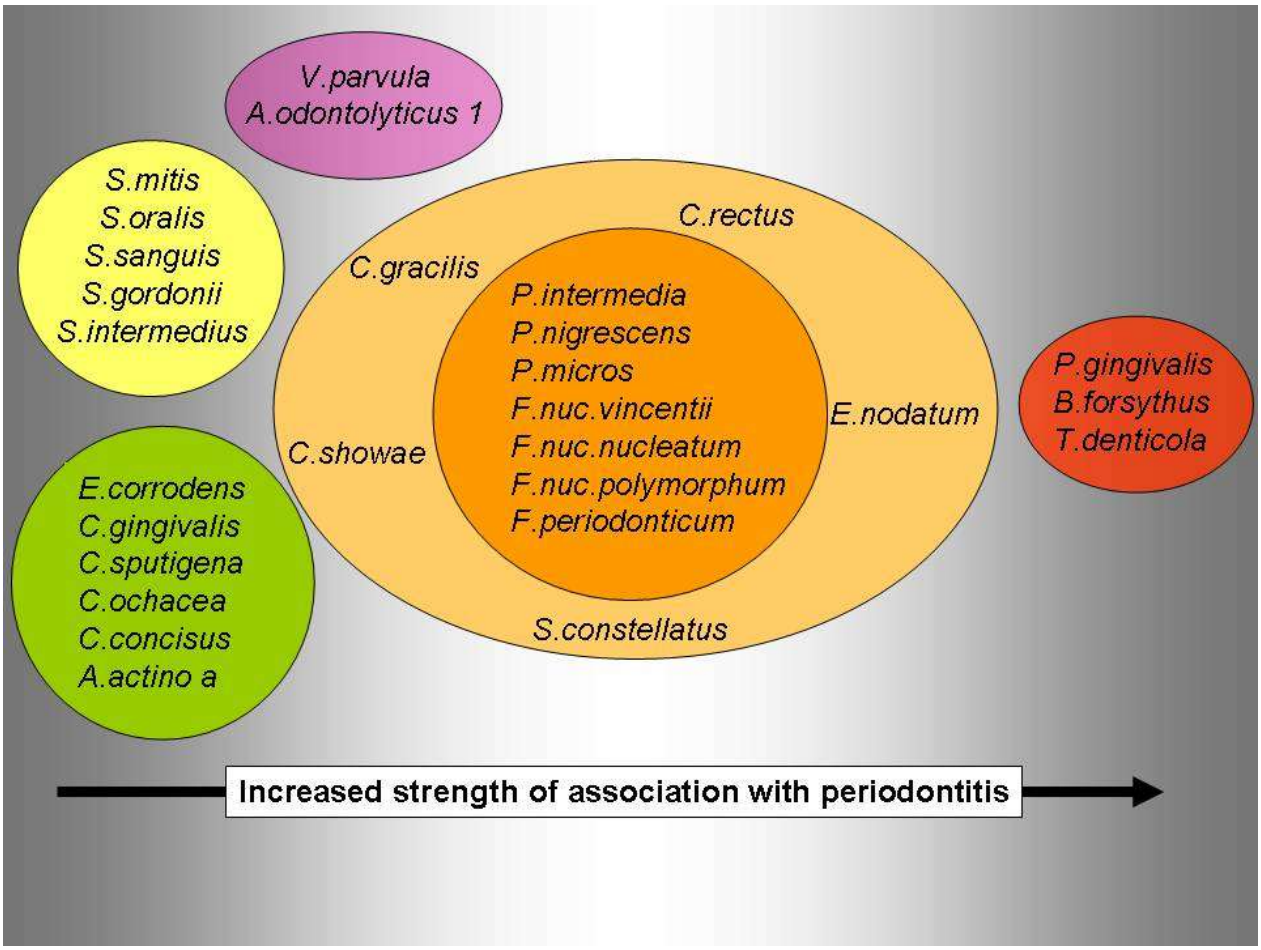

Figure 1.8: The role of reactive oxygen species in normal and dysregulated innate immunity to periodontal bacteria, proposing the role of pocket/sulcular epithelium.

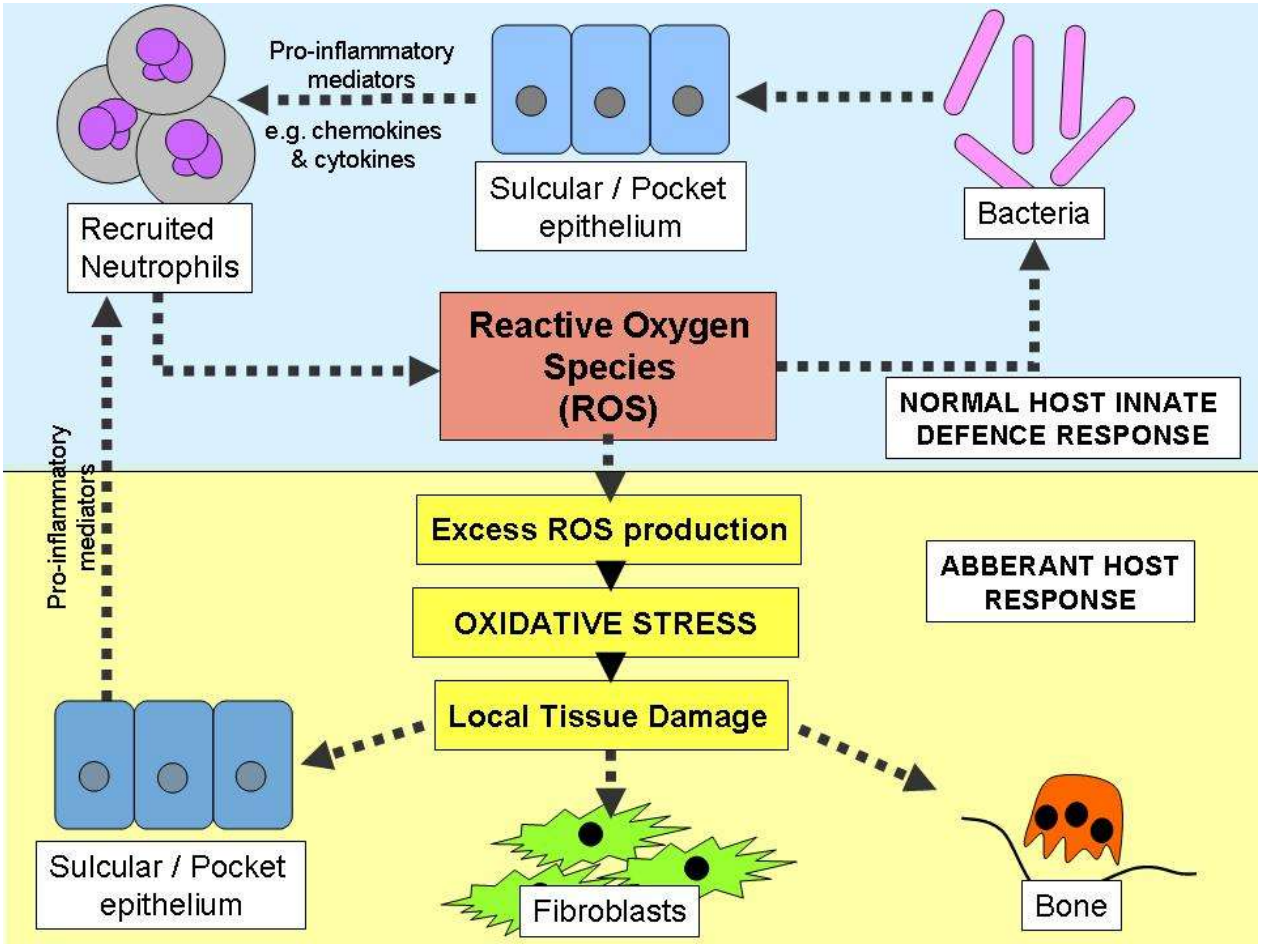

Figure 1.9: Schematic representation of normal tissue homeostasis and oxidative stress due to excess ROS.

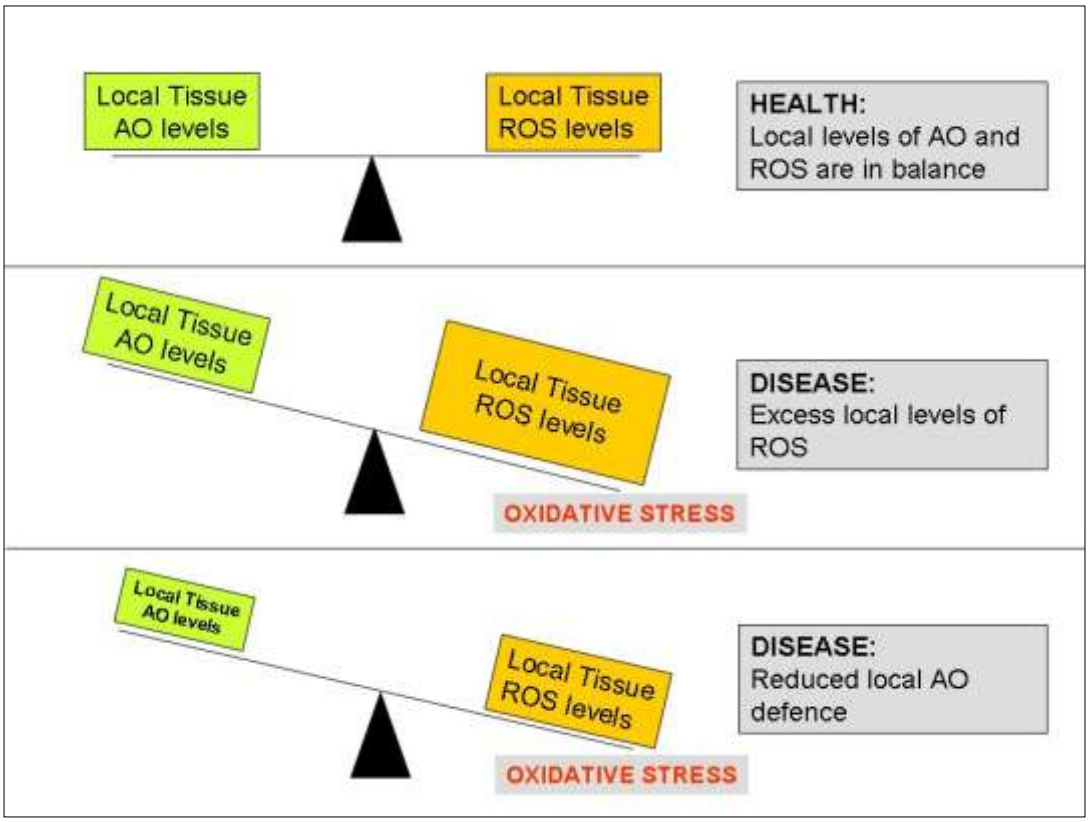

Figure 1.10: Examples of local risk factors; A: root groove, B: overhanging crown margin, C: poorly designed plaque retentive partial upper acrylic denture.

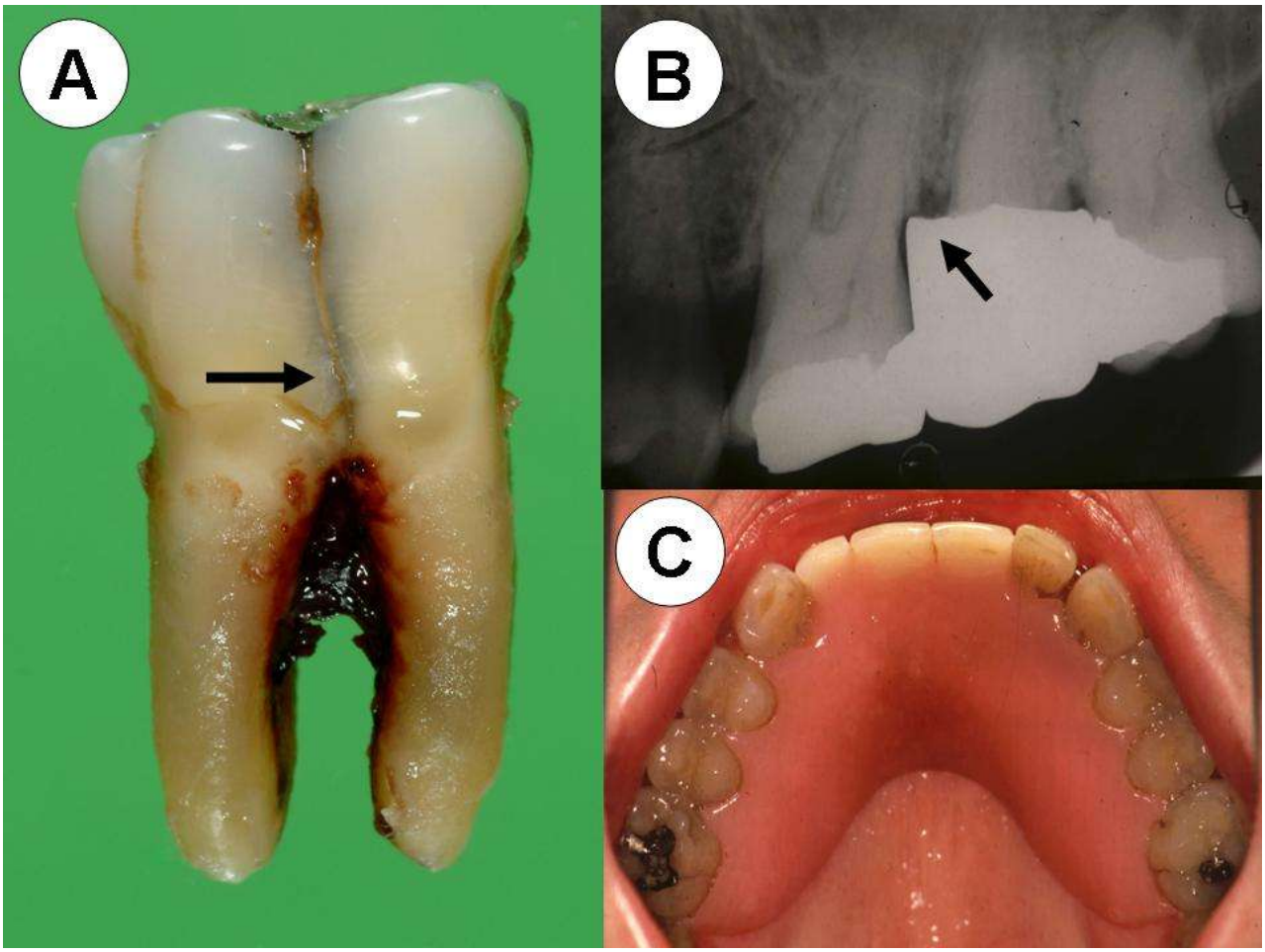

Figure 1.11: Diagram showing the pathway of REDOX sensitive transcription factor activation leading to chronic inflammation. This may represent a normal inflammatory response or if exaggerated may lead to tissue damage.

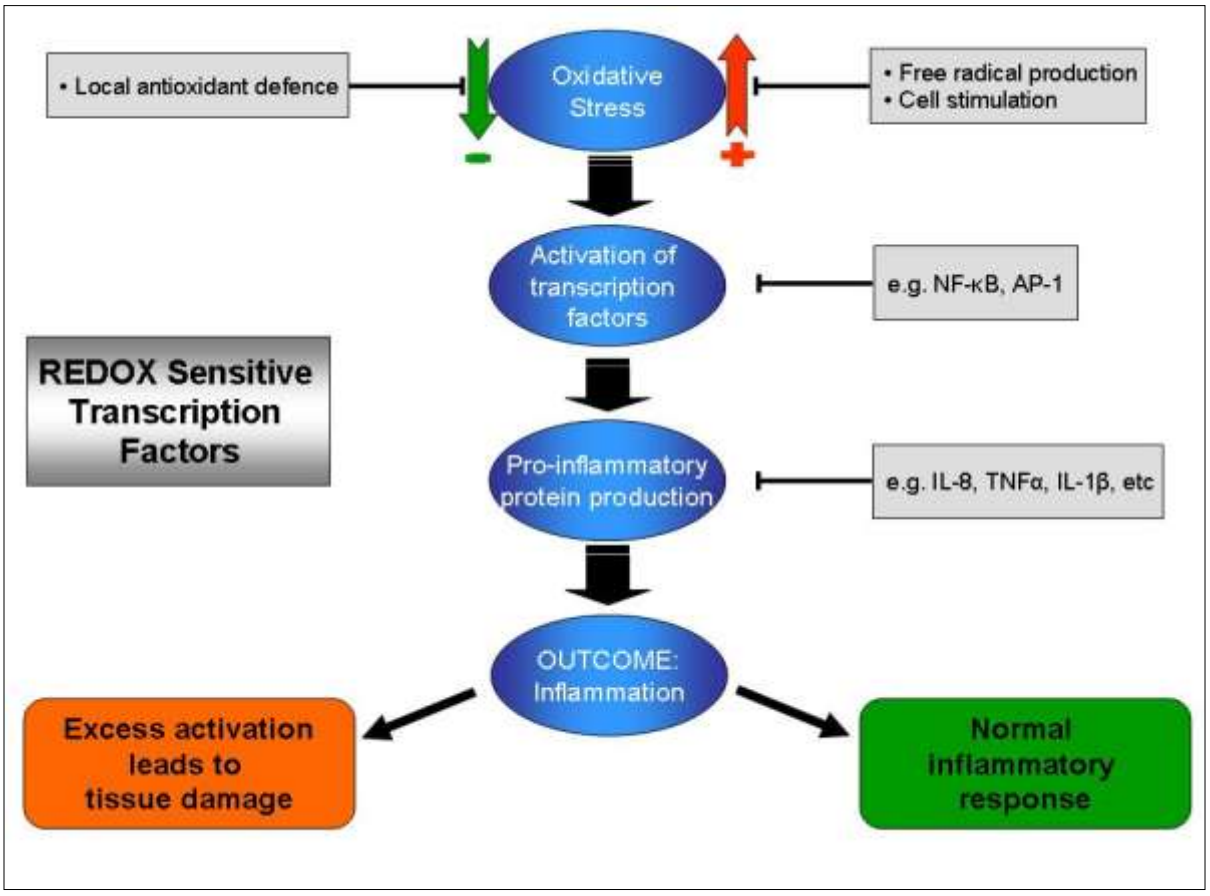

Figure 1.12: Activation of REDOX sensitive transcription factors

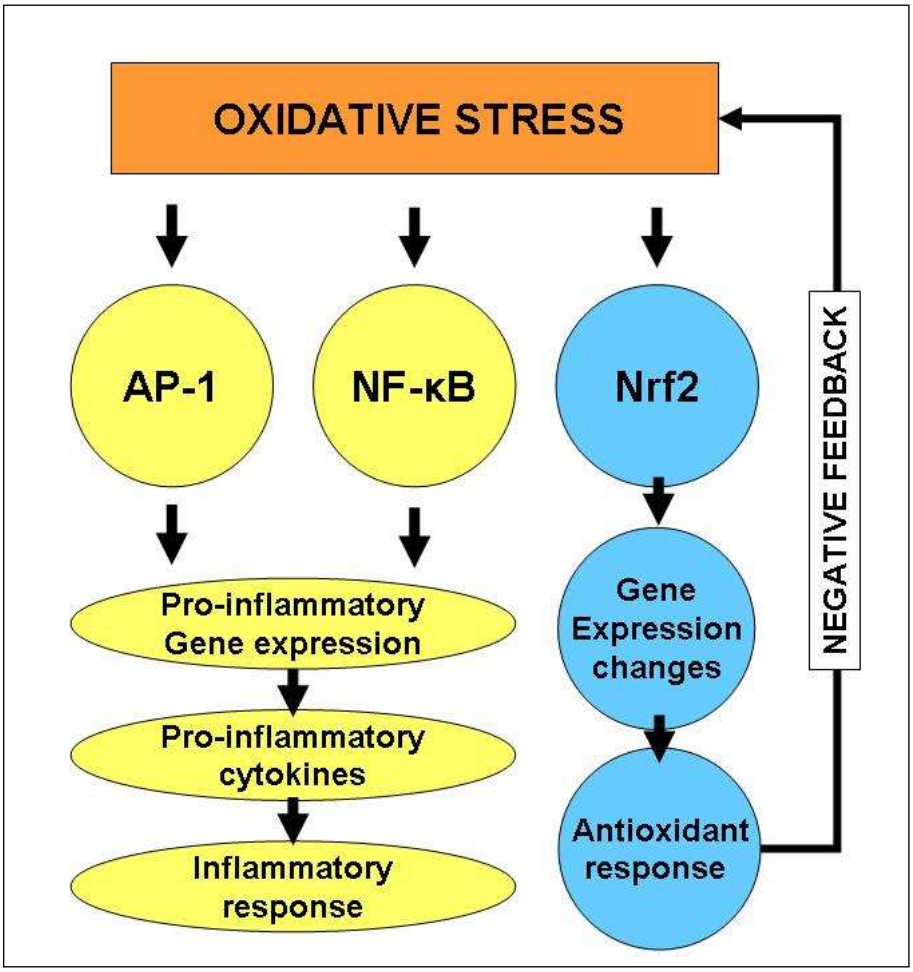

Table 1.3: Examples of diseases where NF-κB dysregulation has been implicated in the aetiology

Disease	Citation
Cardiovascular Disease	Freund et al 2005, Nichols 2004
Pulmonary disease	Christman et al, 2000
Diabetes type 1 & type 2	Eldor et al, 2006, Chen 2005
Kidney disease	Guzik & Harrison 2007
Liver disease	Zima et al 2005
Asthma	Pahl et al 2002
Dermatological diseases	Bell et al 2003
Gut disease	Neurath et al 1998
Tuberculosis	Zea et al 2006
Crohn's disease	Pena et al 2002
Occular allergy / Glaucoma	Bielory et al 2002; Zhou et al 2005
Nasal sinusitis	Xu et al 2006
Parkinson Disease	Soos et al 2004; Mogi et al 2006
Periodontal Disease	Ambili et al 2005; Nichols et al 2001
Rheumatic disease	Okamato et al 2006
Pancreatitis	Weber et al 2001
Inflammatory Bowel Disease	Dijkstra et al 2002

Figure 1.13: Activation of NF-κB leading to pro-inflammatory gene activation.

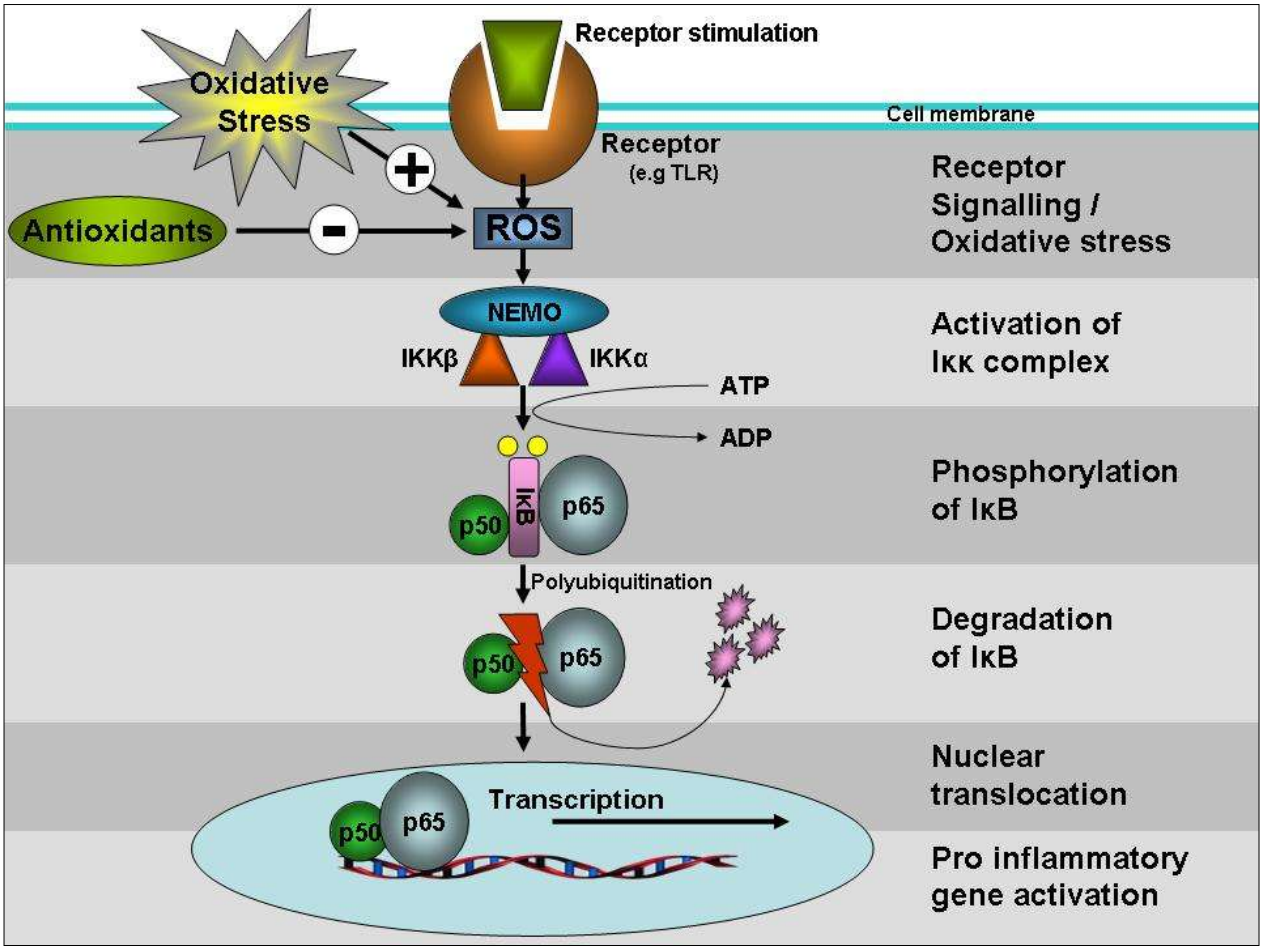

Figure 1.14: Phosphatase pathway limiting NF-κB activation; however ROS inhibition of this pathway encourages NF-κB activation.

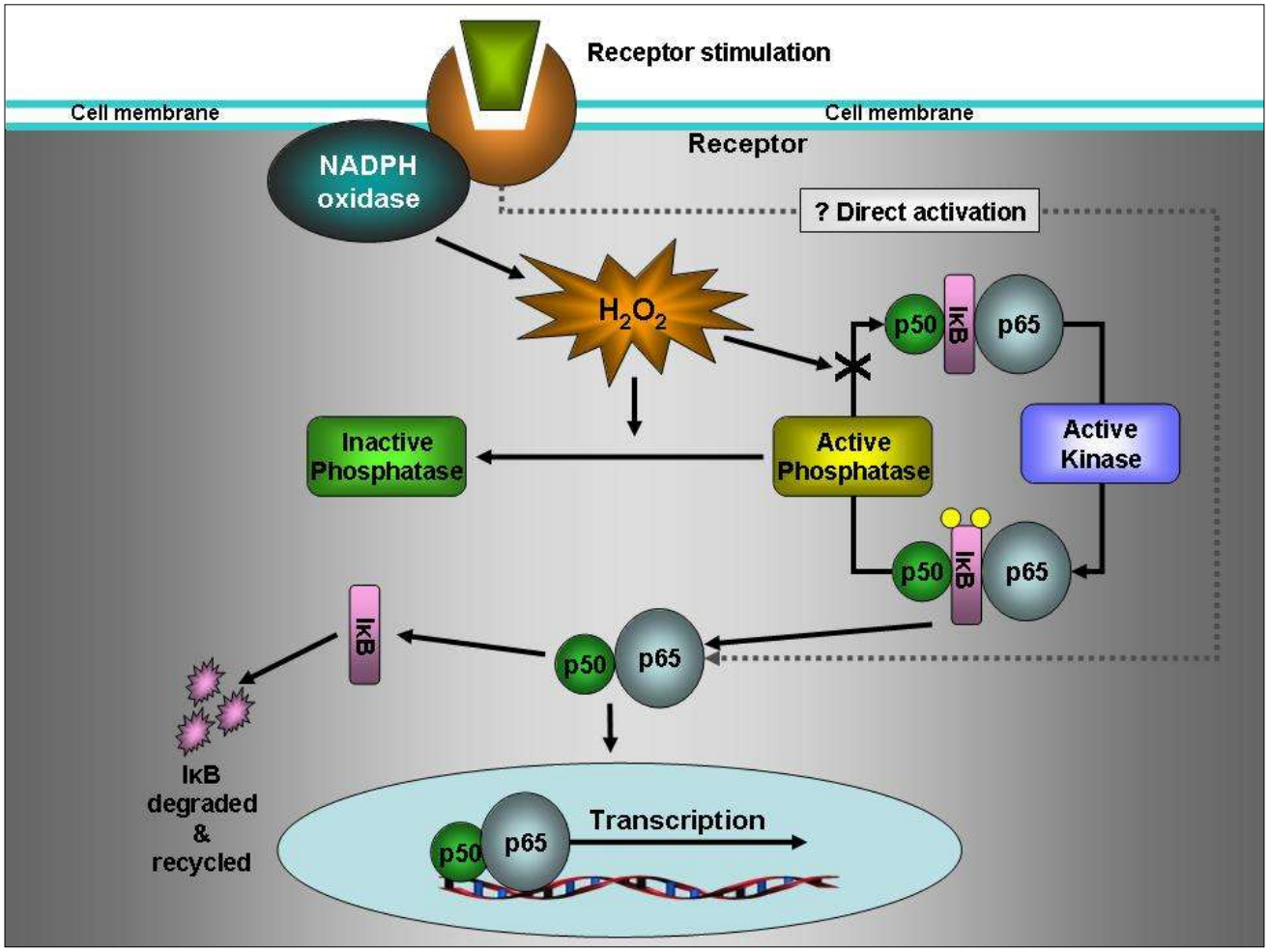

Figure 1.15: Potential NF-κB blocking agents, illustrating their site of action.

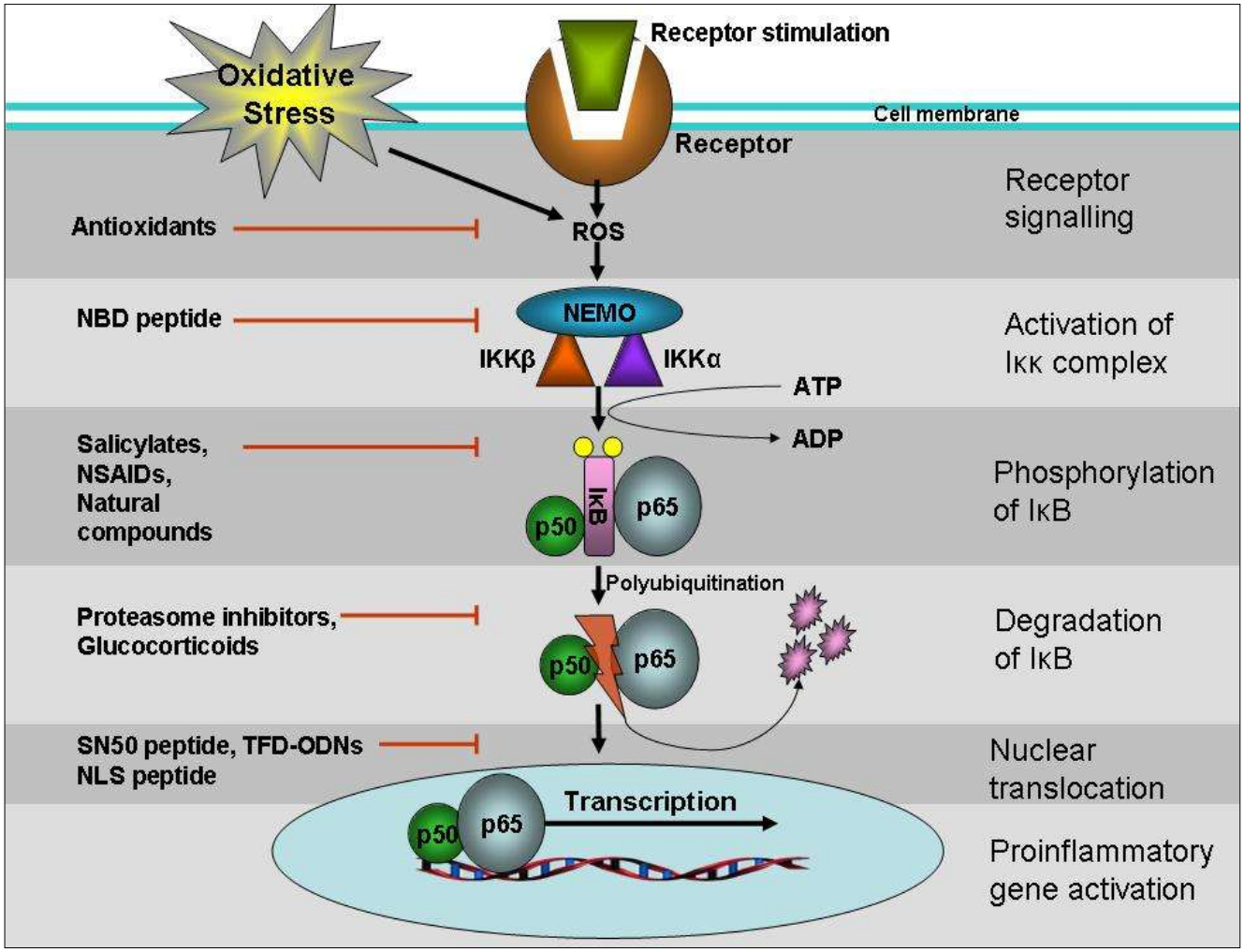

Figure 1.16: Diagram illustrating one mechanism by which antioxidants may block NF-κB activation

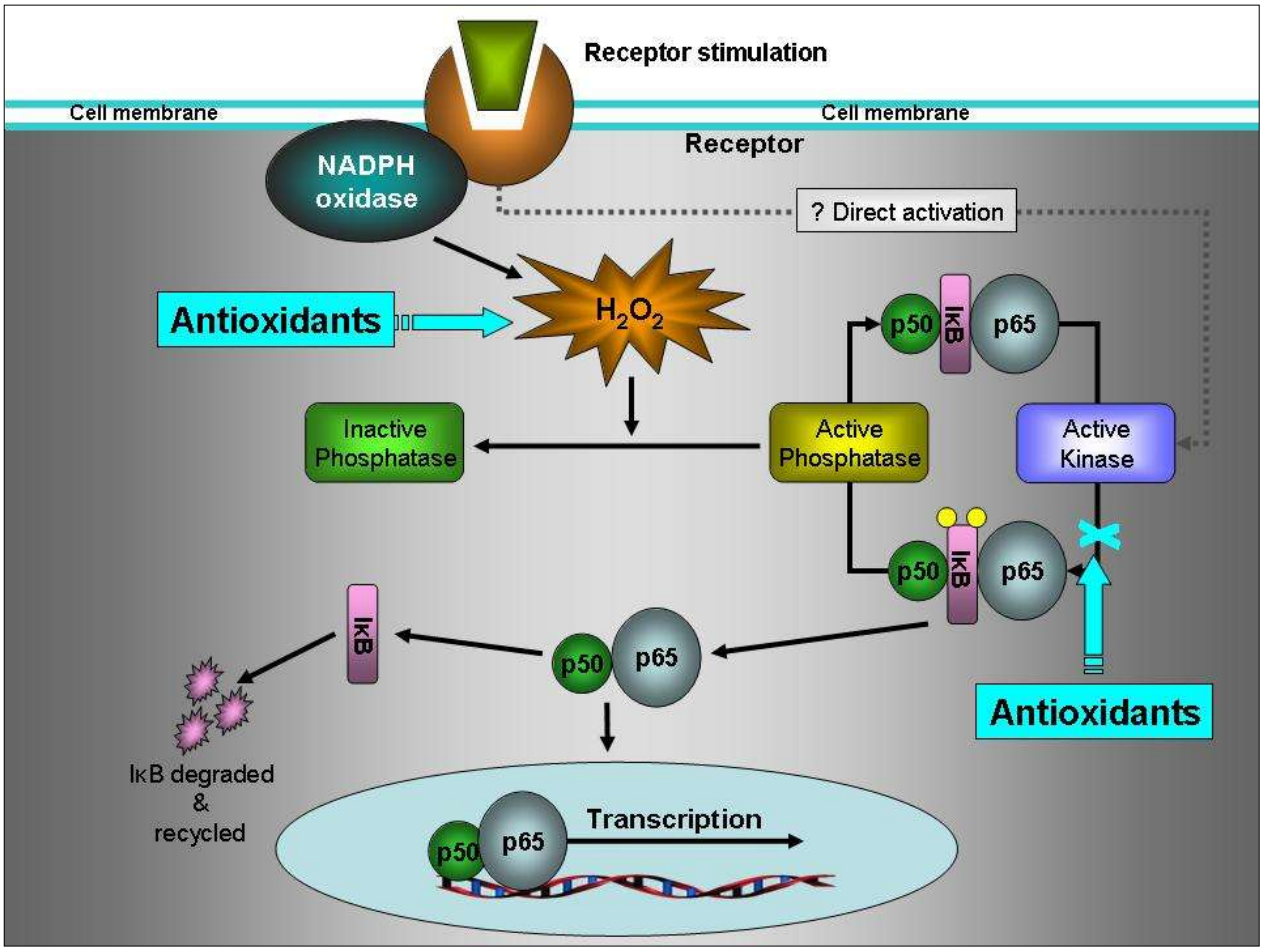

Figure 1.17: Molecular structure of α-lipoate and its reduced form dihydrolipoic acid

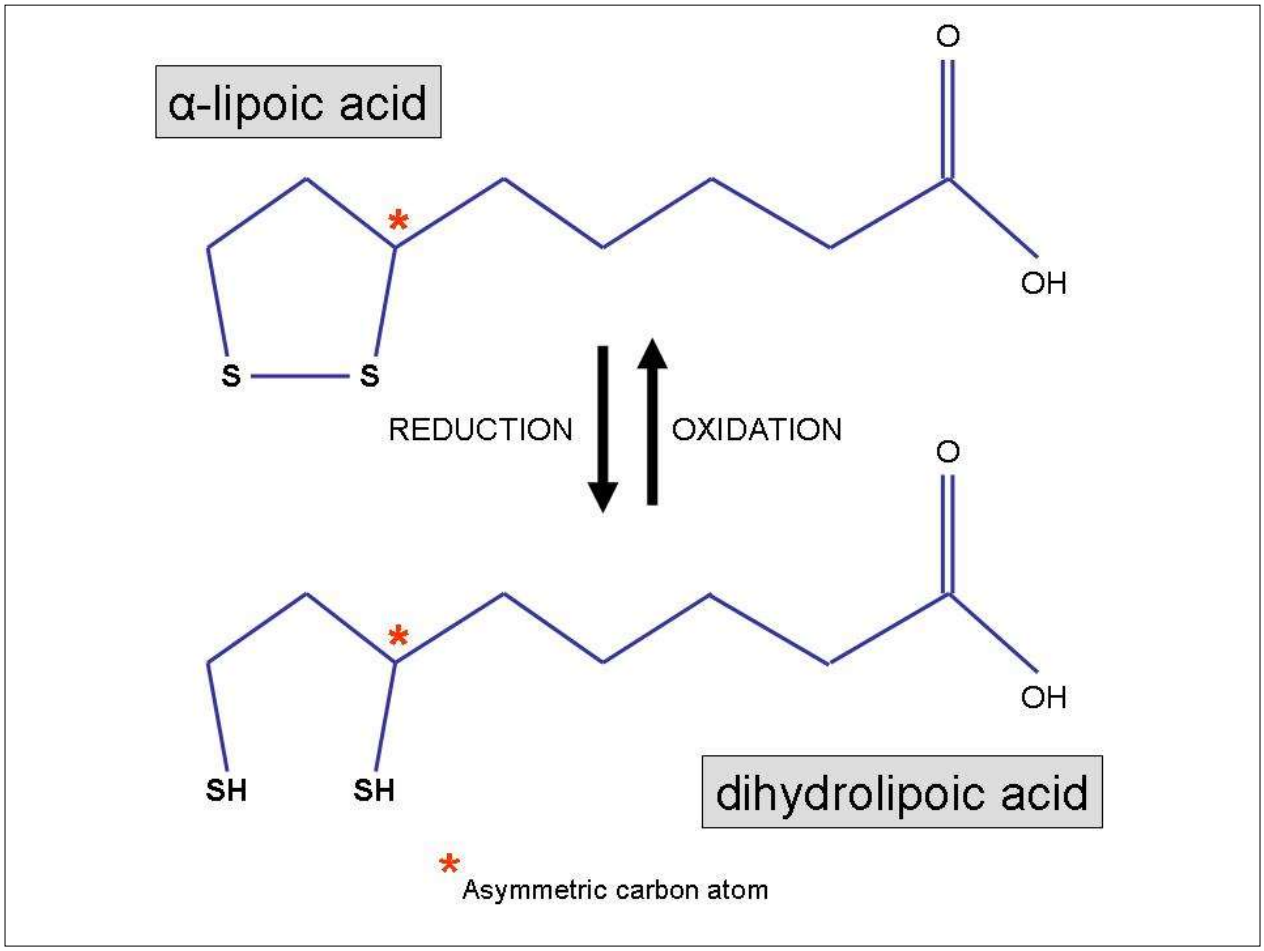

Figure 1.18: The impact α-lipoate on intracellular reduced glutathione

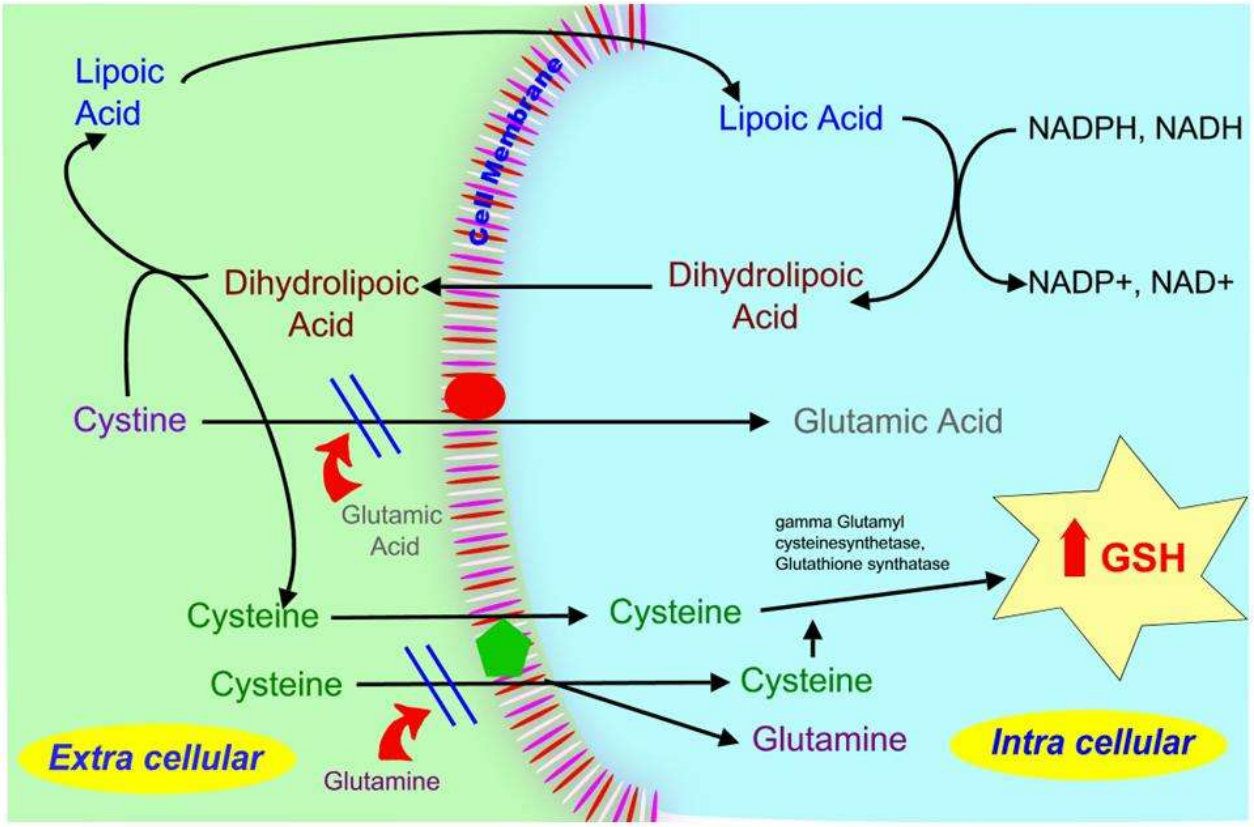

Figure 1.19: α-lipoate re-cycling of antioxidants from their oxidized forms

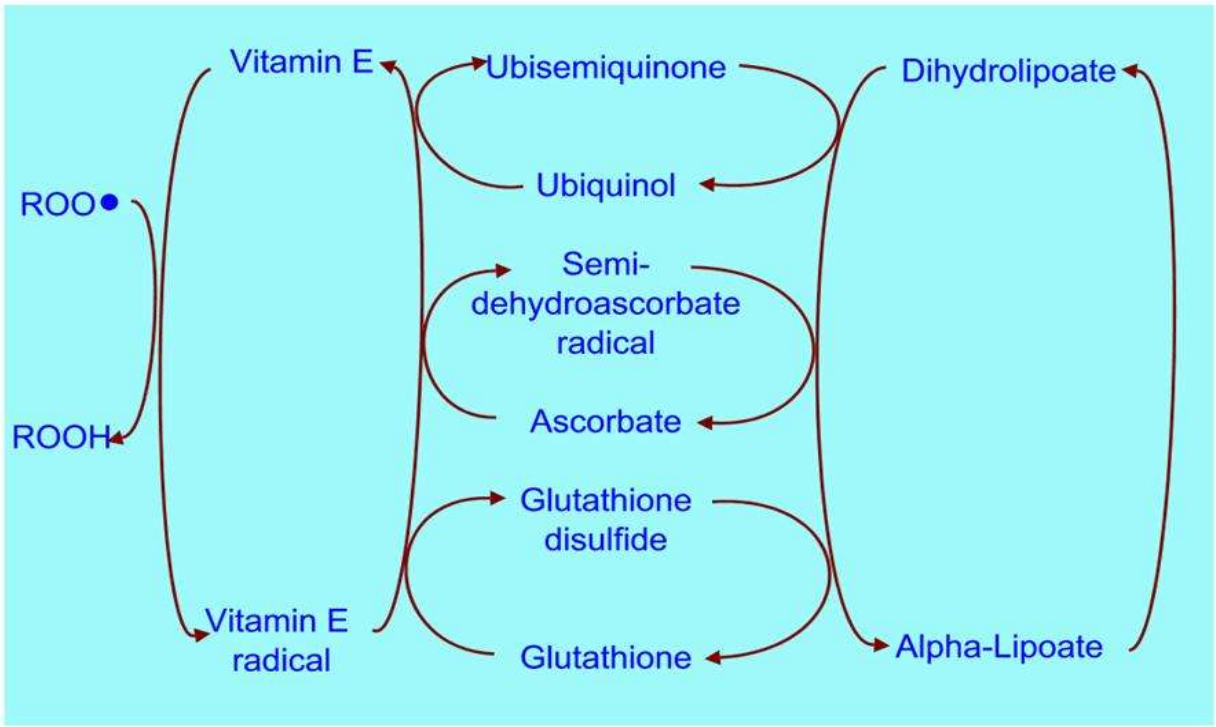

Figure 1.20: The key biological stages following epithelial cell stimulation and activation of the NF-κB pathway. **A**: translocation of NF-κB to the nucleus, **B**: gene expression changes, C: production of cytokines.

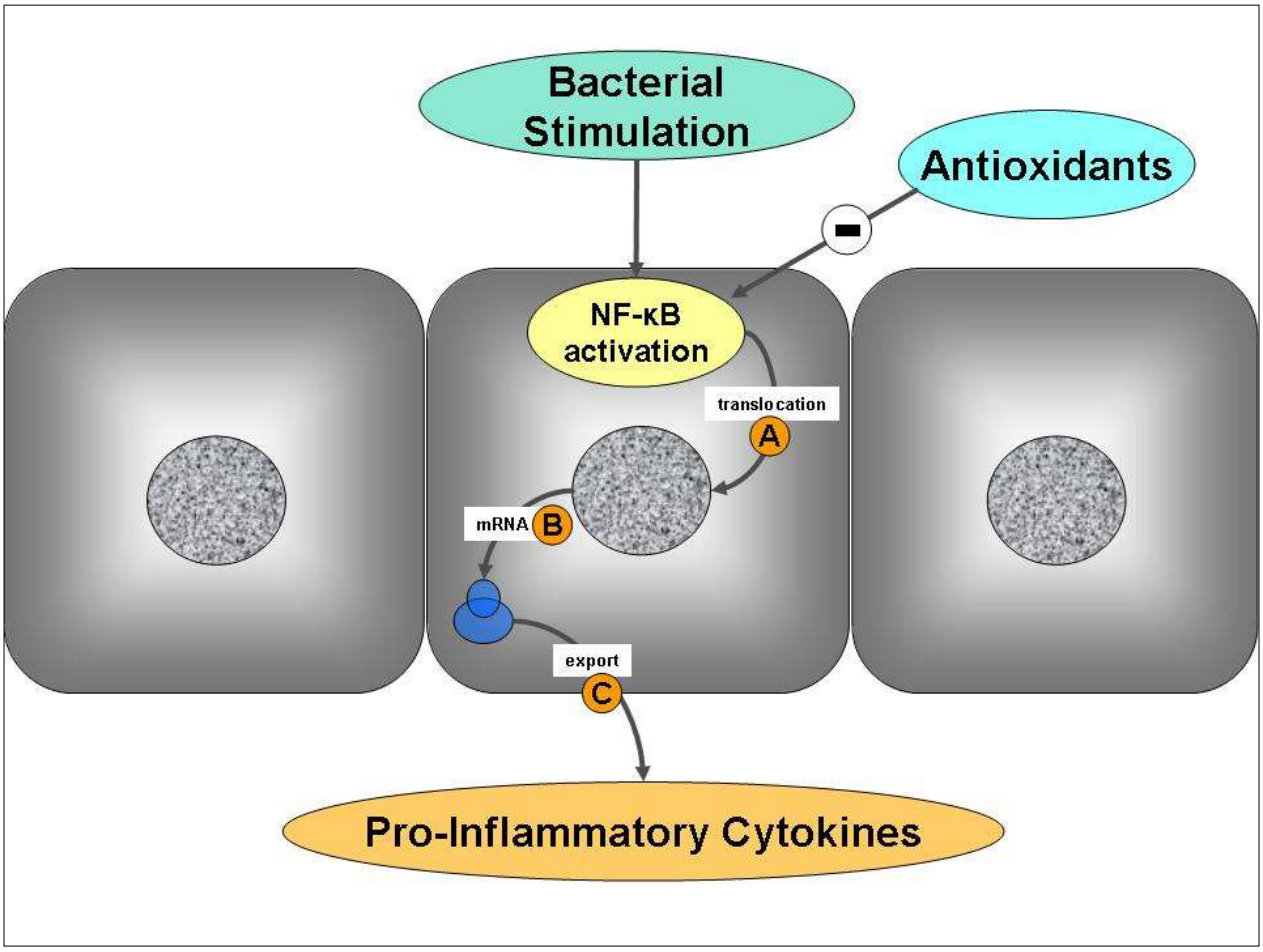

Figure 2.1: Anaerobic chamber (Don Whitley,UK)

Figure 2.2: MSC 12 positive flow cell culture cabinet

Figure 2.3: Substrates for H400 cell growth; **A**: Petri dish with multi-well slide. **B**: Plastic cell culture flask. **C**: Printed four well slide: **D** 96 well flat bottomed plate.

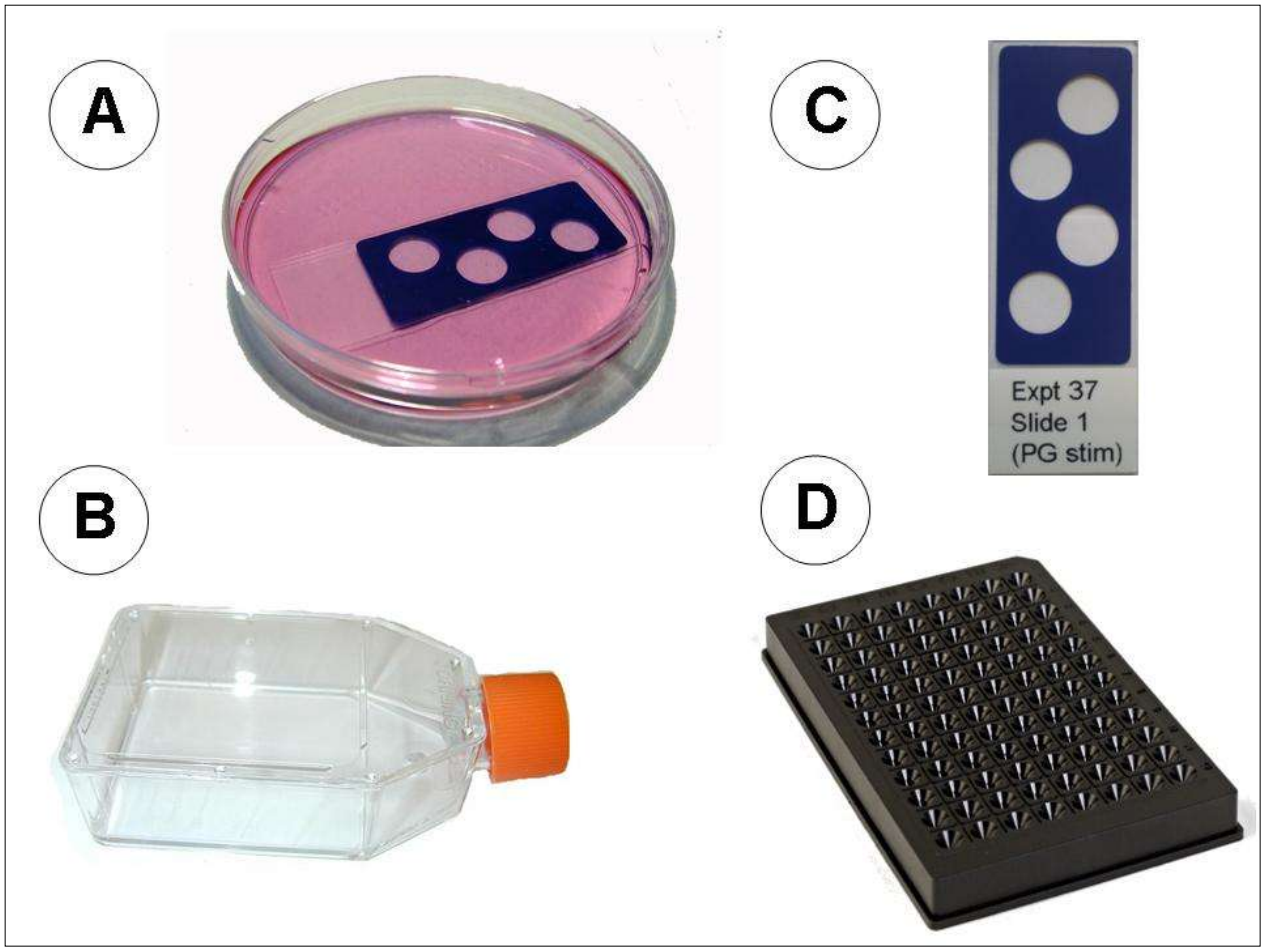

Figure 2.4: Diagrammatic representation of immuno-cytochemical methodology. **1:** cell substrate, **2:** primary monoclonal antibody, **3:** biotinylated secondary antibody (multi-link), **4:** peroxidase linked to streptavidin (label), **5:** diaminobenzidene (DAB)

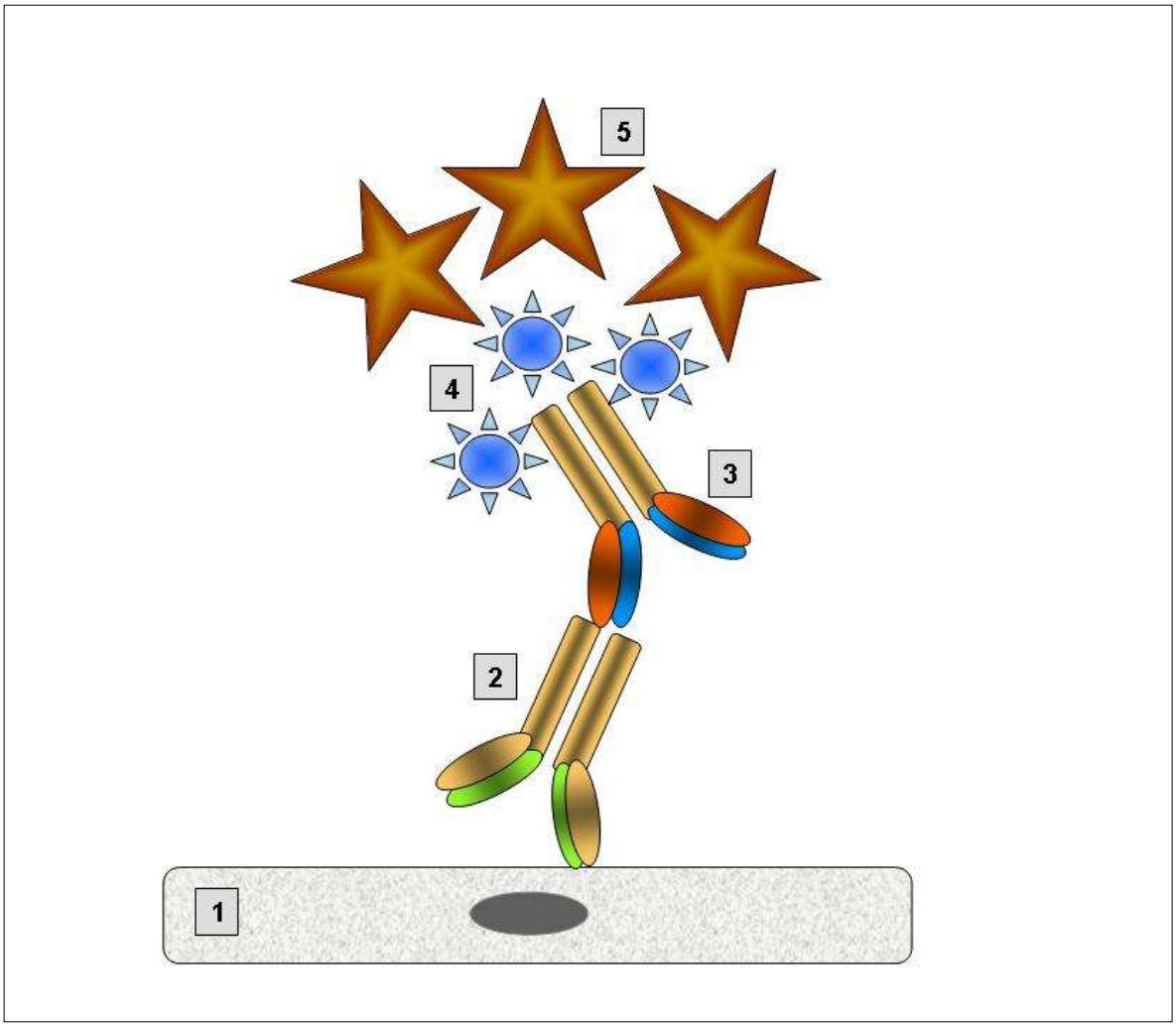

Figure 2.5: Flow diagram summarising the imunocytochemical staining method.

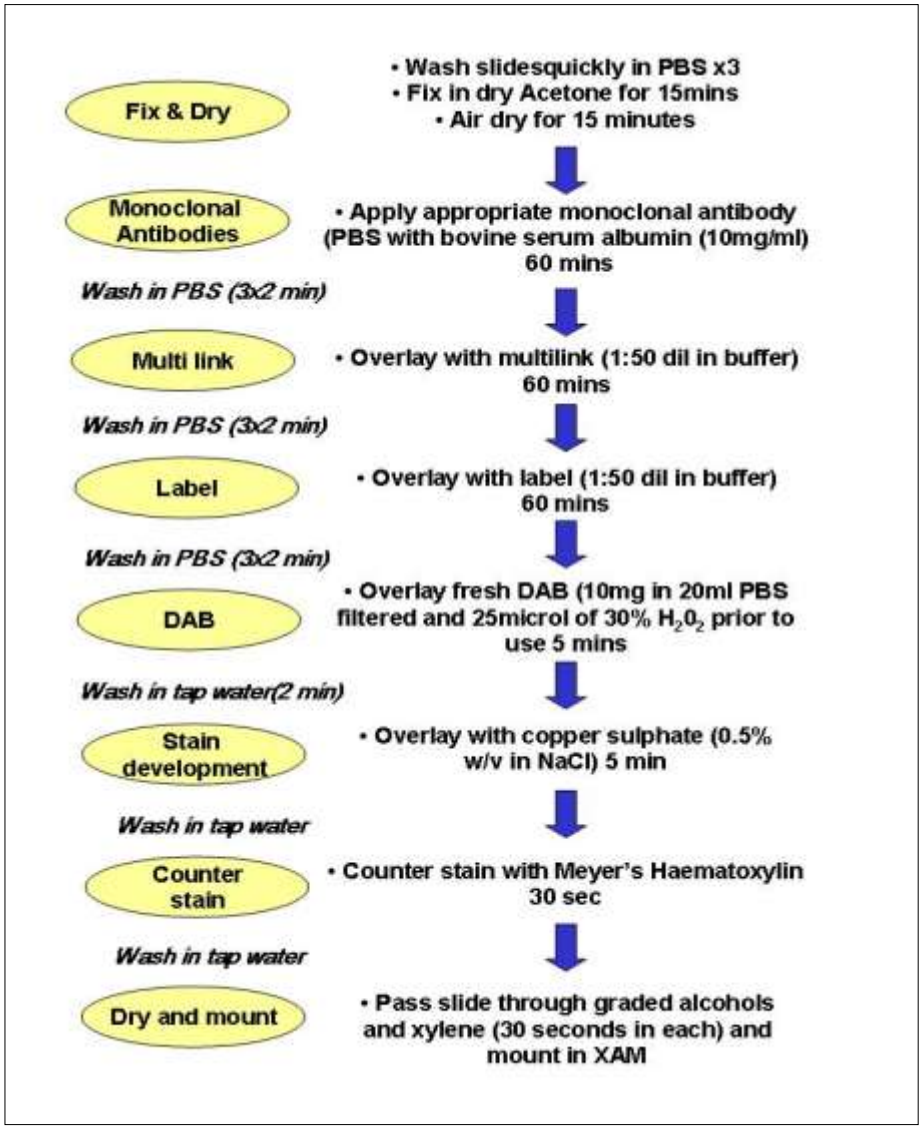

Figure 2.6: **A**: Represents a microscopic field using a graticule to divide into 0.1mm by 0.1mm squares**. B**: Example of a Hunting curve.

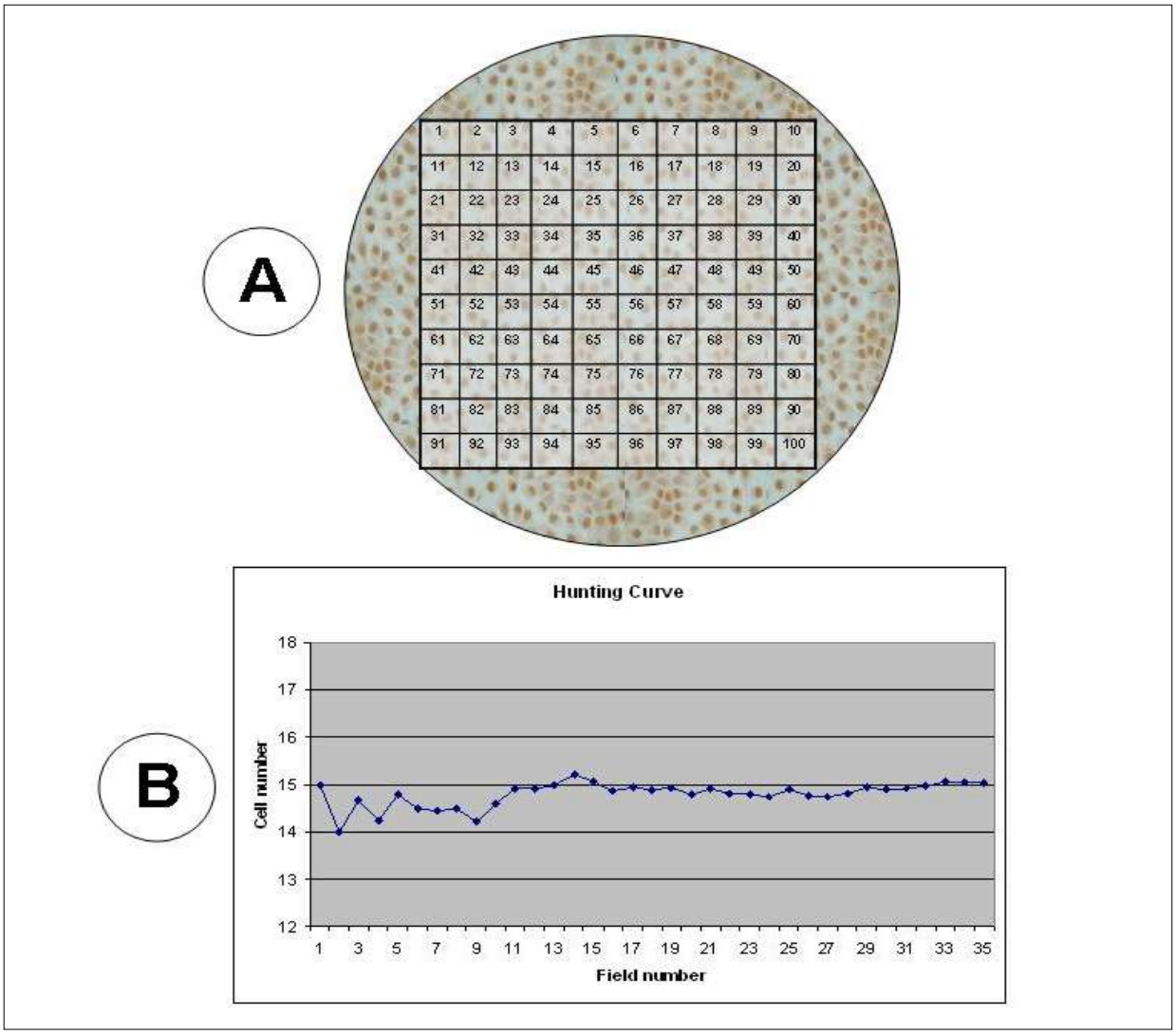

Figure 2.7: Cellomics ArrayScan II imaging cytometer

Figure 2.8: Quantification of nuclear and cytoplasmic intensity; **A** shows a diagrammatic representation of cell compartmentalisation, **B** shows how this is related to an actual scanned image.

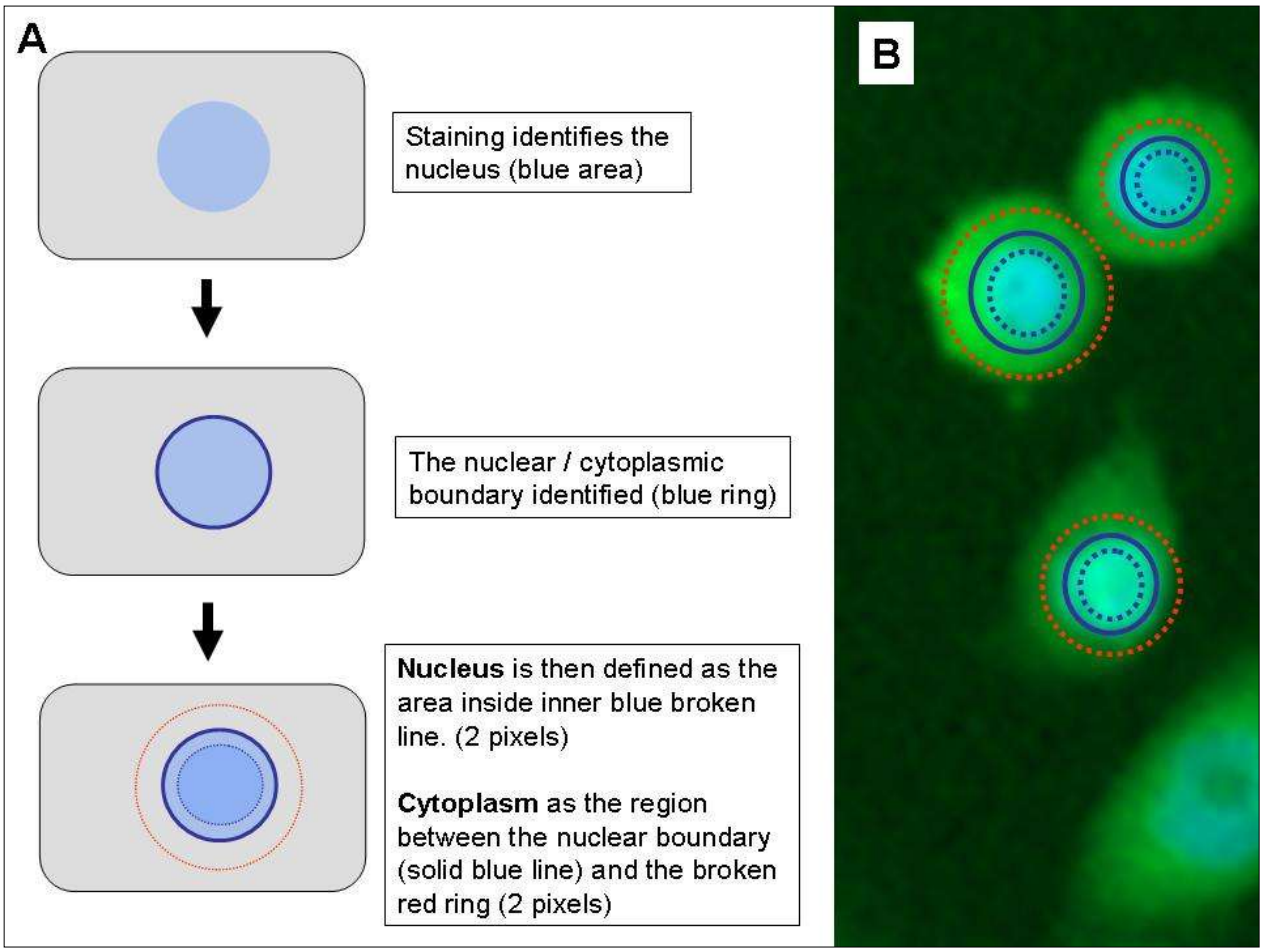

Figure 2.9: Schematic diagram showing the stages in PCR reaction

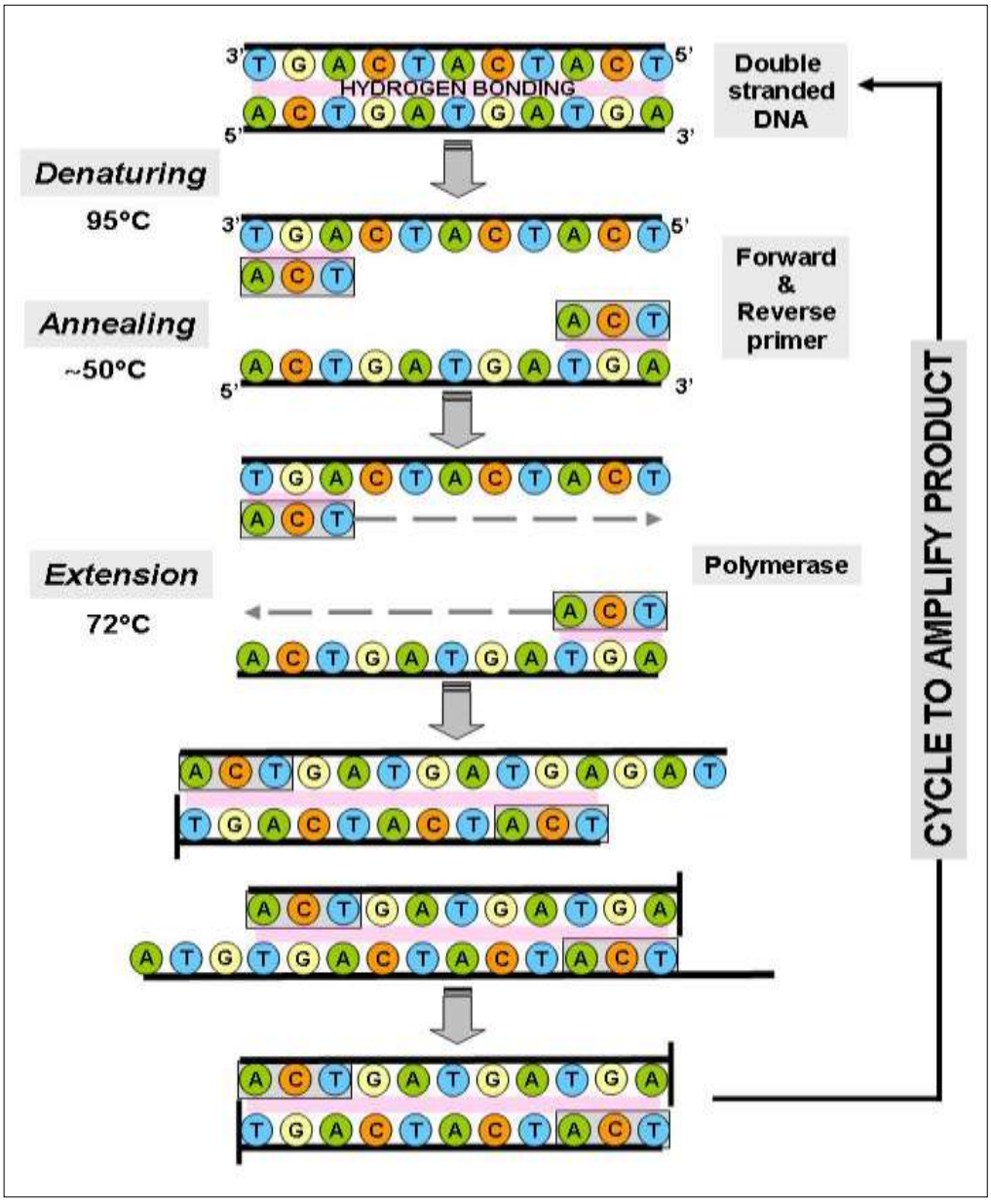

Figure 2.10: Agarose gel electrophoresis plate

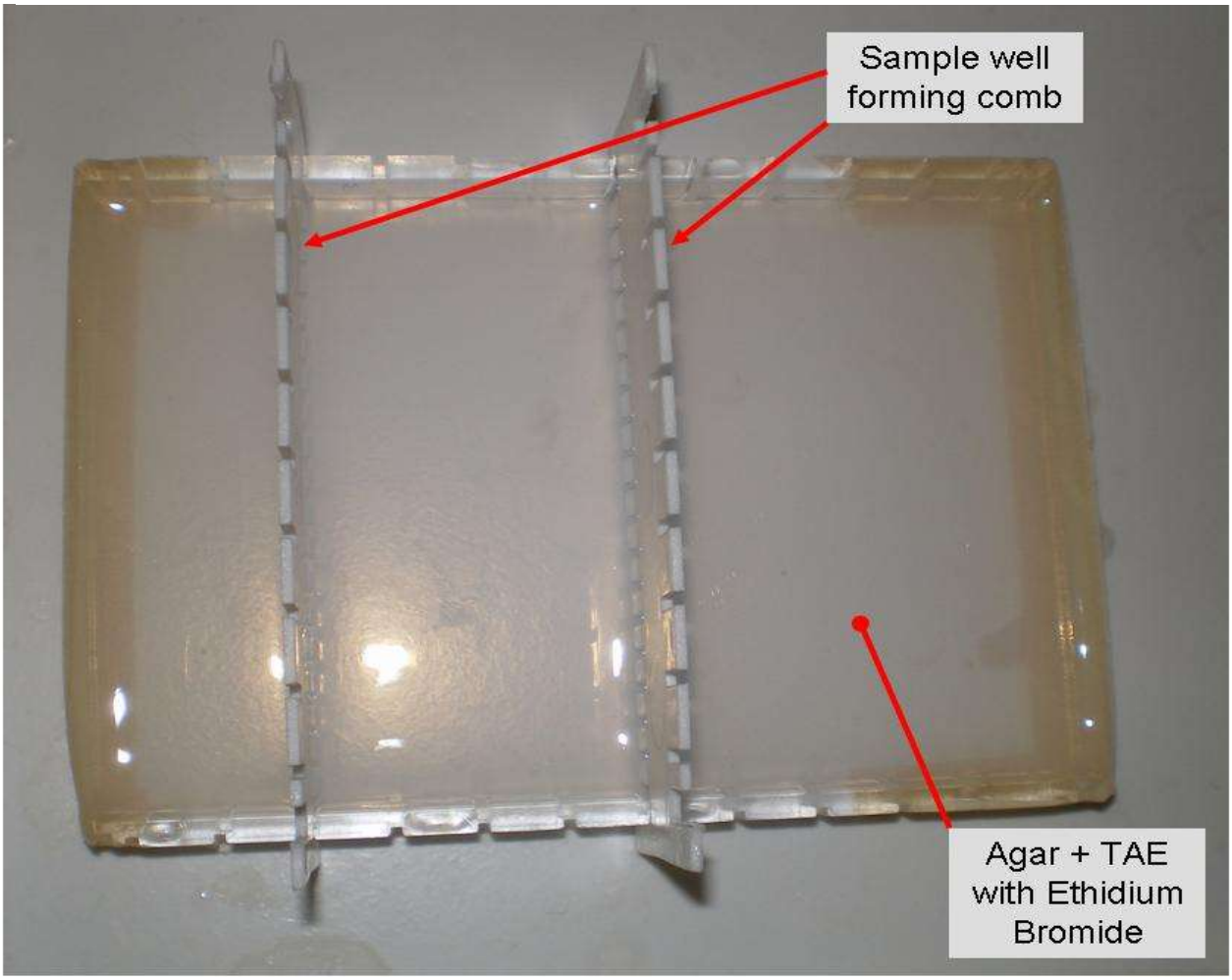

Figure 2.11: Processing of RNA samples for microarray analysis (courtesy of Affymetrix, UK)

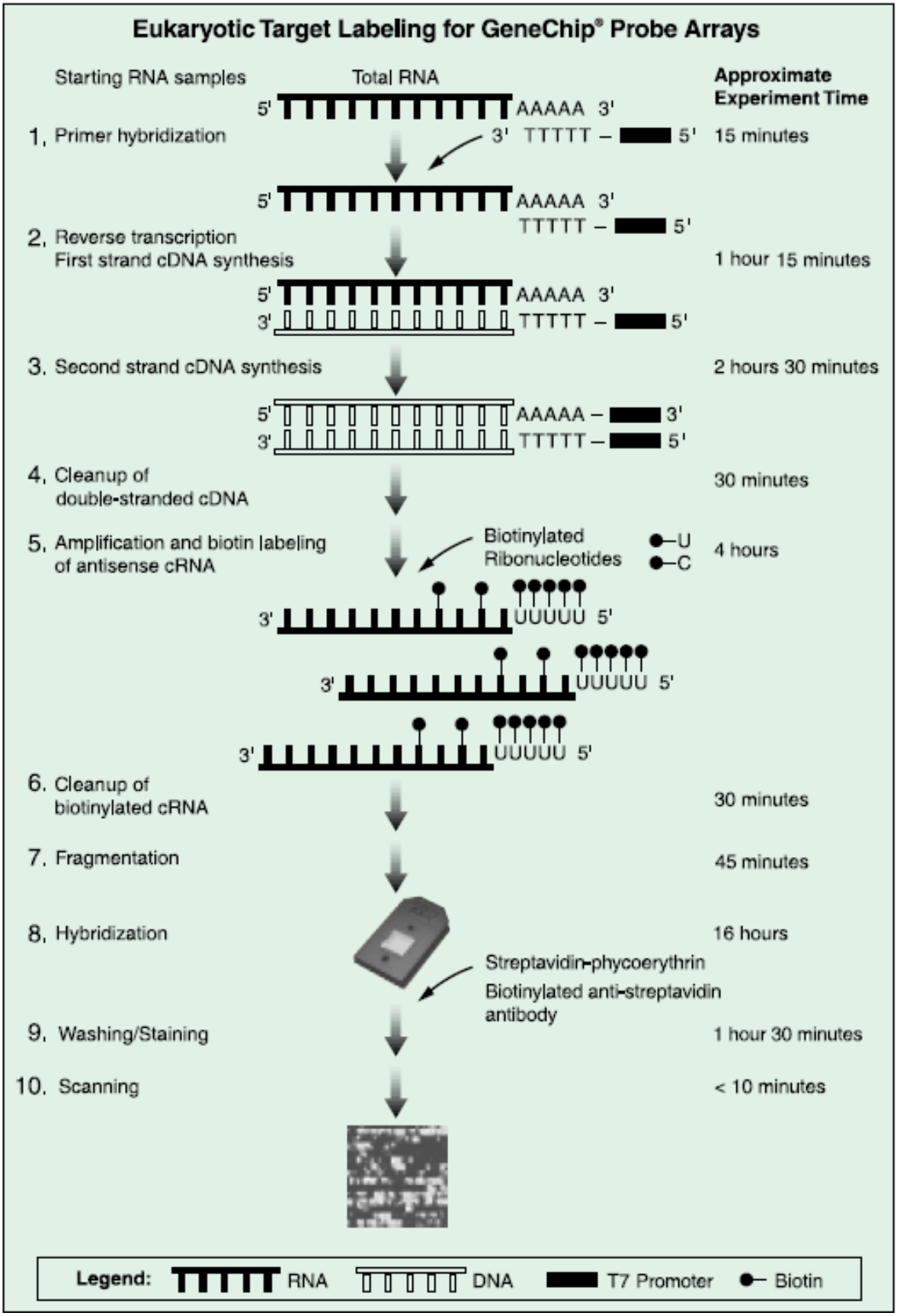

Figure 2.12: Affymetrix microarray test chip

Figure 2.13: Introduction of hybridisation buffer to U133A microarrays. Second pipette tip to allowing venting and ensure complete wetting of the chip

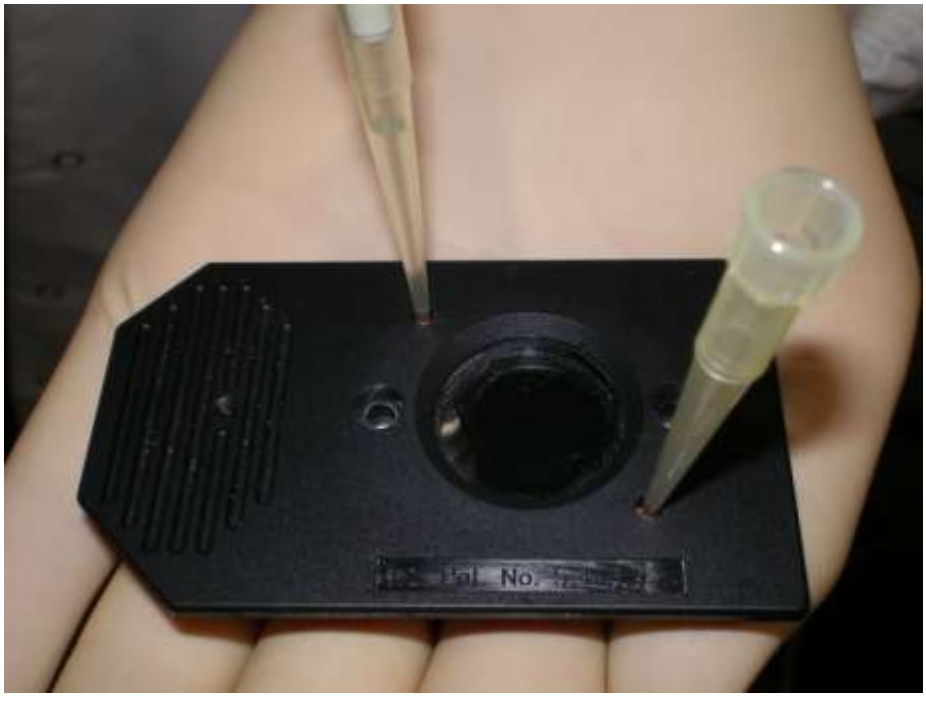

Figure 3.1: Diagrammatic representation of the H400 model indicating the range of investigations employed.

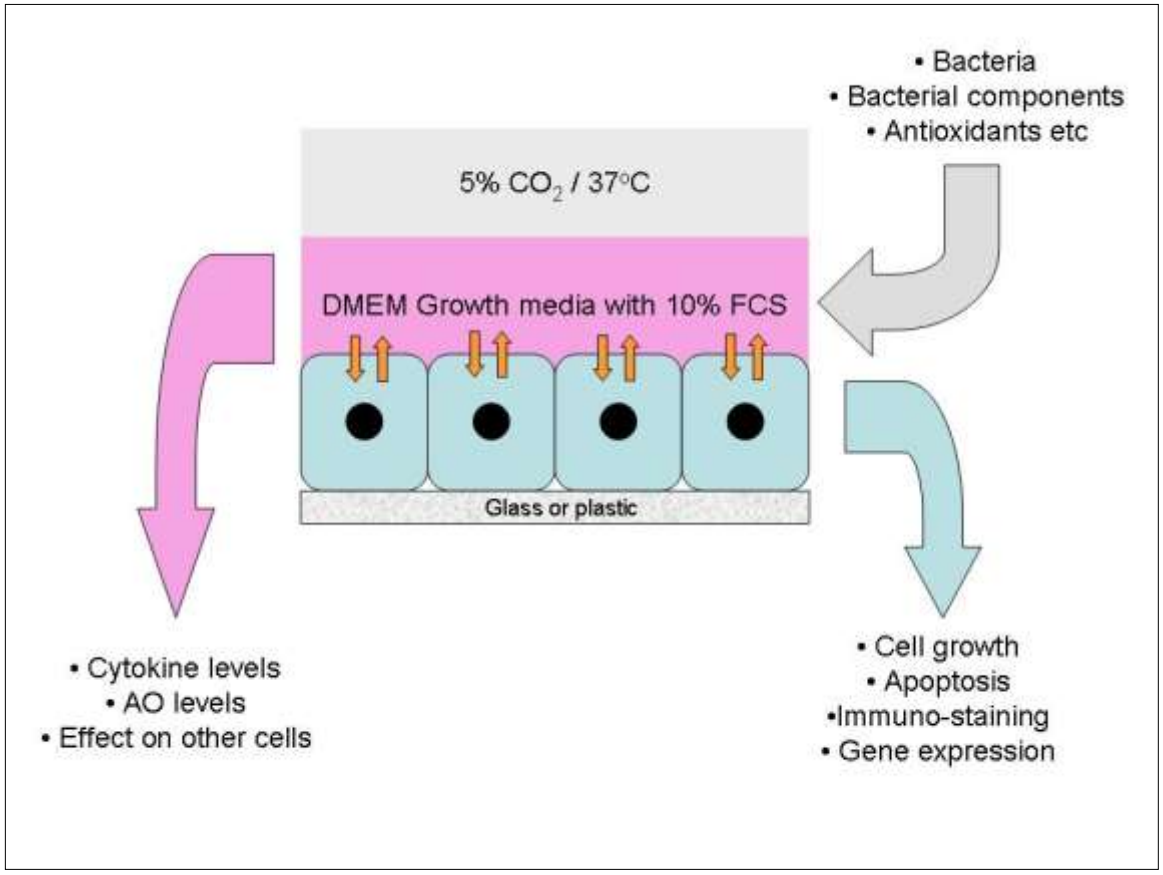

Figure 3.2: H400 cells cultured (mean ± SD, n=3) in DMEM (10% FCS at 37°C in 5% CO_2) for 4 days.

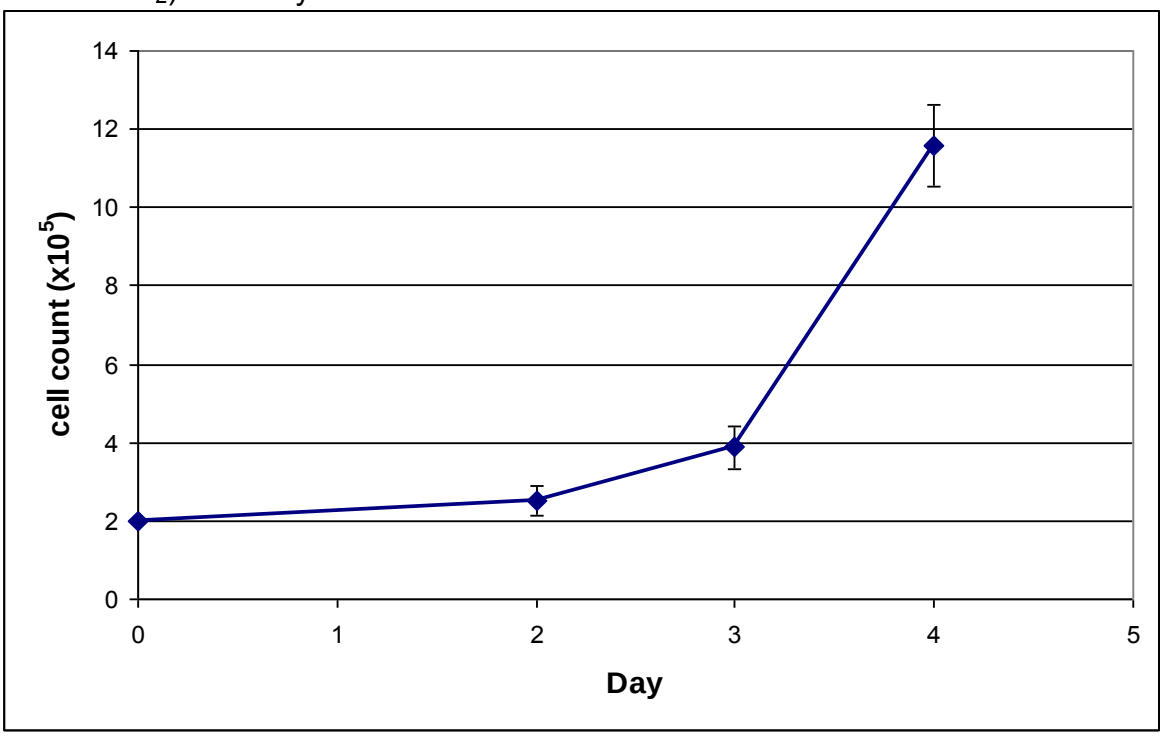

Figure 3.3: Attached H400 cells grown in cell culture flask for 4 days viewed using an inverted microscope

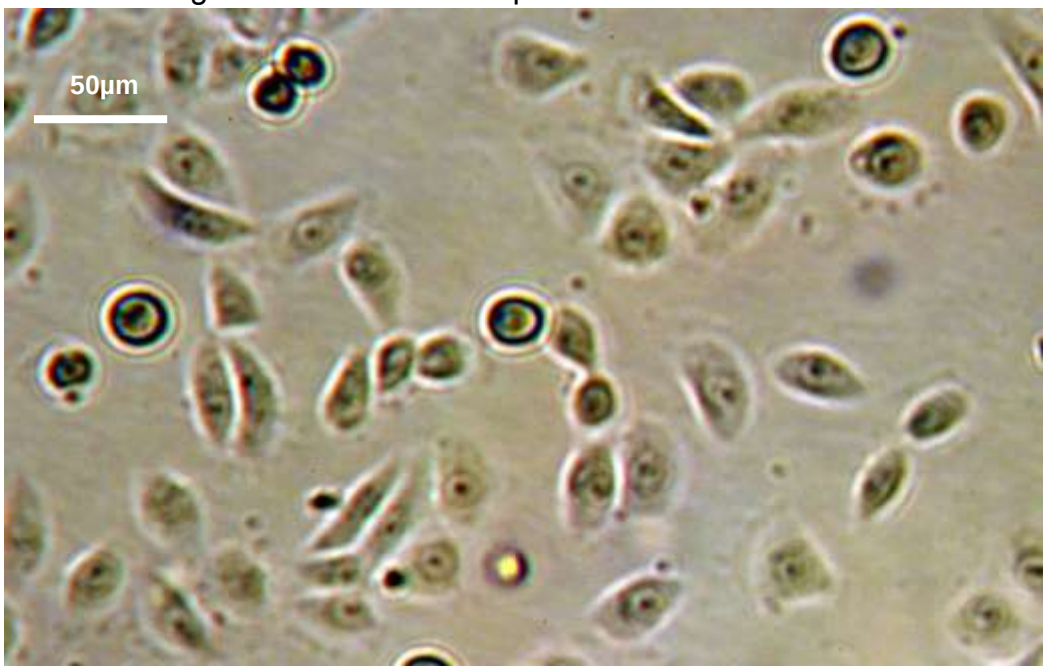

Figure 3.4: Growth characteristics of H400 cells (mean ± SD, n=2) grown in DMEM (10% FCS at 37°C in 5% CO_2) for 9 days

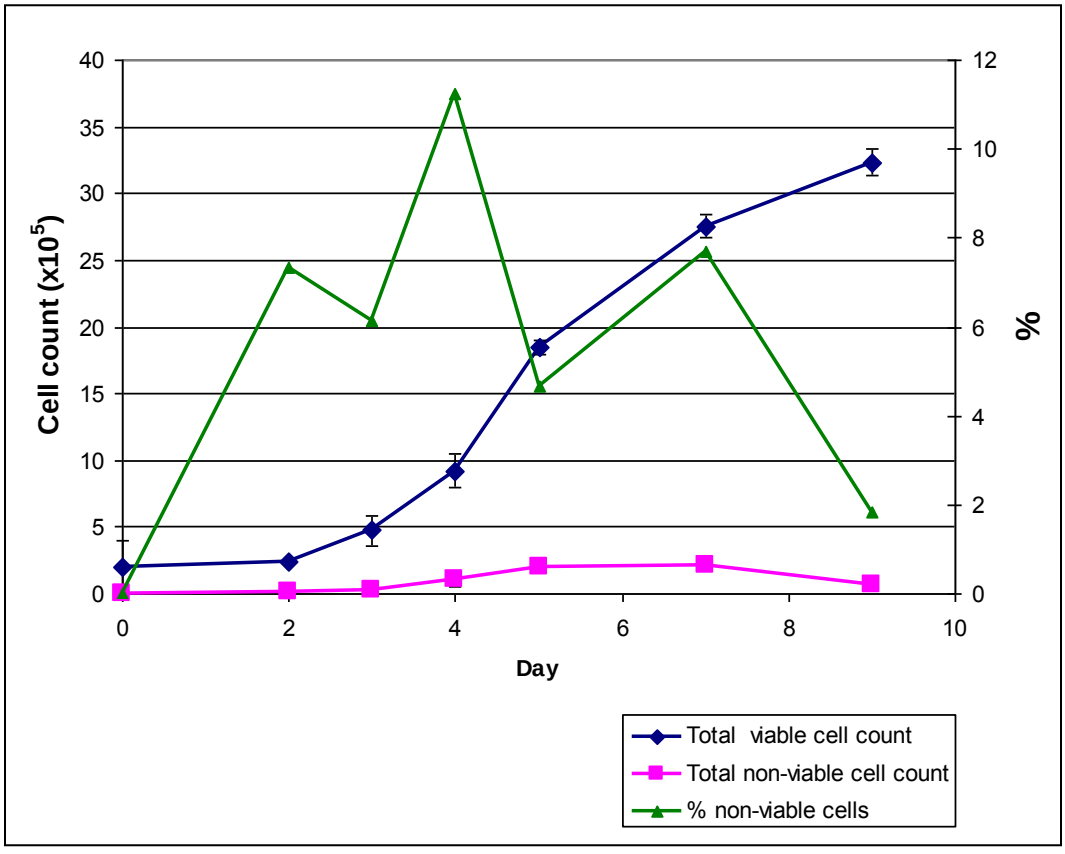

Figure 3.5: Attached H400 cells grown in cell culture flask for 6 days and viewed using an inverted microscope

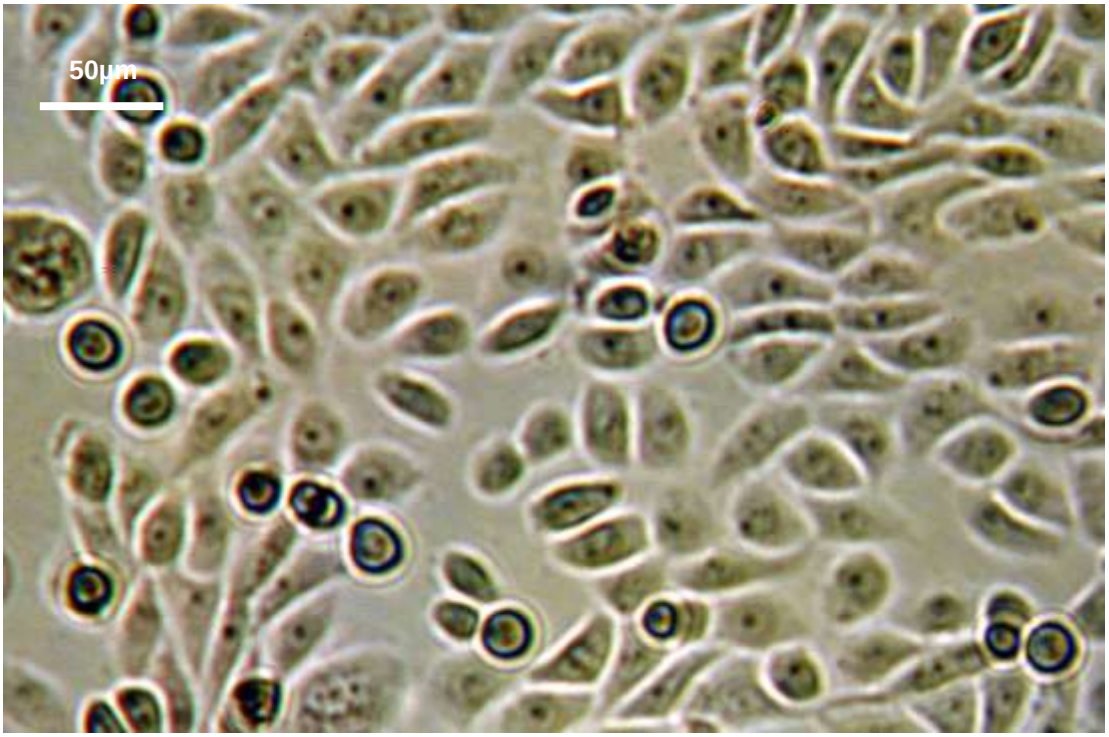

Figure 3.6: Changes in media pH (mean ± SD, n=2 per time point) during H400 cell growth in DMEM (10% FCS at 37°C in 5% CO_2)

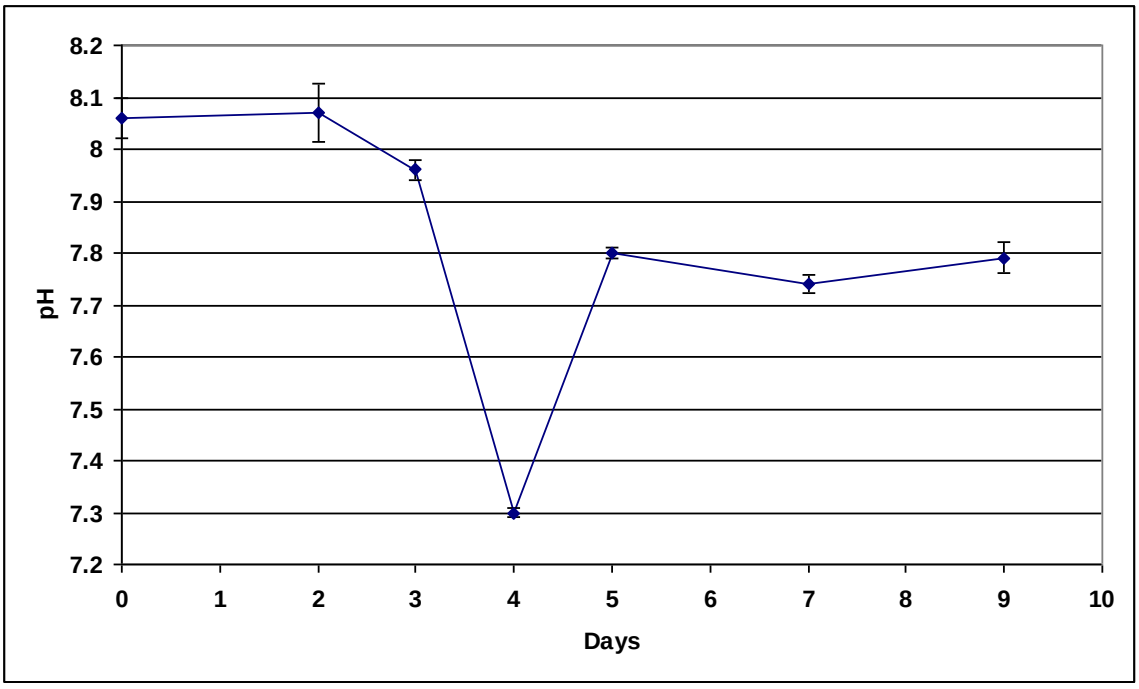

Figure 3.7: Unattached cell count for H400 cells (10% FCS at 37°C in 5% CO_2) grown for 9 days (mean ± SD, n=2 per time point)

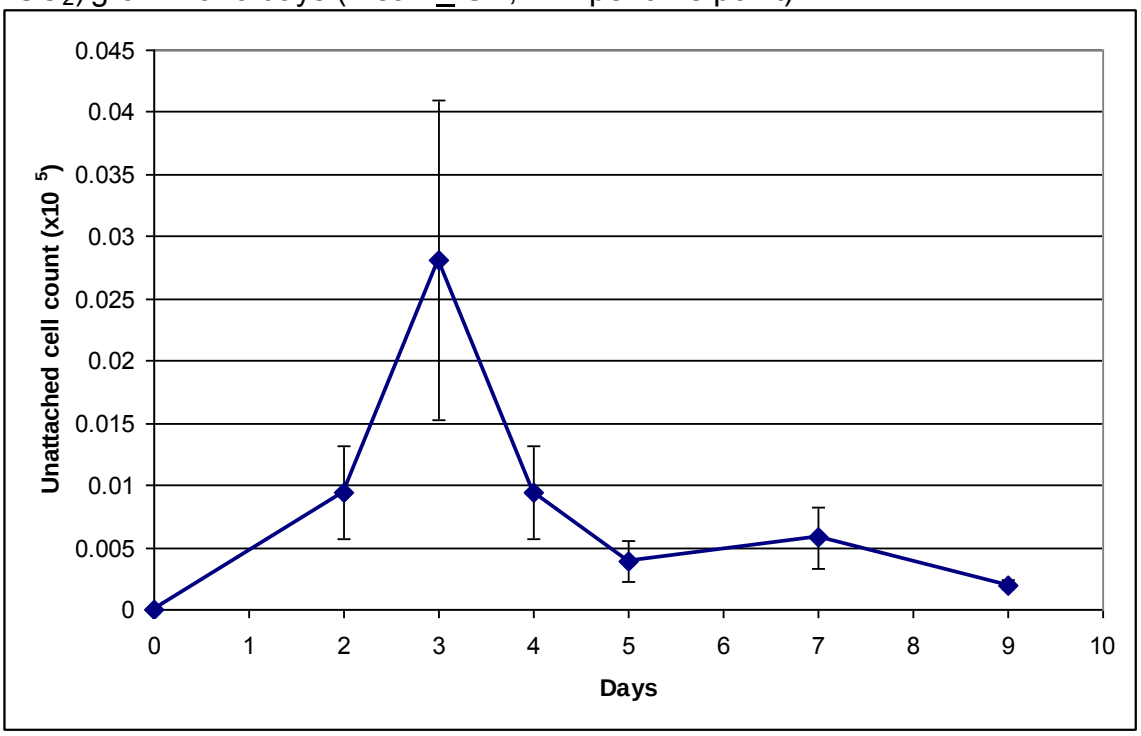

Figure 3.8: H400 cells cultured on glass slides. **A**: initial inoculum of $3x10^5$ cells incubated for 5 days; **B**: initial inoculum of $4x10^5$ cells incubated for 5 days.

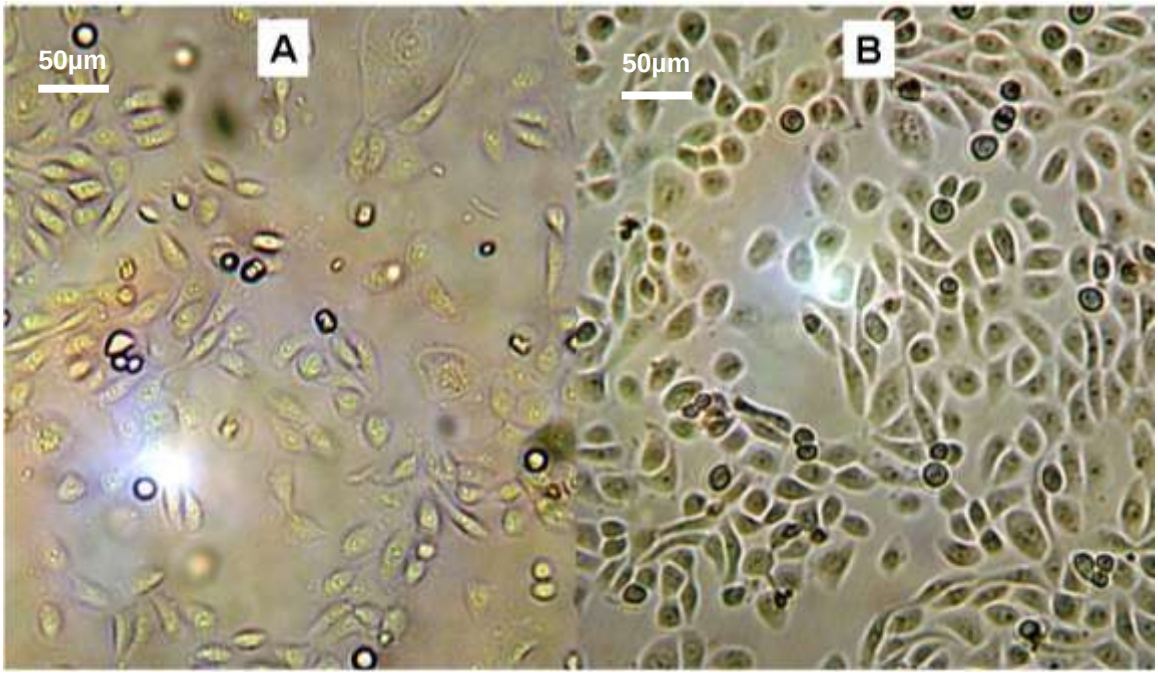

Table 3.1: H400 cells cultured on glass multi-well slides, showing time to reach confluence with varying initial inoculum

Initial inoculum	Days to reach 80% confluence
$3x10^5$	6
$4x10^5$	5
$5x10^5$	4-5

Figure 3.9: H400 cells immuno-cytochemically stained for NF-κB; image **A:** un-stimulated control (NF-κB staining localised in the cytoplasm); image **B** *E.coli* LPS (20μg/ml for 1 hour) stimulated (NF-κB staining localised to the nucleus).

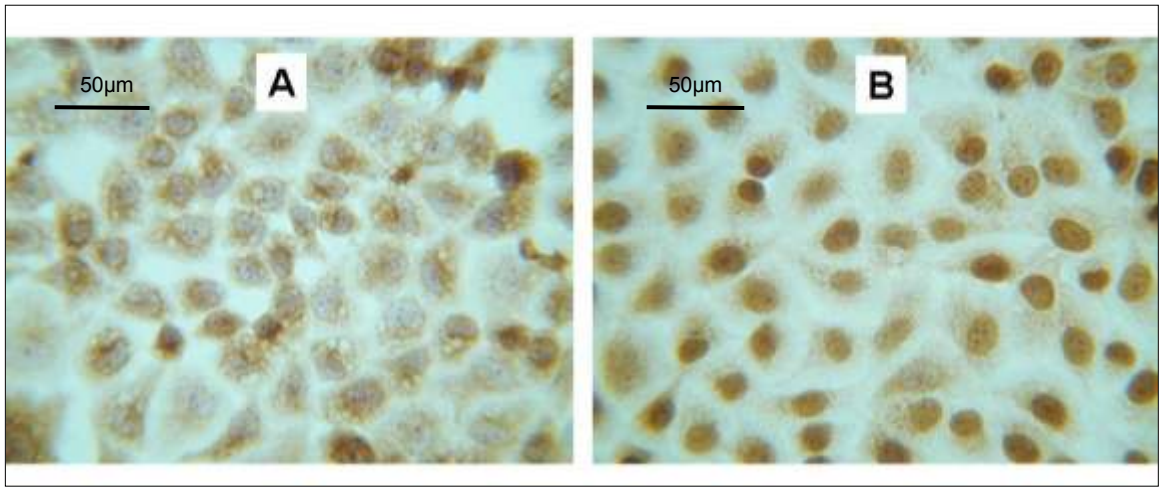

Figure 3.10: Percentage of H400 cells (mean ± SD, n=4) exhibiting NF-κB translocation following stimulation with 10µg/ml *E. coli* LPS for 1 hour.

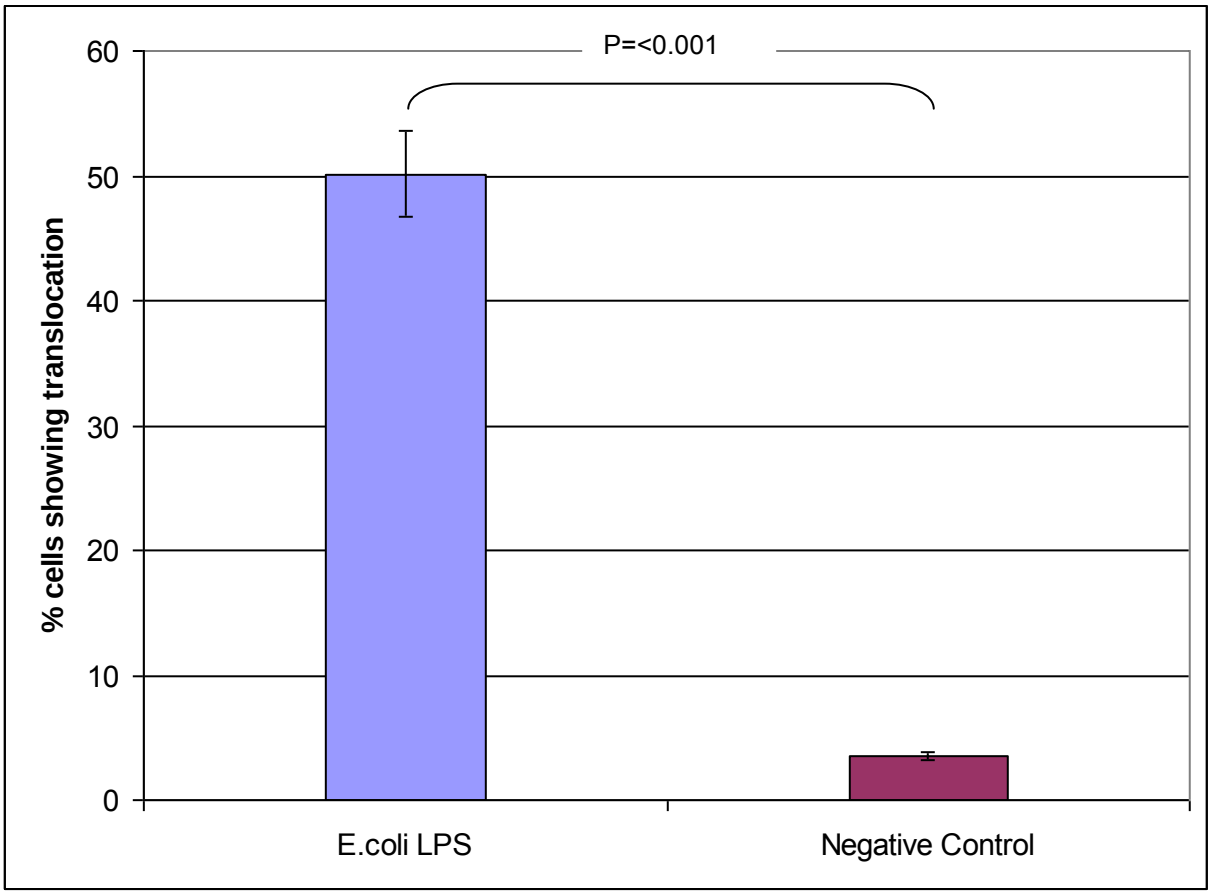

Figure 3.11: H400 cells stimulated with *E. coli* LPS (10µg/ml) at varying time points, showing % NF-κB translocation (mean ± SD, n=4).

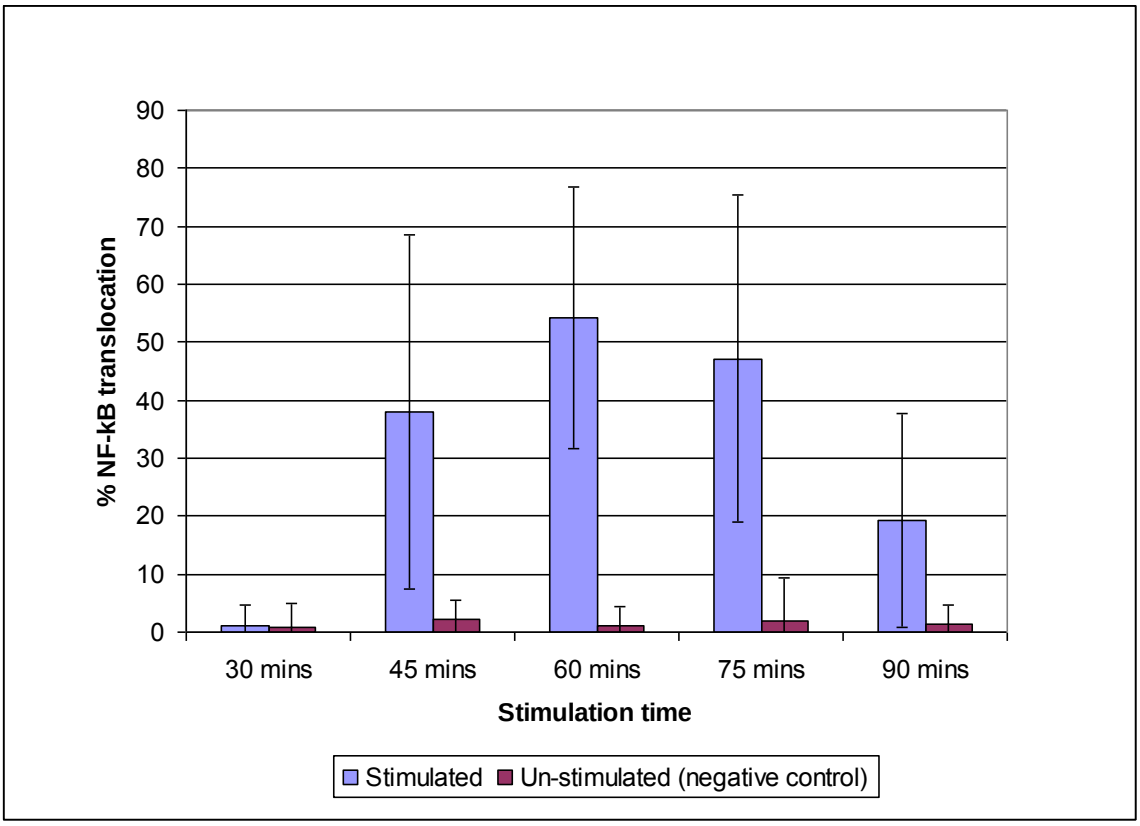

Figure 3.12: H400 cells stimulated for 1 hour with two concentrations of *E. coli* LPS (mean ± SD, n=4).

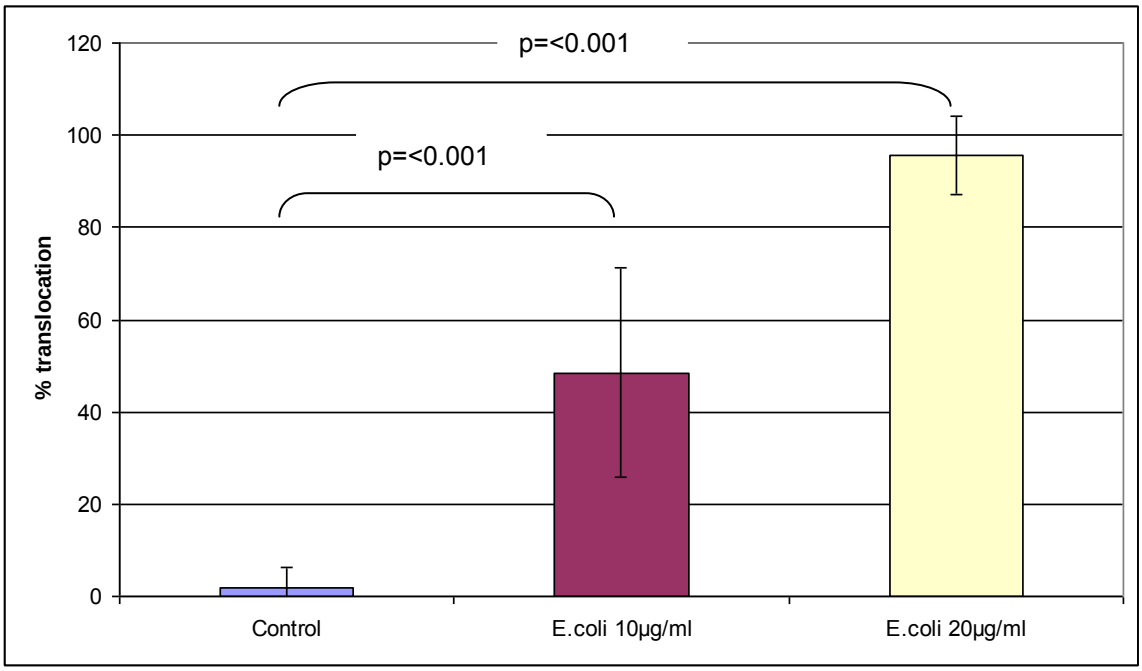

Figure 3.13: Effect of level of cell confluence on NF-κB activation in H400 cells ± stimulation *with E. coli* LPS (20µg/ml) mean ± SD n=4.

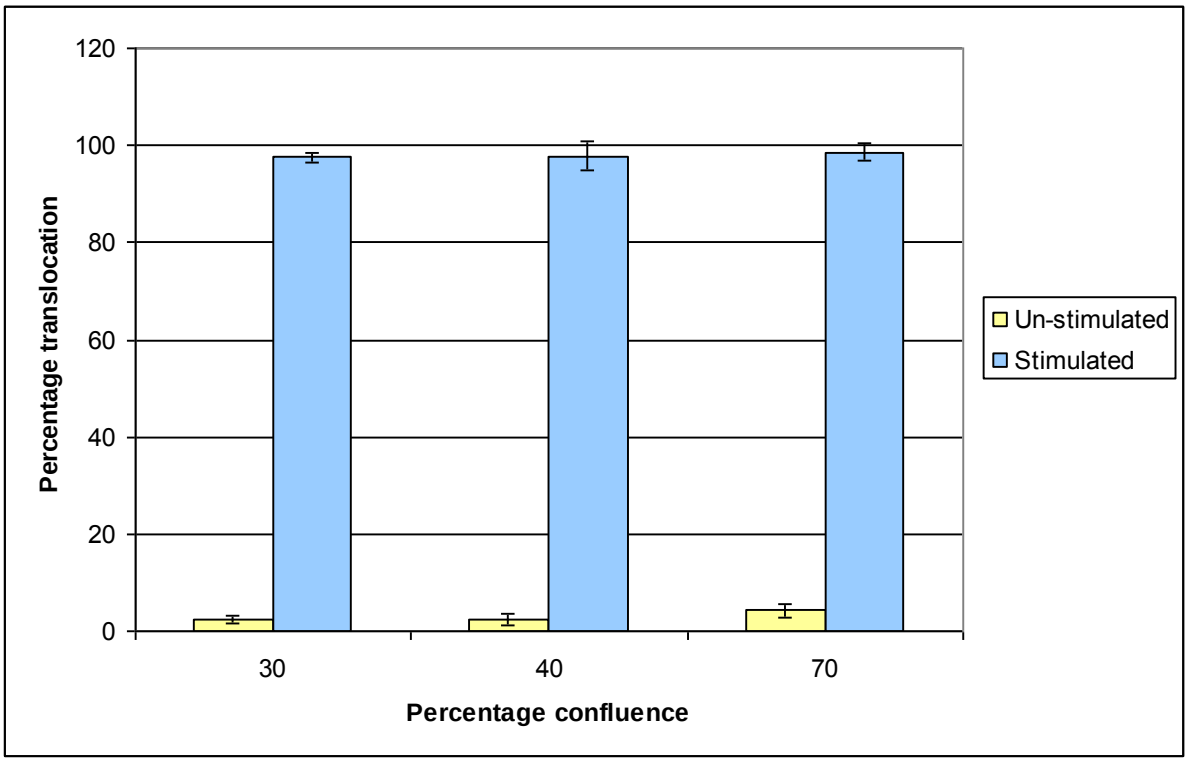

Figure 3.14: NF-κB translocation in H400 cells ± stimulation with *E. coli* LPS (20µg/ml) mean ± SD n=4.

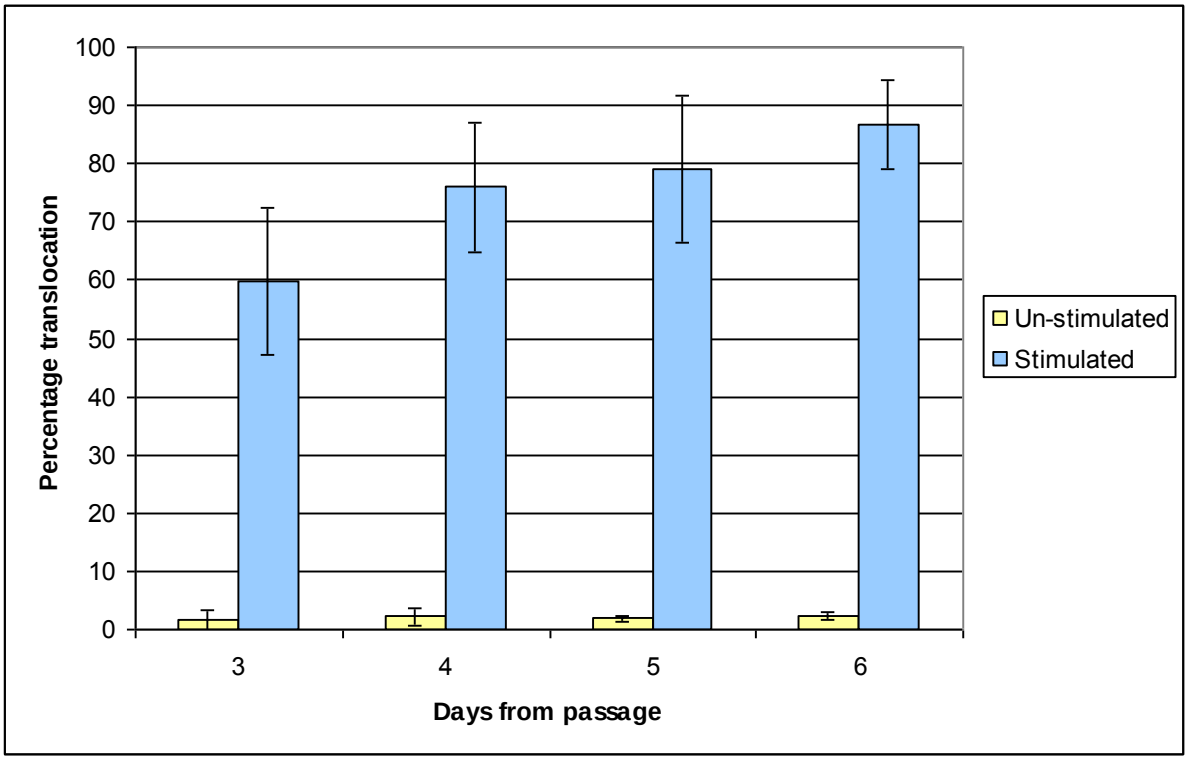

Figure 3.15: Percentage translocation of NF-κB in H400 cells ± 1 hr stimulation with whole dead bacteria (mean ± SD n=4).

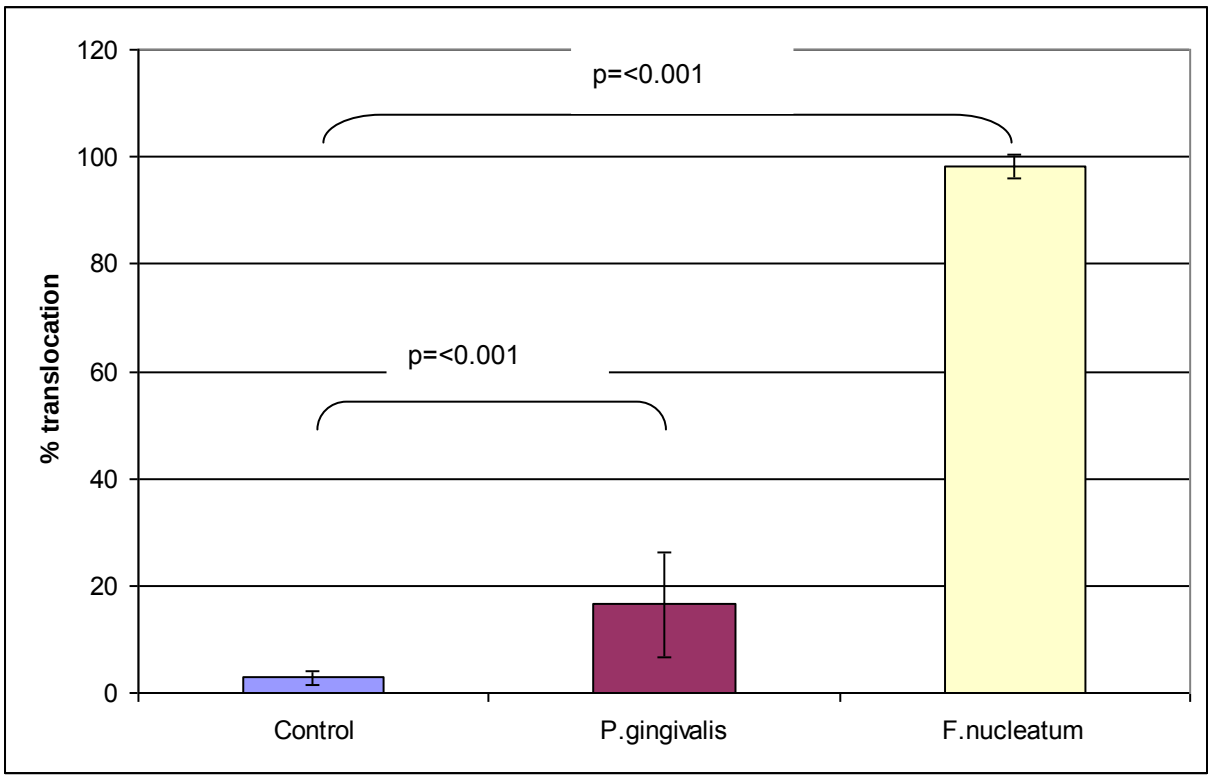

Figure 3.16: Relative expression of nuclear vs. cytoplasmic NF-κB in H400 cells ± 1 hr stimulation by high throughput immuno-cytochemical analysis (mean ± SD n=4).

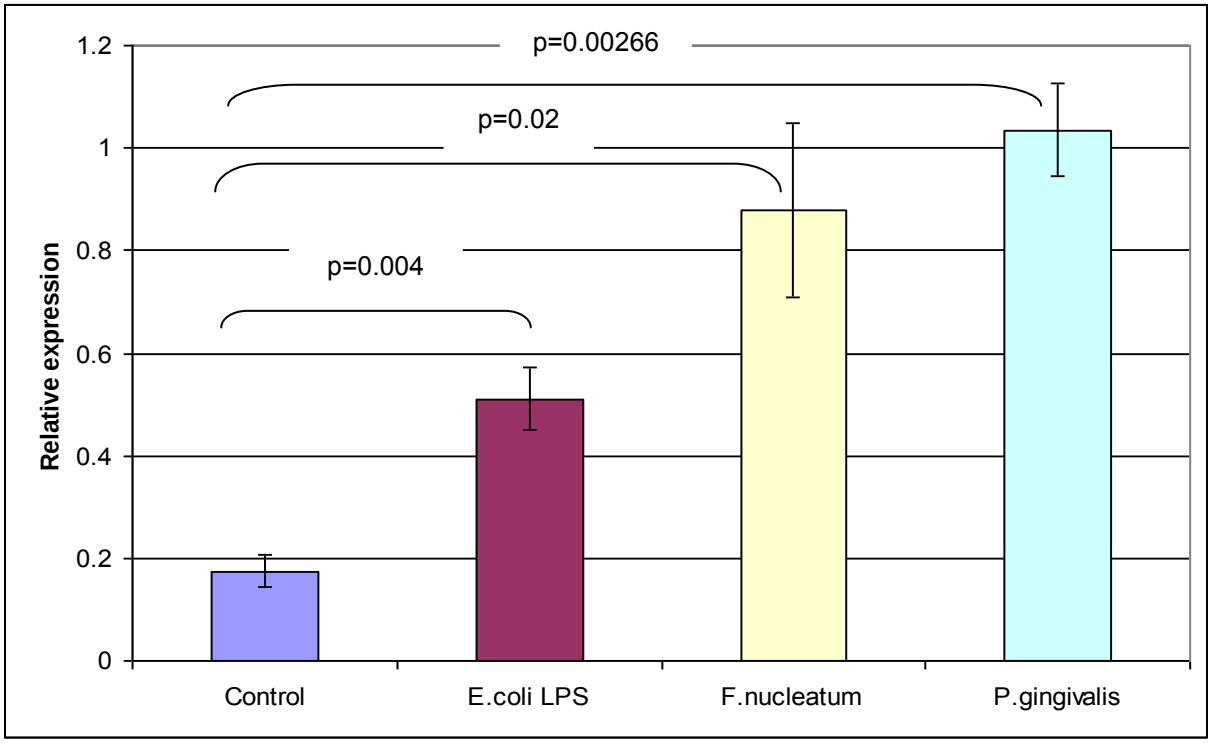

Figure 3.17: Nuclear to cytoplasmic ratio of NF-κB in H400 cells ± stimulation with *P. gingivalis* & *F. nucleatum* over time using high throughput Immuno-cytochemistry (mean ± SD, n=3)

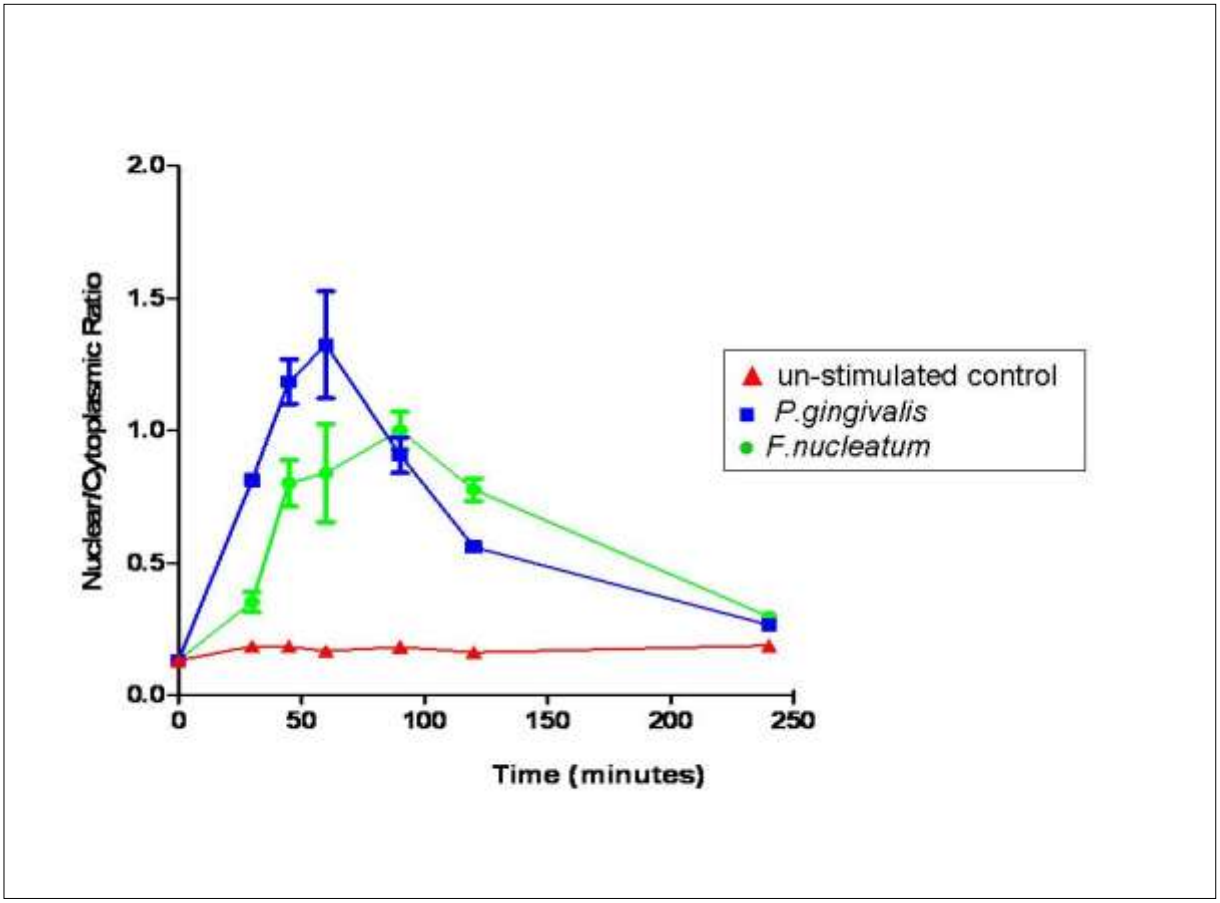

Figure 4.1: Adherent cell count for H400 cells incubated from initial seeding with DMEM supplemented with 1mM α-lipoate (red lines; n=2) or no α-lipoate (blue lines; n=2) (Error bars not included as n=2)

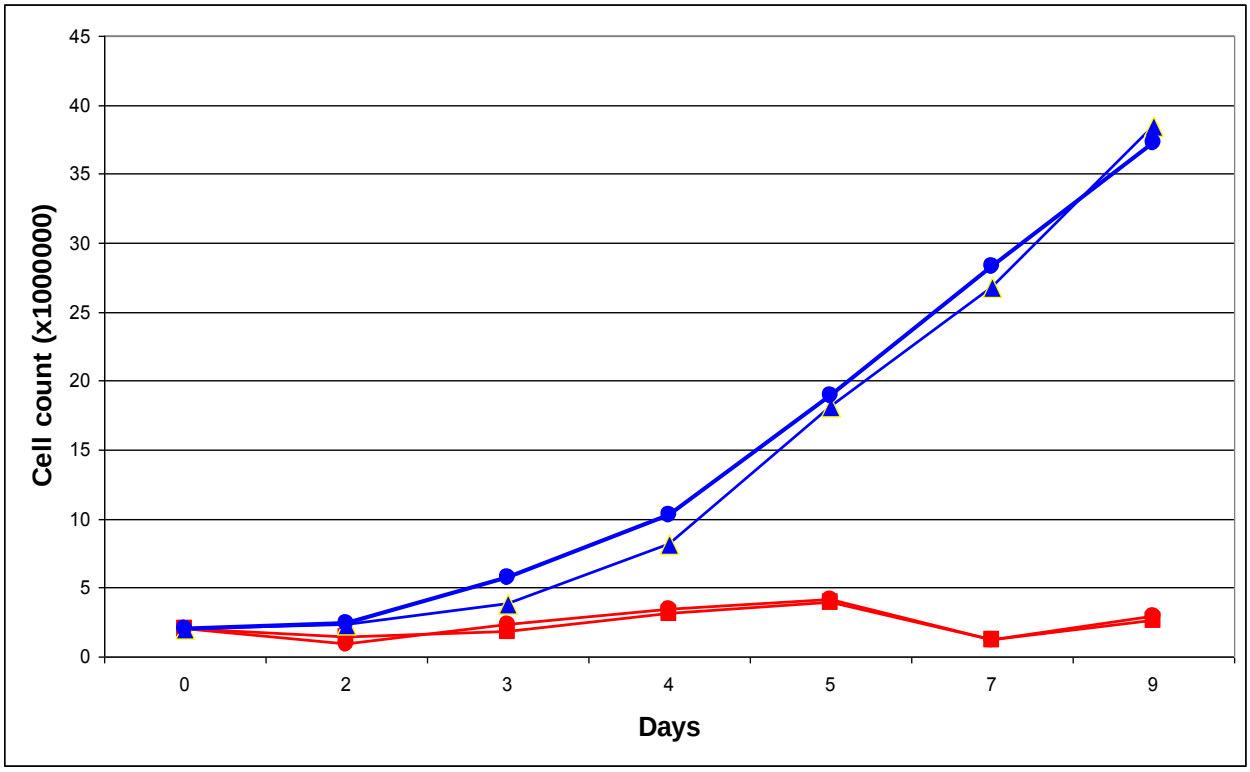

Figure 4.2: Non adherent cell count for H400 cells seeded into DMEM supplemented with 1mM α-lipoate (red lines) or no α-lipoate (blue lines) (Error bars not included as n=2)

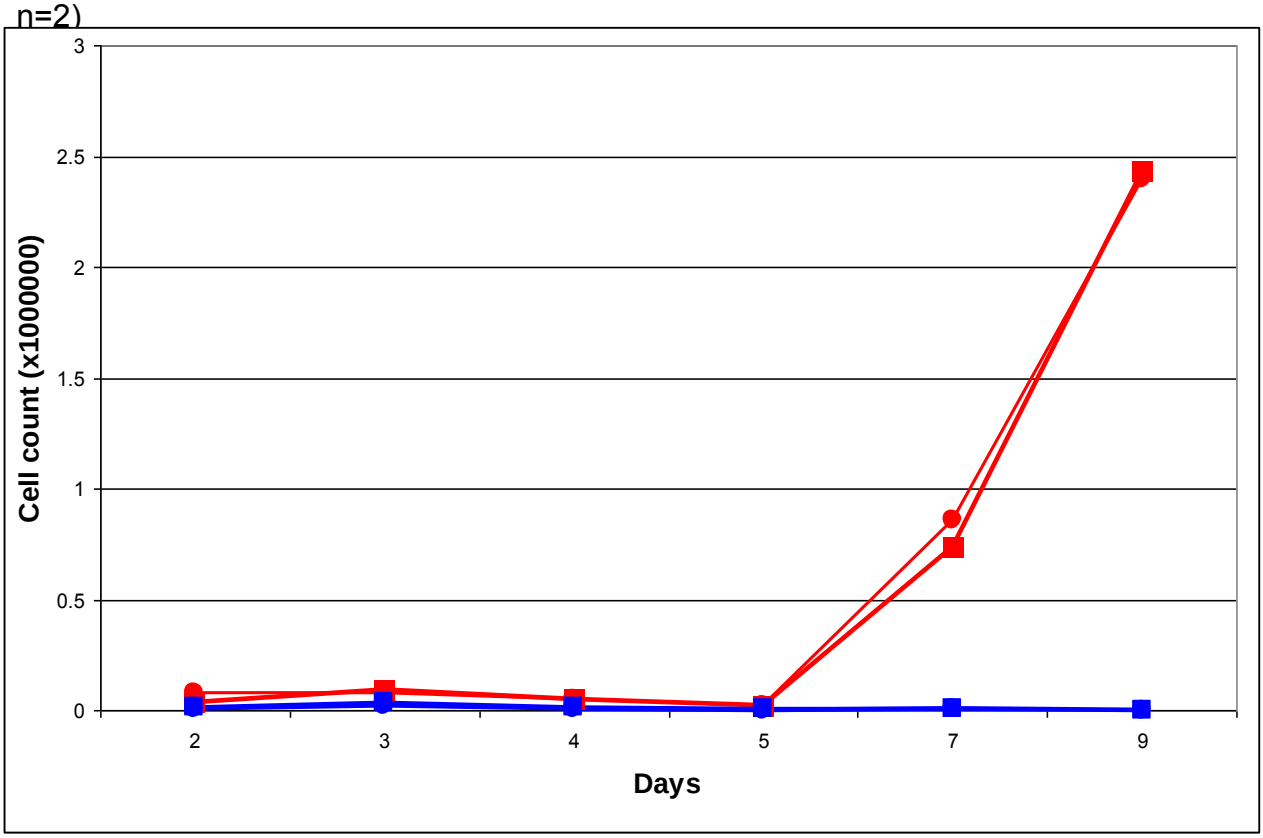

Figure 4.3: Cell viability (trypan blue exclusion) of non attached H400 cells supplemented with 1mM α-lipoate (red lines) or no α-lipoate (blue lines) (Errors not included as n=2)

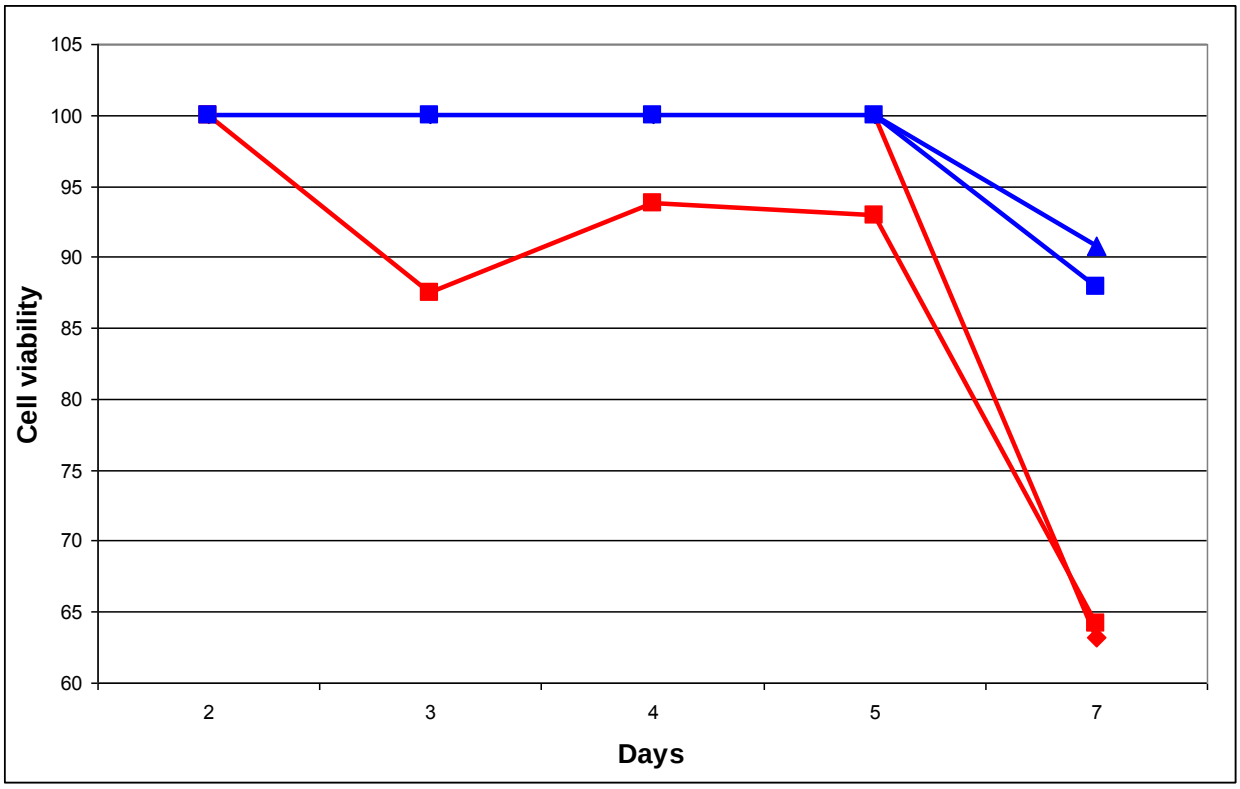

Figure 4.4: Cell viability (trypan blue exclusion) of adherent H400 cells supplemented with 1mM α-lipoate (red lines; n=2) or no α-lipoate (blue lines; n=2)

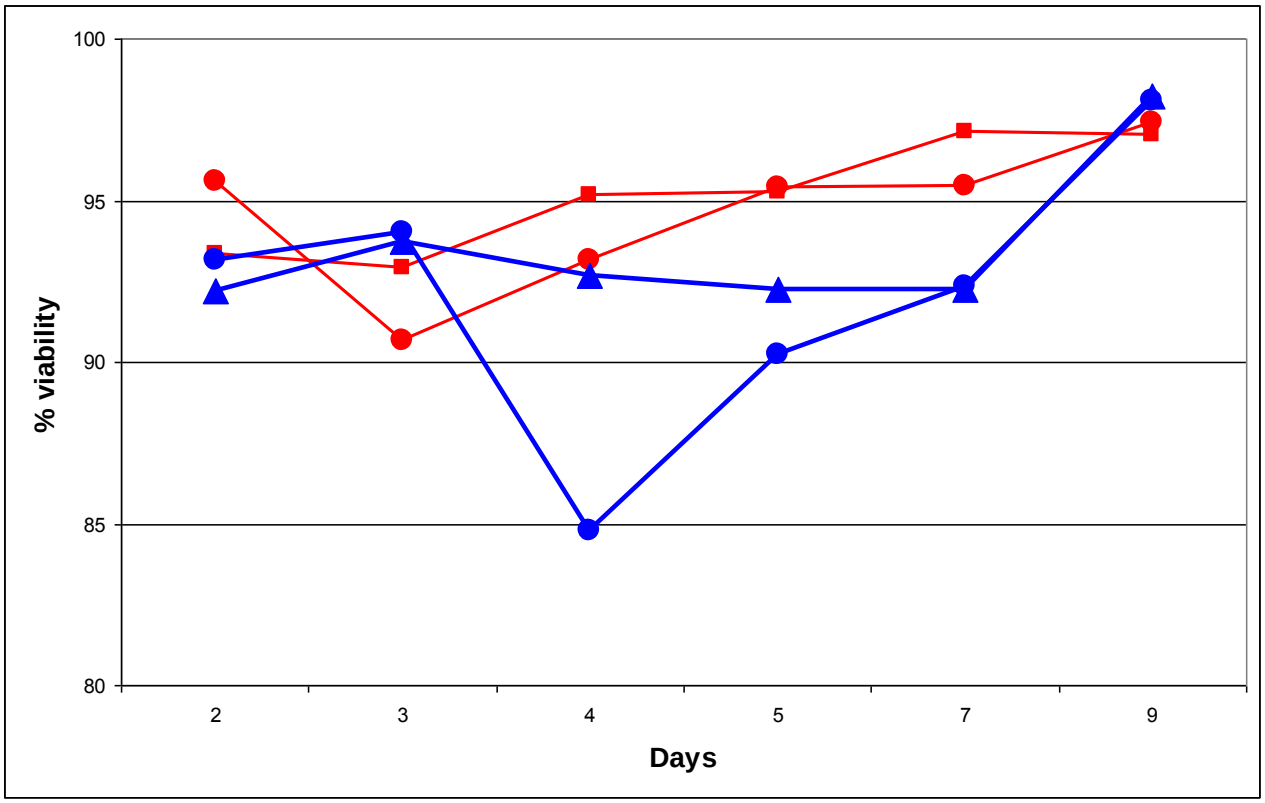

Figure 4.5: H400 cells incubated for 24h with **A**: control solution (negative control); **B**: 4mM α-lipoate.

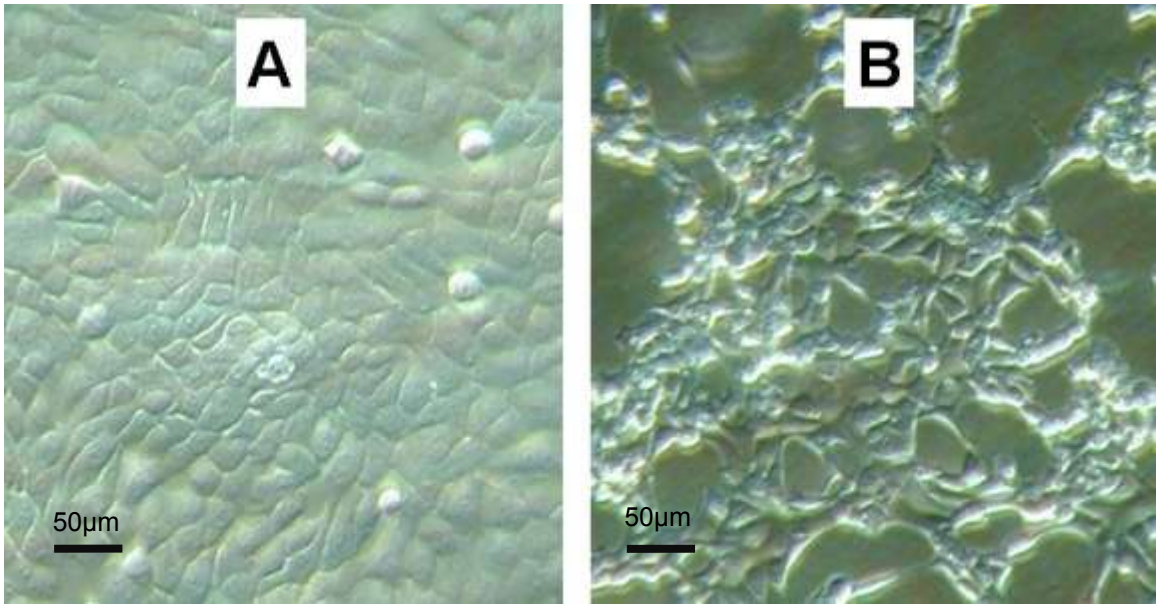

Figure 4.6: Adherent H400 cells exposed to varying α-lipoate concentrations (n=2 per concentration) each value plotted and the mean

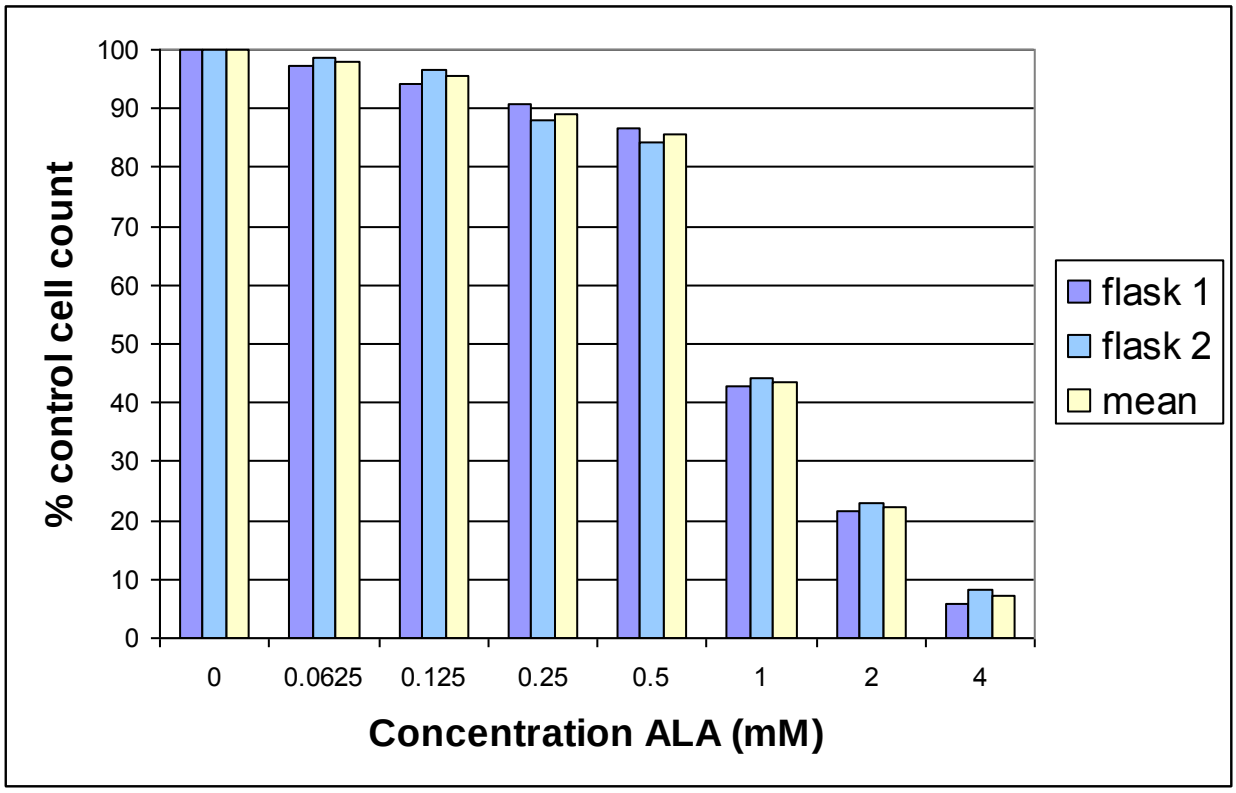

Figure 4.7: Agarose gel electrophoresis of H400 cells exposed to α-lipoate for 24h (n=2; samples from each concentration pooled)

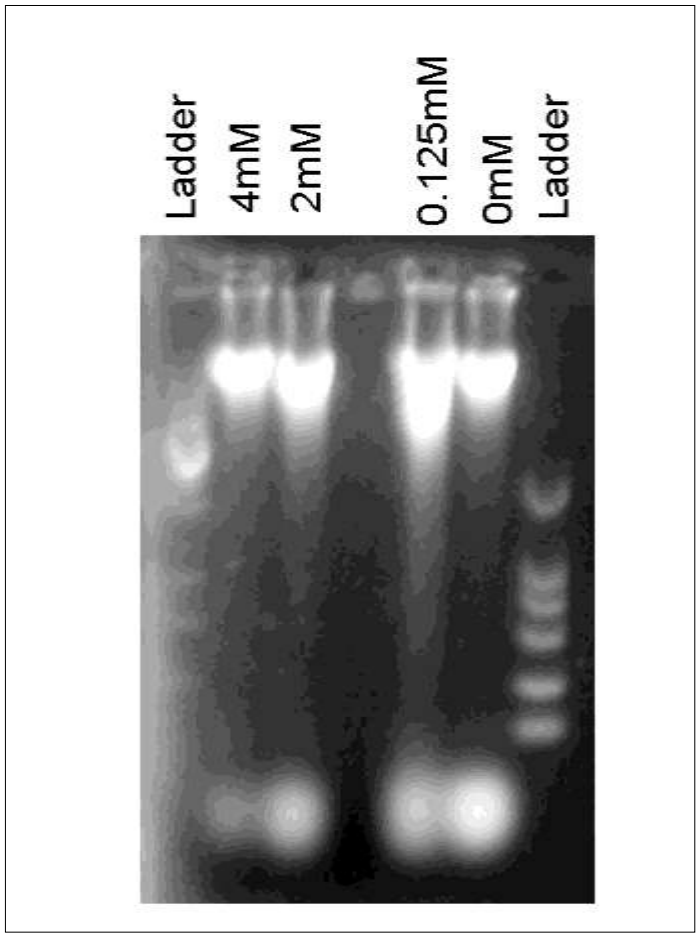

Figure 4.8: Immuno-cytochemical images of H400 cells stained for caspase 3 A= no α-lipoate; B= 1mM α-lipoate for 48h. Caspase positive cell stain red.

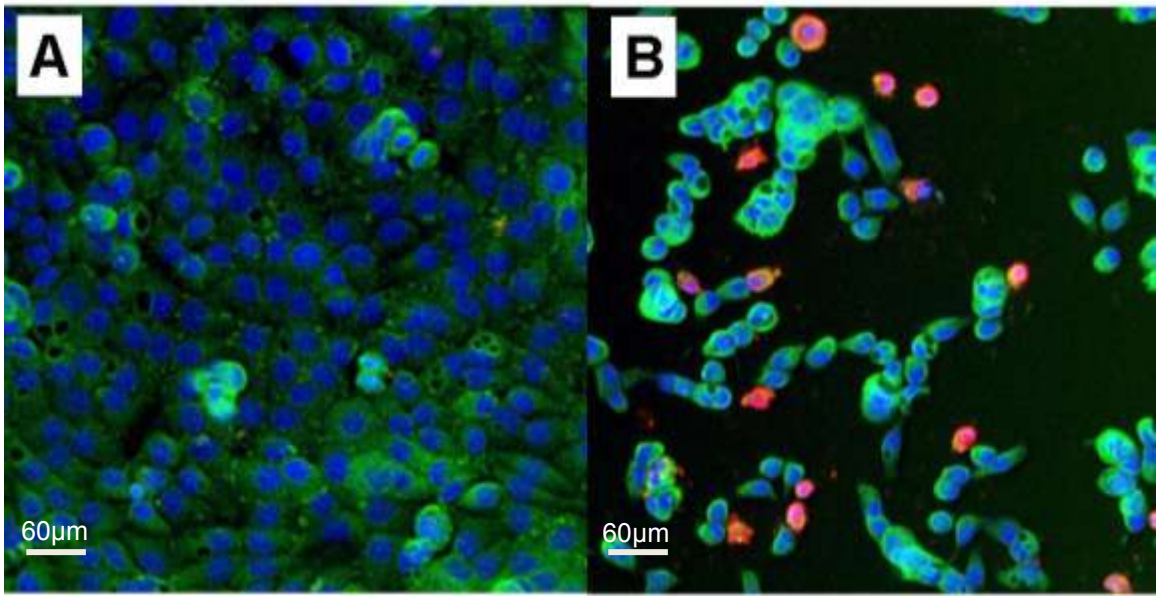

Figure 4.9: Levels of caspase 3 activity in H400 cells incubated for 48h with α-lipoate (mean ± SD; n=3) (* p=0.039)

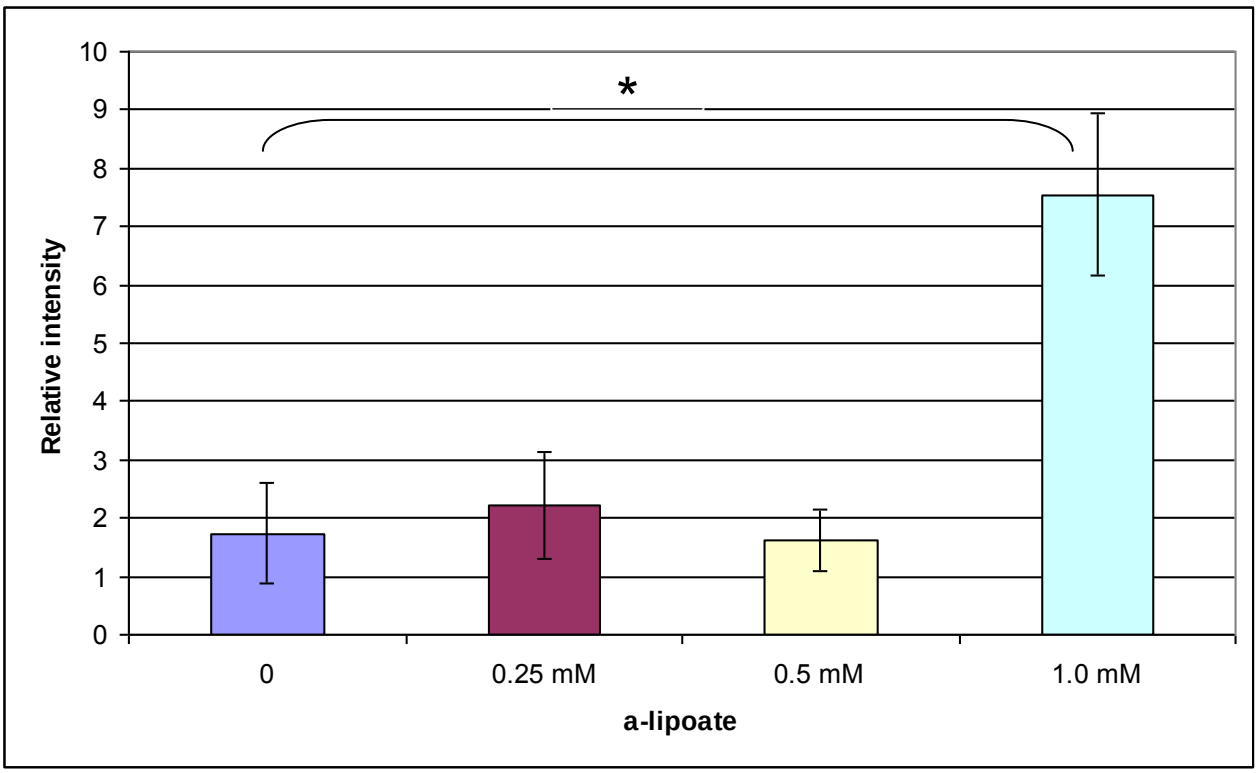

Figure 4.10: Photo-micrograph demonstrating the effect of calcium chloride concentration on attached H400 cell morphology / cell attachment when incubated ± 1mM α-lipoate.

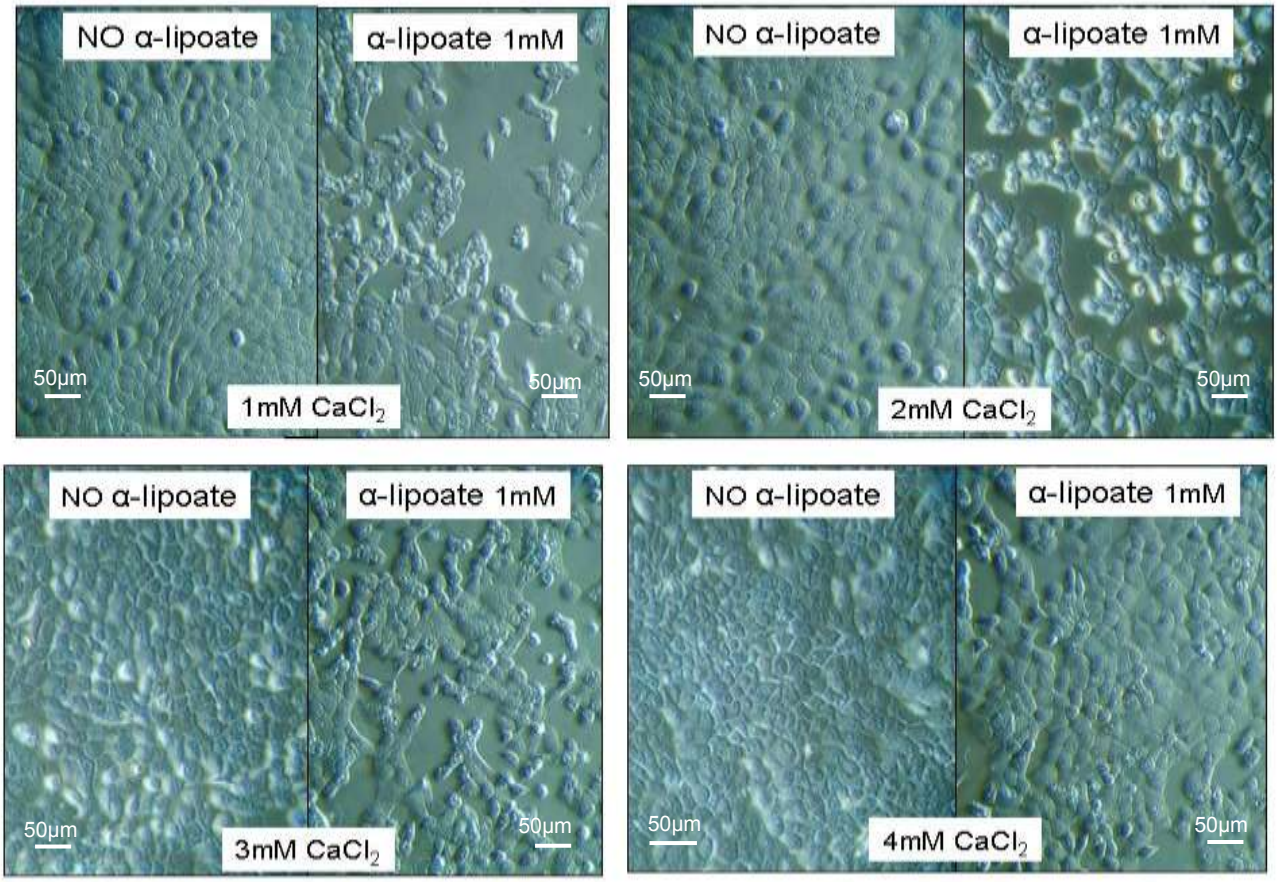

Figure 4.11: Effect of calcium chloride concentration on attached H400 cell count when incubated ± 1mM α-lipoate (n=2; each value and mean plotted)

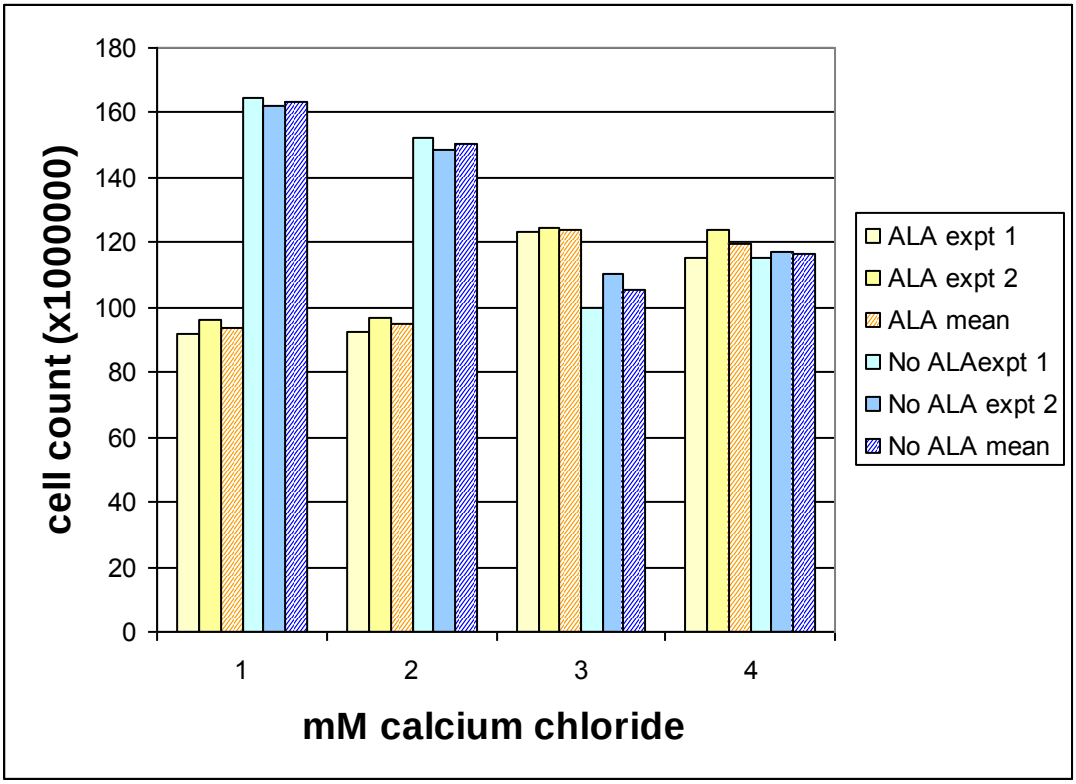

Figure 4.12: H400 cells pre incubated +/- 4mM α-lipoate for 1h, stimulated +/- 20µg/ml *E.coli* LPS for 1hour. (mean % NF-κB translocation ± SD; n=3)

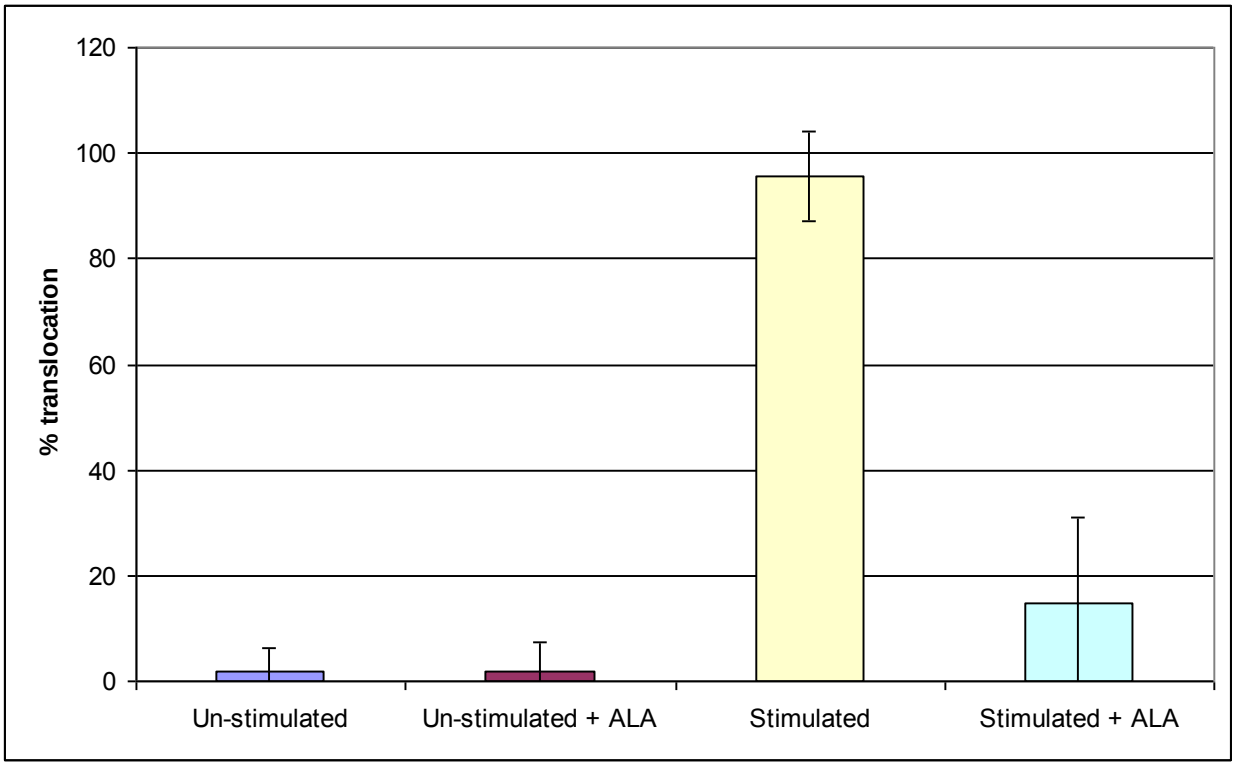

Figure 4.13: H400 cells pre-incubated with 0.5mM α-lipoate for 24h prior to stimulation with *E. coli* LPS for 1h (mean ± SD; n=3)

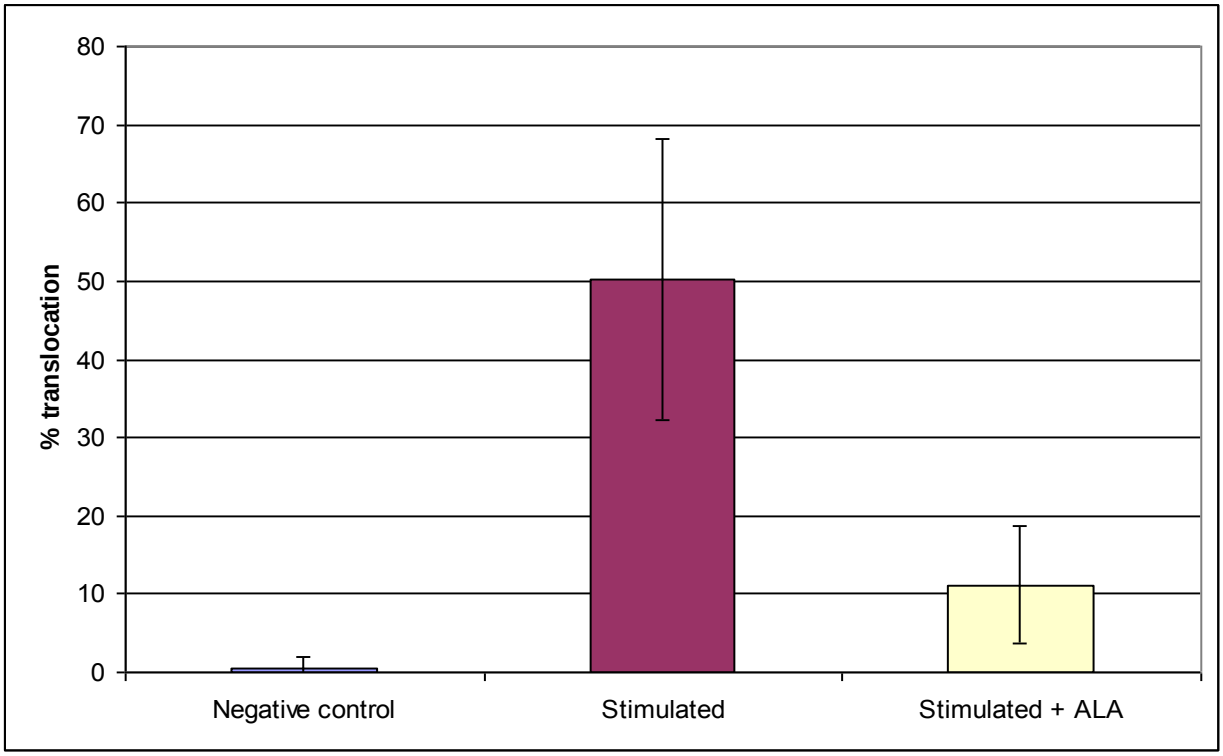

Figure 4.14: H400 cells pre incubated with a range of α-lipoate concentrations for 24h, stimulated with *E.coli* LPS (1h) and immunocytochemically stained for NF-κB. (Negative control is a staining control; no NF-κB monoclonal antibody)

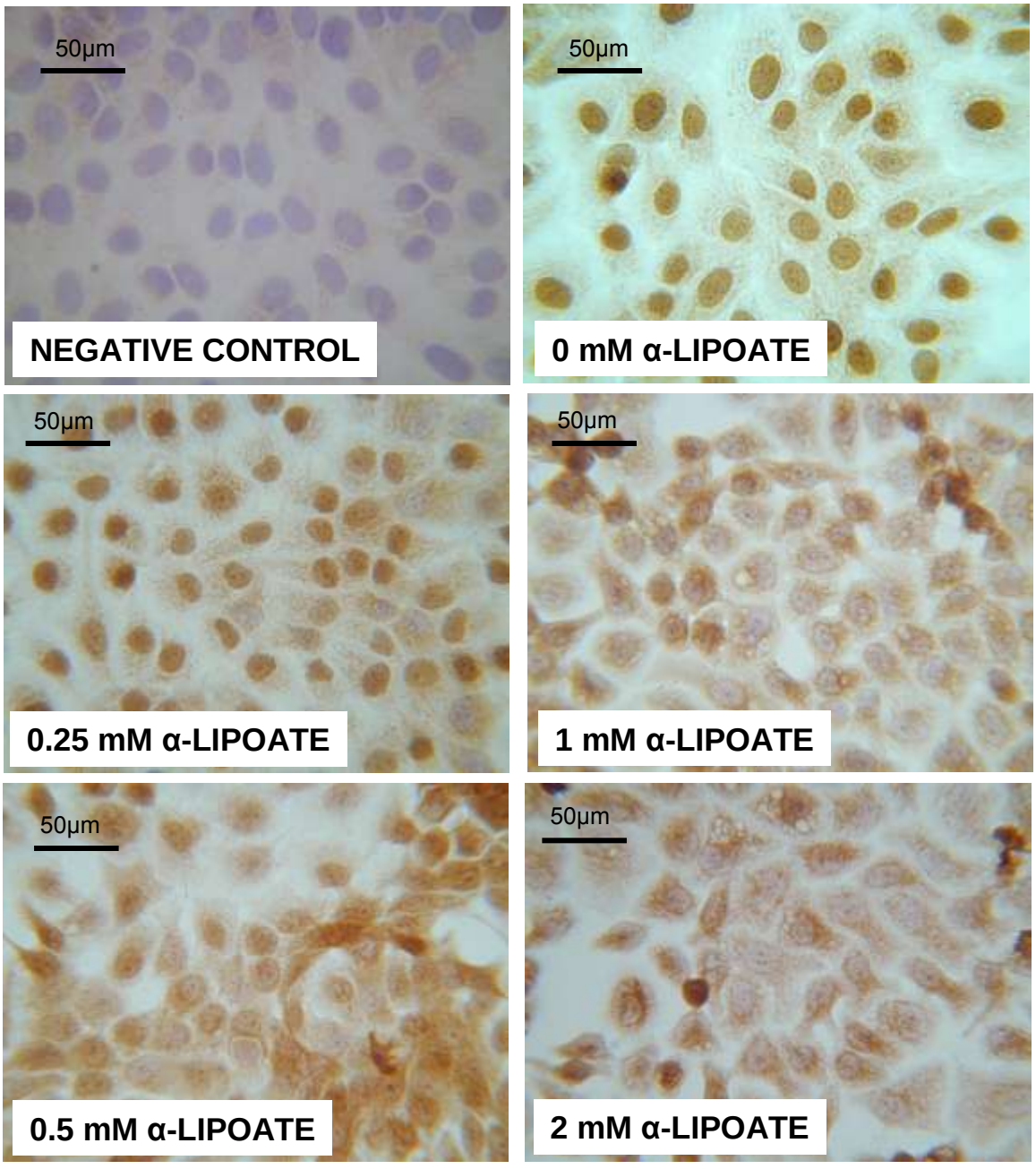

Figure 4.15: H400 cells incubated with a range of α-lipoate concentrations and stimulated with *E.coli* LPS. (n=2, therefore each value and mean plotted)

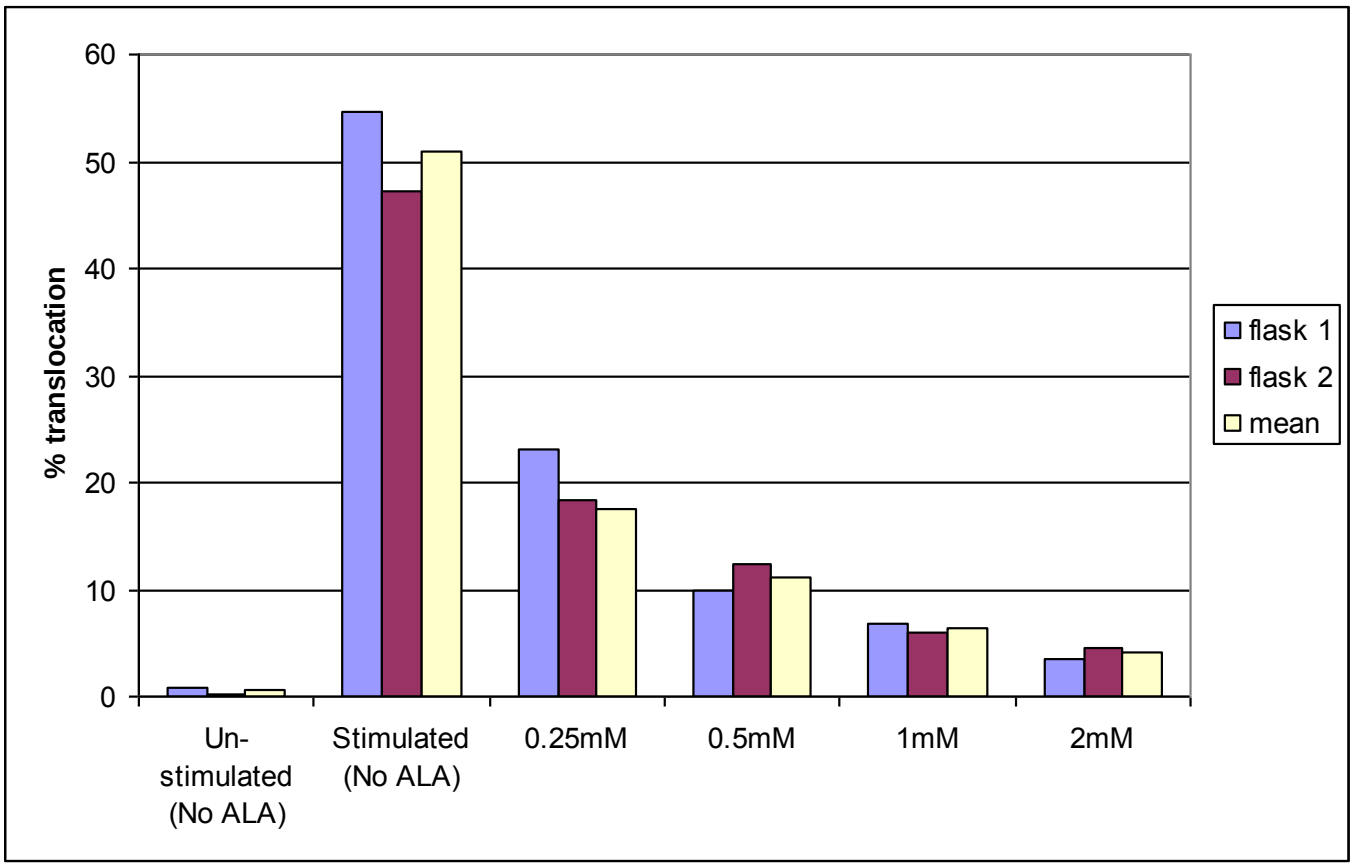

Figure 4.16: A: Images of florescent immuno-cytochemical (high throughput) analysis of H400 cells stimulated with *P. gingivalis* +/- α-lipoate. ***B:*** Diagrammatic representation of colour changes seen.

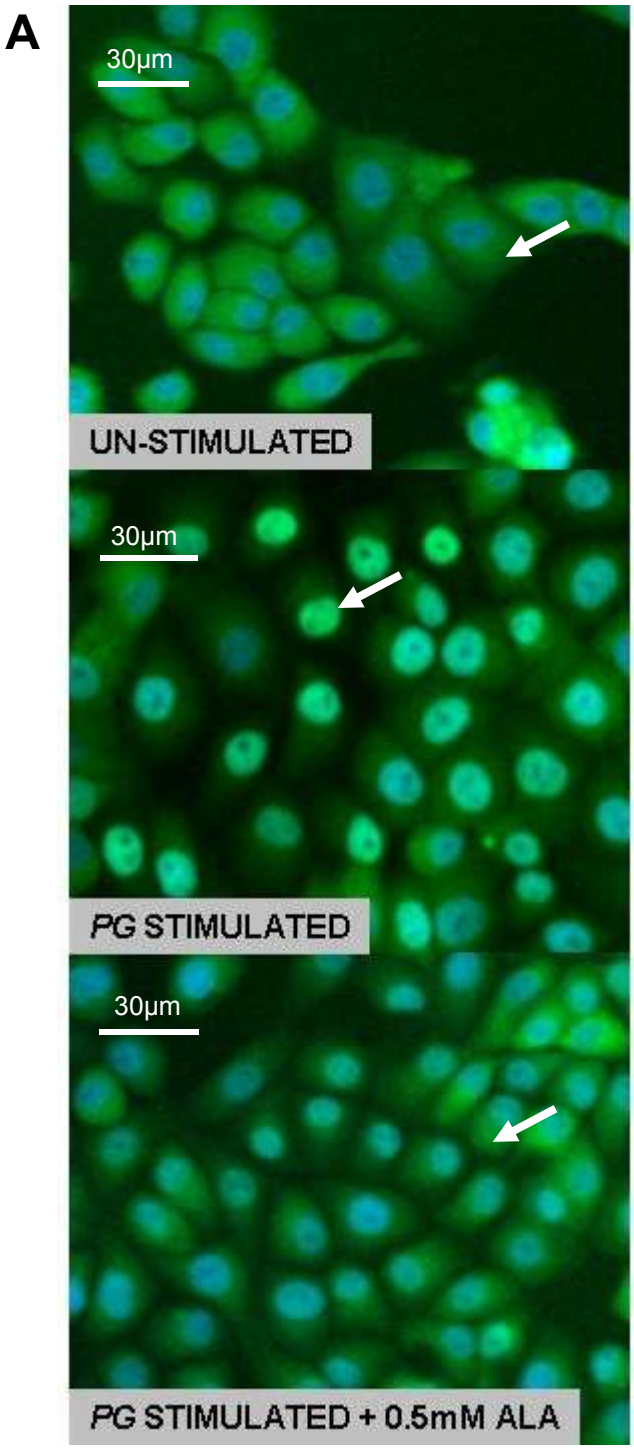

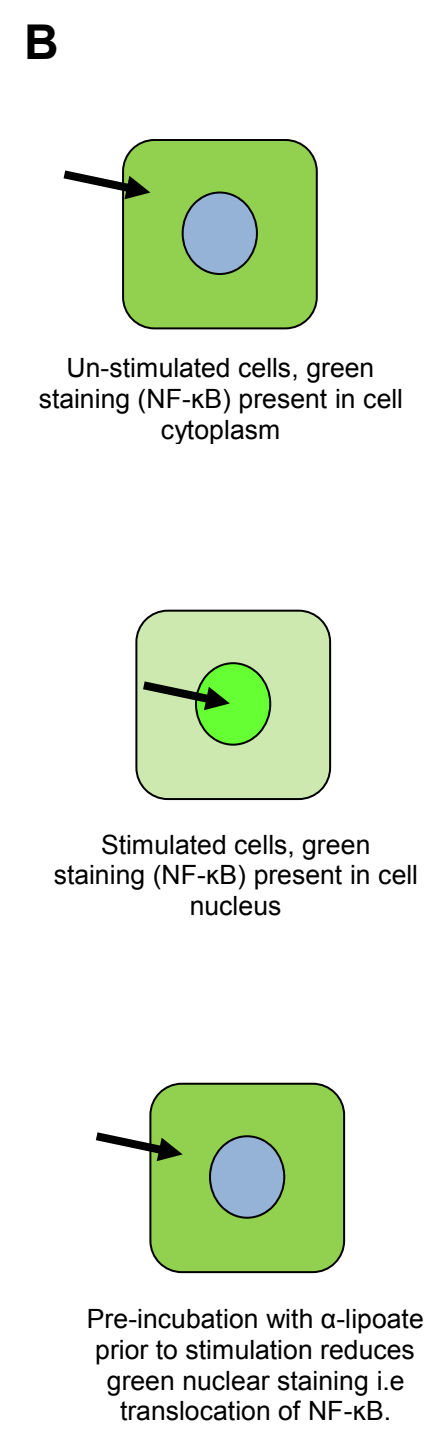

Figure 4.17: Quantitative analysis of high throughput immunocytochemical analysis of H400 cells stimulated with *P. gingivalis* +/- α-lipoate (n=3 ± SD). (* p=0.0016; $^{+}$ p=0.0026)

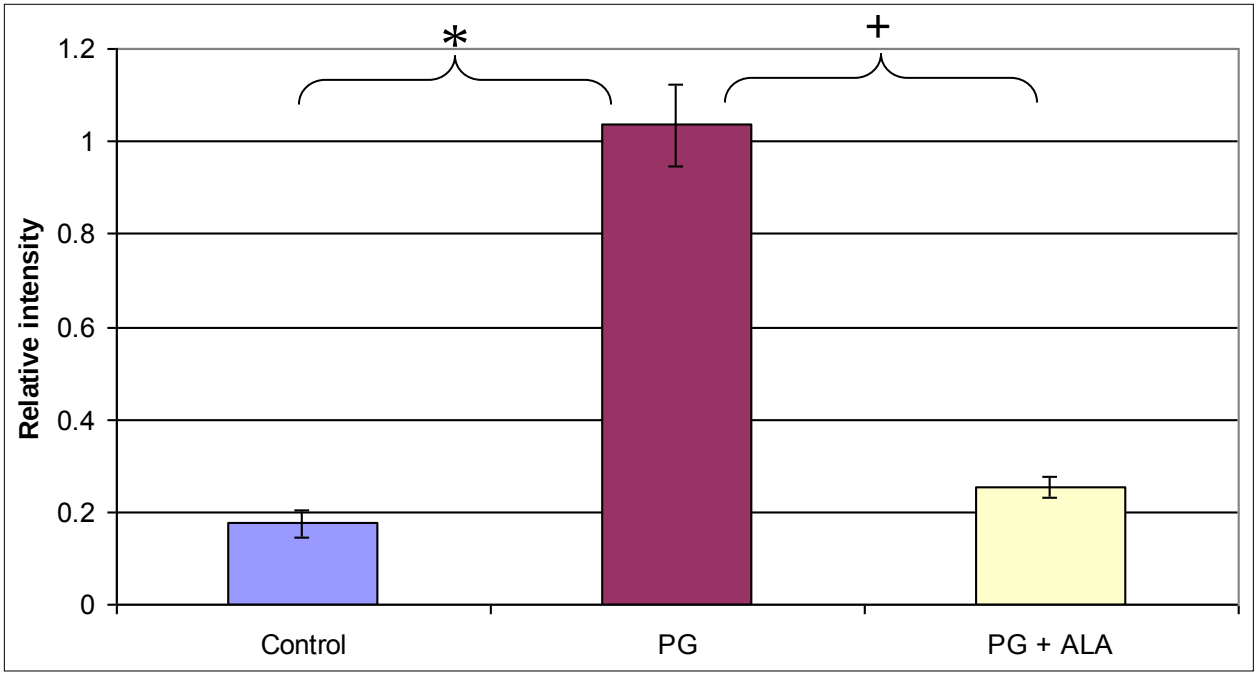

Figure 4.18: A: Fluorescent immuno-cytochemical analysis (high throughput) of H400 cells stimulated with *F. nucleatum* +/- α-lipoate. ***B:*** Diagrammatic representation of colour changes seen.

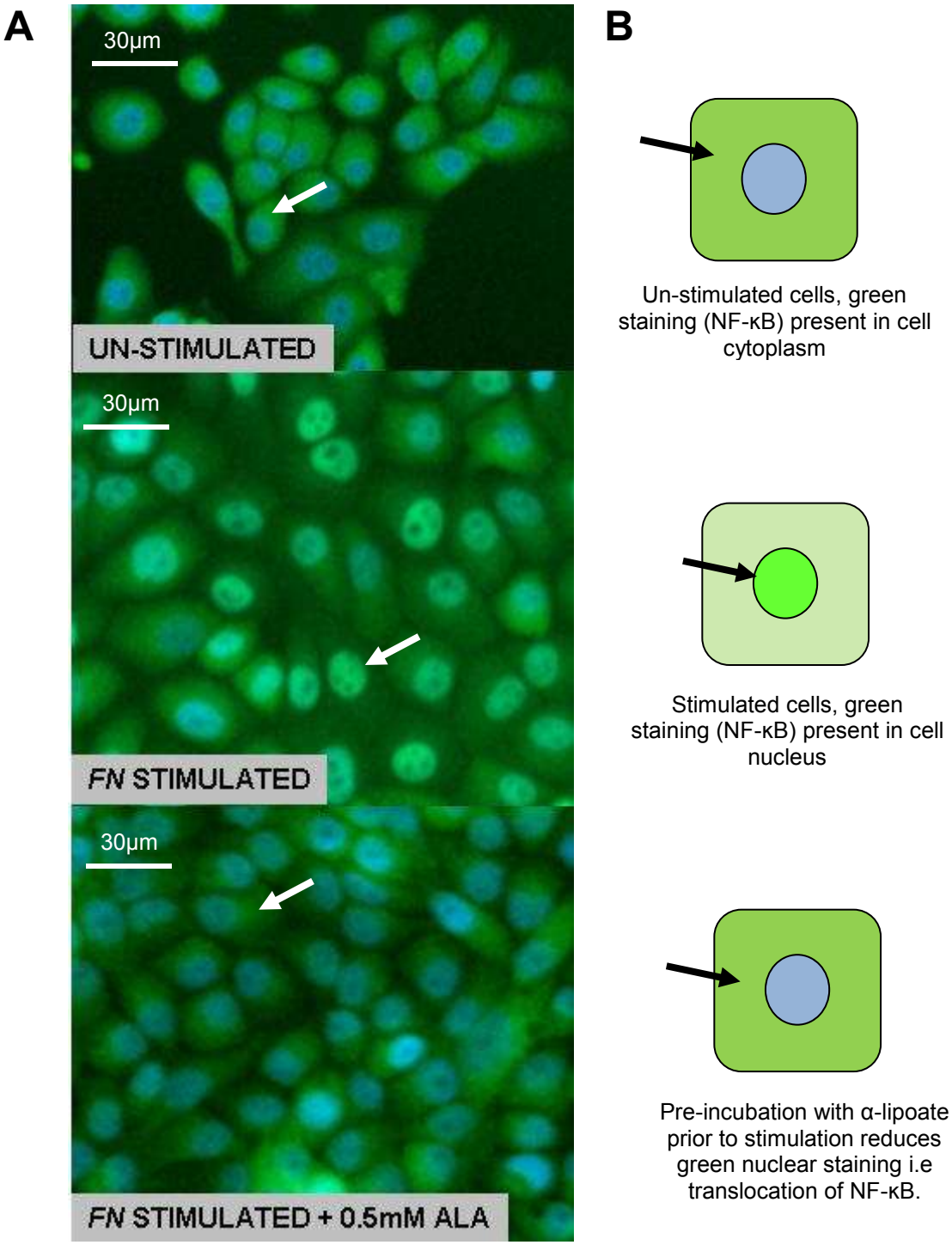

Figure 4.19: Quantitative analysis of high throughput immunocytochemical analysis of H400 cells stimulated with *F. nucleatum* +/- α-lipoate (n=3 ± SD) (* p=0.02; $^{+}$ p=0.008)

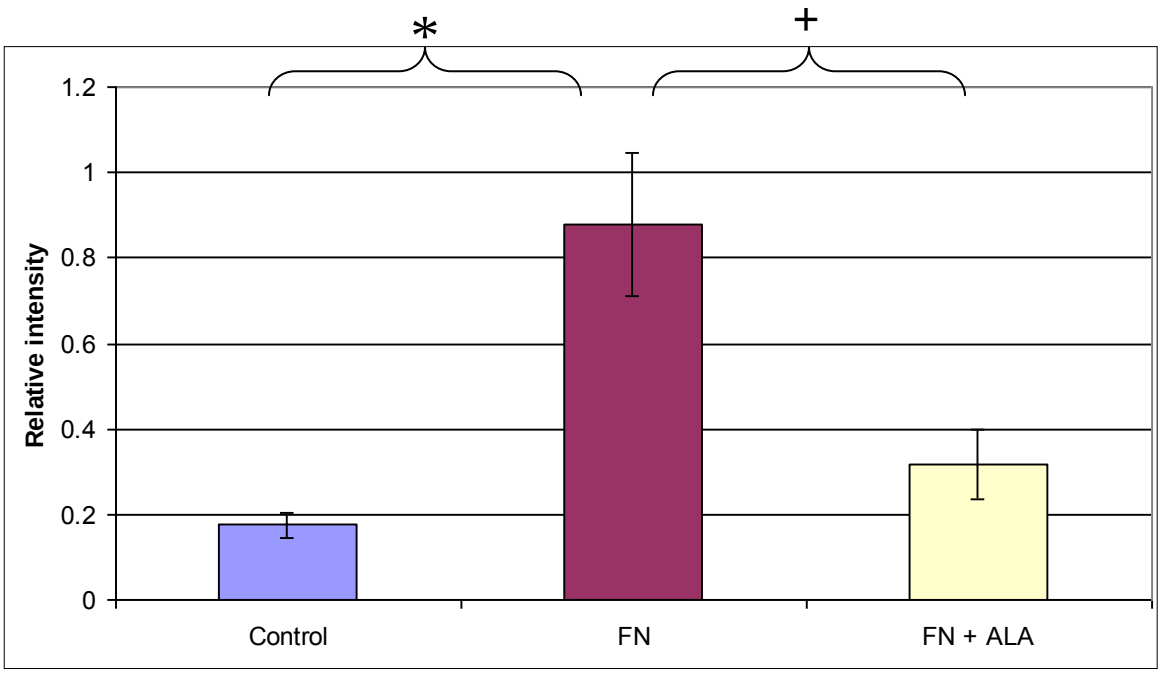

Figure 5.1: Representative gel images of H400 cells stimulated with *F. nucleatum, P. gingivalis* or media for **A**: 24h, **B**: 4h, showing differential expression of pro-inflammatory cytokines

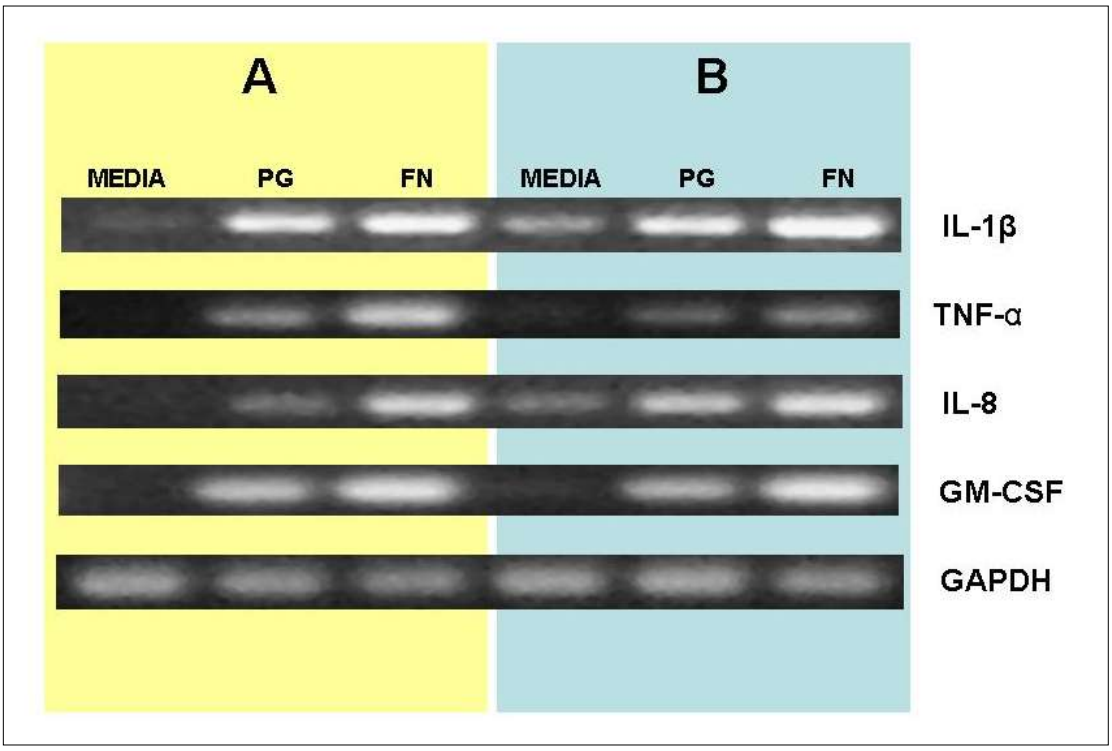

Figure 5.2: Semi quantitative RT-PCR analysis of gel images showing gene expression of H400 cells stimulated with *P. gingivalis*, *F. nucleatum* (or media control) at 4 and 24h.

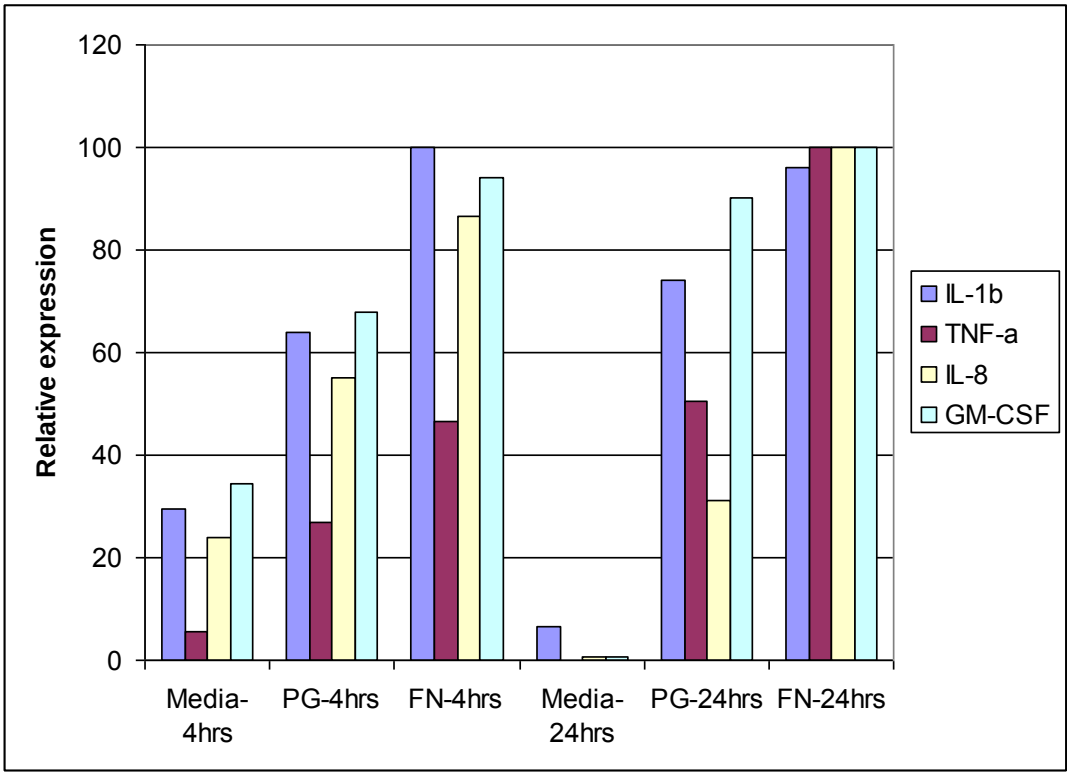

Figure 5.3: Agarose gel electrophoresis of RNA extracted from H400 cells stimulated with *P. gingivalis, F. nucleatum* or media (negative control)

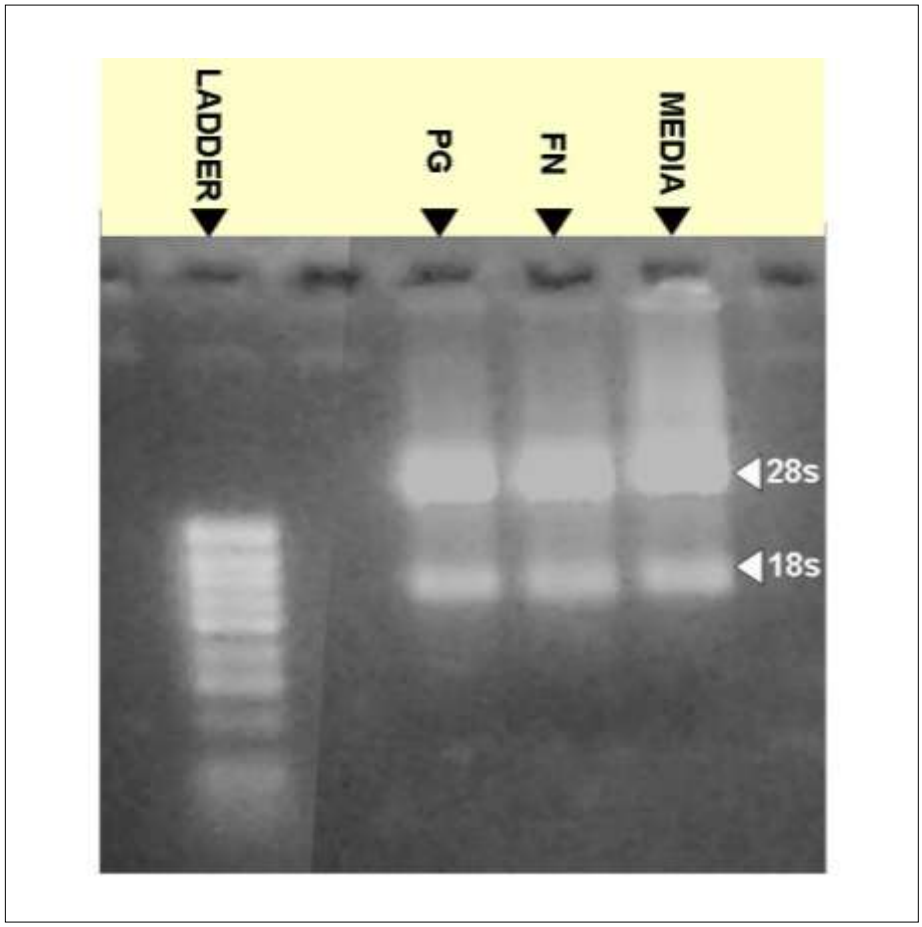

Figure 5.4: Agarose gel electrophoresis to determine success of labelling and fragmentation of cRNA prior to hybridisation onto Affymetrix U133A arrays.

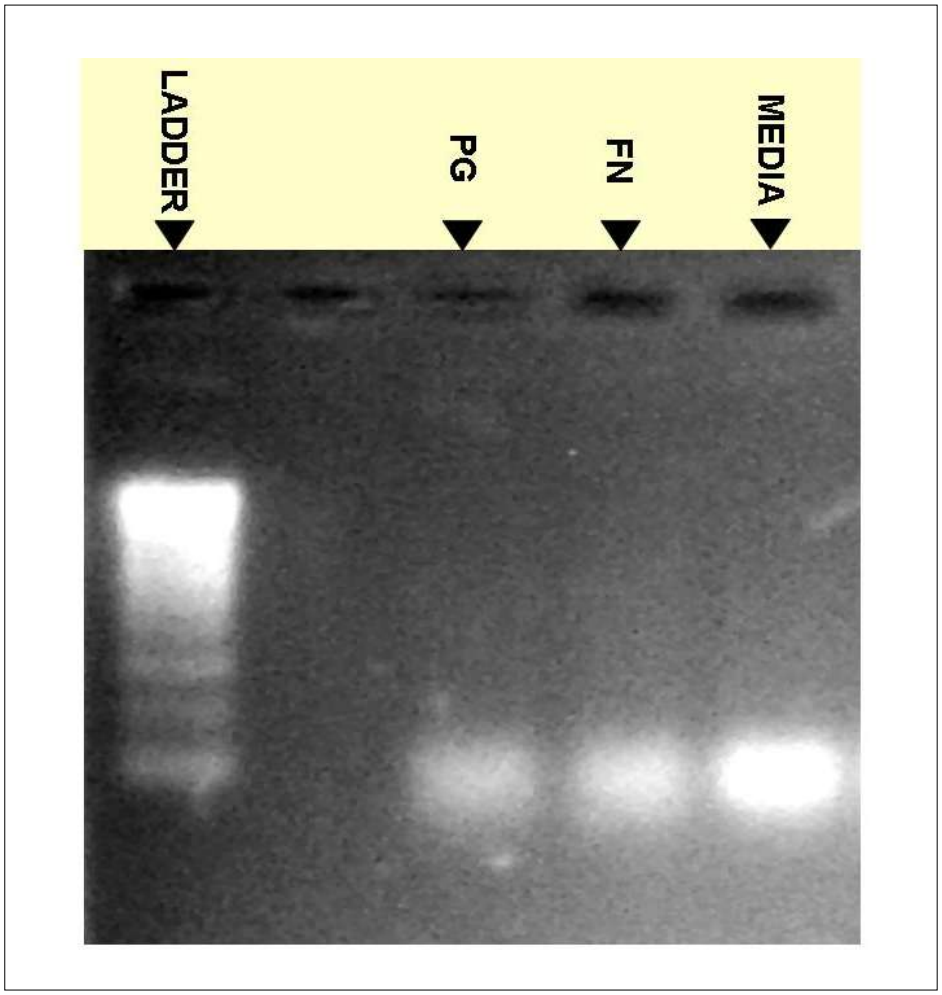

Table 5.1: List of common genes up-regulated (top 25) in H400 cells following *P. gingivalis* and *F. nucleatum* stimulation

Gene (Affymetrix definition)	Fold change	
	FN	***PG***
interleukin 8	33.1	10.2
interleukin 1, alpha	17.5	10.8
interleukin 8	15.6	9.4
tumor necrosis factor, alpha-induced protein 3	15.0	3.0
inhibin, beta A (activin A, activin AB alpha polypeptide)	14.9	6.1
interleukin 1 family, member 9	14.6	3.3
epiregulin	14.3	20.6
tumor necrosis factor, alpha-induced protein 3	13.6	3.8
heparin-binding EGF-like growth factor	12.1	4.4
A kinase (PRKA) anchor protein (gravin) 12	10.6	3.3
a disintegrin and metalloproteinase domain 8	9.8	6.9
interleukin 1, beta	9.8	5.9
interleukin 1, beta	9.7	5.6
arginase, type II	9.3	3.9
amphiregulin (schwannoma-derived growth factor)	8.5	8.6
tenascin C (hexabrachion)	8.5	3.1
microtubule associated monoxygenase	8.1	2.9
serine (or cysteine) proteinase inhibitor,	7.6	3.0
pleckstrin homology-like domain, family A, member 1	7.1	3.8
plasminogen activator, urokinase	7.0	3.7
interleukin 32	6.9	3.7
chemokine (C-X-C motif) ligand 2	6.8	3.3
plasminogen activator, urokinase receptor	6.5	2.6
secretory granule, neuroendocrine protein 1 (7B2 protein)	6.3	4.2
high mobility group AT-hook 2	5.7	3.8

Table 5.2: List of common down-regulated genes (top 25) in H400 cells following *P. gingivalis* and *F. nucleatum* stimulation.

Gene (Affymetrix definition)	Fold change	
	FN	***PG***
integrin, beta 4	-3.3	-3.1
cysteine-rich protein 2	-2.8	-3.2
hydroxyprostaglandin dehydrogenase 15-(NAD)	-3.7	-3.3
epiplakin 1	-3.4	-3.3
Glycoprotein (transmembrane) nmb	-2.5	-3.3
Ribosomal protein L37a	-2.7	-3.3
stoned B-like factor	-3.8	-3.4
FAT tumor suppressor homolog 2 (Drosophila)	-3.2	-3.4
keratin 15	-2.7	-3.5
Unc-5 homolog B (C. elegans)	-2.5	-3.7
integrin, beta 4	-2.4	-3.9
chloride channel, calcium activated, family member 2	-3.9	-3.9
inhibitor of DNA binding 3	-3.6	-4.0
matrix-remodelling associated 5	-5.0	-4.2
myristoylated alanine-rich protein kinase C substrate	-3.7	-4.3
fibroblast growth factor receptor 3	-7.5	-4.3
lysyl oxidase	-2.5	-4.8
chromosome 11 open reading frame 8	-5.2	-4.8
plakophilin 3	-4.2	-5.0
fatty acid binding protein 4, adipocyte	-2.8	-5.7
lysyl oxidase	-4.1	-6.1
keratin 14	-8.6	-6.2
lysyl oxidase	-3.2	-6.9
matrix metalloproteinase 13 (collagenase 3)	-4.0	-7.3
matrix metalloproteinase 12 (macrophage elastase)	-3.2	-9.1

Table 5.3: Genes up-regulated (top 25) in H400 cells following *F. nucleatum* stimulation.

Gene (Affymetrix definition)	Fold change
interleukin 8	33.1
interleukin 1, alpha	17.5
interleukin 8	15.6
tumor necrosis factor, alpha-induced protein 3	15.0
inhibin, beta A (activin A, activin AB alpha polypeptide)	14.9
interleukin 1 family, member 9	14.6
arachidonate 5-lipoxygenase-activating protein	14.5
epiregulin	14.3
hypothetical protein MGC4504	13.9
tumor necrosis factor, alpha-induced protein 3	13.6
activating transcription factor 3	12.7
keratin 6B	12.4
heparin-binding EGF-like growth factor	12.1
chemokine (C-X-C motif) ligand 3	11.0
A kinase (PRKA) anchor protein (gravin) 12	10.6
a disintegrin and metalloproteinase domain 8	9.8
interleukin 1, beta	9.8
interleukin 1, beta	9.7
heparin-binding EGF-like growth factor	9.5
prostaglandin E receptor 4 (subtype EP4)	9.4
arginase, type II	9.3
protein phosphatase 1, regulatory (inhibitor) subunit 15A	9.2
amphiregulin (schwannoma-derived growth factor)	8.5
tenascin C (hexabrachion)	8.5
dual specificity phosphatase 5	8.1

Table 5.4: Genes down-regulated (top 25) in H400 cells following *F. nucleatum* stimulation.

Gene (Affymetrix definition)	Fold change
aldo-keto reductase family 1, member B10	-27.6
KIAA0101	-12.4
histone 1, H4c	-11.5
thymidylate synthetase	-10.9
epidermal growth factor receptor	-9.6
keratin 14	-8.6
epidermal growth factor receptor	-8.4
Rho-related BTB domain containing 3	-8.0
Rho-related BTB domain containing 3	-7.9
epidermal growth factor receptor	-7.8
thymopoietin	-7.7
fibroblast growth factor receptor 3	-7.5
translocated promoter region (to activated MET oncogene)	-7.3
kinesin family member 20A	-7.3
topoisomerase (DNA) II alpha 170kDa	-7.1
solute carrier family 26 (sulfate transporter), member 2	-7.0
ribonucleotide reductase M2 polypeptide	-6.7
lamin B1	-6.1
PDZ binding kinase	-5.9
chromosome 10 open reading frame 3	-5.9
MCM2 minichromosome maintenance deficient 2	-5.7
chromosome 22 open reading frame 18	-5.6
dihydrofolate reductase	-5.6
DKFZP586A0522 protein	-5.5
UDP glucuronosyltransferase 1 family, polypeptide A10	-5.4

Table 5.5: Genes up-regulated (top 25) in H400 cells following *P. gingivalis* stimulation.

Gene (Affymetrix definition)	Fold change
epiregulin	20.6
heme oxygenase (decycling) 1	15.3
cytochrome P450, family 1, subfamily A, polypeptide 1	11.8
interleukin 1, alpha	10.8
interleukin 8	10.2
interleukin 8	9.4
amphiregulin (schwannoma-derived growth factor)	8.6
DnaJ (Hsp40) homolog, subfamily B, member 9	6.9
a disintegrin and metalloproteinase domain 8	6.9
chemokine (C-C motif) ligand 20	6.4
inhibin, beta A (activin A, activin AB alpha polypeptide)	6.1
interleukin 1, beta	5.9
interleukin 1, beta	5.6
cytochrome P450, family 1, subfamily B, polypeptide 1	5.5
FOS-like antigen 1	5.2
interleukin 7 receptor /// interleukin 7 receptor	5.1
SRY (sex determining region Y)-box 9	4.7
cytochrome P450, family 1, subfamily B, polypeptide 1	4.5
DR1-associated protein 1 (negative cofactor 2 alpha)	4.5
heparin-binding EGF-like growth factor	4.4
spastic ataxia of Charlevoix-Saguenay (sacsin)	4.3
secretory granule, neuroendocrine protein 1 (7B2 protein)	4.2
cisplatin resistance-associated overexpressed protein	4.0
neuron navigator 3	4.0
aldo-keto reductase family 1, member C3	4.0

Table 5.6: Genes down-regulated (top 25) in H400 cells following *P. gingivalis* stimulation.

Gene (Affymetrix definition)	Fold change
kelch-like 22 (Drosophila)	-12.5
3-hydroxyisobutyrate dehydrogenase	-10.9
matrix metalloproteinase 12 (macrophage elastase)	-9.1
protocadherin gamma subfamily A, 3	-9.0
matrix metalloproteinase 13 (collagenase 3)	-7.3
lysyl oxidase	-6.9
keratin 14	-6.2
Tumor necrosis factor (ligand) superfamily, member 10	-6.1
lysyl oxidase	-6.1
Consensus includes gb:AW451806	-5.9
matrix metalloproteinase 1 (interstitial collagenase)	-5.8
fatty acid binding protein 4, adipocyte	-5.7
lysosomal-associated membrane protein 1	-5.5
MRNA full length insert cDNA clone EUROIMAGE 21920	-5.3
plakophilin 3	-5.0
olfactomedin 4	-4.9
tumor necrosis factor (ligand) superfamily, member 10	-4.9
tumor necrosis factor (ligand) superfamily, member 10	-4.8
hydroxyprostaglandin dehydrogenase 15-(NAD)	-4.8
chromosome 11 open reading frame 8	-4.8
lysyl oxidase	-4.8
RAD51-like 3 (S. cerevisiae)	-4.5
Consensus includes gb:BF739971	-4.4
fibroblast growth factor receptor 3 (achondroplasia, thanatophoric dwarfism)	-4.3
acetyl-Coenzyme A carboxylase beta	-4.3

Figure 5.5: Venn diagram representing the number of **A:** up-regulated genes, **B:** down-regulated genes and **C:** differentially expressed genes (up & down) from microarray analysis (using a 2 fold cut off) of *P. gingivalis (PG)* and *F. nucleatum (FN)* stimulated H400 cells. Data includes common genes expressed by both periodontal pathogens.

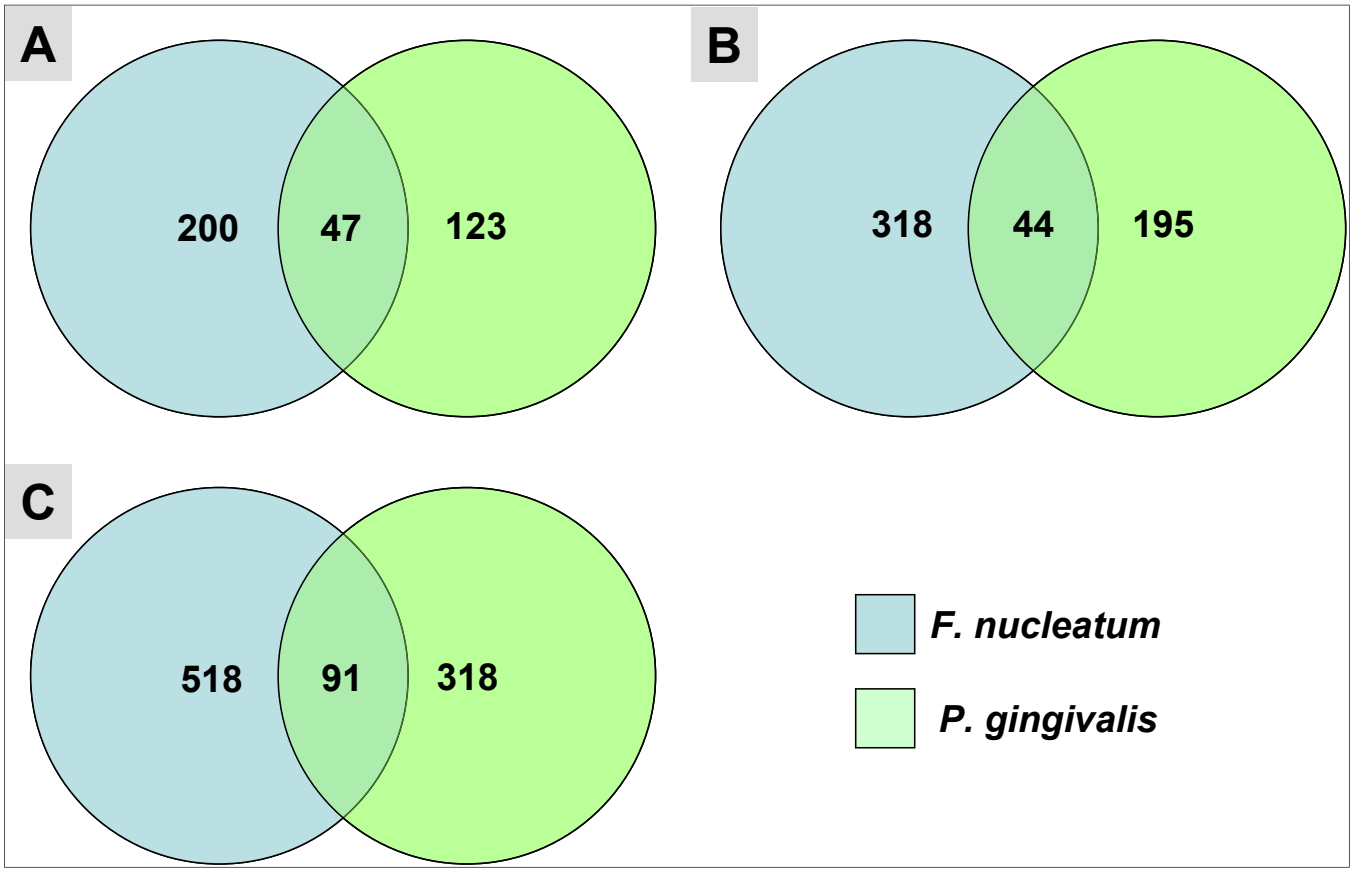

Figure 5.6: Diagram illustrating ontological groups of genes up-regulated by **A**: *F.nucleatum* (247 genes), **B**: *P. gingivalis* (170) & **C**: genes common to *F. nucleatum* & *P. gingivalis* (47 genes). Microarray analysis using a 2 fold change gene expression cut off.

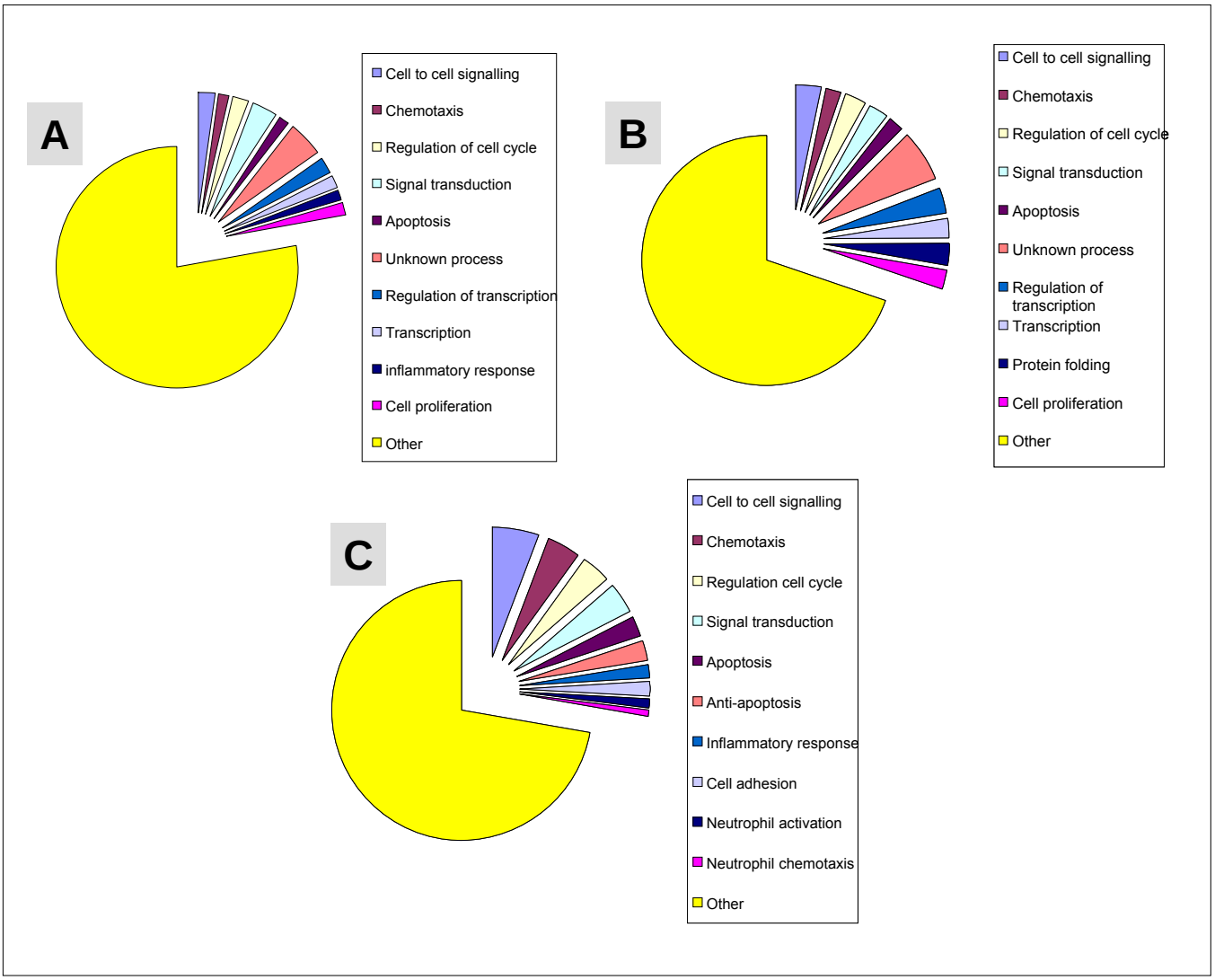

Figure 5.7: Common up-regulated genes (2-fold or greater) for H400 cells stimulated with *P. gingivalis* and *F. nucleatum*. Genes listed in ontological groups (higher level of expression between *PG* & *FN* highlighted in grey).

GO Annotation	Affymetrix ID	GENE	Gene Symbol	Fold change *PG*	Fold change *FN*
Immune / Inflammatory / chemotaxis response	211506_s_at	interleukin 8	*IL8*	10.2	33.08
	210118_s_at	interleukin 1, alpha	*IL1A*	10.77	17.45
	202859_x_at	interleukin 8	*IL8*	9.37	15.61
	220322_at	interleukin 1 family, member 9	*IL1F9*	3.28	14.59
	205067_at	interleukin 1, beta	*IL1B*	5.92	9.79
	39402_at	interleukin 1, beta	*IL1B*	5.59	9.69
	211668_s_at	plasminogen activator, urokinase	*PLAU*	3.73	6.95
	203828_s_at	interleukin 32	*IL32*	3.72	6.9
	209774_x_at	chemokine (C-X-C motif) ligand 2	*CXCL2*	3.25	6.77
	210845_s_at	plasminogen activator, urokinase receptor	*PLAUR*	2.61	6.45
	205476_at	chemokine (C-C motif) ligand 20	*CCL20*	6.39	5.7
	204420_at	FOS-like antigen 1	*FOSL1*	5.17	4.09
Cell cycle / proliferation / differentiation	210511_s_at	inhibin, beta A (activin A, activin AB alpha polypeptide)	*INHBA*	6.14	14.87
	205767_at	epiregulin	*EREG*	20.59	14.29
	205239_at	amphiregulin (schwannoma-derived growth factor)	*AREG*	8.55	8.51
	203414_at	monocyte to macrophage differentiation-associated	*MMD*	2.95	4.45
	202147_s_at	interferon-related developmental regulator 1	*IFRD1*	2.65	3.31
	200953_s_at	cyclin D2	*CCND2*	2.59	3.15
	202146_at	interferon-related developmental regulator 1	*IFRD1*	2.69	2.67
	202934_at	hexokinase 2	*HK2*	2.63	2.58
	208892_s_at	dual specificity phosphatase 6	*DUSP6*	3.08	2.37
Protein metabolism / processing	205180_s_at	a disintegrin and metalloproteinase domain 8	*ADAM8*	6.85	9.84
	203889_at	secretory granule, neuroendocrine protein 1 (7B2 protein)	*SCG5*	4.23	6.26
	202843_at	DnaJ (Hsp40) homolog, subfamily B, member 9	*DNAJB9*	6.91	4.94
	215009_s_at	SEC31-like 1 (S. cerevisiae)	*SEC31L1*	2.36	2.89
	213262_at	spastic ataxia of Charlevoix-Saguenay (sacsin)	*SACS*	4.32	2.56
	217168_s_at	homocysteine-inducible, endoplasmic reticulum stress-inducible, ubiquitin-like domain member 1	*HERPUD1*	2.92	2.37
Signal transduction	202644_s_at	tumor necrosis factor, alpha-induced protein 3	*TNFAIP3*	3.01	15.01
	202643_s_at	tumor necrosis factor, alpha-induced protein 3	*TNFAIP3*	3.84	13.61
	203821_at	heparin-binding EGF-like growth factor	*HBEGF*	4.37	12.12
	210517_s_at	A kinase (PRKA) anchor protein (gravin) 12	*AKAP12*	3.25	10.58
	221577_x_at	growth differentiation factor 15	*GDF15*	3.58	2.81
Apoptosis / Anti-apoptosis	204614_at	serine (or cysteine) proteinase inhibitor, clade B (ovalbumin), member 2	*SERPINB2*	3.02	7.59
	217997_at	pleckstrin homology-like domain, family A, member 1	*PHLDA1*	3.77	7.11
	218000_s_at	pleckstrin homology-like domain, family A, member 1	*PHLDA1*	2.56	4.49
	210538_s_at	baculoviral IAP repeat-containing 3	*BIRC3*	2.52	2.43
Transcription regulation	208025_s_at	high mobility group AT-hook 2 /// high mobility group AT-hook 2	*HMGA2*	3.84	5.72
	202936_s_at	SRY (sex determining region Y)-box 9	*SOX9*	3.2	4.71
	36711_at	v-maf musculoaponeurotic fibrosarcoma oncogene homolog F (avian)	*MAFF*	3.23	3.4
Cell adhesion	201645_at	tenascin C (hexabrachion)	*TNC*	3.12	8.47
	203562_at	fasciculation and elongation protein zeta 1 (zygin I)	*FEZ1*	3.21	3.68
Metabolism	212473_s_at	microtubule associated monoxygenase, calponin and LIM domain containing 2	*MICAL2*	2.93	8.09
	210041_s_at	phosphoglucomutase 3	*PGM3*	2.79	3.53
Nitric oxide / oxidative stress response	203946_s_at	arginase, type II	*ARG2*	3.89	9.25
	215223_s_at	superoxide dismutase 2, mitochondrial	*SOD2*	2.57	4.69
Autophagy / Cytolosis	203827_at	WD40 repeat protein Interacting with phospholnositides of 49kDa	*WIPI1*	3.01	3.24

Figure 5.8: Common down-regulated genes (2-fold or greater) for H400 cells stimulated with *P. gingivalis* and *F. nucleatum*. Genes listed in ontological groups (higher level of expression between *PG* & *FN* highlighted in grey).

Go Annotation	Affymetrix ID	GENE	Gene Symbol	Fold change *PG*	Fold change *FN*
Protein metabolism / processing / proteolysis	209596_at	matrix-remodelling associated 5	*MXRA5*	-4.18	-4.99
	221215_s_at	receptor-interacting serine-threonine kinase 4	*RIPK4*	-3.02	-4.88
	213640_s_at	lysyl oxidase	*LOX*	-6.07	-4.14
	205959_at	matrix metalloproteinase 13 (collagenase 3)	*MMP13*	-7.34	-4.02
	204580_at	matrix metalloproteinase 12 (macrophage elastase)	*MMP12*	-9.05	-3.19
	204298_s_at	lysyl oxidase	*LOX*	-6.92	-3.17
	214041_x_at	Ribosomal protein L37a	*RPL37A*	-3.34	-2.68
	215446_s_at	lysyl oxidase	*LOX*	-4.75	-2.48
Cell cycle / growth / proliferation	211607_x_at	epidermal growth factor receptor	*EGFR*	-2.72	-8.42
	210984_x_at	epidermal growth factor receptor	*EGFR*	-2.85	-7.83
	204379_s_at	fibroblast growth factor receptor 3	*FGFR3*	-4.34	-7.48
	202718_at	insulin-like growth factor binding protein 2, 36kDa	*IGFBP2*	-2.37	-3.99
	213413_at	stoned B-like factor	*STON1*	-3.39	-3.78
	209784_s_at	jagged 2	*JAG2*	-3.01	-2.5
	32137_at	jagged 2	*JAG2*	-2.98	-2.48
	201141_at	glycoprotein (transmembrane)	*GPNMB*	-3.29	-2.46
Cell adhesion / motility	209872_s_at	plakophilin 3	*PKP3*	-4.95	-4.17
	201668_x_at	myristoylated alanine-rich protein kinase C substrate	*MARCKS*	-4.3	-3.74
	211905_s_at	integrin, beta 4	*ITGB4*	-3.11	-3.33
	208153_s_at	FAT tumor suppressor homolog 2	*FAT2*	-3.42	-3.19
	201107_s_at	thrombospondin 1	*THBS1*	-2.9	-2.7
	201107_s_at	thrombospondin 1	*THBS1*	-2.9	-2.7
	204989_s_at	integrin, beta 4	*ITGB4*	-3.92	-2.37
Epidermis development	209351_at	keratin 14	*KRT14*	-6.17	-8.63
	213240_s_at	keratin 4	*KRT4*	-2.59	-4.89
	222242_s_at	kallikrein 5	*KLK5*	-2.51	-3.38
	204734_at	keratin 15	*KRT15*	-3.47	-2.67
	207935_s_at	keratin 13	*KRT13*	-2.71	-2.49
Fatty acid / lipid metabolism	211548_s_at	hydroxyprostaglandin dehydrogenase 15-(NAD)	*HPGD*	-3.26	-3.69
	211708_s_at	stearoyl-CoA desaturase (delta-9-desaturase)	*SCD*	-2.8	-3.38
	203980_at	fatty acid binding protein 4, adipocyte	*FABP4*	-5.72	-2.79
	203914_x_at	hydroxyprostaglandin dehydrogenase 15-(NAD)	*HPGD*	-2.57	-2.75
Nervous system signalling / development	205413_at	chromosome 11 open reading frame 8	*MPPED2*	-4.76	-5.19
	200648_s_at	glutamate-ammonia ligase (glutamine synthase)	*GLUL*	-2.75	-3.78
	217202_s_at	glutamate-ammonia ligase (glutamine synthase)	*GLUL*	-3.07	-3.46
Transcription regulation	207826_s_at	inhibitor of DNA binding 3	*ID3*	-4.01	-3.61
	210892_s_at	general transcription factor II, I	*GTF2I*	-2.67	-3.31
	212016_s_at	polypyrimidine tract binding protein 1	*PTBP1*	-2.45	-3.18
Transport	206165_s_at	chloride channel, calcium activated, family member 2	*CLCA2*	-3.94	-3.89
Unclassified	207761_s_at	DKFZP586A0522 protein	*METTL7A*	-2.9	-5.47
	221805_at	neurofilament, light polypeptide 68kDa	*NEFL*	-2.43	-3.57
	208156_x_at	epiplakin 1 /// epiplakin 1	*EPPK1*	-3.27	-3.41
	213075_at	olfactomedin-like 2A	*OLFML2A*	-2.83	-2.99
	208978_at	cysteine-rich protein 2	*CRIP2*	-3.22	-2.77
	213069_at	HEG homolog 1 (zebrafish)	*HEG1*	-2.58	-2.74
	213100_at	Unc-5 homolog B (C. elegans)	---	-3.71	-2.51

Figure 5.9: Comparative analyses of microarray and PCR data (right hand y scale represents microarray fold change (normalised); left hand y scale represents RT-PCR relative expression).

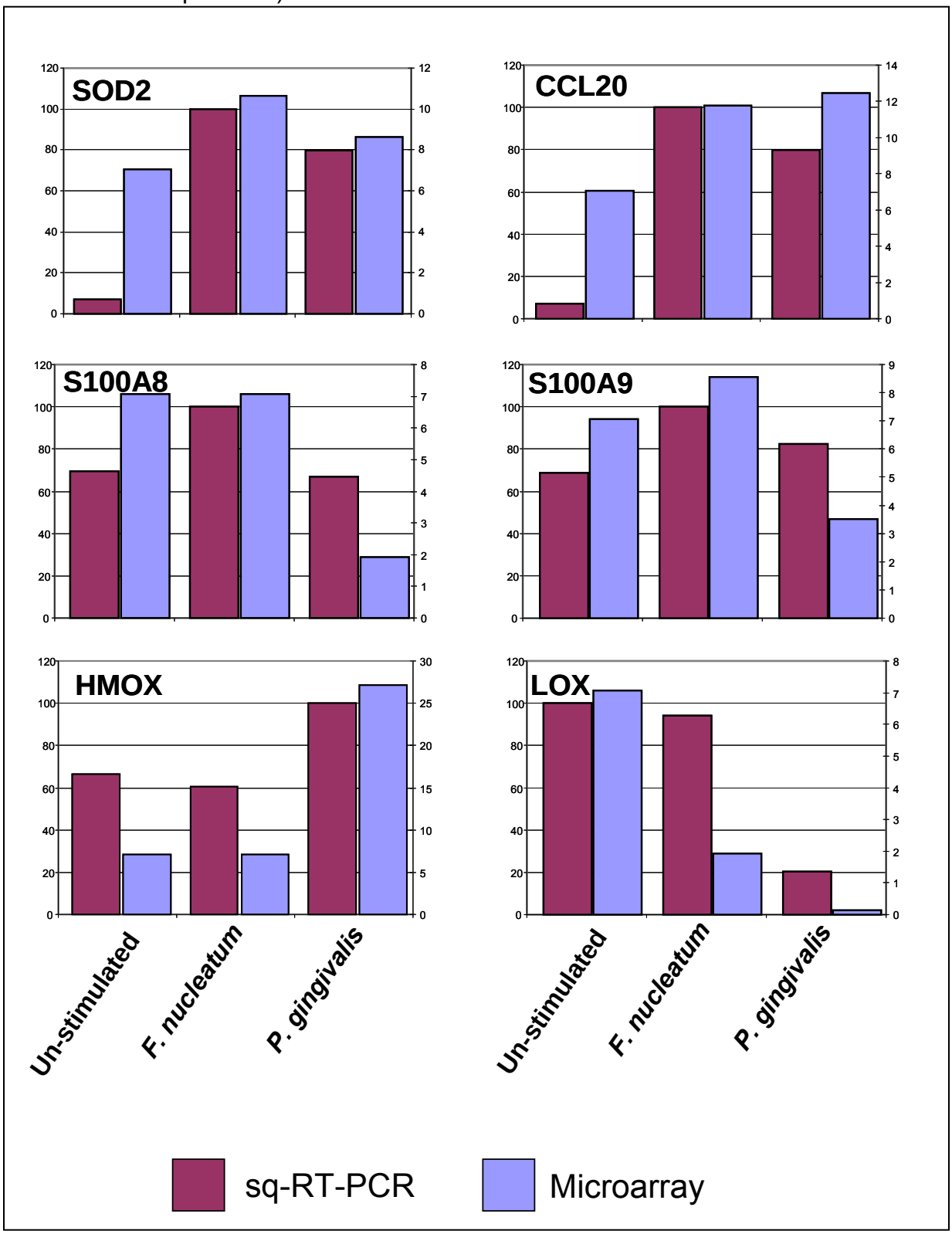

Figure 6.1: SQ RT-PCR gel images of H400 cells pre incubated with α-lipoate or vehicle control; and stimulated with *P. gingivalis, F. nucleatum* or media control. All samples normalised to GAPDH.

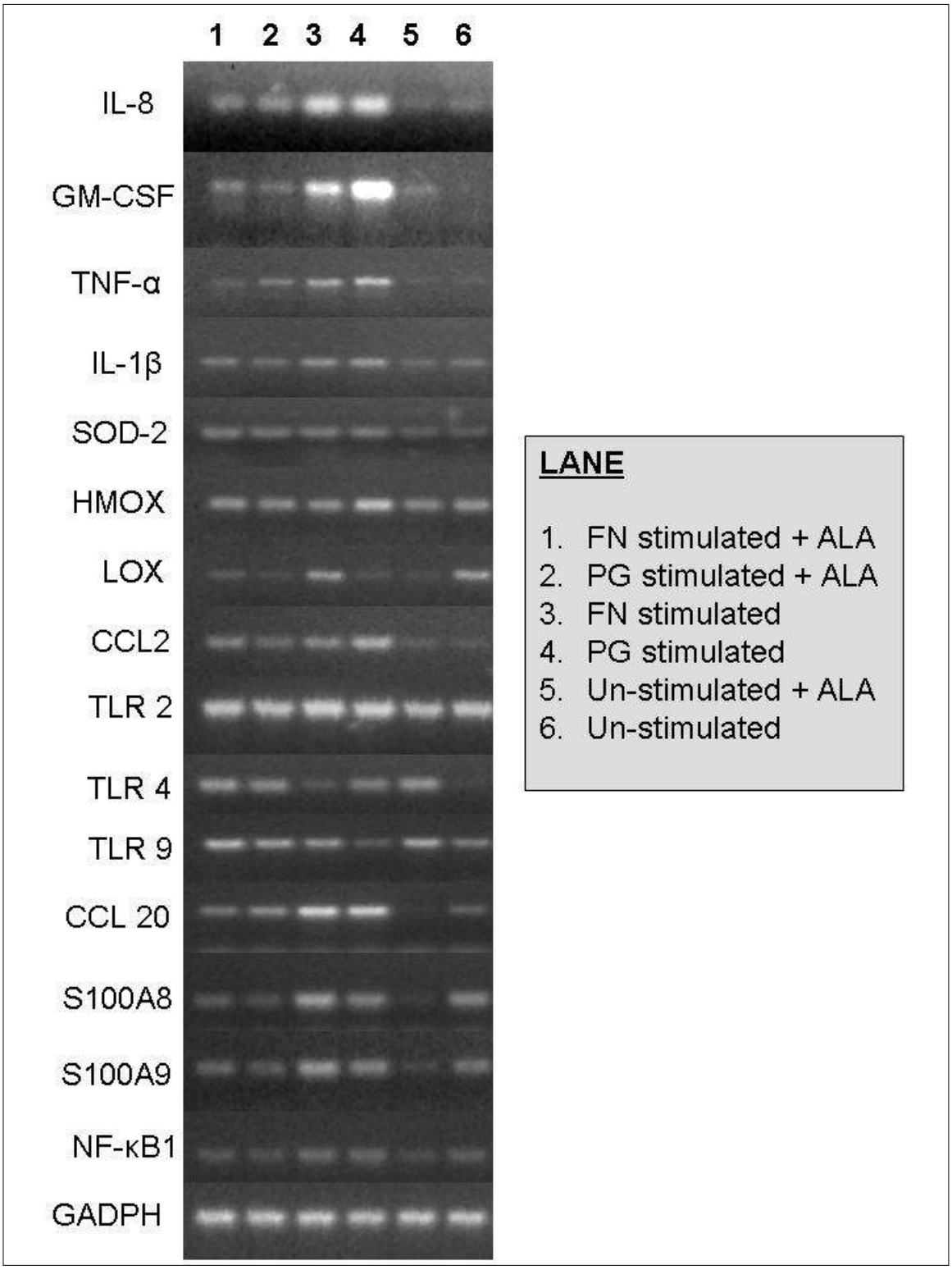

Figure 6.2 Pro-inflammatory gene expression changes determined by sq-RT-PCR in H400 cells pre-incubated with 0.5mM α-lipoate (24h) or vehicle control, stimulated with *P. gingivalis, F. nucleatum* or media (negative control). Mean values of duplicate analyses are shown.

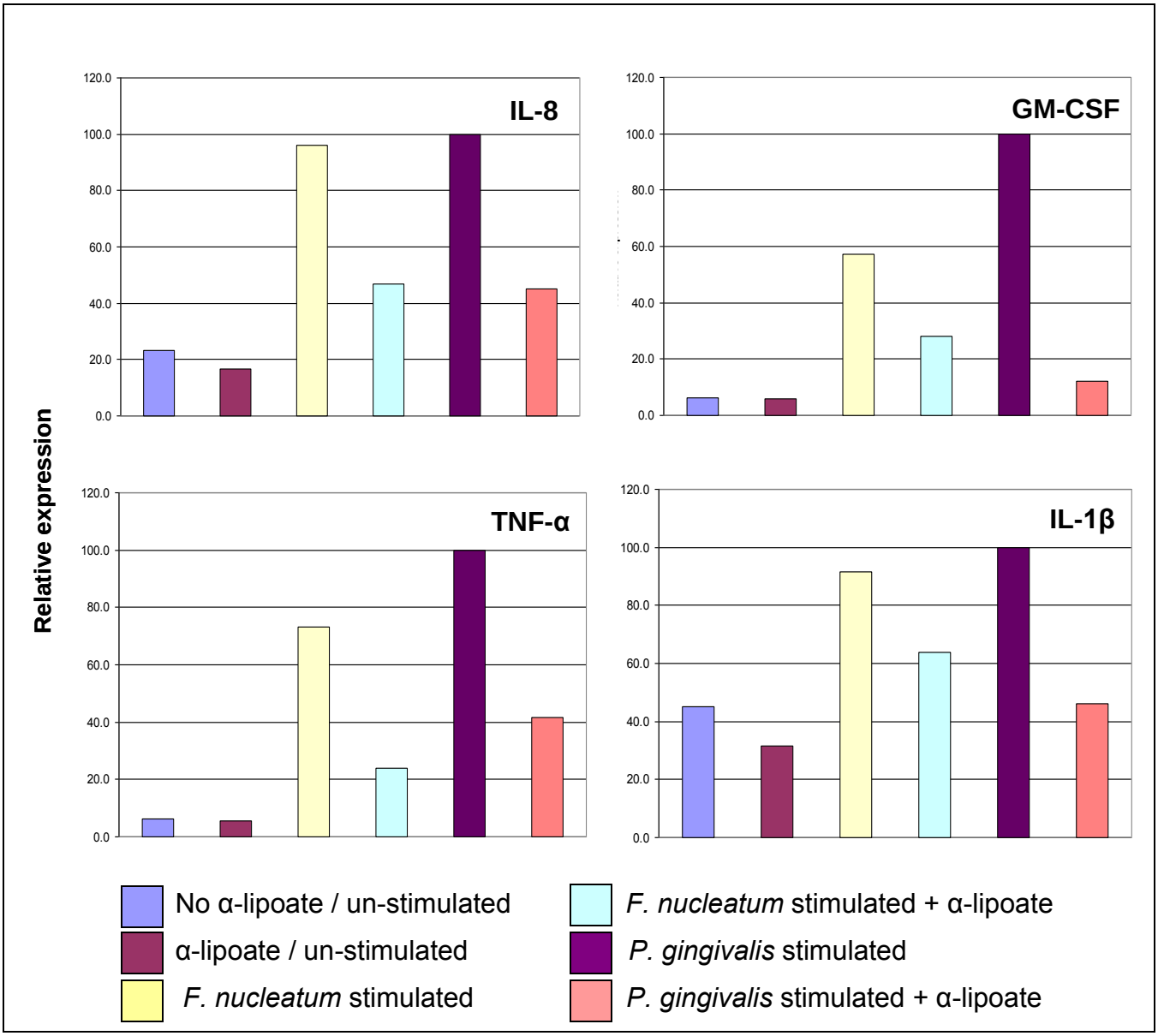

Figure 6.3 Bacterial recognition (Toll-like receptor) gene expression changes determined by sq-RT-PCR in H400 cells pre-incubated with 0.5mM α-lipoate (24h) or vehicle control, stimulated with *P. gingivalis, F. nucleatum* or media (negative control). Mean values of duplicate analyses are shown.

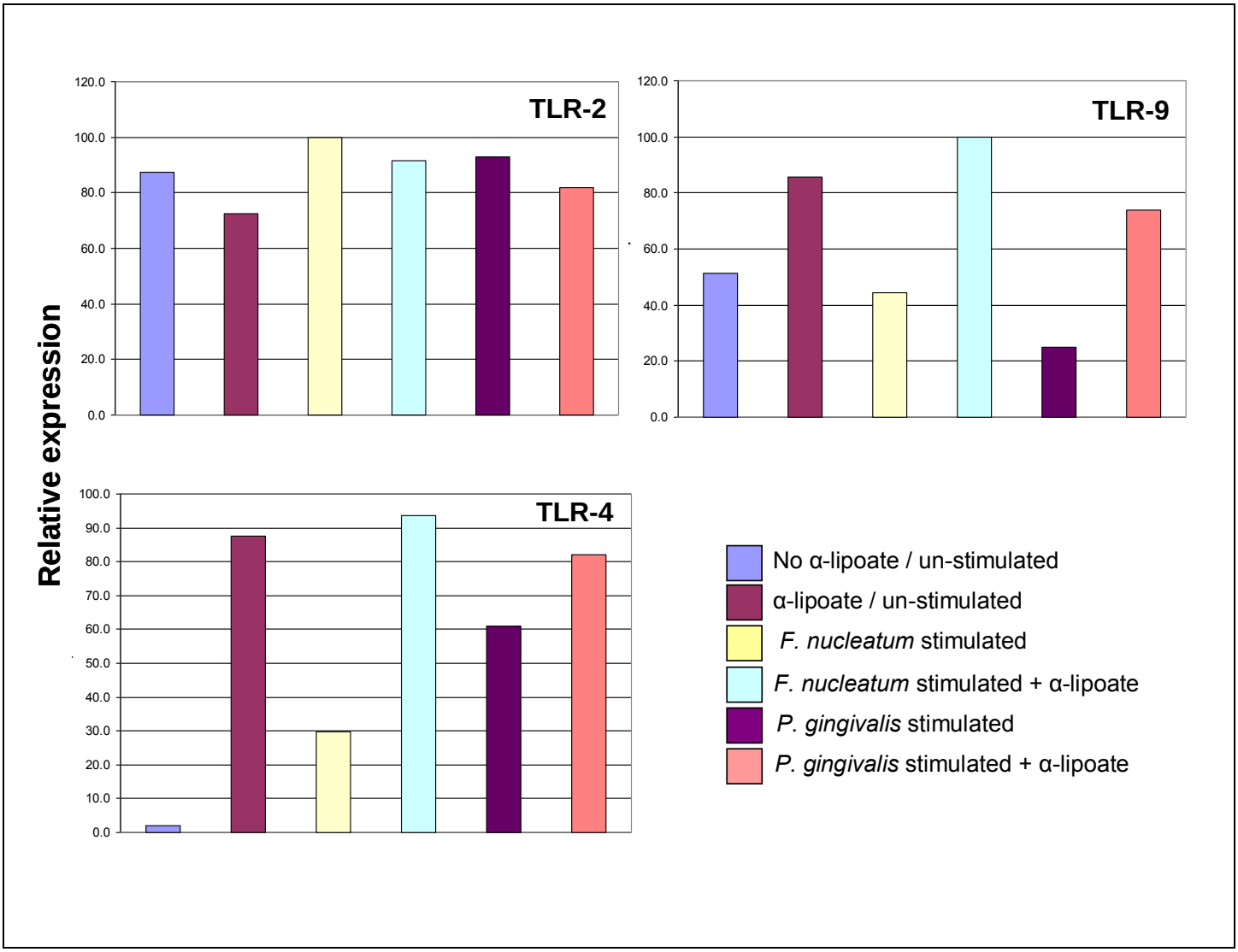

Figure 6.4 Epithelial protective gene expression changes determined by sq-RT-PCR in H400 cells pre-incubated with 0.5mM α-lipoate (24h) or vehicle control, stimulated with *P. gingivalis, F. nucleatum* or media (negative control). Mean values of duplicate analyses are shown.

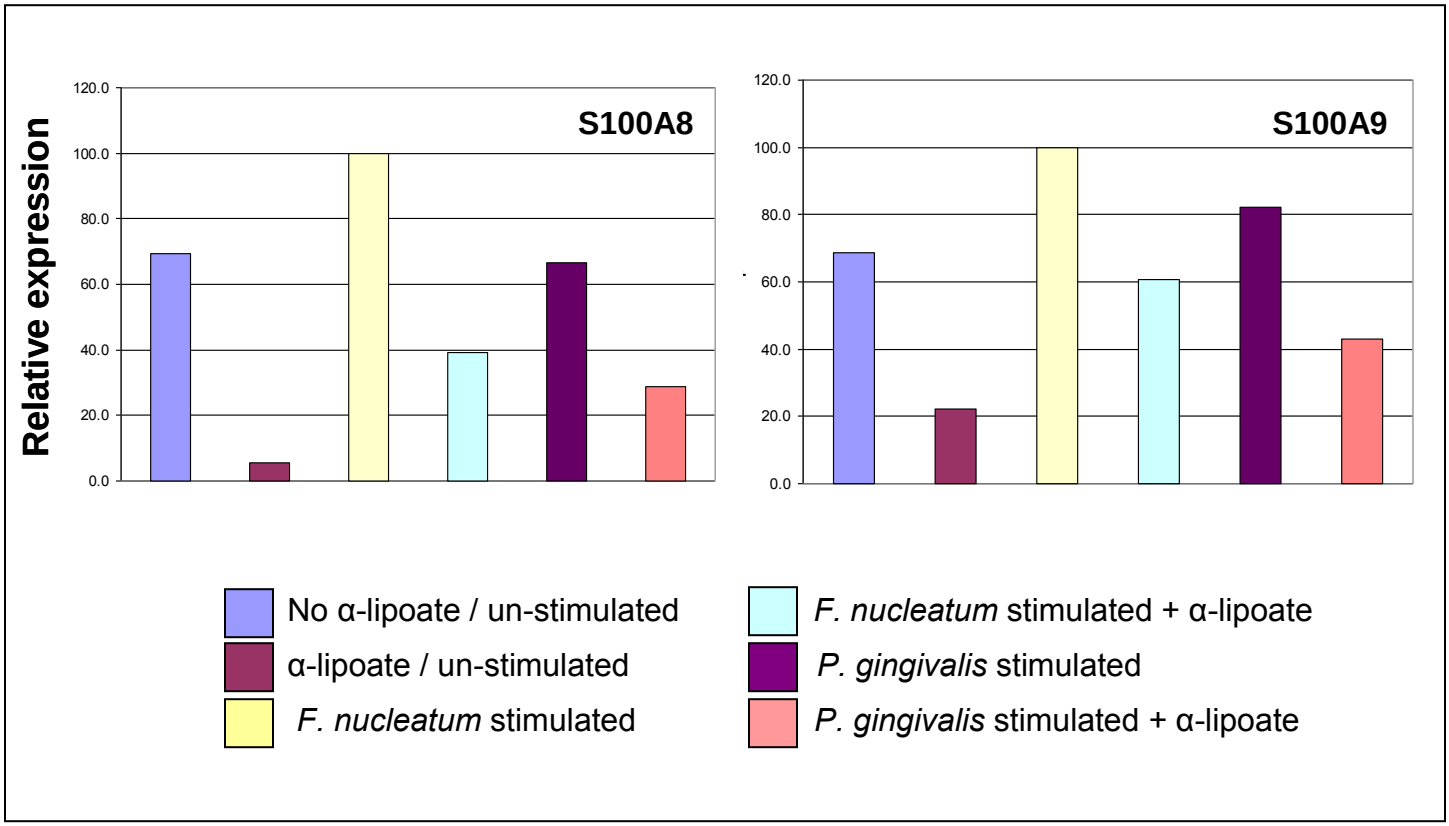

Figure 6.5 Anti-oxidant gene expression changes determined by sq-RT-PCR in H400 cells pre-incubated with 0.5mM α-lipoate (24h) or vehicle control, stimulated with *P. gingivalis, F. nucleatum* or media (negative control). Mean values of duplicate analyses are shown.

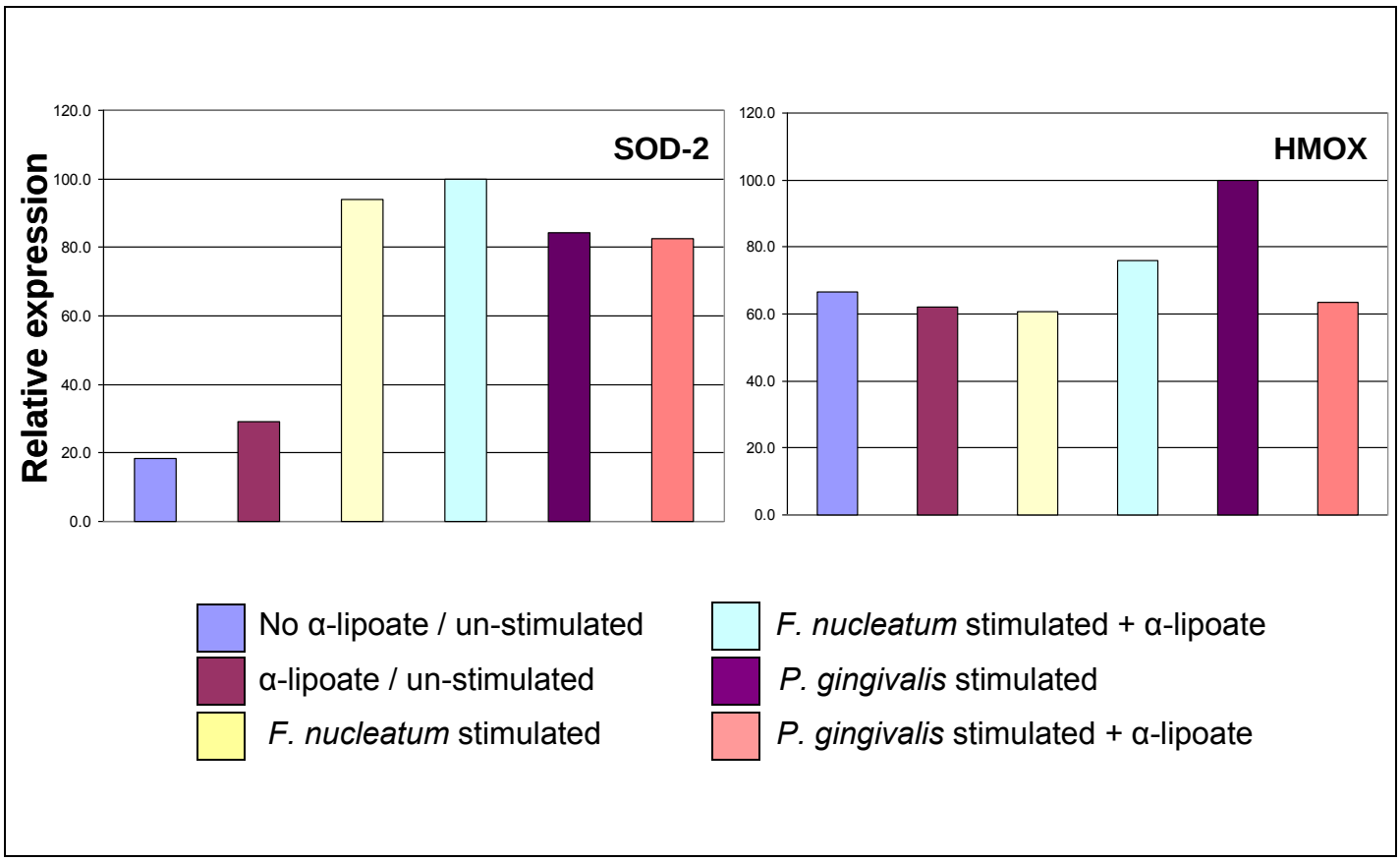

Figure 6.6: LOX gene expression changes determined by sq-RT-PCR in H400 cells pre-incubated with α-lipoate (24h) or vehicle control, stimulated with *P. gingivalis, F. nucleatum* or media (negative control). Mean values of duplicate analyses are shown.

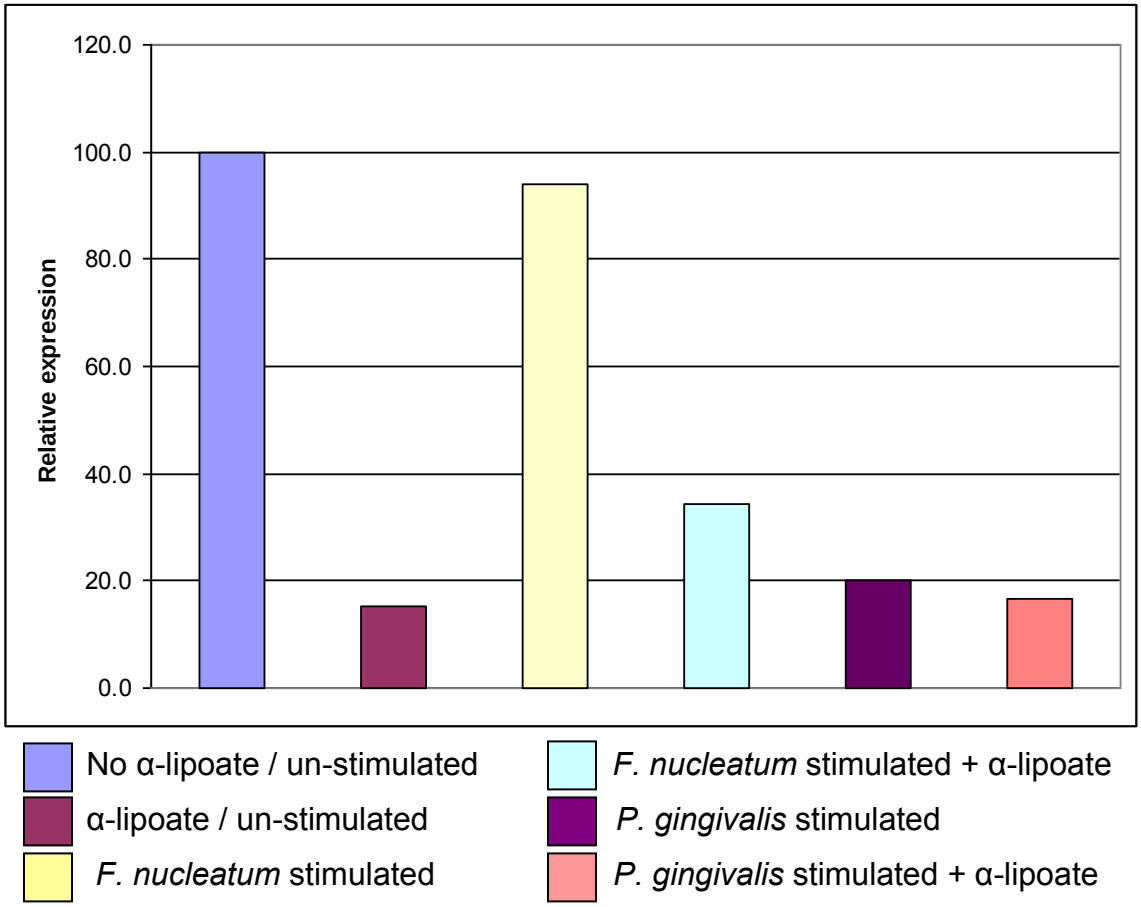

Figure 6.7 CCL-2 & CCL-20 gene expression changes determined by sq-RT-PCR in H400 cells pre-incubated with α-lipoate (24h) or vehicle control, stimulated with *P. gingivalis, F. nucleatum* or media (negative control). Mean values of duplicate analyses are shown.

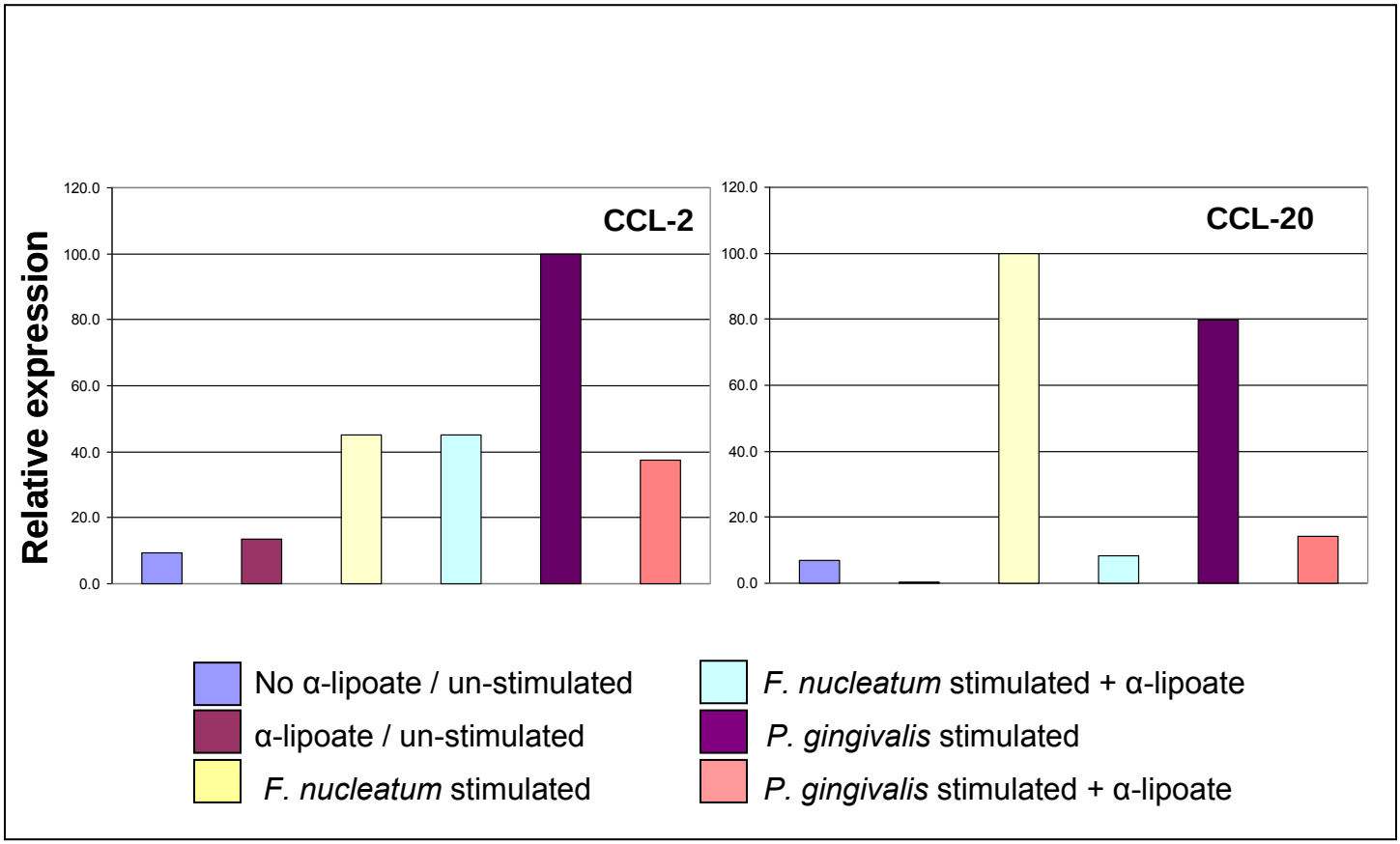

Figure 6.8: NF-κB$_1$ gene expression changes determined by sq-RT-PCR in H400 cells pre-incubated with 0.5mM α-lipoate (24h) or vehicle control, stimulated with *P. gingivalis, F. nucleatum* or media (negative control). Mean values of duplicate analyses are shown.

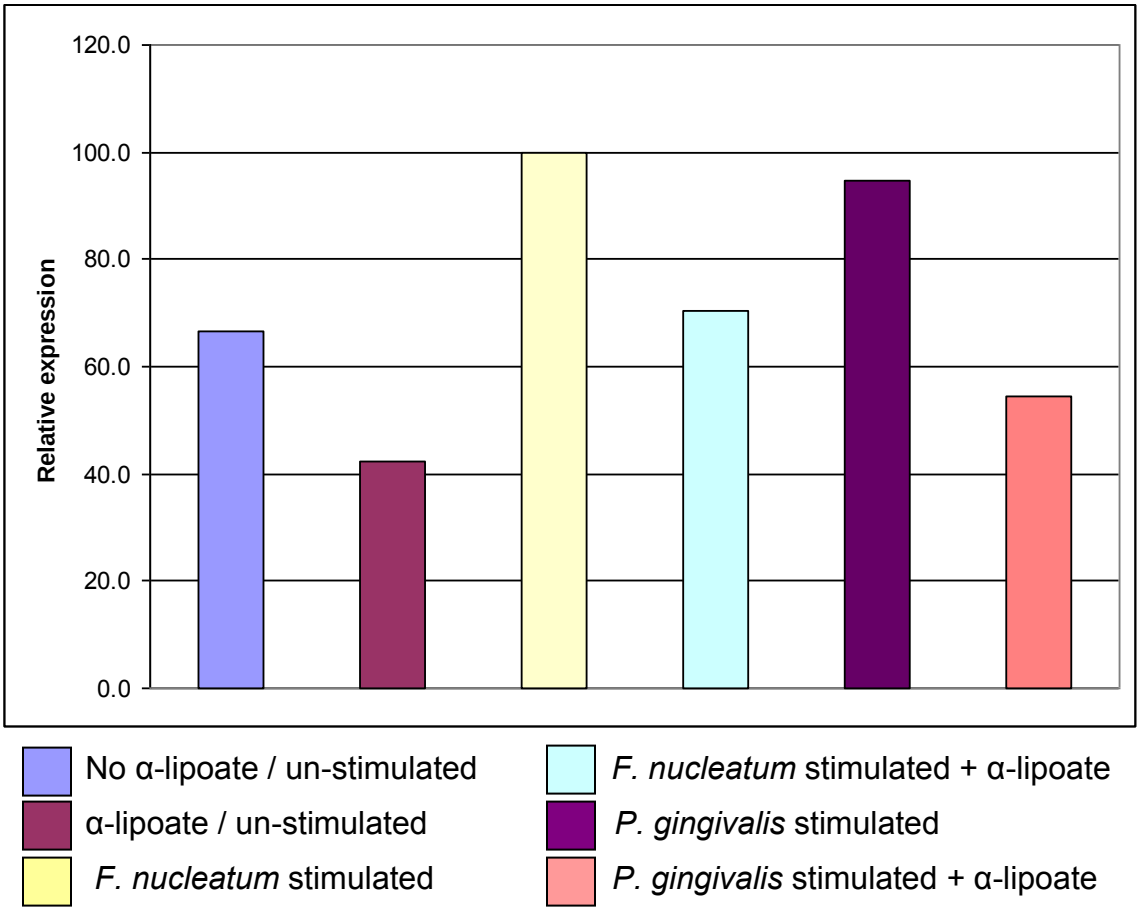

Figure 6.9 Cytokine levels in H400 cells pre-incubated with 0.5mM α-lipoate or vehicle control (24h) and stimulated with *P. gingivalis, F. nucleatum* or media (negative control). Samples run in duplicate with each value plotted.

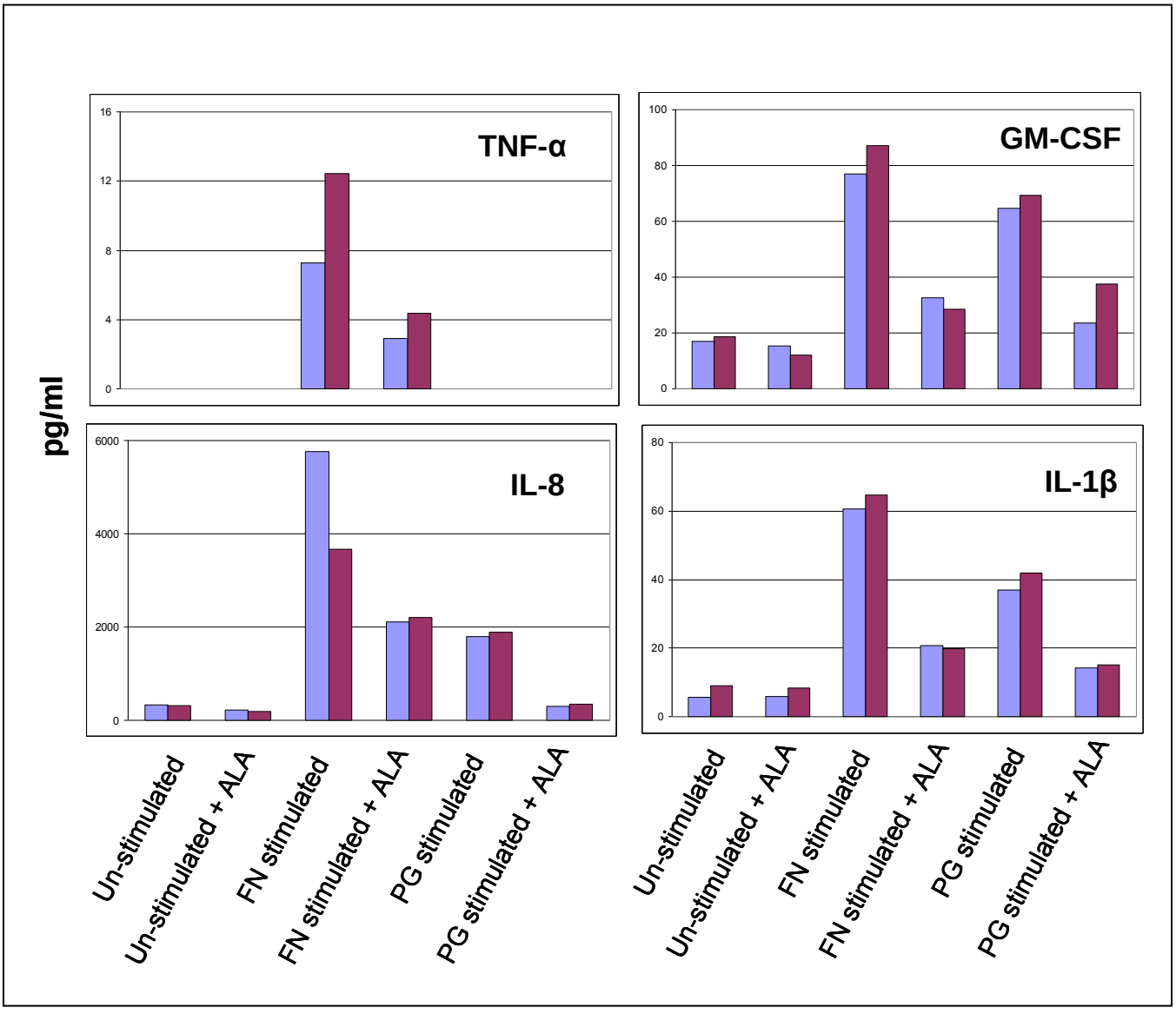

Figure 7.1 Diagrammatic representation of the epithelial model system identifying the stages investigated in cell activation. **1**: Activation of NF-κB; **2**: Gene expression changes; **3**: Pro-inflammatory cytokine production. Reduced activation of NF-κB by α-lipoate is also included (**4**).

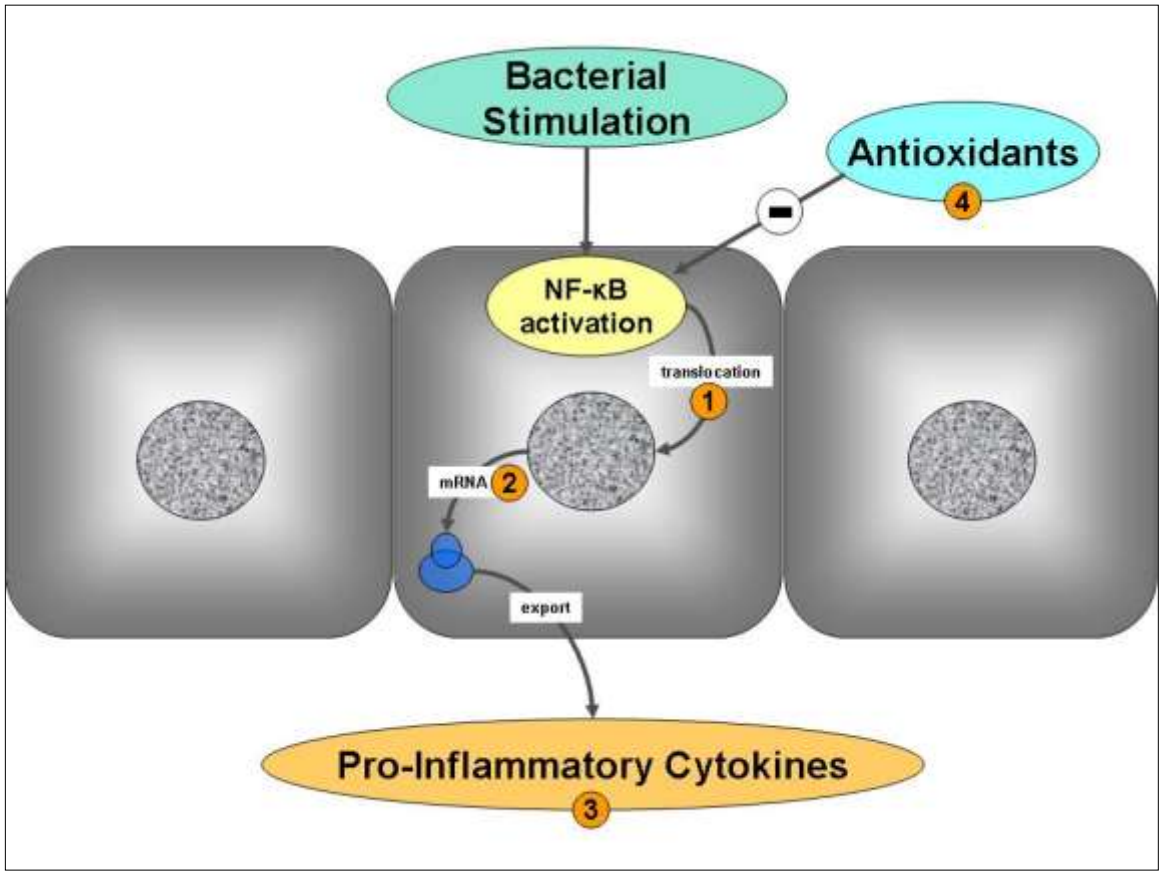

Figure 7.2: Diagram illustrating ontological groups of genes up-regulated by **A**: *F.nucleatum* (247 genes), **B**: *P. gingivalis* (170) & **C**: genes common to *F. nucleatum* & *P. gingivalis* (47 genes). Microarray analysis using a 2 fold change gene expression cut off.